Functional analysis of the histone methyltransferase SET9 in androgen receptor regulation and prostate cancer

Thesis submitted to Newcastle University for the degree of Doctor of Philosophy by

Nan Wang

Northern Institute for Cancer Research

Submitted October 2010

Abstract

Prostate cancer is the leading cause of cancer-related death in western men and results in approximately 10,000 deaths in the UK per year (Cancer Research UK). The androgen receptor (AR) plays a prominent role in both androgen-dependent (AD) and androgen-independent (AI) disease, but treatments that attempt to inactivate the receptor are in-effective. There is a requirement therefore to develop new therapies that permanently disrupt AR function and attenuate disease progression. Hence, identification of new targets within the AR signalling cascade is vital. Numerous AR co-regulators have been identified that regulate AR activity and several of these proteins have been suggested to play a role in the progression of AD and AI disease. In this project, using CaP cell lines, different aspects of the histone methyltransferase enzyme SET9 were studied including its phenotypic influence, expression dynamics and also the molecular mechanisms it mediates in CaP cells.

Our previous data demonstrated that SET9 enhances AR activity by directly methylating the receptor at lysine (K) residue 632 in the KLKK motif within the hinge domain of the receptor, and this affected co-activator-AR interaction in LNCaP prostate cancer cells. To assess the physiological role of SET9 in CaP cells, SET9 expression in LNCaP cells was reduced by siRNA interference and the effects on proliferation and apoptosis were investigated. Interestingly, SET9 knockdown reduced LNCaP cell proliferation and up-regulated apoptosis, implicating a role for SET9 in driving CaP progression. Moreover, a combination of SET9 knockdown and treatment with the DNA-damaging agent Doxorubicin in LNCaP cells synergised to increase apoptosis suggesting SET9 may be a potential therapeutic target for advanced CaP.

Using a GFP-SET9 fusion protein and immunofluorescence, incorporating an anti-SET9 antibody, SET9 was demonstrated to be predominantly cytoplasmic in LNCaP and U2OS cells, suggesting additional, non-nuclear roles for SET9. To address this issue, and also to explore novel mechanisms of SET9 regulation, the enzyme was immunoprecipitated from LNCaP cells and the immunoprecipitated material was subjected to in solution based protein

separation (OFF-GEL fractionation) followed by LC-MS/MS analysis to identify novel SET9 interacting proteins. Amongst several SET9 interacting partners, FXR1 was identified as a pro-apoptotic protein that facilitates SET9 knockdown mediated apoptosis in response to Doxorubicin. A predominantly cytoplasmic co-localisation pattern was confirmed for FXR1 using confocal microscopy, which was consistent with the data obtained from prostate clinical specimen using immunohistochemistry. Moreover, FXR1 was shown to function through AR to repress SET9 mediated co-activation of AR in reporter assays. More surprisingly, FXR1 displayed potent repressive effects on AR without the induction of SET9.

In summary, this data highlights SET9 as a novel AR co-regulator that is important for prostate cancer cell growth. Further characterisation of SET9-interacting proteins including FXR1 may also provide novel protein targets for CaP therapy.

Acknowledgement

I would first and foremost like to thank my family, particularly my father and mother who supported me from all aspects (in daily life and in the lab) since the first time I came to the UK and throughout the 5 years from the time I was undertaking the master degree up to the present when I am approaching the end of my PhD. Without your kind concern and regard throughout this time, I would never have completed. I would also like to give a special thank-you to my wife who has been helping me and encouraging me to get through this hard time and with the dilemmas I have encountered during my pursuit of the PhD.

I have to pay my highest respect to my two supervisors, Prof. Craig Robson and Dr. Luke Gaughan for giving me the opportunity to carry out my PhD in their group and in fact since the first day I arrived at their lab in December 2005 for my master project. In the past 5 years, I appreciated your endless enthusiasm and patience to guide me through from a “naive child” in scientific research to a molecular biology scientist equipped with solid and broad background knowledge both theoretically and practically. I also did greatly appreciate your positive attitudes, wiseness and personalities during the entire supervision for my PhD. Just as a proof of what I have been seeing in the past 5 years, Craig has not failed to cycle to work any single day, a well featured example reflecting his continuity not only in working but also in daily life.

Herein, I also can not forget to mention other members of our group Drs. Steven Darby, Kelly Armstrong, Emma Clark, Ian Logan (previous and current member), Fadhel Shaheen, other PhD students, including Stuart Williamson, Dhuha Alkharaif, Hollie Lumsden and former members of the lab, Jacqueline Stockley, Lynsey Rogerson and Hesta McNeill and to members of the Ovarian cancer group, Richard Edmondson, Sarah Wilkinson and Ann Fisher for their kind help and friendship. In addition, I would also like to thank my annual PhD assessors Profs. John Lunec and Derek Mann (Newcastle University) for their thought-provoking suggestions for my PhD project.

Another special thank-you goes to a group of people at North East Proteomic Analysis Facility (NEPAF) based in Newcastle University including its scientific manager Prof. Achim Treumann (Northumbria University), program manager Dr. Glen Kemp for their kind concern and intuitive suggestions for my PhD project and Karen Lowdon and David Blinco and Kavah Emami for their warm-hearted attitude and serious-minded contribution towards my project in their lab. This collaboration built up a strong tie between me and their lab, which subsequently provided me an opportunity to work for their company since June 2010 on an interesting project. It is also worth mentioning this familiar phrase from them “how is the thesis going?” as a non-stopping encouragement for me to complete my writing. A significant mention is needed for Dr. Brian Shenton and Dr. Trevor Booth at the Flow Cytometry and Confocal Microscopy core facilities at the Medical School, respectively for their technical and analytical support for my PhD project.

Last but not least, I would like to thank all my lovely PhD friends from the Marie Curie CANCURE consortium and the program organizers for constructing such a wonderful PhD project and I do remember every time we spent together in the past 4 years.

I complete my acknowledgement with the quote from Dr. James Watson “One could not be a successful scientist without realizing that, in contrast to the popular conception supported by newspapers and mothers of scientists, a goodly number of scientists are not only narrow-minded and dull, but also just stupid.”

Table of contents

List of figures and tables

Abbreviations

°C	Degree Celsius
Å	Angstrom, unit of molecular distance
7-AAD	7-Aminoactinomycin D
A	Alanine
AAH	Atypical adenomatous hyperplasia
AR	Androgen receptor
AD	Androgen-dependent
AI	Androgen-independent
AIB1	Amplified in Breast Cancer 1
AF	Activation function
AMACR	Alpha-methylacyl-CoA racemase
APC	Adenomatous polyposis coli
AREs	Androgen response elements
ATCC	American type culture collection
ATP	Adenosine-5'-triphosphate
BAF	BRG1-associated factor
Bp	Base pair
BPH	Benign Prostate Hyperplasia
BRCA1/2	Breast cancer ½
BRM	Brahma gene
BRG1	Brahma-related gene 1
BrdU	Bromodeoxyuridine
$CaCl_2$	Calcium chloride
CaP	Prostate cancer
CARM1	Coactivaotor-associated arginine methyltransferase
CBP	cAMP response element (CREB) binding protein
CDK	Cyclin dependent kinase
cDNA	Complimentary DNA
ChIP	Chromatin immunoprecipitation
CHX	Cycloheximide
CIP	Calf Intestinal Phosphatase
CMV	Cytomegalovirous
CO_2	Carbon dioxide
CoREST	Corepressor to REST (RE1 silencing transcription factor)
CRPC	Castrate-resistant prostate cancer
CTD	C-terminal domain
D	Aspartic acid
DAPI	4',6-diamidino-2-phenylindole
DBD	DNA binding domain
DEPC	Diethylpyrocarbonate
DHT	Dihydrotestosterone
DMEM	Dulbecco's Modified Eagle Medium
DMSO	Dimethyl sulfoxide
DRE	Digital rectal exam
DSC3	Desmocollin 3
E Coli.	*Escherichia coli*
EBP1	ErBb3 binding protein 1
EDTA	Ethylenediaminetetraacetic acid
ER	Estrogen receptor

ERA	Early target of retinoid acid
ERF1	Ets-domain transcription factor
ERG	Ets Related Gene
ETS	E-twenty six
ETV1	ETS translocation variant 1
EZH2	Enhancer of Zeast Homolog 2
F	Phenylalanine
FACS	Fluorescence activated cell sorting
FCS	Fetal calf serum
FHL2	Four and a half LIM-domain protein 2
FITC	Fluorescein isothiocyanate
FM	Full medium
FSH	Follicle-stimulating hormone
G418	Geneticin
GAPDH	Glyceraldehyde 3-phosphate dehydrogenase
GASC1	Gene amplified in squamous cell carcinoma 1
GFP	Green fluorescent protein
GIPC1	GAIP C-terminus-interacting protein
GnRH	Gonadotropin-releasing hormone
GR	Glucocorticoid receptor
GRIP1	Glucocorticoid receptor-interacting protein 1
GSTpi	Glutathione S-transferase pi 1
h	Hour
HAT	Histone acetyltransferase
HCl	Hydrochloric acid
HDAC1	Histone deacetylase 1
HDM	Histone demethylase
HMT	Histone methyltransferase
HPC1	Hereditary prostate cancer 1
HPRT1	Hypoxanthine phosphoribosyltransferase 1
HREs	Hormone response elements
HRP	Horseradish peroxide
HSP	Heat shock protein
IF	Immunofluorescence
IGFBP-1	Insulin-like growth factor binding protein
IHC	Immunohistochemistry
IL-6	Interleukin-6
IP	Immunoprecipitation
JHDM2A	Jumonji domain-containing protein 1A
K	Lysine
KCl	Potassium chloride
kDa	Kilo-Dalton
L	Leucine
LB	Luria Bertani
LBD	Ligand binding domain
LH	Luteinizing hormone
LHRH	Luteinizing-hormone-releasing hormone
LSD1	Lysine specific demethylase 1
M	Molar
MAPK	Mitogen activated protein kinase

MEF	Mouse embryonic fibroblast
$MgCl_2$	Magnesium chloride
MR	Mineralocorticoid receptor
mRNA	messenger RNA
min	Minute
miRNA	micro RNA
MMTV	Mouse mammary tumor virus
MUT	Mutant
NaCl	Sodium chloride
Na_2CO_3	Sodium carbonate
NF-kβ	Nuclear factor kappa β
NICE	National institute for health and clinical excellence
NLS	Nuclear localization signal
NR	Nuclear Receptor
NSD1	Nuclear receptor binding SET domain protein 1
NuRD	Nucleosome remodeling and deacetylase
ONPG	O-nitrophenyl-β-D-galactoside
P/CAF	p300/CBP associated factor
PAP	Prostatic acid phosphatase
PARP1	Poly [ADP-ribose] polymerase 1
PBS	Phosphate buffered saline
PCR	Polymerase chain reaction
PGS	Protein G Sepharose
PI	Propidium Iodide
PIN	Prostate intraepithelial neoplasia
PKC	Protein kinase C
PMSF	phenylmethylsulfonyl fluoride
PR	Progesterone receptor
PRMT1	Protein arginine methyltransferase
PSA	Prostate specific antigen
PSCA	Prostate stem cell antigen
PSMA	Prostate specific membrane antigen
PTEN	Phosphatase and tensin homolog
PTGS2	Prostaglandin-endoperoxide synthase 2
Q	Glutamine
R	Arginine
Rb	Retinoblastoma
RIP140	Receptor interacting protein 140
RIZ1	Rb-interacting zinc finger gene
RLU	Relative light unit
RNA	Ribonucleic acid
RPB	RNA polumerase II gene
RPM	Revolutions per minute
RPMI	Roswell Park Memorial Institute
RT	Room temperature
RUNX3	Runt-related transcription factor 3
RXR	Retinoid X receptor
s	Second
S	Serine
SAM	S-adenosyl-methionine

SLC45A3	Solute carrier family 45, member 3
SD	Steroid depleted
SDS-PAGE	Sodium dodecyl sulphate polyacrylamide gel electrophoresis
SET	Su(var) Enhancer of zeast, Trithorax
SHBG	Steroid hormone binding globulin
SLPI	Secretory leukocyte protease inhibitor
SRC1	Steroid receptor coactivator 1
SWI/SNF	SWItch/Sucrose NonFermentable
T	Threonine
TAE	Tris-acetate-EDTA
TAF	TBP (TATA box protein) associated factor
TBS	Tris-buffered saline
TF	Transcription factor
TD	Tansactivation domain
TIP60	Tat interacting protein 60
TK	Tyrosine kinase
TMPRSS2	Transmembrane protease, serine 2
TNF	Tumor necrosis factor
Tris	Tris-(hydroxymethyl)aminomethane
TRUS	Transrectal ultrasound
TRITC	Tetramethylrhodamine Isothiocyanate
TSA	Trichostatin A
TTBS	Tween-20 TBS
UV	Ultra-violet
V	Voltage
WB	Western blotting
WT	Wild-type
X	Any amino acid

Chapter 1

Introduction

1.1 The Prostate

1.1.1 Basic Anatomy of the Prostate

The human prostate is a composite organ made up of tubuloalveolar secretory glands and non-glandular elements which are tightly constructed together within a common capsule. It is roughly a walnut sized and shaped gland and located just beneath the urinary bladder and in front of the rectum with neurovascular bundles branching and rejoining from the lateral border of the prostate near the base and with lymph vessels drainage into the internal iliac nodes. The prostate mainly functions to store and secrete fluids which constitute partial volumes of the semen. Since it plays such roles in helping with semen secretion in the human body, it is a part of the male reproductive system and is classed as a secondary sex organ.

i Prostate Morphology

The prostate is subdivided into three parts (Figure 1.1). The large peripheral zone is composed of a glandular epithelium which extends from the base of the verumontanum to the prostatic apex. This area is the site of origin of approximately 64 percent of prostate cancers. The central zone comprising 25 percent of the volume of the glandular prostate surrounds the ejaculatory ducts and is responsible for about 2.5 percent of the prostate cancer, especially more aggressive cases. A transitional zone surrounds the proximal urethra and comprises about 5 to 10 percent of the glandular prostate. This region grows constantly throughout life, accounts for 34 percent of prostate cancer and is also responsible for benign prostate hyperplasia (BPH) (McNeal et al., 1988; McNeal, 1969) .

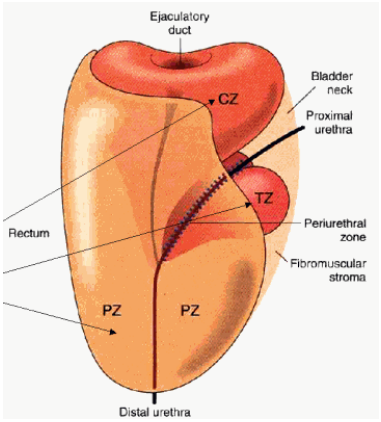

Figure 1.1 Schematic representation of the zonal classification of the prostate. PZ: Peripheral zone TZ: Transitional zone. CZ: Central zone. (Figure from online resources)

ii Prostate Histology

The histological structure of the prostate can be explained based on the zone structure of the prostate. In all three zones, both ducts and acini are lined by secretory epithelium which is composed of three epithelial cell populations (Figure 1.2). The luminal cells are the predominant cell population of the prostatic epithelium and are classified by expression of androgen receptor (AR) and secretion of prostate specific antigen (PSA) as well as other secretory proteins such as cytokeratins 1 and 18 and cell surface marker CD57. The basal cells are the second largest population of prostate epithelial cells located between luminal cells and the basement membrane and express cytokeratins, CD44 and anti-apoptotic regulators Bcl2, but without prostatic secretory proteins (Liu et al., 1997). A third population is a small portion of neuroendocrine cells which are thought to support luminal cell development as it is presumed that prostate epithelial stem cells arise in this compartment. In between the duct-acinar system lies the prostatic stroma, which contains bundles of smooth muscle cells (Abate-Shen and Shen, 2000). The three prostate zones differ from each other histologically and biologically. One of the major distinguishing features between individual zones is the size of the ducts and acini. In the peripheral zone and transitional zone, ducts and acini are usually 0.15 to 0.3 mm in diameter and tend to present simple rounded contours which are not perfectly circular shaped due the random undulations of the surrounding epithelial layers. Whereas, in the central zone, ducts and acini are larger with the diameter up to 0.6mm and display a polygonal structure (McNeal, 1978). Another disparity between individual zones is the ratio of epithelium to stroma.

The central zone has the higher epithelium composition and the most compact stromal structure, whereas the peripheral and transitional zone stroma is loosely woven and contains irregularly arranged smooth muscle bundles. Although it is generally feasible to distinguish these zones by their histological characteristics, it should be noted that with the organ becoming older or disease orientated, it becomes harder to distinguish those zones histologically.

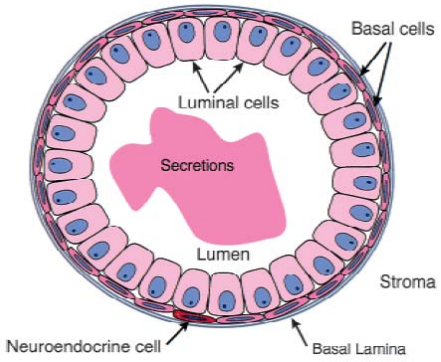

Figure 1.2 Schematic depiction of the cell types within a human prostatic duct. (Figure from Abate-Shen and Shen, 2000)
Note that the rare neuroendocrine cells are morphologically indistinguishable from basal cells

iii Prostate development and pathogenesis

From a time course view of the embryonic development of the prostate, the male urogenital system remains identical to the female system within the first 6 weeks of embryo formation, which is then followed by a period of differentiation whereby the urinary bladder, ejaculatory ducts and prostatic urethra begin to emerge. The increased cellularity of the internal layer of mesoderm surrounding the proximal part of the urethra is the first line of evidence to indicate prostate formation and it is the prostatic part of the urethra from which the mature prostate develops. At week 10, the androgen responsive urogenital sinus triggers the budding of the prostatic urethra epithelium, subsequently giving rise to the initial presumptive peripheral and internal glandular areas of the prostate. By week 11, endodermal differentiation leads to the formation of lumens and acini, whereas the mesenchyme differentiates into smooth muscle, fibroblasts and blood vessels. Following proliferation of the epithelium and stroma, by week 15, the high concentration of testosterone causes vigorous epithelial mesenchyme interactions leading to the further maturation of the epithelium. Within a week, luminal secretory cells start to function with the presence of basal and neuroendocrine cell populations (Ingber, 2002; Xia et al., 1990;

Kellokumpu-Lehtinen, 1985; Kellokumpu-Lehtinen et al., 1980; Siiteri and Wilson, 1974). The maturation process continues until the embryonic testosterone level falls, when the prostate enters a homeostatic state.

The second round of the prostate development begins during puberty, which is featured by the growth of epithelium stimulated by the elevated androgen level. During this phase, the prostate doubles in size with the fully differentiated cell phenotypes and the expression of androgen receptor by secretory cells. This will be discussed in section 1.1.3.

1.1.2 Diseases of the prostate

The prostate encounters different disorders and the most common syndromes are prostatitis, benign prostate hyperplasia (BPH) and prostate cancer. Prostatitis is inflammation of the prostate and has different categories depending on their etiological factors (McNeal, 1968). Benign prostate hyperplasia (BPH) refers to the enlargement of the prostate due the proliferation of the epithelial and stromal cells. This disease normally happens in middle-aged and elderly men and is believed to be androgen-related, although there are controversies on the direct link between androgen and BPH. In addition, other hormones such as estrogens have also been shown to account for BPH pathogenesis (McNeal, 1969). Unlike BPH, which is a non-malignant neoplasm of the prostate, prostate adenocarcinoma is the malignant transformation of the prostate and accounts for most of the prostatic disease related deaths in men. Although the specific causes of prostate cancer still remain unclear, the incidence of prostate cancer is correlated with risk factors such as age, genetics, racial background, diet, lifestyle and medications (Hsing and Chokkalingam, 2006; Hankey et al., 1999). One common syndrome which is thought to be highly associated with prostate cancer is prostatic intraepithelial neoplasia (PIN), as this condition represents confined localized cancerous clumps within different zones of the prostate and is also featured by the thickening of the epithelial layer and loss of the basal layer (Montironi et al., 2007; McNeal and Bostwick, 1986). However, direct evidence is still lacking to prove that PIN is a bona fide tumour precursor of the prostate. Among the risk factors, age and

genetic abnormality contribute primarily to prostate cancer and these will be discussed.

1.1.3 Function of the Prostate

The prostate has two main functions based on its histological structure. As its stromal compartment contains smooth muscle cells, the prostate is able to help expel semen during ejaculation and control the flow of urine during urination. Given that prostate epithelial cell layer is composed of a large amount of secretory cells, it plays important exocrinological roles within the human body and also has strong endocrinological cross-talk networks with other organs (Aumuller and Seitz, 1990).

i Secretions of the prostate

The prostate stores and secretes a slightly alkaline fluid which constitutes 25-30% of the volume of semen and contains a variety of molecules secreted specifically by the prostate including proteolytic enzymes, prostatic acid phosphatase (PAP), citrate and prostate-specific antigen (PSA) (Abrahamsson and Lilja, 1990). One primary purpose for the secretion is to serve as a medium for sperm transport and protection and thus to increase the mobility, viability and oxygen consumption of sperm (Toyama et al., 1995; Lindholmer, 1974).

Apart from the protective effect of the prostatic fluid, many prostatic secretory proteins possess various enzymatic activities with the major activity being proteolysis. One well-known and intensely studied protease is prostate specific antigen (PSA). This enzyme is a 34kDa serine protease belonging to the human glandular kallikrein (hGK-1) superfamily and is secreted by epithelial cells as well as the periurethral gland (Ban et al., 1984; Wang et al., 1979). PSA gene expression is androgen regulated. Due to its trypsin-like activity, it functions with another protease, pepsinogen to dissolve the major seminal gel-forming proteins semenogelin A and fibronectin thus liberating entrapped sperm (Lee et al., 1989; Lilja, 1985). PSA is also proposed to be involved in the breakdown and modulation of the insulin-like growth factor binding protein (IGFBP-1) and the degradation of secretory leukocyte protease inhibitor (SLPI) in the ejaculate

(Birnbaum et al., 1994; Cohen et al., 1994). From a clinical standpoint, PSA remains the only serum biomarker recommended for use in the clinical screening of prostatic malignancies, although there are many other markers potentially available such as prostate specific membrane antigen (PSMA), and prostate stem cell antigen (PSCA) (Bradford et al., 2006; Smith et al., 2005).

ii Endocrinology of the prostate

The prostate undergoes dynamic endocrinological regulation by various hormones. It contains endocrine responsive tissue and its development and maintenance are hormone dependent with a major influence by androgens. There are different types of androgens within the human body; the most emphasized and crucial one is testosterone which is produced primarily in the testes in men and also with small quantities generated by adrenal glands in males and ovaries in females. It is a member of the steroid hormone family and is derived from cholesterol. Upon generation by the Leydig cells in the testes, testosterone is circulated in the blood and concentrates in spermatic veins, where 60-70 percent of it binds to a plasma protein named steroid hormone binding globulin (SHBG), 25-30 percent binds to albumin and only 2 percent in free form. Biologically active forms which are either albumin bound or free can target their functioning organs including the prostate, whereas the SHBG associated testosterone is difficult for uptake and thus needs dissociation to carry out its function (Anderson, 1974). Although, testosterone is the primary androgen affecting the growth and homeostasis of the prostate, a conversion from testosterone to the more potent form, dihydrotestosterone (DHT) is necessary for it to carry out its ultimate function and this reducing step is stimulated by 5α-reductase within the prostate cells (Edwards and Bartlett, 2005a).

Evidence for androgen-dependent prostate regulation is largely derived from both human and animal model studies and have shown a permissive and active role for prostate regulation both pre-natally and post-natally. Removal of the foetal testis prior to sexual differentiation inhibits prostate development and the growth of other male internal sex glands. Castration experiments on pre-pubertal mice indicated that ablation of testosterone results in the prevention of

further development of the prostate and this effect can be reversed by administration of testosterone (Cunha et al., 1987; Berry and Isaacs, 1984). It was also demonstrated that with the exogenous testosterone treatment, the speed of prostate growth is accelerated in immature rats with earlier completion of the formation of the mature prostate (Berry and Isaacs, 1984).

There are different mechanisms that are involved in this phenomenon. Back in the 19th Century, scientists were aware that castration halts the prostate growth and causes the shrinkage of the prostate and this was more explicitly explained and postulated as a result of dysregulation of RNA and proteins, which led to the concept of “programmed cell death” in the prostate reviewed by Lee, C. (1981). Not only does this explain the growth inhibition of the prostate, but also that differentiation and proliferation contribute to the fate of prostate under testosterone manipulation. It has been clarified that stimulation by testosterone increases DNA synthesis and in turn the production of proteins predominantly via androgen receptor mediated axis, which then initiates prostatic cell proliferation by regulating the cell cycle and other pathways (Balk and Knudsen, 2008).

In the normal prostate, apoptosis and proliferation are maintained in a homeostatic state, however, once this balance is destroyed by elimination of androgens, striking regression of the prostate will occur. Other than testosterone, levels of other hormones are also responsible for prostatic growth. These include adrenal androgens, estrogen, glucocorticoids, growth hormone and other hormones (Ellem and Risbridger, 2009). The physiological effect of those hormones resides in their capability to assist prostate growth and maintenance, consequently influencing the abnormal pathological changes of the prostate, especially prostate cancer. Discussed in detail in section 1.2.

iii Regulation of prostate growth

As androgen is an indispensible prerequisite and is the single most important mitogenic hormone responsible for prostatic cell growth, the production of androgen is vital in controlling the prostatic functions. This is mainly governed by the hypothalamic pituitary axis. The anterior pituitary gland secretes several

hormones including gonadotropins, follicle-stimulating hormone (FSH) and luteinizing hormone (LH) which are involved in regulation of androgen production in the testis. Release of LH and FSH from the anterior pituitary with subsequent androgen production from the testicular Leydig cells is modulated by gonadotropin-releasing hormone (GnRH) produced by the hypothalamus. The feedback mechanism of the sex steroids on gonadotropin release rises from the testis and occurs at both the hypothalamic and pituitary level. This is controlled by testosterone and estradiol. Testosterone exerts this negative effect by slowing the hypothalamus pulse generator and subsequent release of LH and estradiol produces equal inhibition of both LH and FSH in the hypothalamus and pituitary gland (Vacher, 1995).

1.1.4 Mechanisms and Importance of Androgenic Action in the Prostate

The mechanism of androgen regulated cellular functions is predominantly mediated by androgen receptor (AR) which is a ligand dependent transcription factor belonging to the nuclear hormone receptor superfamily. This multi-step metabolic pathway involves the following cascade. Upon entry of free testosterone (the main form of male androgen) into target prostate cells, it is subsequently converted to more active dihydrotestosterone (DHT) by 5α-reductase. DHT subsequently binds to the AR to induce a conformational change of the AR from its inactive state through the binding of Steroid Hormone Binding Globulin (SHBG) to active state and enables formation of AR homo-dimer, which is also accompanied by other regulations of AR at the molecular level (Edwards and Bartlett, 2005a). This process stabilizes the homo-dimer and facilitates the translocation of the AR to the nucleus, where it subsequently binds to androgen responsive elements (AREs) within target genes and drives their expression (Edwards and Bartlett, 2005b; Suzuki et al., 2003). As the single most important mitogenic hormone, androgen impacts significantly on prostate development, growth and homeostasis and this influence is generally achieved by modulating different cellular compartments within the prostate. Androgen stimulates stromal cell proliferation and the production of various growth factors involved in the regulation of epithelial growth and proliferation. It is also postulated that androgen targets epithelial cells via autocrine and paracrine pathways to promote cell differentiation and growth (Cunha et al.,

2004; Cunha et al., 1987). This is not only applicable to normal prostate development and growth balance control, but is also one of the main driving forces contributing to prostate carcinogenesis.

1.2 Prostate cancer (CaP)

1.2.1 Incidence and etiology of prostate cancer

Prostate cancer (CaP) is the second most common cause of cancer death in men in Western countries. In the UK, it accounts for 13% of male death from cancer with significantly increasing mortality with aging (Office for National Statistics, 2007 Mortality Statistics: Cause, 2005). Possible etiological factors associated with the incidence and disease predisposition include genetics, racial background, diet, aging and hormone. Prostate cancer incidence rises dramatically with age with approximately three quarters of cases occurring in males over 65 and only 0.1% diagnosed under the age of 50 (Gronberg, 2003; Parkin et al., 2001). Evidence from biopsy-based studies also indicates that prostate cancer is detected in 30% of men in their 30's, 50% of men in their 50's and more than 75% from men older than 85 (Sakr et al., 1993). However, other epidemiological findings suggest that the risk of dying from prostate cancer is 50% in patients over 70 who have clinically localized CaP (Narain et al., 2002).

Ethnicity represents an important risk factor for CaP. Intensive studies indicate that African American, Caucasian and Scandinavian males have the highest incidence (137 cases per 100,000 per year) while Chinese and Japanese have the lowest rates (1.9 cases per 100,000 per year) (Parkin et al., 2001). Geographic variation is another factor contributing towards the incidence of CaP. Chinese from the mainland have the lowest rates in the world (1.3 per 100,000) compared to Hong Kong Chinese having a rate five times higher and Chinese in the United States having a rate 16 times higher (Muir et al., 1991).

In addition to age, ethnicity and environmental factors, genetic predisposition is another well established risk factor for prostate cancer and this is largely associated with early onset of the disease. Findings from case-control analysis suggest that there was a 2.4 and 2.1 fold age-adjusted relative risk in men with

an affected first or second degree relatives, respectively (Spitz et al., 1991). Men who have brothers affected by prostate cancer are more prone to develop prostate cancer (Monroe et al., 1995). Studies of twins in Scandinavia suggest that 40% of prostate cancer risk can be explained by inherited factors (Lichtenstein et al., 2000). So far, many prostate cancer susceptibility genes and loci have been found in the human genome. Although no single gene is fully responsible for prostate cancer, several key genes have been shown to play important roles during CaP development, including BRCA1/2, androgen receptor, PTEN, ELAC2 and HPC1 and loci on chromosome X, 1, 5, 8, 17 and 20 (Gronberg, 2003; Simard et al., 2002; Abate-Shen and Shen, 2000; Struewing et al., 1997).

Other epidemiological studies imply dietary agents as risk factors for prostate cancer. Although, the findings are conflicting, it has been highlighted that intake of multi-vitamins such as D/E/B6 may have preventive effect for CaP, whereas high alcohol intake and over-consumption of fatty acids may cause increased the risk of prostate cancer (Shannon et al., 2009; Berquin et al., 2007; Lawson et al., 2007; Weinstein et al., 2007). Another postulated risk factor responsible for prostate cancer is hormones. Many lines of evidence suggested that androgen ablation causes the regression of the cancer and therapeutic intervention using anti-androgens such as 5-alpha reductase inhibitor reduce the prevalence of prostate cancer (Kramer et al., 2009; Hsing and Comstock, 1993).

1.2.2 Pathology and molecular mechanisms of prostate cancer

i Overview of the pathogenesis of prostate cancer

Prostate cancer is largely characterized as an adenocarcinoma which accounts for 95% of cases and originates due to transformation of epithelial cells in the prostate gland; predominantly from the peripheral zone of the organ. (Shah and Getzenberg, 2004). Prostate intraepithelial neoplasia (PIN), which is characterized by the conformational change of prostatic cells and in the thickening of the epithelial layer and loss of the basal layer (Gelmann, 2002)

represents a potential precursor to CaP. This lesion is distinguishable architecturally and cytologically from various other histological abnormalities of prostate epithelium, including benign prostate hyperplasia (BPH) and atypical adenomatous hyperplasia (AAH), which are not believed to be pre-malignant states for CaP (McNeal and Bostwick, 1986). Caused by the inappropriate balance between cell proliferation and apoptosis as well as multifocal histological transformation, PIN has the potential to develop to CaP eventually, which is due to a series of alteration at both genetic and cellular level (Abate-Shen and Shen, 2000). Some of those altered genes include Alpha-methylacyl-CoA racemase (AMACR), Telomerase, Hespin, BRCA1, E-cadherin and C-met, which show either reduced or increased expression during the transition from PIN to prostate carcinoma suggesting PIN represents a bona fide precursor to CaP (Rubin and De Marzo, 2004; Abate-Shen and Shen, 2000).

The initial stage of cancer formation is followed by further malignant changes which drive the tumour to grow from clinically localized prostate cancer to metastatic disease via local invasion to the surrounding tissues and organs or via circulation through the bloodstream and lymphatic system.

ii Molecular genetics of prostate cancer

CaP is believed to result from a series of genetic alterations (Figure 1.3). Proliferative inflammatory atrophy (PIA) has been postulated to the precursor of high-grade PIN due to the finding of the merging atrophic epithelium in the same duct and acinus as high-grade PIN. This early prostatic lesion is associated with decrease of p27 ^{KIP}, increase of bcl-2 and carcinogen detoxification enzyme GSTP1 (Putzi and De Marzo, 2000). PIN formation is frequently associated with the loss of chromosome 8p and in particular the deletion of NKX3.1, which is believed to play a role in normal prostate differentiation (Abate-Shen and Shen, 2000; Bhatia-Gaur et al., 1999; Chang et al., 1994). Additional chromosomal aberrations that are implicated in the subsequent development of CaP are, among many, loss of chromosome 10q and in particular 10q23 where PTEN is located. PTEN encodes a lipid phosphatase whose substrate is PIP3. Loss of PTEN leads to activation of PKB/Akt pathway which in turn desensitizes the response to cell death causing

the tumour growth and triggers cell proliferation (Di Cristofano and Pandolfi, 2000; Sun et al., 1999; Carter et al., 1990).

The loss of Rb on chromosome 13q is also present in 50% of prostate cancer including both clinical localized and invasive cases (Abate-Shen and Shen, 2000; Cooney et al., 1996). In prostate cancer, it has been found that the Rb tumour suppressor is responsible for regulation of apoptosis and cell cycle via the androgen receptor mediated pathways (Balk and Knudsen, 2008; Abate-Shen and Shen, 2000; Zhao et al., 1997). Another intensively studied oncogenic

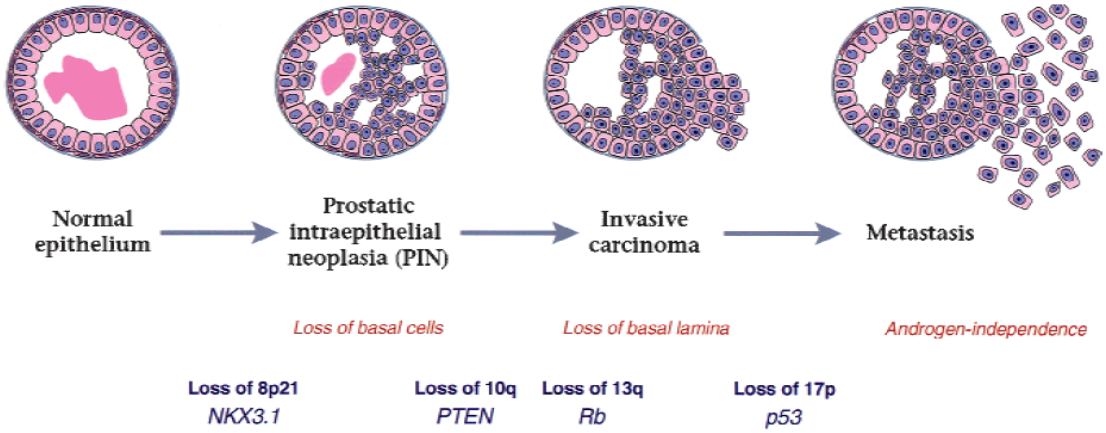

Figure 1.3 Representative development of the prostate cancer with sequential and accumulative loss and mutation of genes. (Figure from Abate-Shen and Shen, 2000)

pathway of prostate cancer concerns the tumor suppressor p53. p53 is a transcription regulator of many key genes engaged in oncogenesis of various tumour types and this gene is frequently mutated or deleted during tumour progression. Some of the regulated genes by p53 include p21, MDM2, BAX, p73 and Proliferating Cell Nuclear Antigen (PCNA) (Riley et al., 2008). Amongst those p53 target genes, MDM2 functions as a pivotal mediator of p53 by negatively regulating p53 turnover in a feedback manner. The mode of p53 directed transcription activation requires the binding of p53 to its consensus response element on DNA and the follow-up recruitment of general transcription proteins such as TAFs and other histone acetyltranferase CBP, p300 and PCAF to the promoter –enhancer regions (Gu and Roeder, 1997; Farmer et al., 1996). The main outcomes of p53 mediated gene regulation include apoptosis, senescence and cell-cycle arrest. In prostate, p53 is frequently altered in normal prostate, precursor lesion and prostatic intraepithelial neoplasia resulting in the cancer predisposition and this is due to the overexpression of mdm2 and HPV-

E6 (Downing et al., 2003). In p53 wide-type LNCaP cells, p53 activation and phosphorylation in response the DNA damaging agent such as selenium trigger caspase-dependent apoptosis indicative of its importance mediating the prostate cancer regression (Jiang et al., 2004).

1.2.3 Diagnosis and treatment of prostate cancer

Prostate cancer is generally curable when it remains indolent and has organ-confined status, but is sometimes neglected as it shares some common symptoms with other non-malignant prostate diseases. Nowadays, early detection of prostate cancer is aided by the combination of the serum prostate specific antigen (PSA) test and digital rectal exam (DRE), while other methods are also available and effective for different stages of cancer diagnosis ranging from basic physical examination, transrectal ultrasound (TRUS), prostate biopsies and bone scans (Lemaitre et al., 2006; Martinez de Hurtado et al., 1995; Berman and Clark, 1992). The PSA test emerged as a gold standard for the detection and monitoring of CaP in the late 1970s (Wang et al., 1979). The diagnostic sensitivity in asymptomatic men has been reported to be 80% when serum PSA levels are above 4ng/ml with a positive predictive value of elevated serum ranging between 28-35% (Lilja et al., 2008; Catalona et al., 1994; Catalona et al., 1993). Although increased PSA level is indicative of cancer presentation, it is not a definitive and distinctive parameter for the cancer diagnosis and staging, as many BPH patients and patients with architecturally normal prostate present with high level of PSA (Oesterling, 1991).

The treatment of prostate cancer is largely dependent upon the diagnostic outcomes. Since the life expectancy of many patients with evidence of CaP is less than 10 years and some patients have no obvious symptom presentation, a no treatment therapy called “watchful waiting” may be applied. Currently, there is no consensus on the best therapeutic option for early CaP, however, according to the guidance from NICE (National Institute for Health and Clinical Excellence), if detected in early or organ confined status, the disease can be treated individually based upon risk stratification of patients into low, intermediate or high risk. Patients with organ confined CaP are most likely to undergo radical prostatectomy or radiation therapy depending on the disease

aggressiveness and the physical state of the patient. At this stage, some other therapies may also be used as treatment regimes such as cryosurgery and high intensity focused ultrasound. Regardless of the beneficial outcomes from those therapies, the treatments are always plagued with side effects such as impotency, pain during urination, diarrhoea and incontinence.

While clinical localized CaP can be treated by above-mentioned therapeutic intervention, CaP unfortunately becomes invasive to adjacent tissues and may metastasize, primarily to the bone, this is usually lethal. Metastatic prostate cancer can be primarily controlled by hormone therapy (androgen ablation) that abrogates androgen-stimulated cancer cell growth. Removal of hormone, mainly testosterone, by various methods remains the first line treatment for advanced prostate cancer. Apart from conventional surgical castration, many anti-androgens are used normally in combination with surgical operation as effective treatment of invasive cancer. Anti-androgens include Bicalutamide which blocks DHT binding to the AR which in turn prevents activation of androgen regulated genes (Furr, 1996; Narayana et al., 1981) and Cetrorelix acetate, an antagonist of LHRH, which reduces LH production from pituitary and subsequently testosterone secretion (Reissmann et al., 2000). Ultimately, within a median time of two years, a population of cells escapes from androgen-dependence to androgen independence leading to hormone-refractory prostate cancer or castrate-resistant prostate cancer (CRPC) a disease that currently has limited remedies, resulting in an overall high risk of mortality and reduced survival (Edwards and Bartlett, 2005a; Berman and Clark, 1992). Current medical solutions for hormone refractory prostate cancer include the application of combinational Mitoxantrone and corticosteroids, combinations of Estramustine, etoposide and cisplatin, and Docetaxel with its combinations which show improved life quality and overall survival although only by 2-4 months maximum (Petrylak et al., 2004; Smith et al., 2003; Kantoff et al., 1999; Tannock et al., 1996).

1.3 The Androgen Receptor

1.3.1 The nuclear hormone receptor super-family

The family of nuclear hormone receptors function as transcription factors that specifically regulate target genes involved in metabolism, development and reproduction. Nuclear hormone receptors primarily function to mediate transcriptional response to hormones and these include substances with lipophilic properties such as sex steroids, adrenal steroids, vitamin D3 and thyroid and retinoid hormones (McKenna et al., 1999). More than 100 nuclear receptors are known to exist in metazoans with around 48 found in the human genome (Robinson-Rechavi et al., 2001). The nuclear receptor superfamily is composed of three structurally-related families depending on their mechanisms of action and sub-cellular distribution. Type I receptors bear ligand dependent activation property and ligand binding of the receptors lead to the dissociation from heat shock proteins, homo-dimerization, translocation from the cytoplasm into the cell nucleus, and binding to specific sequences of DNA known as hormone response elements (HREs). Type I nuclear receptors bind to HREs consisting of two half-sites separated by a variable length of DNA, and the second half-site has a sequence inverted from the first (inverted repeat). Examples include the androgen receptor, estrogen receptors, glucocorticoid receptor, and progesterone receptor. Type II receptors, in contrast to Type I, are retained in the nucleus regardless of the ligand binding status and in addition bind as hetero-dimers (usually with RXR) to DNA. Examples include the retinoic acid receptor, retinoid X receptor and thyroid hormone receptor. Type III nuclear receptors (principally NR subfamily 2) are similar to type I receptors in that both classes bind to DNA as homo-dimers. However, type III nuclear receptors, in contrast to type I, bind to direct repeat DNA sequences instead of inverted repeat HREs. Examples include various orphan receptors (Novac and Heinzel, 2004; Mangelsdorf et al., 1995).

Tyne I receptors which are also called steroid hormone receptors, including receptors to androgens and estrogens are composed of several independently functioning domains, including: an N-terminal transactivation domain, a DNA binding domain (DBD), a hinge region and a C-terminal ligand binding domain (LBD/AF-2). The AF-1 (TD) domain alone weakly regulates the transactivation of genes, however it synergizes with AF-2 domain to trigger a robust gene transcription, however there is an exception for AR as its transcription activity is mainly contained in AF-1 (TD). The highly conserved DNA binding domain

contains 2 zinc fingers which bind to specific DNA sequences that contain hormone responsive elements (HREs). The hinge region is designated for intracellular trafficking and localization as it harbours a nuclear localization signal (NLS) or at least some elements of a functional nuclear localization signal. The AF-2 domain is responsible for ligand binding, receptor dimerization and association with several nuclear hormone coregulators (McEwan, 2009; McKenna and O'Malley, 2002; McKenna et al., 1999). Type I receptors mainly includes those for progestins (PR), estrogens (ER), androgens (AR), glucocorticoids (GR), and mineralocorticoids (MR). Different from other types of nuclear receptors, this group of receptors in the absence of ligand is sequestered in cytoplasm in an inactive state by association with heat shock proteins (HSPs) and they are converted to active state via ligand binding and then translocate to the nucleus to bind to their cognate DNA sequences. The transcriptional machineries mediated by nuclear hormone receptors are thought to be due to communication between the receptors, RNA pol II and surrounding coregulators. It has been shown that the structural changes and folding of the transactivation domain AF-1 in response to specific protein-protein interactions create a platform of subsequent interaction which favours the assembly of a competent transcriptional activation complex and the formation of the complex increases the resistance of the general transcription factor TFIIF towards protease digestion suggesting its role in the regulation of basal transcriptional machinery (Reid et al., 2003). Subsequently it was shown that the interaction between RAP74, a component of TFIIF and AR induces significantly higher helical content in the AF-1 domain which in turn facilitates the interaction of AR with SRC-1 suggesting the cooperative transcription mechanism executed by AR basal transcription machinery and surrounding AR co-regulators (Kumar et al., 2004).

1.3.2 Characteristics of the androgen receptor

i Expression patterns of the androgen receptor

The androgen receptor gene is located on chromosome X at Xq11-12 (Chang et al., 1988a). The major site for regulating expression of AR is present 1.1kb upstream of the initiator methionine where the promoter region is situated. This

region lacks the typical “TATA” and “CAAT” motifs but lies in a “GC-rich” region and a putative SP1 binding site, a proposed “housekeeping” promoter sequence. In addition, it also possesses a 44bp alternating A/G residue sequence (Tilley et al., 1990). Androgen receptor is auto-regulated by androgen. Studies have shown that in the androgen-dependent LNCaP prostate cancer cell line, administration of androgen causes down-regulation of AR mRNA level whereas the protein level of AR is stabilized, a phenomenon due to elevated translational efficiency (Krongrad et al., 1991). In addition to the antagonistic auto-regulation of the receptor at the transcriptional level, other negative regulatory mechanisms affect AR gene at transcript level. It has been reported that the AR has relatively low expression in most tissues other than reproductive organs and this is possibly due to the repression of AR gene transcription by the negative regulatory complex containing the ubiquitous transcription factor NFI and two other nuclear factors (Song et al., 1999).

ii Structure and action of the androgen receptor

The human androgen receptor is composed of 8 exons encoding a protein of 919 amino acids. Like other nuclear hormone receptors, the AR consists of four distinct domains, including an N-terminal transactivation domain (TD) (1-559aa) a highly conserved DNA binding domain (DBD) (560-624aa), a hinge region (625-674aa) and a C-terminal ligand binding domain (LBD) (675-918aa) (Tenbaum and Baniahmad, 1997; Weigel, 1996) (Figure 1.4). These regions have specific functions: the DBD and hinge region are responsible for DNA-bindings at androgen responsive elements (AREs) and the hinge region also harbours a nuclear localization signal to mediate the cellular movement of the receptor. The DBD contains a 68 amino acid region which folds into two “zinc coordinated finger” structure and binds to target DNA (Chang et al., 1988b). The LBD containing the activation function 2 (AF2) functional domain, that regulates ligand-dependant receptor activation and functions in conjunction with transcription co-regulators containing the LXXLL or FXXFL motifs. The TD carrying the AF1 domain is characterized by its role in transactivation and as a coactivator binding mediator. In addition, this N-terminal region contains a FXXFL motif which binds to the LBD via an intramolecular interaction that reduces androgen dissociation and facilitates co-regulator interaction thus

enhances receptor activity (Dubbink et al., 2004; Gelmann, 2002; Gnanapragasam et al., 2000). Furthermore, structural analysis revealed that the LBD contains several helical structures (12 α-helixes) which forms the ligand binding pocket mediating the receptor binding to testosterone and dihydrotestosterone and is involved in receptor dimerization and transcription regulation (Gelmann, 2002; Thornton and Kelley, 1998).

The mechanism of AR activation is a multi-step process that initiates with the binding of DHT to the receptor in the cytoplasm. This induces a conformational change within the AR from its inactive to active state and enables formation of the AR homo-dimer, which is also accompanied by the phosphorylation of the AR by various kinases (Edwards and Bartlett, 2005b; Weigel, 1996). This process stabilizes the AR homo-dimer and exposes the nuclear localization signal within the hinge domain that allows translocation of the receptor to the nucleus, interaction with a cohort of AR co-regulators and binding to AREs in androgen-regulated genes to regulate transcriptional output (Edwards and Bartlett, 2005a; Lee and Chang, 2003b; Suzuki et al., 2003) (Figure 1-5).

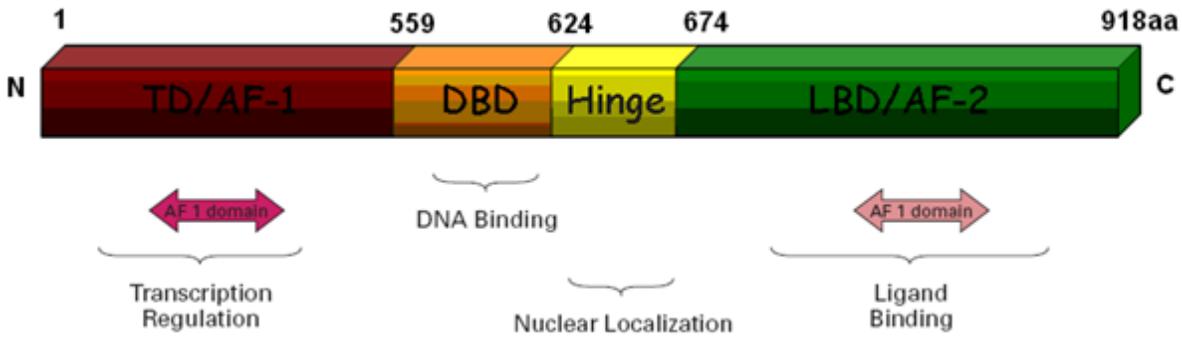

Figure 1.4 Schematics of androgen receptor structure and functions of domains.
Schematics of structure of human AR, individual domains are indicated in different colours.

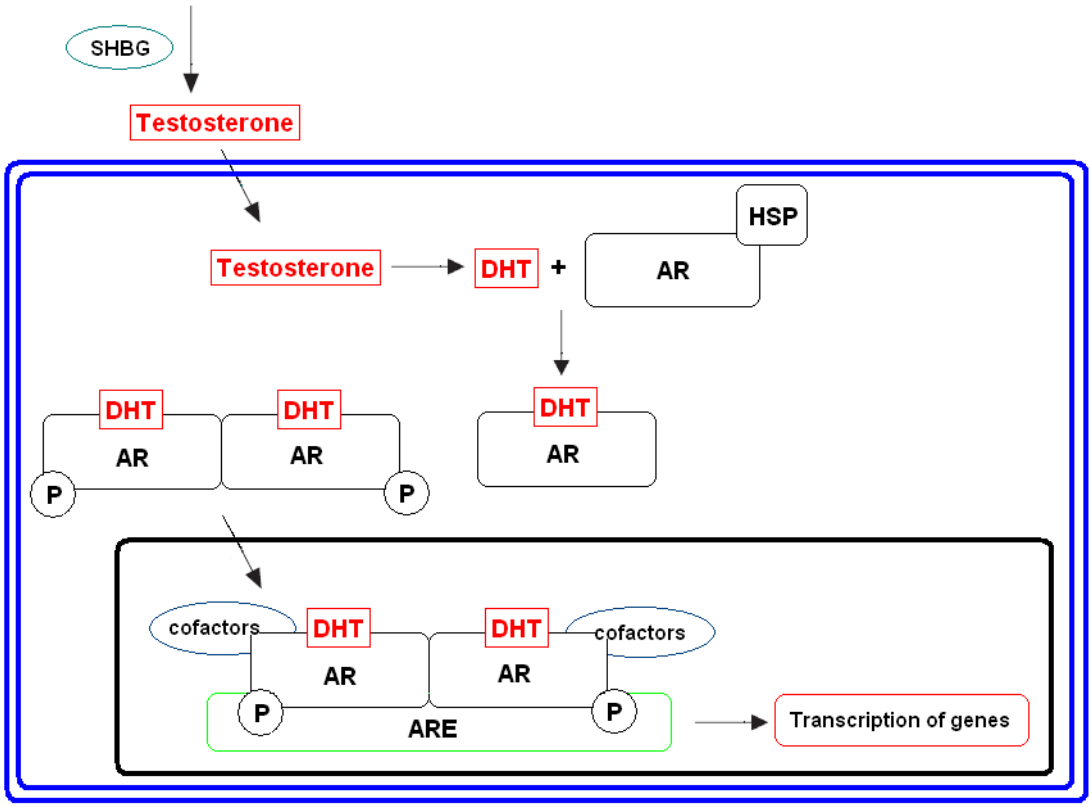

Figure 1.5 Mechanisms of androgen receptor signaling pathway.
Conventional AR activation pathway is schematically shown.

1.3.3 Transcriptional regulation by the androgen receptor

i AR-regulated genes

The AR regulates vital aspects of prostate growth and function including cellular proliferation, differentiation, apoptosis, metabolism, and secretary activity. Since the application of gene microarray analyses in androgen-dependent LNCaP and CWR22 cell lines, among others, there have been more than 600 androgen regulated genes identified (Velasco et al., 2004; Karan et al., 2002; Nelson et al., 2002). Many of those genes play significant roles in the pathogenesis of prostate cancer and contribute towards the transformation from androgen dependent to independent disease (Mehra et al., 2008; Massie et al., 2007; Velasco et al., 2004). As discussed, the most studied androgen regulated gene is PSA which serves as a serum marker in prostate cancer diagnosis, monitoring of treatment response and detection of disease recurrence (Lilja et al., 2008). Researchers have identified 3 functionally active AREs at the androgen promoter and enhancer regions. There are two proximal promoter

sequences mapped at the position -170 (AREI) and -394 (AREII) and a putative ARE as enhancer region at -3.7kb (AREIII) (Cleutjens et al., 1997; Cleutjens et al., 1996). Of particular interest, the AREIII has strong affinity for the receptor binding as it showed 1000-fold transcription activity in the presence of synthetic androgen R1881 and mutation analysis in this motif almost abolished the promoter activity of the PSA gene (Cleutjens et al., 1997).

Many other reports have shown the importance of individual androgen regulated genes in the progression of prostate cancer. The cyclin dependent kinase inhibitor p21 is up-regulated in response to androgenic treatment and this is potentially mediated by the putative ARE residing within the 2.4kb promoter region of the gene (Lu et al., 1999). Another group of key androgen-regulated genes are the TMPRSS2-ETS fusions which have been found in both clinically localized and aggressive stages of the cancer (Mehra et al., 2008; Tomlins et al., 2005). This fusion gene is formed by abnormal translocation of the androgen regulated serine protease TMPRSS2 and the ETS family transcription factor (Nam et al., 2007). The fusions of TMPRSS2 with ERG, ETV1 and ETV4 have been identified in large portion of prostate cancer cohorts and the TMPRSS2-ERG fusion has been implicated as a predictive marker for the recurrence of prostate cancer in patients with clinical localized cancer after surgery (Nam et al., 2007). Probing into the molecular mechanisms linking the TMPRSS2-ERG rearrangement and the cancer aggression, it has been found that androgenic stimulation may trigger oncogenic C-MYC up-regulation by ERG and the abrogation of epithelial differentiation genes PSA and SLC45A3, which together may contribute to the neoplastic process of CaP (Sun et al., 2008).

In addition to direct androgen regulation on transcription, reports also indicate that androgen signalling is able to up-regulate the micro-RNA (miRNA) miR-125b which in turn stimulates the androgen independent growth of cancer cells by attenuating Bak1 expression (Shi et al., 2007). Moreover, proteomic approaches interrogating the androgenic network in LNCaP cells identified 1024 up-regulated proteins in response to synthetic androgen R1881 suggestive of the comprehensive role and multi-tasking of androgen in coordinating the various cellular components during cancer progression (Wright et al., 2003).

ii Regulatory patterns of AR-mediated transcription

Dynamic transcriptional regulation by AR is tightly co-ordinated through cis-acting androgen responsive elements (AREs). This 15bp palindromic sequence consists of two hexameric half-sites (5'-AGAACA-3') arranged as an inverted repeat with a 3-bp spacer in between (Shaffer et al., 2004). Although there are over 500 perfect palindromic AREs identified in the human genome, the degeneracy of functional AREs has also been implicated as some reports have found some near-consensus sequence with matches of 9- to 12 nucleotides or a single AR half-site which would favour the AR binding under a cellular context (Horie-Inoue et al., 2004; Nelson et al., 2002). One study using Chip-on-Chip analysis on gene promoter tiling arrays, containing 24275 promoter elements, identified over 1500 AR binding sites. A substantial proportion of these sites consisted of 6-bp AR half-sites and many of the AR-binding sites were associated with the ETS1 transcription factor suggesting that AR-mediated DNA binding may be influenced by or act in conjunction with other factors in the nucleus (Massie et al., 2007).

Like other nuclear hormone receptors, the AR modulates dynamics of transcription initiation through the interaction with components of the basal transcription machinery and altering the chromatin landscape in the vicinity of the promoter to facilitate transcription. It has been found that ligand-bound AR dimers are recruited to both enhancer and promoter regions of PSA gene, which brings the enhancer into proximity of the promoter near transcriptional start site and this process is subsequently followed by the ordered and coordinated recruitment of AR co-regulators p160, CBP, p300 and RNA polymerase II holoenzyme to build up the AR containing transcription complex to facilitate transcription initiation (Shang et al., 2002) (Figure 1.6). The direct interaction between AR and RPB2 (the second largest RNA polymerase II subunit) was documented and this association might facilitate transcription factors and enhance AR mediated transactivation (Lee and Chang, 2003a). In addition to the contact with the initiation complex, the direct interactions between AR and the general transcription factors. TFIIF, TFIIH and P-TEFb have been discovered using co-immunoprecipitation from LNCaP cells and this inter-molecular association enhances polymerase II CTD phosphorylation in

turn causing the elevated efficiency of the elongation procedure (Lee and Chang, 2003a). The interplay between AR and basal transcription machinery is either direct protein-protein interaction or indirect association modulated by AR co-factors - discussed below.

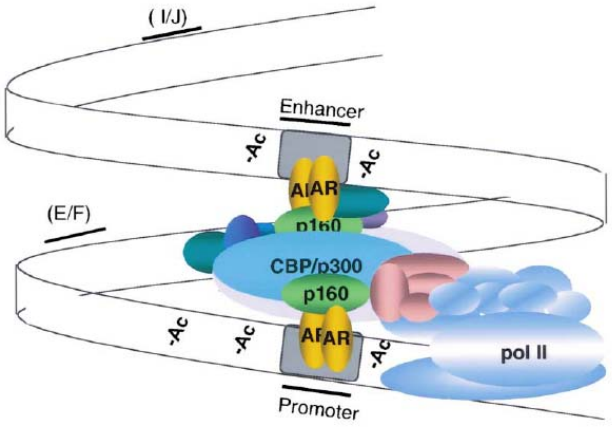

Figure 1.6 Formation of androgen receptor transcription complex. (Figure from Shang et al., 2002)

1.3.4 Transcriptional co-regulation by androgen receptor associated proteins

i Modulation of androgen receptor activity by co-regulators

Regulation of AR during transcription is multifaceted and involves divergent molecular processes coupling signalling transduction molecules and the activity of co-activators and co-repressors that regulate AR function upon target genes (Culig et al., 2004; Taplin and Balk, 2004). At target gene promoters, co-regulators participate in AR regulation in three ways: 1. Direct modification of DNA and/or histone proteins, 2. Remodeling of the local chromatin structure through the communication with chromatin modifying enzymes and complexes. 3. Direct involvement of the recruitment of basal transcriptional machinery. However, transcriptional co-regulation is not the only regulatory principle applied by co-factors and many AR co-regulators function through other mechanisms such as modulation of AR ligand binding capacity, AR nuclear/cytoplasmic trafficking and AR protein stability control. The most up-to-date overview of putative AR co-regulators suggests that more than 170 members exist in human cells and they display a diverse array of functions and

are involved in distinct cellular pathways (Heemers and Tindall, 2007). Amongst the entire group of AR co-regulators, those involved directly in transcriptional control are of particular interest and this remains an extremely intensive area of research.

Active transcription initiation demands the unpacking and loosening of the tight DNA-histone structure of the nucleosome to favour the accession of transcription factors and basal transcriptional elements. Some AR co-regulators have been identified as components of chromatin remodelling complexes to exert their function to open up the tightly packed chromatin, in turn facilitating AR-mediated transcription. The SWI/SNF chromatin remodelling complex contains several AR modulators which potently govern receptor activity. These ATP-dependent chromatin remodelling complexes utilize ATP to modify chromatin structures. Alternative models include ATP-dependent movement of histone octamers in cis along the DNA, transfer of histone octamers from one nucleosomal array to another or replacement of nucleosomal histones (Reisman et al., 2009). The net result of the chromatin remodelling imposed by SWI/SNF complexes is the pre-disposition towards nuclease digestion and increased affinity to transcription factors and basal transcriptional machinery. In the case of AR, the ATPases Brahma related gene 1 (BRG1) and human homolog of Drosophila brm gene (hBRM) were shown to robustly stimulate AR activity and depending on the chromatin template contexts, BRG1 and hBRM regulate designated subsets of androgen responsive genes (Marshall et al., 2003). The BRG1 associated factor (BAF57) subunit, another component of the SWI/SNF complex, binds to AR directly and activates AR regulated genes while inhibition of the gene attenuates LNCaP cell proliferation. The gene regulatory mechanism involves the synergistic effect between BAF57 and p160 HAT coactivator SRC-1 or is alternatively through non-160 AR coactivators, such as ARA70 (Link et al., 2005). Another well studied SWI/SNF component is the SWI3-related gene product (SRG3/BAF155) which interacts with the DBD region of AR and exists in a complex containing the AR at gene promoter regions and it functions by recruiting steroid hormone receptor co-activator 1 (SRC-1) independent of BRG1 and hBRM (Hong et al., 2005). Overall, these components function as part of the chromatin remodelling complex to alter the

structure and topology of the DNA-histone interface rendering AR mediated transcription.

Apart from the alteration of the chromatin structure and repositioning of transcription-related components by remodelling complexes, another widely established mechanism is the direct modification of histone proteins. This relatively elaborate and precise control over the local chromatin and nucleosome contributes to regulation of receptor action. Such modifications include acetylation, methylation, phosphorylation, ubiquitination and sumoylation. For brevity, only acetylation and methylation will be discussed in the next section.

Modified forms of histone residues cause changes of the net charges of the nucleosome which in turn causes the restructuring or remodeling of DNA-histone and DNA-protein in the local environment. For instance, lysine acetylation of histones neutralizes the positive charges, which consequently abrogates the interaction with negatively charged DNA, resulting in reduced nucleosome-nucleosome interaction allowing for enhanced promoter access. For example, members of p160 family of co-activators bearing histone acetyltransferase (HAT) activity, such as steroid receptor coactivator 1 (SRC-1), has been identified to interact with AF-1 and AF-2 of AR to enhance receptor transcriptional activity. This mechanism may be due to the modification on proteins, allowing the alteration of the topology of chromatin resulting in the access of basal transcriptional machinery, or stabilizing the pre-initiation complex (Culig et al., 2004; Powell et al., 2004). Another well-known transcription co-activator, p300, a histone acetyltransferase (HAT), has the potential to acetylate histone and non-histone proteins including AR to enhance AR-mediated transactivation (Gong et al., 2006). TIP60, another HAT enzyme also up-regulates AR activity in a HAT-dependent manner. Moreover, the antagonistically functioning histone deacetylase 1 (HDAC1) has been shown to repress AR activity by counteracting the activity of TIP60 (Gaughan et al., 2002; Brady et al., 1999; Heery et al., 1997).

Another group of potent histone modifiers is the histone methyltransferases that function to either activate or inactivate genes in a highly discriminate manner

that depends upon the exact site of modification within histones H3 and H4. Compared to the acetylation on histone proteins, methylation is more complicated as this modification can be either active or inactive and the position of modification on histones especially histone tails protruding out of the core histones is vital to dictate the outcome of downstream events. For example, H3 lysine 4, H3 arginines 2, 17 and 26 and histone H4 arginine 3 are generally associated with gene activation whereas H3 lysines 9, 27 and 36 and H4 lysine 20 are broadly linked with gene silencing (Lee et al., 2005a). On histone residues, both lysine and arginine can be potentially methylated and in particular lysine residues can be mono-, di- or tri- methylated. The status of the modification correlates with the transcriptional activity and this will be discussed in detail below On the contrary, although histone methylation has been considered as a stable modification for some time, recent discoveries indicated that reversal of histone methylation can be achieved through histone demethylases and some of these enzymes show dynamic regulation in androgen receptor mediated transcriptional pathway. So far, many methyltransferases and demethylases associated with AR activity have been identified.

The well characterized arginine methyltransferases CARM1 and PRMT1 are engaged in AR mediated transcriptional regulation in different contexts. CARM1 has been identified as a secondary AR co-regulator through the interaction with SRC co-activators (Chen et al., 1999). CARM1 has been found to be recruited to AREs upon ligand stimulation of the receptor and additional mechanisms involve methylation of other AR co-regulators, including p300/CBP and some RNA binding proteins and interaction with p160 group proteins of AR co-regulators. CARM1 mediated co-activation is dependent on enzymatic activity since the methylation-dead mutant is unable to induce AR activation (Koh et al., 2001). PRMT1 has also been shown to be a component of the AR transcriptional complex and stimulates receptor activity (Wang et al., 2001b).

In addition to arginine methylation, lysine methylation is another key component during transcriptional regulation of the AR. The histone H3 lysine 9 methyltranferase G9a functions as an AR co-activator in spite of the repressive feature of H3 lysine 9 methylation. G9a synergizes with GRIP1, CARM1 and

p300 to facilitate AR mediated transcription. The methyltransferase activity of CARM1, but not G9a is fully required for the synergistic effect to take place (Lee et al., 2006a). Moreover, G9a recruitment to AR responsive regions in the genome is apparent both in the presence or absence of androgens suggestive of a role for G9a in the progression of hormone insensitive prostate cancer (Lee et al., 2006a). Another example is the bi-functional nuclear receptor co-activator NSD1 (ARA267) which methylates both H3 lysine 36 and H4 lysine 20 (Huang et al., 1998). This protein interacts with the DBD-LBD of AR and up-regulates the transactivation in a ligand-dependent manner, although the involvement of relevant local histone modification is not yet proven (Huang et al., 1998).

The importance of histone demethylation in androgen receptor mediated transcriptional regulation has recently been established by the discovery of the first AR associated demethylase LSD1 (Metzger et al., 2005). LSD1-mediated specific demethylation of mono- and di-methylated histone H3 lysine 9, a repressive marker for transcription, leads to activation of AR-dependent transcription (Metzger et al., 2005). LSD1 recruitment to AR-regulated genes, including PSA, coincides with robust reduction of H3 lysine 9 methylation (Metzger et al., 2005). Regardless of its role as an AR co-activator, additional lines of evidence indicate the context-dependent regulatory mechanism by LSD1 as it has also been identified in the CoREST complex containing HDAC activity that targets histone H3 lysine 4 for demethylation (Wang et al., 2007).

Similar to LSD1, the histone demethylase JHDM2A demethylates mono- and di-methylated H3 lysine 9 in a hormone dependent manner. Functional assays support the notion that status of methylation mediated by JHDM2A is key in AR mediated ligand dependent activation of AR target genes (Yamane et al., 2006). Of interest, another jumonji domain containing demethylase JMJD2C (GASC1) which specifically demethylates tri- and di-methylated H3 K9 has been identified as an AR co-regulator which functions in cooperation with LSD1 to demethylate trimethylated Histone H3 lysine 3 in turn causing the loading of acetylation on histones to boost the assembly of AR containing complex at the promoter regions (Wissmann et al., 2007; Cloos et al., 2006). These observations indicate that transcriptional control of the AR requires the coordinative and concomitant function of multiple enzymatic activities, including the opposing

actions of HATs, and HDACS together with HMT and HDM enzymes. The current full list of AR co-regulators can be found in an excellent review (Heemers and Tindall, 2007).

ii Expression and regulation of androgen receptor co-factors

The crucial roles of AR co-regulators in the receptor mediated transcription regulation have been suggested and it has also been highlighted that aberrant expression of some co-regulatory proteins may be involved in the development and progression of prostate cancer (Urbanucci et al., 2008; Culig et al., 2004; Fujimoto et al., 2001). Thus far, the expression and regulation of some AR co-regulators have been correlated to the androgenic stimulation and various clinical and pathological parameters. The well-known AR co-activator SRC-1 is elevated in patients with poor response to endocrine therapy and the expression level is higher compared to patients with BPH or androgen-dependent prostate cancer (Fujimoto et al., 2001). The SRC-family member TIF2 was also found to be up-regulated in relapsed CaP patients; the effect of which was simulated in the CWR22 xenograft model, where the expression of SRC-1 and TIF2 decreased after castration and increased again at the time of relapse (Fujimoto et al., 2001). Another well-characterized AR co-activator, p300 has been implicated in androgen independent prostate cancer. This mechanism was linked with IL-6 mediated ligand independent AR activation as over-expression of p300 in LNCaP cells attenuated AR inhibition by MAPK inhibitor PD 98059, a pathway activated through IL-6 (Debes et al., 2002). Tip60 has been demonstrated to exhibit significant nuclear accumulation in the majority of sample obtained from patients with castrate-resistant prostate cancer, (Halkidou et al., 2003).

In addition to the altered expression patterns of some AR co-regulators, it has been found that several AR co-regulators are themselves androgen regulated. In one study, using LNCaP cells stably transfected with the AR as a model of amplified AR expression in CaP, several potential AR regulated co-regulators have been identified, including AIB1, CBP, MAK and BRCA1 (Urbanucci et al., 2008). Taken together, the above lines of evidence support the notion of the mutual interplay between AR and its co-regulators, whereby AR can up-regulate

co-activator expression which in turn may cause sustained tumour growth under low androgen environment.

1.4 Epigenetic regulation and prostate cancer

1.4.1 An overview of epigenetics

i The concepts and theories of epigenetics

The term epigenetics refers to mechanisms that permit the stable transmission of cellular traits without alterations in DNA sequence or amount and this can be fulfilled by different mechanisms including DNA methylation, RNA interference, genomic imprinting and histone modifications.

Histone proteins are composed of 5 classes including linker histones H1/H5, and 4 core histones H2A, H2B, H3 and H4. Two of each core histones assemble to constitute one histone octamer with 147 base pairs of DNA wrapped around. This structure is termed a nucleosome. The linker histone H1 functions to binds the nucleosome and the entry and exit sites of the DNA, thus locking the DNA into place and rendering the formation of higher order structure. Here the basic ‘beads on a string’ structure of chromatin is formed (Luger et al., 1997). This model enables the compaction to suit large genomes of eukaryotes inside cell nuclei. Besides, this highly ordered structure called chromatin is also associated with regulation of many essential biological processes, including replication, transcriptional, DNA repair, DNA recombination and chromosome segregation (de la Cruz et al., 2005; Strahl and Allis, 2000). Dynamic changes to chromatin compaction is required for each of these processes and is largely mediated by two distinct pathways: (1) Covalent modification of histones including acetylation, methylation, phosphorylation, ubiquitination and sumoylation; (2) Alteration of the nucleosomal positioning by enzymes utilizing energy from ATP hydrolysis (de la Cruz et al., 2005; Holbert and Marmorstein, 2005). Histone tails protruding from the histone octamer, which are the main targets for the aforementioned post-translational modifications, have been broadly studied and their functional significance have been deciphered over the

past decade (Mersfelder and Parthun, 2006). Histone octamers especially H3 and H4 tetramers have long tails protruding the nucleosome and they are the hot spots for various post-translational modifications which play essential roles in regulating cellular functions in many aspects. Histone H3 N-terminal tail extends from the central globular domain and is subject mostly to post-translational modification including the covalent attachment of methyl or acetyl groups to lysine and arginine amino acids and the phosphorylation of serine or threonine. Such examples include H3 lysine 4 methylation and H3 lysine 9 acetylation. Likewise, histone H4 is also a preferred target for these covalent modifications, including H4 lysine 20 methylation and H4 arginine 3 methylation. On the contrary, histone H2A and H2B are not as favoured as H3/H4 for post-translational modifications, although certain modifications show important functions in cells such as ubiquitination at core site lysine 119 of H2A and lysine 5 of H2B (Wang et al., 2004; Myers et al., 2003). Detailed modifications on histone tails are described below in Figure 1.7.

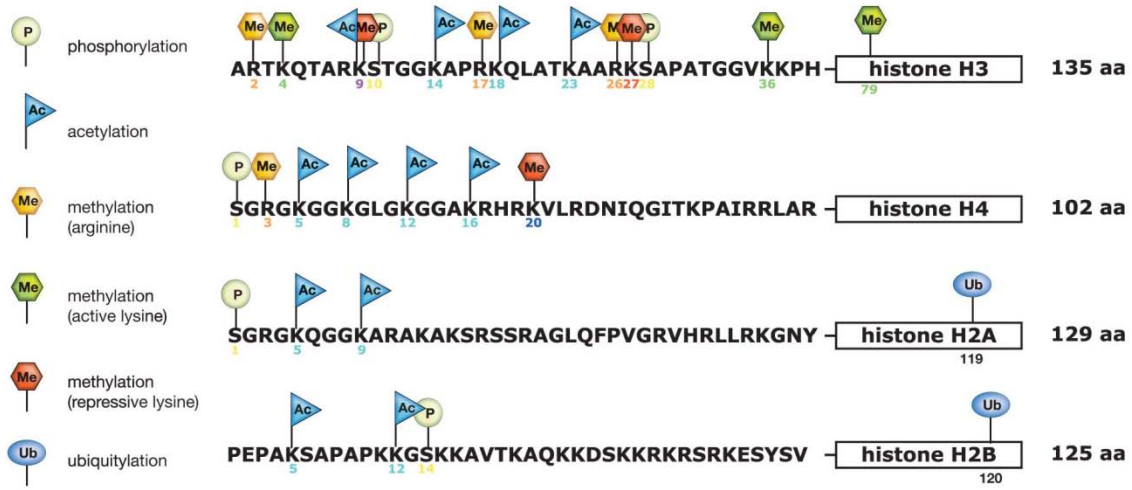

Figure 1.7 Sites of histone tail modifications. (Figure from online resources)

Early studies proposed that modified histones can act as recognition signals to direct binding of non-histone proteins to specific sites within chromatin, thus establishing local DNA-protein or protein-protein conformational changes which link the alteration of chromatin structure to cell cycle progression, DNA replication, DNA damage and its repair, and transcription regulation (Jenuwein and Allis, 2001). More recently, based on abundant evidence, the histone code hypothesis, which indicates that specific tail modifications and/or their combinations constitute a code that act in concert to bring about unique

downstream events, has become generally accepted. This putative epigenetic histone code hypothesis has been strongly supported firstly and mostly by experimental studies investigating lysine acetylation of histones H3 and H4 including the cooperative acetylations between H3 K9 and K14 and H4 K4, K8, K12 and K16 (Peterson and Laniel, 2004). Some acetylated histone residues facilitate further lysine acetylation at adjacent residues, the phenomenon which has been observed in many organisms. For instance, histone H4 K16 acetylation is accompanied by an increase of contiguous lysine acetylation and is associated with a 2-fold increase of transcriptional up-regulation of genes on male X in Drosophila (Turner, 2000). The notion of the histone code was further emphasized by studies demonstrating histone H3 serine 10 phosphorylation and histone H4 lysine 16 acetylation may set up a combinatorial mark leading to the enhanced transcripton of male X chromosome (Strahl and Allis, 2000). Interestingly, antagonizing enzymes such as demethylases, deubiquitinases and phosphatases also exist (Holbert and Marmorstein, 2005). The net effect of both sets of enzymes in combination with simultaneous or subsequent modifications generate a distinct readout of chromatin that can either reconfigure chromatin structure or modulate binding affinity of chromatin-associated proteins. Such changes have the capacity to impact on chromatin metabolism, including transcription and DNA repair.

Although the mechanistic links between histone modification and chromatin function still remain largely elusive, several chromatin-interacting protein motifs have been identified, including bromodomains that interacts with acetylated lysines; chromodomains that target methylated lysines, and SANT domains that recognizes unmodified lysine residues (Holbert and Marmorstein, 2005). Many identified HAT, HMT and HDM enzymes have been shown to contain these domains that constitutes a mechanism of controlling substrate specificity of these proteins. For example, heterochromatin-binding protein 1 (HP1), a methyl-lysine binding protein, interacts with SUV39H1, a histone H3 K9 HMT and the methylation of H3 K9 by SUV39H1 creates a binding site to allow the access of the HP1 protein to execute its repressive property to silence genes and this procedure also synergistically relies upon the suppressive activity of Rb protein (Lachner et al., 2001; Nielsen et al., 2001). Likewise, human $TAF_{II}250$ which is the largest subunit of TFIID contains two bromodomain modules that

bind selectively to multiple acetylated histone H4 peptides (Jacobson et al., 2000). This evidence again supports that multiple modification patterns of histones, not a single acetylated lysine, is required for deciphering an epigenetic code and hints at a new and unexpected role for $TAF_{II}250$ upon hyperacetylated histone H4 due to its accessory role in RNA polymerase II mediated transcription.

In summary, although a large amount of data are suggestive and indicative of the function of multiplex histone modifications, the mysteries of post-translational marks that decorate histone tails are by no means deciphered. Understanding the rules and the consequences of this histone code may impact on many, if not all, DNA-templated processes with far-reaching implications for human biology and diseases (Strahl and Allis, 2000). A list of histone modifications and their correlation with transcription regulation is comprehensively represented in Table 1.1.

Summary table of the HAT-, HMT-, and ATP-dependent chromatin-remodelling enzymes carrying bromodomains, chromodomains or SANT domains as part of their sequence, in different organisms

Protein activity	Domain	Organism	Gene	# Domains	Residue specificity			Molecular function
Chromatin Remodeling	BROMO	*D. melanogaster*	BRM	1				*Transc. coactiv./corepres.*
		H. sapiens	BRM	1				*Transc. coactiv./corepres.*
			BRG1	1				*Transc. coactiv./corepres.*
		S. cerevisiae	SWI2/SNF2	1				*Transc. coactiv./corepres.*
			STH1	1				*Transc. coactiv./corepres.*
Histone Acetyltransferase	BROMO	*A. thaliana*	GCN5	1	—			*Transc. coactiv.*
		C. elegans	1E91	1	—			*Transc. coactiv.*
			CBP-1	1	—			*Transc. coactiv.*
		H. sapiens	P300	1	H3: K14, K18	H4: K5, K8	H2A, H2B	*Transc. coactiv.*
			PCAF	1	H3: K14	H4: K8		*Transc. coactiv.*
			CBP	1	H3: K14, K18	H4: K5, K8	H2A, H2B	*Transc. coactiv.*
			TAF250	2	H3: K14	H4	H2A	*Transc. coactiv.*
			GCN5	1	H3: K14	H4: K8, K16		*Transc. coactiv.*
		M. musculus	GCN5	1	H3: K14	H4: K8, K16		*Transc. coactiv.*
			PCAF	1	H3: K14			*Transc. coactiv.*
			CBP	1	H3: K14, K18	H4: K5, K8	H2A, H2B	*Transc. coactiv.*
			LOC330129	1	—			*Unknown*
Histone Methyltransferase	BROMO	*H. sapiens*	MLL	1	H3: K4			*Transc. coactiv.*
Chromatin Remodeling	CHROMO	*A. thaliana*	CHD-3	2				*Transc. corepres.*
		C. elegans	LET-418 (Mi-2 like)	2				*Transc. corepres.*
			CHD-3	2				*Transc. corepres.*
		D. melanogaster	CHD-3	2				*Transc. corepres.*
		H. sapiens	CHD-3	2				*Transc. corepres.*
			CHD-4	2				*Transc. corepres.*
			CHD-5	2				*Unknown*
		O. sativa	P0018C10.33	2				*Unknown*
Histone Acetyltransferase	CHROMO	*H. sapiens*	CDY-1	1	—			*Transc. corepres.*
			CDY-2	1	—			*Transc. corepres.*
			TIP60	1	H2A: K5	H3: K14	H4: K5, K8, K12, K16	*HIV tat interaction*
			MORF4L1	1	H4: K5, K8, K12, K16		H3	*Transc. coactiv.*
		D. melanogaster	CG6121	1	—			*Unknown*
		M. musculus	MORF4L1	1	—			*Unknown*
		R. norvegicus	TIP60	1	H2A: K5	H3: K14	H4: K5, K8, K12, K16	*HIV tat interaction*
		S. pombe	SPAC637.12C (Myst family)	1	—			*Unknown*
		S. cerevisiae	ESA1	1	H4: K5, K8, K12, K16	H3	H2A	*Cell Cycle Regulator*
Histone Methyltransferase	CHROMO	*D. melanogaster*	SU(VAR)3-9	1	H3: K9			*Heterochr. Formation/Transc. corepres.*
		H. sapiens	SUV39H1	1	H3: K9			*Heterochr. Formation/Transc. corepres.*
			SUV39H2	1	H3: K9			*Heterochr. Formation/Transc. corepres.*
		M. musculus	SUV39H1	1	H3: K9			*Heterochr. Formation/Transc. corepres.*
			SUV39H2	1	H3: K9			*Heterochr. Formation/Transc. corepres.*
		R. norvegicus	SUVAR39-1	1	H3: K9			*Heterochr. Formation/Transc. corepres.*
			SUVAR39-2	1	H3: K9			*Heterochr. Formation/Transc. corepres.*
		S. pombe	CLR4	1	H3: K9			*Heterochr. Formation/Transc. corepres.*
Chromatin Remodeling	SANT	*S. cerevisiae*	ISW1	2				*Transc. coactiv./corepres.*
			ISW2	2				*Transc. coactiv./corepres.*
		D. melanogaster	ISWI	2				*Transc. coactiv./corepres.*
		H. sapiens	SNF2L	2				*Transc. coactiv./corepres.*
			SNF2H	2				*Transc. coactiv./corepres.*
Histone Methyltransferase	SANT	*A. thaliana*	MEDEA	1	—			*Gene Silencing*
			EZA1	1	—			*Gene Silencing*
		D. melanogaster	E(Z)	2	H3: K27			*Gene Silencing*
		H. sapiens	EZH1	2	H3: K27			*Gene Silencing*
			EZH2	2	—			*Gene Silencing*
		M. musculus	EZH1	2	H3: K27			*Gene Silencing*
			EZH2	2	—			*Gene Silencing*
		Z. mays	EZ1	1	—			*Gene Silencing*
			EZ2	1	—			*Gene Silencing*
			EZ3	1	—			*Gene Silencing*

Table 1.1 List of epigenetic modifications and regulatory effects on transcription. (Table from (de la Cruz et al., 2005)

ii The link between epigenetics and prostate cancer

Insight into the relationship between epigenetic modifications and CaP revealed the abnormal phenotypic manifestations in CaP as consequences of gene expression alterations could be partially attributed to certain epigenetic

phenomenon (Schulz and Hoffmann, 2009; Schuettengruber et al., 2007). DNA methylation is one mechanism of gene silencing which is known to be important in prostate cancer (Dobosy et al., 2007; Pang et al., 2006; Patra et al., 2002). The other driving force of epigenetic regulatory mechanism in prostate cancer is the covalent modification of histone proteins or non-histone proteins, mainly catalyzed by HATs and HMTs and their opposing enzymes HDACs and HDMTs, respectively (Seligson et al., 2005). Increased HAT activities have a myriad of effects that may alter prostate cancer growth in positive and negative fashion (Dobosy et al., 2007). For example, the previously mentioned HATs p300, PCAF and TIP60 up-regulate AR activity leading to increased AR signalling in the presence of trace amount of ligands (Halkidou et al., 2003; Debes et al., 2002). In addition, the level of TIP60 is up-regulated in CWR22 CaP xenograft model and AIB1 another AR co-activator has also shown increased expression in prostate cancer clinical specimens (Halkidou et al., 2003; Gnanapragasam et al., 2001). Counteractively, removal of acetyl groups from lysines by HDACs, are a family of enzymes whose expression is frequently up-regulated in prostate cancer (Patra et al., 2001). For instance, high levels of HDAC1 have been seen in metastatic CaP cells including LNCaP, PC3 and DU145 and intriguingly in LNCaP cells the co-regulation of HDAC1 and Tip60 has been observed at AR responsive PSA promoter (Halkidou et al., 2004b; Gaughan et al., 2002). Furthermore, the link between the expression of HDACs and CaP has also been established. It was shown that HDAC1 was up-regulated in pre-malignant and malignant lesions, with the most robust increase in expression in hormone insensitive cancer (Halkidou et al., 2004b). Additionally, HDAC4 expression showed a predominant occupancy in the nucleus in hormone refractory CaP compared to the large cytoplasmic distribution of the protein in androgen sensitive primary tumour (Halkidou et al., 2004a).

Co-localization of AR and the HDM LSD1 has been observed and it relieves the repressive state of methylated H3 K9, thereby leading to de-repression of AR target genes (Metzger et al., 2005). Other evidence also suggests that LSD1 in cooperation with a half LIM-domain protein 2 (FHL2) showed elevated expression in high risk prostate tumours and might serve as a predictive biomarker of CaP aggression (Kahl et al., 2006). Likewise, another strong candidate a histone methyltransferase, EZH2 displays significant over-

expression in hormone refractory and metastatic CaP and is essential for cancer cell proliferation, being a strong marker to distinguish indolent prostate cancer from those at risk of lethal progression (Varambally et al., 2002). Furthermore, although NSD1, a bi-functional transcriptional intermediary factor, interacts directly with LBD of several nuclear receptors, its correlation with AR is still lacking (Huang et al., 1998). However, it is worth mentioning that it bears a putative SET domain and exhibits both repressive and activating function via a novel variant motif FXXLL, which differs from the previous conserved box LXXLL identified in many AR cofactors (Huang et al., 1998; Heery et al., 1997). In fact, NSD1 is amongst the three catalytic SET motif-containing HMTs that are linked to nuclear receptor mediated transcription: the other two are G9a and RIZ1, both H3 K9 HMTs which are implicated in human cancer. G9a being an AR co-activator that synergizes with CARM1 and GRIP1 to regulate AR activity (Lee et al., 2006a; Carling et al., 2004).

Despite the CpG island hypermethylations at specific gene promoters as cancer diagnostic markers such as the hypermethylated promoters of GSTpi, RUNX3, APC and PTGS2 genes, certain histone modifications may also predict the risk of prostate cancer recurrence (Richiardi et al., 2009). These include the widespread changes of acetylation status at three residues on histone H3 and H4, which could potentially serve as independent parameters to predict the outcome of tumour stage, preoperative PSA levels and capsule invasion (Seligson et al., 2005). Altered expression and activity of epigenetic modifying enzymes may provide another avenue for therapeutic prevention of CaP. Many agents have been discovered and tested for their therapeutic potentials such as MTase inhibitor (Decitabine and Zebularine) and HDAC inhibitors (Trichostatin A and Depsipeptide). One study showed that HDAC1 inhibitors trichostatin A (TSA), FR901228 or depsipeptide induced LNCaP and DU-145 cell death and exhibited several apoptotic features such as cellular shrinkage nuclear condensation, and poly(ADP)ribose polymerase cleavage. Another study using a novel Phenylbutyrate-Based Histone Deacetylase Inhibitor, (S)-HDAC-42 showed significant suppression of PC-3 tumor xenograft growth with the reduction of intra-tumoural levels of phospho-Akt and Bcl-xL (Dobosy et al., 2007; Schmidt and McCafferty, 2007; Kulp et al., 2006; Fronsdal and Saatcioglu, 2005). These lines of evidence together suggest the promising potential of

therapeutic intervention for CaP through the mechanisms of epigenetic regulation.

In all, since global modifications of histones and their versatile functions acting extensively on a variety of proteins involved in significant biological processes establish a hallmark for human cancer (Jacobson and Pillus, 1999), their contributive roles in prostate cancer development is under intensive investigation (reviewed in (Lonard and O'Malley, 2005), (Culig et al., 2004), (McKenna et al., 1999) (Seligson et al., 2005)).

1.4.2 The role of histone methyltransferases in prostate cancer

i Protein lysine methylation by histone methyltransferases

Methylation of histone predominantly occur on H3 and H4. Arginine methylation and lysine methylation are catalyzed by two groups of enzymes: PRMT family and SET (Suppressor of variegation 3-9, the Polycomb-group chromatin regulator Enhancer of zeste, and the Trithorax-group chromatin regulator Trithorax) domain containing family, respectively and the correlations between the individual modifications and their effects on transcription regulation are listed (Dillon et al., 2005). The functional significance of arginine methylation includes transcriptional regulation via chromatin remodelling, interplay between histone acetylation, interaction with diverse types of transcriptional activators or co-activators and coordination with ATP dependent enzyme complexes and signal transductions (Lee et al., 2005a).

Lysine methylation which is mediated largely by SET domain-containing HMT enzymes contributes to both transcriptional activation and repression depending upon the discriminate modification of specific lysine residues in histones H3 and H4 (Dillon et al., 2005; Lachner and Jenuwein, 2002). Thus far, functional studies on histone H3 lysine 4 (H3 K4), K9, K36 and K79 revealed both antagonizing and agonizing effects on transcription by either direct or indirect mechanisms. In contrast, H3 K27 and H4 K20 methylation is associated with gene silencing (Lee et al., 2005a). The precise regulatory mechanisms

underlying these effects may be due to three key mechanisms: (1) Inhibiting binding of proteins (or other nucleosome) to histone tails or inhibiting binding or activities of enzymes that make additional modifications of histone tails or other proteins. (2) Creating a binding site for the recruitment of specific proteins involved in chromatin remodelling or enhancing activities of certain enzymes to make additional modifications. (3) Reprogramming nucleosome conformation, thus reconfiguring its association with other proteins or nucleosomes (Schuettengruber et al., 2007; Lee et al., 2005a). A list of key histone methylations on H3 and H4 and their correlation with transcription regulation is presented in Table 1.2.

Methylation	H3	K4	Set1 (yeast)	Permissive euchromatin (di-Me)
			Set9 (vertebrates)	Active euchromatin (tri-Me)
				Transcriptional elongation/memory (tri-Me)
				Transcriptional activation
			MLL, Trx	Transcriptional activation
			Ash1 (*D. melanogaster*)	Transcriptional activation
		K9	Suv39h, Clr4	Transcriptional silencing (tri-Me)
				DNA methylation (tri-Me)
			G9a	Transcriptional repression
				Imprinting
			SETDB1	Transcriptional repression (tri-Me)
			Dim-5, Kryptonite	DNA methylation (tri-Me)
			Ash1 (*D. melanogaster*)	Transcriptional activation
		R17	CARM1	Transcriptional activation
		K27	Ezh2	Transcriptional silencing
				X inactivation (tri-Me)
		K36	Set2	Transcriptional elongation
				Transcriptional repression?
		K79	Dot1p	Euchromatin
				Transcriptional elongation / memory
	H4	R3	PRMT1	Transcriptional activation
		K20	PR-Set7	Transcriptional silencing (mono-Me)
			Suv4-20h	Heterochromatin (tri-Me)
			Ash1 (*D. melanogaster*)	Transcriptional activation
		K59	?	Transcriptional silencing?

Table 1.2 Individual histone methylations on H3 and H4 and their correlation with transcription regulation. (Table from Craig L. Peterson and Marc-Andre Laniel, Magazine)
Corresponding histone modification enzymes are also listed.

ii The link between HMTs and prostate cancer

Several HMTs have been shown to have a potential role in prostate transformation. For example, the intensively studied Poly-Comb Group SET domain containing HMT EZH2 is over-expressed in malignant prostate tissue,

especially metastatic CaP and may serve as an independent cancer biomarker useful in predicting patient outcome after treatment at early stages of disease (Sellers and Loda, 2002; Varambally et al., 2002). Studies have also shown this highly expressed protein may play a role in regulating cell cycle progression, cell self-renewal and apoptosis by controlling transcription of genes such as cyclin-A and DAB2IP, a potent growth inhibitor in prostate cancer (Chen et al., 2005; Tonini et al., 2004). Another Poly-Comb candidate is BMI1, whose expression is elevated in CaP (Berezovska et al., 2006). Likewise, the SET domain containing tumour suppressor protein RIZ1 is inactivated by promoter hypermethylation based on studies using pathological samples. G9a, a histone H3 K9 HMT, has been shown to function as an AR coactivator for genes such as PSA and methylation of its histone substrate suppressed expression of anti-metastatic tumour suppressor genes, including desmocollin 3 (DSC3) and MASPIN, suggesting its cancer pathogenesis potential (Lee et al., 2006a; Suzuki et al., 2006; Wozniak et al., 2006).

1.5 The histone lysine methyltransferase SET9

1.5.1 Characteristics of SET9

i The discovery of SET9

Two pilot papers published in 2002 identified and characterized a novel histone H3 K4 methyltransferase SET9 (Nishioka et al., 2002; Wang et al., 2001a). Originally purified from HeLa cells, SET9 was shown to methylate histone H3 lysine 4 *in vitro*, whereas it failed to methylate histone assembled into nucleosome *in vitro* suggesting it's *in vivo* capability requires other factors (Wang et al., 2001a). Depletion and point mutation analyses demonstrated that the SET domain and its adjacent sequences are required for SET9-mediated HMT activity, although it lacks the pre- and post-cysteine rich regions, which is found in many other SET domain containing HMTs (see Figure 1-8) (Wang et al., 2001a). Functional analysis revealed that SET9 functions as a transcriptional co-activator via several mechanisms; (1) Methylation of H3 K4 displaces the HDAC containing transcription silencing complex NuRD at silenced chromatin regions; (2). Methylation of H3 K4 by SET9 and methylation of H3 K9 by

SUV39H1 inhibit each other and the latter modification is largely involved in transcription repression; (3). Methylation of H3 K4 by SET9 favours subsequent deposition of p300 on histone H4, both phenomena together indicative of gene activation (Nishioka et al., 2002; Wang et al., 2001a).

ii SET9 protein structure and the catalytic mechanism

SET9 consists of 324 amino acids with the catalytic SET domain located at the C-terminus of the protein between residues 227 and 335 (Figure1.8). Mutational analysis revealed that histidine 297 within the SET9 domain is required for SET9-mediated methylation. In line with other histone methyltransferases, the catalytic mechanisms of SET9 relies upon the transfer of methyl group(s) from the cofactor S-adenosyl-methionine (SAM) to the specific substrate lysine 4 on histone H3 (Figure 1.9) (Hu and Zhang, 2006). The high-resolution crystal structure of a ternary complex of human SET7/9 with a histone peptide and cofactor reveals that the peptide substrate and cofactor bind on opposite surfaces of the enzyme and the target lysine accesses the active site within the enzyme and S-adenosyl-methionine cofactor by inserting its side chain into a narrow channel that runs through the enzyme, connecting the two interfaces (Xiao et al., 2003). Proteomic and structural analysis also indicated it is a histone mono-methyltransferase as the structure shows that the arrangement of protein side chains in the active site of SET7/9 is such that it can only catalyse the addition of a single methyl group to the lysine amine (Couture et al., 2006). In addition to the original feature of recognizing histone R-T-K-Q sequence as the primary substrate, crystal structure analysis using TAFIID (a SET9 substrate) bound SET9 also revealed that in the case of non-histone proteins, it has a recognizable motif K/R-S/T/A preceding the lysine substrate and has a propensity to bind asparagine and aspartate on the C-terminal side of the lysine target (Couture et al., 2006).

MDSDDEMVEEAVEGHLDDDGLPHGFCTVTYSSTDRFEGNFVHGEKNGRGK 50
FFFFDGSTLEGYYVDDALQGQGVYTYEDGGVLQGTYVDGELNGPAQEYDT 100
DGRLIFKGQYKDNIRHGVCWIYYPDGGSLVGEVNEDGEMTGEKIAYVYPD 150
ERTALYGKFIDGEMIEGKLATLMSTEEGRPHFELMPGNSVYHFDKSTSSC 200
ISTNALLPDPYESERVYVAESLISSAGEGLFSKVAVGPNTVMSFYNGVRI 250
THQEVDSRDWALNGNTLSLDEETVIDVPEPYNHVSKYCASLGHKANHSFT 300
PNCIYDMFVHPRFGPIKCIRTLRAVEADEELTVAYGYDHSPPGKSGPEAP 350
EWYQVELKAFQATQQK 366

Figure 1.8 Full-length SET9 amino acid sequence containing a SET domain.
Underlined sequences are identified by mass spectrometry. SET-domain residues are in blue, and histidine 297 is highlighted in red.

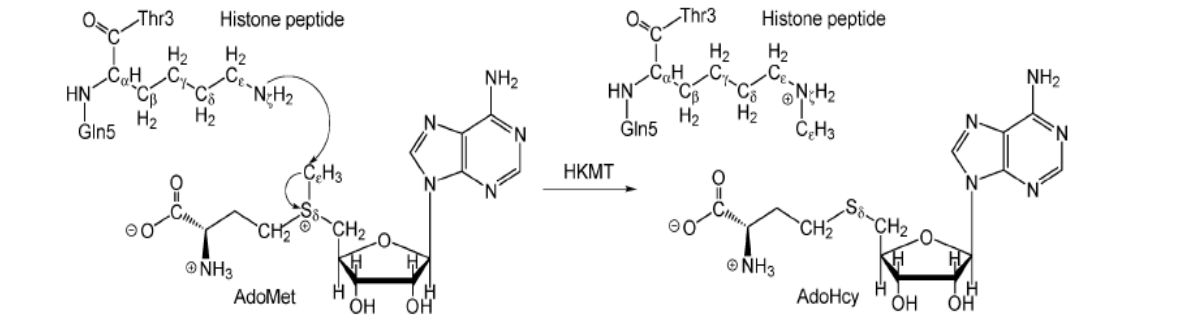

Methyl-transfer reaction catalyzed by SET7/9, in which one methyl group is transferred from AdoMet to the histone-lysine residue H3-K4.

Figure 1.9 Chemical mechanisms of histone lysine methyltransferase.
A methyl group is transferred from S-adenosylmethionine (AdoMet) to the substrate Histone H3 K4.

iii Molecular and cellular functions of SET9

In keeping with the computational-based SET9 putative target identification supported by above crystal structure based evidence, it was subsequently suggested that SET9 can not only mediate the methylation of histone proteins but truly can also methylate or interact with some non-histone proteins. Interestingly, it was shown that SET9 enhances p53 transcriptional activity by directly methylating p53. Methylation of lysine 372 of p53 by direct SET9 interaction stabilizes p53 protein and facilitates p53-mediated transcription of p21, BAX and MDM2 and indeed exerts effect on the cell phenotype such as apoptosis in response to chemotherapeutic intervention doxorubicin (Chuikov et al., 2004). This molecular biology property of SET9 has been proven in vivo using null allele SET9 mouse model, where deletion of SET9 caused the pre-disposition to oncogenic transformation upon induction with DNA damage through p53 mediated pathway. More interestingly, SET9 methylation of p53 in

vivo potentiates acetylation of p53 by TIP60 suggesting a mechanistic link between methylation and acetylation of proteins (Kurash et al., 2008). Another line of evidence in pancreatic β cells suggested that Pdx-1-mediated insulin gene transcription is synergistically up-regulated due to -methylation of both Pdx-1 protein and histone H3 K4. This also linked its relationship with basal transcription machinery, as methylated H3 K4 correlated with RNA polymerase II recruitment at the insulin promoter, but not the myoD1 promoter in which H3 K4 methylation is not enriched (Francis et al., 2005; Chakrabarti et al., 2003). A similar mechanism is observed for the collagenase gene, where SET9 functions to modify histone H3 K4 with subsequent ordered recruitment of other modifying enzymes, including p300, RSK2 kinase and Brg-1, all of which constitute a putative readable code recognized by TATA binding protein, c-jun/c-fos and RNA polymerase II (Martens et al., 2003). Additionally, supporting these findings a physical interaction between SET9 and TAF10, and subsequent TAF10 methylation (a component of the general transcription factor TFIID) has been observed. This association increases the affinity between TFIID and RNA polymerase II facilitating some, but not all corresponding gene transcription, including ERA and ERF1 (Kouskouti et al., 2004). Recently, it has been found that SET9 can directly methylate estrogen receptor (ER) at a single lysine residue, 302 in the lysine-rich RSKK motif. Similar to the story between SET9 and p53, SET9 methylated ER shows enhanced stability. Methylation at this site is a pre-requisite for efficient ER recruitment at the promoter of target genes and their subsequent transcription. Interestingly, a breast cancer associated mutation at the 303 (lysine to arginine) alters SET9-methylation at adjacent 302 both in vitro and in vivo suggesting the importance and influence of surrounding structure at the hinge region to favour the essential modification (Subramanian et al., 2008). SET9 has also been shown to be a regulator of NF-kB. Down-regulation of SET9 by siRNA caused abolishment of TNF-α induced NF-kβ recruitment at inflammatory gene promoters and corresponding transcription in monocytes and this also impacts on monocyte adhesion (Li et al., 2008). Recent findings indicate that methylation of NF-kB occurs on the p65 subunit of the protein complex at lysine 37, which is responsible for TNF- α and lL1-β induced promoter binding of p65 (Ea and Baltimore, 2009). In addition, subsequent findings suggest that NF-kB is also methylated by SET9 at the lysine residues 314 and 315 of the RelA/p65 subunit and these modifications

inhibit NF-kB action by inducing the proteasome-mediated degradation of promoter-associated RelA in vitro and in vivo. This suggests an alternative mechanism whereby NF-kB is differentially regulated by SET9 (Yang et al., 2009).

1.5.2 SET9 and cancer

As discussed above, the potential role of SET9 as a non-histone protein modifier expands the diversity of the protein in regulating key components in cancer biology. The role of SET9 as a p53 stabilizer and participation in pro-apoptotic gene activation suggests its role as a tumour suppressor. However, during breast cancer progression, SET9 may act as a cancer facilitator by stabilizing estrogen receptor protein to allow constitutive stimulation of target gene expression. Thus the effect of SET9 on positive/negative regulation in cancer development might be dependent upon the cellular and molecular complex therein. To date, although the function of SET9 in CaP is largely unknown, due to the discovery and characterization of many AR co-activators combined with their intrinsic effects of targeting specific histone residues at numerous gene loci, a role for HMT function in AR activity remains to be established. The finding that H3 K4 methylation stimulates the PSA promoter in response to androgen suggests an involvement of a H3 K4 HMT in AR mediated transcription regulation and signalling, which provides supporting evidence of the likelihood of SET9 involvement in prostate cancer progression (Kim et al., 2003). In line with the hypothesis, our early data suggested a direct interaction between SET9 and AR in LNCaP cells and this interaction imposed a direct methylation of the receptor by SET9 at lysine residue 632 in the KLKK motif of the hinge domain. Luciferase reporter assays using the AREIII at the PSA promoter suggested its function as an AR co-activator again emphasizing the potential role of SET9 as a pivotal mediator in the development of prostate cancer (Gaughan et al, 2010).

Aims

Although SET9 was initially characterized in cancer cells and shown to be an important co-regulator protein for numerous transcription factors, including p53 and the estrogen receptor, mechanisms that regulate this methyltransferase enzyme remain undefined. Pioneering experiments performed in the Urology Research Group, Newcastle University, demonstrated a role for SET9 in androgen receptor regulation. To further extrapolate the SET9 project in androgen receptor signaling and prostate cancer, the first aim of this studentship is to investigate the regulatory mechanisms of SET9 in the AR signaling cascade and assess the impact of SET9 on cell cycle regulation and apoptosis in cell line models of prostate cancer.

To gain a more detailed insight into regulatory processes that impact on SET9 activity in prostate cancer cells, SET9-interacting proteins will be identified and their impact on SET9-mediated co-activation of the AR and prostate cell growth will be investigated.

In all, the work conducted herein has the potential to highlight novel mechanisms of SET9 activity in the AR signaling cascade and prostate cancer progression that may further validate the enzyme as a potential therapeutic target in this disease. Moreover, by examining protein-interacting partners of the histone methyltransferase, it is postulated that control mechanisms of SET9 will be identified and thus improve our understanding of this enzyme in epigenetic regulation in numerous cellular systems.

Chapter 2

General materials and methods

2.1 General reagents and chemicals

All general reagents and chemicals detailed in this thesis were purchased from the following manufacturers (table 2.1)

Names	Suppliers
Methanol, Ethanol, Isopropanol, NaCl, Glycine, Tris(hydroxymethyl)aminomethane, Sodium dodecyl sulfate, Glycerol, Acidic acid	Fisher Scientific
Triton X-100, Tween-20, Chloroform, Whatman paper, Harris's Haematoxylin	BDH, VWR
Nonidet P-40	CalBiochem
Na_3VO_4, Dimethyl sulfoxide, NaOH, phenylmethanesulfonylfluoride, Dithiothreitol, Aluminium potassium sulfate, Bromophenol blue, T4 DNA polymerase, RPMI 1640 medium (HEPES modification), DMEM, 3,3'-Diaminobenzidine tablet, EDTA, plasmid DNA purification kit, L-Glutamine, Ampicillin, Kanamycin, X-gal, Isopropyl Thio-β-D-Galactoside, Foetal bovine serum , DHT, R1881, Trypsin	Sigma Aldrich
Yeast extract, Tryptone, Agar bacteriological, PBS tablets	OXOID
Saran wrap	SLS
PCR buffer, dNTPs, Hyperladder I and IV,	Bioline
Oligo dT, Luciferase assay lysis buffer and luciferase substrate, MMLV reverse transcriptase and buffer	Promega
G418, SYBER green, SYBR safe DNA staining reagent, T4 DNA ligase	Invitrogen
Nuclear/cytoplasmic extraction kit	Perbio Science
X-ray film	GR1
G418, SYBR green	Invitrogen
Nuclear/cytoplasmic extraction kit	Perbio Science
Dextran-charcoal-stripped serum	Hyclone
Protease inhibitor tablet	Roche
Avidin-biotin-complex kit	Pierce
Maxiprep, Miniprep Gel extraction kit	Qiagen

Table 2.1 List of general chemicals and reagents and relevant suppliers.

All reagents and chemicals specifically used for individual experimental purposes are described below in individual sections. Description of techniques used in generating the results within this thesis is provided below. Manufacturer's protocols are referenced where appropriate if the work was performed strictly according to those protocols.

2.2 General molecular cloning methods

2.2.1 Molecular cloning methods

i Agarose gel electrophoresis

Agarose gel electrophoresis was routinely performed as a pre-requisite for DNA/RNA separation. Agarose (Invitrogen) was dissolved in TAE (Tris Acetate EDTA) buffer and gels were subsequently poured onto clean class plates with perspex combs overhang in order to form sample wells for loading. Gels were placed into electrophoresis tank (Bio-Rad). DNA samples were mixed with 5x DNA sample buffer (30% sucrose, 100mM EDTA, pH 8, 0.05% bromophenol blue, New England Biolabs) at appropriate ratio and loaded into wells alongside DNA molecular weight markers (Bioline). Electrophoresis was performed at 100 volts for 30-60 mins. Gels were then stained in SYBR SAFE at 1 in 10,000 dilution (Invitrogen) for 10 mins and analyzed using a GelDoc video imaging system (Bio-Rad).

ii E.coli culture

Genetically modified chemical competent *E.coli* strains (Top10 and NEB 5-α) were routinely cultured in autoclaved Luria Bertani (LB) medium. pH value of the LB medium was adjusted according to manufacturer's recommendation for competent *E.coli* cells prior to autoclaving. Antibiotics were also added to LB medium immediately before culturing in accordance with the resistance property of the transformed plasmid vectors for amplification. Ampicillin and kanamycin were used as routine antibiotic selection methods for related cloning works.

Chemical	Conc. for medium	Conc. for plate	Conc. for plate for blue-white selection
tryptone	10.0g/L	10.0g/L	10.0g/L
yeast extract	5.0g/L	10.0g/L	10.0g/L
sodium chloride	5.0g/L	5.0g/L	5.0g/L
Agar powder	--	15.0g/L	15.0g/L
distilled H_2O	diluent	diluent	diluent
IPTG	--	--	100µl/plate

			(stock:100mM)
X-Gal	--	--	40µl/plate (stock: 20mg/ml)

Table 2.2 Composition of Luria Bertani (LB) medium.

iii Plasmid DNA vector preparation

All *E.coli* cells were cultured at 37°C with constant horizontal shaking at approximately 180 rpm overnight. Alkaline lysis method was used to extract plasmid DNA from bacteria. This was carried out routinely by using Maxiprep or Miniprep kit (Qiagen) according to manufacturer's protocols. Quality of extraction was controlled by either agarose gel electrophoresis or UV spectrophotometry measuring 260 Å light absorbance using Nanodrop ND-1000.

iv Endonuclease DNA digestion

BamH1 and Kpn1 endonucleases were used in this work during subcloning and positive clone selection. Suppliers of these enzymes included Roche, New England Biolabs, and Fermentas. Digest reactions were set at either 30°C or 37°C according to each enzyme's properties. Incubation was typically performed for 1 hour using 3-5 units of enzyme per microgram plasmid DNA.

v Ligation of DNA fragments and alkaline phosphatase treatment

T4 recombinant bacteriophage DNA ligase (Invitrogen) was used routinely in all DNA ligation reactions. Typical ligation reactions were performed at RT or 14°C from 1 hour up to overnight according to manufacturer's recommendation. For subcloning work, digested vectors were treated with Calf intestine phosphatase (CIP) (New England Biolabs) for 15 mins at 37 °C according to manufacturer's protocol. The purpose was to remove phosphate groups from the 5 prime ends of digested vectors preventing the digested vectors from self-religation.

vi E.coli transformation and plasmid verification

Competent bacteria transformation was carried out according to manufacturer's protocol (Invitrogen or New England Biolabs). Transformed *E.coli* cells were selected by growing *E.coli* on antibiotic (stated above) containing LB agar culture plates overnight at 37 °C. Qualities of the plasmid constructs were verified by DNA sequencing and mammalian cell transfection and subsequent western blotting for the expressed proteins before functional application of these vectors. Sequencing primer sets (Cogenics) are listed below in table 2.3.

vii Gel extraction

Gel extraction was performed using Qiagen gel extraction kit. Gel pieces containing the vectors or inserts were weighted and counted as one volume. Gels were subsequently dissolved in three volumes of Buffer QG and incubated at 50 °C for 10 mins. 1 volume of isopropanol was then added and mixed to allow sufficient precipitation of DNA if the DNA fragments were longer than 4 kb. Otherwise melted gels were transferred to spin columns and spun at 13000 rpm for 1 min. Resultant DNA bound columns were washed with 500 µl of buffer QG and centrifuged at 13000 rpm for 1 min. Columns were then filled with 750 µl of PE buffer and left for 3 mins before centrifugation. Resultant DNA containing columns were then placed in fresh effendorf tubes and 20-30 µl of EB buffer was added and stood for 1 min to elute DNA from the columns. Finally, DNA was spun off from the columns and collected in new tubes for future use.

2.2.3 Conventional PCR amplification

Polymerase chain reaction (PCR) was carried out using T4 DNA polymerase (Sigma) and PCR kit (Bioline) according to the manufacturer's protocols. Some products resulting from PCR were subcloned into linearised plasmid vector constructs. The primers used to clone these inserts are listed in Table 2.3. All vectors used in this project are listed in Table 2.4. The Flag-tagged pcDNA3.1-hSET9 vector (GeneBank accession No AF462150) was kindly provided by Danny Reinberg. 1081bp full-length hSET open reading frame was PCR-amplified using the BamH1 site-containing primers shown in Table 2.3. Primer pairs used for cloning were purchased from Sigma-Aldrich.

No.	Name	Sequence
1	3×FLAG-SET9 forward	5’-GGA TCC ATG GAT AGC GAC GAC GAG-3’
2	3×FLAG-SET9 reverse	5’-GGA TCC TCA CTT TTG CTG GGT GGC-3’
3	GFP-SET9 forward	5’-ATG ATG GAA TTC GAT AGC GAC GAC GAG ATG-3’
4	GFP-SET9 reverse	5’-ATG ATG GAA TTC TCA CTT TTG CTG GGT GGC-3’
5	CMV 30 sequencing primer forward	5′-AAT GTC GTA ATA ACC CCG CCC CGT TGA CGC-3′
6	3×FLAG-SET9 sequencing reverse	5’-GGA TCC TCA CTT TTG CTG GGT GGC-3’
7	GFP-SET9 sequencing forward	5’-GCC CCT TGA AGA TCA GTCT CCC ATC TGT-3’
8	GFP-SET9 sequencing reverse	5’-ATG ATG GAA TTC TCA CTT TTG CTG GGT GGC-3’

Table 2.3 List of primers for cloning work.

No.	Vector Type	Insert Type	Mutation	Tag
1	pcDNA 3.1	SET9 WT	n/a	n/a
2	pCR 2.1	SET9 WT	n/a	n/a
3	P3×FLAG-CMV-10	SET9 WT	n/a	N-terminus 3×FLAG
4	pEGFP-C2	SET9 WT	n/a	N-terminus GFP
5	pEGFP-C2	HDAC1 WT	n/a	N-terminus GFP
6	pcDNA 3.1	SET9 WT	n/a	N-terminus FLAG
7	pcDNA 3.1	SET9 MUT	H297A	N-terminus FLAG
8	pcDNA 3.1	FXR1 E WT	n/a	n/a
9	pcDNA 3.1	FXR1 F WT	n/a	n/a
10	pcDNA 3.1	FXR1 G WT	n/a	n/a
11	p3×FLAG-CMV-10	EBP1 WT	n/a	N-terminus 3×FLAG
12	pEGFP-C1	EBP1 WT	n/a	N-terminus GFP
13	pcDNA 3.1-FLAG	GIPC1 WT	n/a	N-terminus FLAG
14	pcDNA 3.1-FLAG	GIPC1 MUT	L142A/G143E	N-terminus FLAG
15	pAREIII-luc	Luciferase	n/a	n/a

16	pCMV	β-gal	n/a	n/a
17	pAD-Gal4	HDAC1WT	n/a	N-terminus Gal4
18	TK-GAL4UASLuc	Gal-4 responsive Luciferase	n/a	n/a
19	pCMVβ	p300 WT	n/a	n/a
20	pCDNA3	AR WT	n/a	n/a

Table 2.4 List of vectors for cloning work and mammalian cell transfection.

2.3 RNA preparation and analysis methods

2.3.1 Total RNA extraction

Trizol reagent (Invitrogen) was applied directly to cell monolayers and total RNA extraction was performed by a series of chloroform, isopropyl alcohol and ethanol treatments, and finally, re-dissolved in DEPC water (detailed description in the manufacturer's protocol).

2.3.2 Reverse transcription and SYBR green and TaqMan real-time PCR analysis

Prepared RNA was heated at 65 ℃ to remove RNA secondary structure and subjected to reverse transcription process for cDNA synthesis using the Mouse Moloney Leukemia Virus Reverse Transcriptase (Promega) with oligo 'dT' as primer hybridizing to polyA tails of mRNA (protocols from Promega). After 1 hour incubation at 37 ℃, cDNAs were used as templates for absolute quantification using SYBR Green I or TaqMan gene expression real-time PCR analysis according to manufacturer's instruction (Sigma Aldrich and Applied Biosystem). GAPDH or HPRT1 (Sigma) were routinely used for normalization in relative quantification and the same setup with polymerase enzyme replaced by water was routinely used as negative control. ABI 7900HT real-time PCR system was used and data was analysed by SDS2.2 software (Applied Biosystem). The primer sets used are listed in Table 2.5.

No.	Name	Sequence
1	PSA forward	5’-GGTGCATTACCGGAAGTGGAT-3’
2	PSA reverse	5’TGGTCATTTCCAAGGTTCCAAG-3’
3	GAPDH forward	5’CGACCACTTTGTCAAGCTCA-3’
4	GAPDH reverse	5’GGGTCTTACTCCTTGGAGGC-3’
5	TaqMan SET9 forward	n/a
6	TaqMan SET9 reverse	n/a
7	p21 forward	5'-GACTCTCAGGGTCGAAAACGG-3'
8	p21 reverse	5'-GCGGATTAGGGCTTCCTCTT-3'
9	Mdm2 forward	5’- CAAGTTACTGTGTATCAGGCAGGG-3’
10	Mdm2 reverse	5’-TCTGTTGCAATGTGATGGAAGG-3’
11	Bax forward	5'-ACTCCCCCCGAGAGGTCTT-3'
12	Bax reverse	5'-GCAAAGTAGAAAAGGGCGACAA-3'
13	HPRT1 forward	5’-TTGCTTTCCTTGGTCAGGCA-3’
14	HPRT1 reverse	5’-AGCTTGCGACCTTGACCATCT-3’

Table 2.5 List of primers used for real-time PCR quantification of target genes.

2.4 Cell biology techniques

2.4.1 General mammalian cell culture methods

Cell lines used in this work are listed in Table 2.6 with their origin stated. All cell lines were originally purchased from American Type Culture Collection (ATCC) and tested to be free of mycoplasma on a bimonthly basis. Cells were routinely propogated in a humidified incubator (5% CO2) in RPMI1640 culture medium supplemented with 10% foetal calf serum (FCS), 1% glutamine or in DMEM medium supplemented with 10% FCS (HeLa cells). For transfection purposes, basal medium (BM) (RPMI 1640 with L-glutamine) was used. Steroid-depleted (SD) medium (RPMI 1640 plus10% charcoal-stripped foetal calf serum and 1% L-glutamine) were used to assess AR activity. Freezing medium (complete medium supplemented with 10% DMSO and 10% FCS) was used for long-term storage of cell lines. During cell passage, PBS was used to wash cells at approximately 80% confluency once before a thin layer of trypsin/EDTA (0.05%/0.02%) was applied to detach cells from culture flasks. Centrifugation for 3 minutes at 200g was applied to pellet the cells. The cells were then resuspended in fresh growth medium and a fraction of the resuspended cells were counted and re-seeded into new flask to achieve approximately 10% confluency for routine culture purpose.

No.	Cell Line	Origin/year isolated and references	Growth Medium
1	LNCaP	Human lymph node metastasis 1980 (Horoszewicz et al., 1983)	RPMI1640 10% FBS
2	U2OS	Human osteosarcoma 1964 (Heldin et al., 1986)	RPMI1640 10% FBS
3	HEK293T	Human embryonic kidney 1970 (Pear et al., 1993)	RPMI1640 10% FBS
4	DU145	Human brain metastasis 1978 (Stone et al., 1978)	RPMI1640 10% FBS
5	HeLa	Human cervical cancer 1951 (Masters, 2002)	DMEM 10% FBS
6	PC3M	Derivative of Human bone metastasis 1979 (Kaighn et al., 1979)	RPMI1640 10% FBS

Table 2.6 List of cell lines used.
RPMI-1640 medium Dulbecco modified eagle medium (DMEM), were purchased from Sigma-Aldrich, UK. Foetal bovine serum (FBS) was purchased from Gibco, UK.

2.4.2 Generation of stable expression clones

For stable Flag-SET9 transfection, HeLa cells were cultured in 90mm dishes until 60-80% confluence and then transfected with 5µg DNA using the transient transfection procedure stated below. Geneticin (G418) selection was applied onto the plates 48 hours post-transfection at a final concentration of 500µg/ml. Cells were then incubated for approximately two weeks with routine replacement of antibiotic containing medium every 4-5 days. Resistant clones were then transferred onto 24-well plates and continually grown under antibiotics selection prior to transfer onto 6-well plates for expansion. Protein expression was then checked by Western blotting. For long-term storage, positive clones were transferred to freezing medium and stored at -80oC. For routine culture, antibiotic selection was continually applied.

2.4.3 Transient transfection

i DNA plasmid transfection

For DNA transient transfection, mammalian cells were routinely grown until required cell densities were reached (approximately 60-80%). Appropriate amounts of DNA for transfection were mixed with serum-free medium with either Superfect transfection

reagent (Qiagen) or Lipofectamine LTX (Invitrogen) transfection reagent according to manufacturer's recommendations. For Superfect mediated transfection after 2 hrs incubation with plasmid tranfection mix, cells were washed with PBS to remove any potential toxicity induced by transfection reagent and incubated in full media at varying time periods according to different experimental purposes. For Lipofectamine LTX mediated transfection, forward transfection was used. Reagent and DNA mixture was incubated at RT for 30 mins and then applied to cultured cells (at approximately 50-60% confluence). Cells were grown for 48 hours before experimental procedures. Lipofectamine LTX Plus reagent (Invitrogen) was occasionally used to enhance the transfection rate. To achieve this, basal medium containing plasmid DNA was first mixed with Plus reagent for 5 mins at RT (as recommended by manufacturer) and the above-mentioned transfection procedure was followed.

ii siRNA transfection

Gene knockdown was performed using siRNA oligos (Sigma) as described in the protocol provided by the manufacturer. A scrambled siRNA was used as a negative control (Sigma). For siRNA transfection, reverse transfection was undertaken using Lipofectamine RNAi MAX transfection reagent (Invitrogen). siRNA oligos were diluted in serum-free medium and mixed with RNAi duplex at an appropriate ratio according to manufacturer's recommendation. Mixtures were then added into designated wells and incubated for 10-20mins at 37 ℃. Appropriate amount of cells were then plated into each well to give 30-50% confluence and cells were subsequently incubated for various times according to individual experimental requirements prior to assays. All transfection conditions are listed below in Table 2.7 and the siRNA oligonucleotide sequences are listed in Table 2.8.

No.	Reagent Name	Manufacturer	Ratio: DNA/RNA versus transfection reagent
1	Lipofectamine LTX/ Plus reagent	Invitrogen	500 ng/1.5 µl for U2OS, H293T and HeLa cells/0.5 µl Plus reagent 500 ng/3 µl for LNCaP cells/ 1.5 µl Plus reagent
2	Lipofectamine RNAi MAX	Invitrogen	1 µl siRNA/3 µl of RNAi MAX for all cell lines

Table 2.7 Transfection conditions during experimental procedures.

No.	Target gene name	sequences	Conc. in medium
1	SET9	5'-CAUUAGGCAGUAGCAGGUCCACG-3'	25 nM

2	p53	5’-GACUCCAGUGGUAAUCUAC-3’	20 nM
3	FXR1	5’-AUGUCGAAGGCCUUGCGAG-3’	25 nM
	GIPC1	5’-UCAGGGAAGGCAAAGUCAC-3’	25 nM
	EBP1	5’-AGAAUAUAAUCCUGGUCGCUU-3’	25 nM
	Scramble control	5’-ACGUGACACGUUCGAGAA-3’	Same as target Conc.

Table 2.8 List of siRNA oligonucleotide sequences for knockdown experiments.

2.4.4 Luciferase reporter assay

Firefly (Photinus pyralis) luciferase gene and b-gal reporter gene were used in this work to carry out luciferase assays. The product of the luciferase gene catalyzes the luciferin oxidization using ATP/Mg^{2+} as a co-substrate, in turn causing chemical energy conversion leading to the light emission quantitatively measured by plate-reading Luminometers (PerkinElmer).

i Chemiluminescent lysate preparation

Transfected cells grown in 24-well plates were washed once with room temperature PBS and then reporter lysis buffer (Promega) was used to harvest cell lysates containing co-over-expressed proteins of interest, luciferase reporter plasmid and β-Galactosidase plasmid. Cell lysates were snap-frozen at -80 ℃ for 20 mins and subsequently warmed to RT by incubating on 37 ℃ hot block for 5 mins. The thawed cell lysates were immediately used for chemiluminescence detection.

ii Chemiluminescence detection

10 µl of lysates from each tested condition was transferred into 96-well opaque plates which were then placed in a luminometer. Lysates were provided with luciferin substrates and reaction buffer mix (Promega UK) before the luminescence signal was read at 560nm wavelength for firefly luciferase signal. Luminescence signal strength was recorded by the luminometer as relative light unit (RLU) and subsequently transfection efficiency was corrected by dividing firefly luminescence values by β-Galactosidase readout values.

iii β-Galactosidase assay

The Luciferase reporter studies were designed with an internal loading control. β-Galactosidase gene-containing vector was always co-transfected with firefly vector and other gene vectors to be studied. This internal control rules out the difference in over-expression efficiencies and pipette errors during lysate loading. β-Galactosidase is encoded by the lacZ gene of the lac operon in E. coli. The enzyme functions by cleaving lactose to glucose and galactose so that they can be used as carbon/energy sources. The synthetic compound o-nitrophenyl-β-D-galactoside (ONPG) is also recognized as a substrate and cleaved to yield galactose and o-nitrophenol which has a yellow color. When ONPG is in excess over the enzyme in a reaction, the production of o-nitrophenol per unit time is proportional to the concentration of β-Galactosidase; thus, the production of yellow color can be used to determine enzyme concentration. Experimentally, 10 µl of cell lysates from each sample was mixed with equal volume of β-Galactosidase reagent (2 mM $MgCl_2$, 100 mM β-mercaptoethanol, 1.33 mg/ml o-nitrophenyl-β-D-galactoside and 200mM sodium phosphate buffer. pH 7.3) and left at RT in a 96 well flat-bottomed plate for 20-30 mins. The reaction was then terminated by adding 50 µl 1M Na_2CO_3 and the A450nm measured using 1 MR500 plate reader. Luciferase readouts were divided by β-Galactosidase results to generate normalized luficerase counts.

2.5 Protein analysis

2.5.1 SDS polyacrylamide gel electrophoresis (SDS-PAGE) and western blotting

Adherent cells were lysed by mixing with SDS sample buffer with 10% β-mercaptoethanol and lysates were then denatured and loaded into gels consisting of appropriate concentration of acrylamide. Samples were separated according to their molecular weights and proteins were transferred overnight onto Hybond-C nitrocellulose membrane (Amersham Biosciences) at 30V. Membranes were blocked with 5% non-fat milk in Tris-buffered saline (TBS) for 1 hour to prevent non-specific protein-binding of antibodies and subsequently

incubated with primary antibodies in diluent (0.1% non-fat milk in TTBS [1% Tween/TBS]) for 1 hr at room temperature. Primary antibody complexes were detected using HRP-conjugated secondary antibodies and protein bands were visualized by enhanced chemiluminescence (ECL, Amersham) under the exposure to photographic film (Amersham Pharmacia Biotech). Antibodies used in experiments are listed in table 2.9. Acidic antibody stripping buffer was used to remove associated antibodies from nitrocellulose membrane for re-blotting in some circumstances. Membranes were stripped in stripping buffer (82 ml d-water, 6.5 ml of 1M Tris-HCl PH 6.7, 10 ml of 20% of SDS and 780 µl of b-mercaptoethanol) at 50 ℃ for 40 mins with shaking and followed by washing twice in TTBS with each time 10 mins. The antibody stripped blots were then subject to second round of immunoblotting using protocol described above.

No.	Primary antibody name	Supplier	Conc. to use in WB	Application
1	Rabbit polyclonal SET9	Upstate	1:2000	WB/IP/IF
2	Mouse monoclonal SET9	Abcam	1:1000	IF
3	Mouse monoclonal p53	Calbiohem	1:1000	WB
4	Goat polyclonal FXR1	Abcam	1:500	WB/IHC/IF/IP
5	Goat polyclonal GIPC1	Abcam	1:500	WB/IHC/IF/IP
6	Goat polyclonal EBP1	Abcam	1:200	WB
7	Mouse monoclonal α-Tubulin	Sigma	1:2000	WB
8	Mouse monoclonal HDAC1	Upstate	1:1000	WB/IP
9	Goat polyclonal PSA	Santa-Cruz	1:400	WB
10	Mouse monoclonal Androgen receptor	Santa-Cruz	1:1000	WB/IP
11	Mouse monoclonal p21	Oncogene	1:1000	WB
12	Mouse monoclonal PARP1	Santa-Cruz	1:500	WB
13	Rabbit polyclonal p72	Cell signalling	1:300	WB
14	Mouse monoclonal Lamin A/C	Santa-Cruz	1:500	WB
15	Mouse monoclonal RACK1	BD-transduction	1:500	WB
16	Mouse monoclonal FLAG M2	Sigma	1:2000	WB
17	Rabbit polyclonal GFP	Santa-Cruz	1:500	WB
18	Mouse monoclonal Cyclin B1	BD pharm	1:1000	WB
No.	Secondary antibody name	Supplier	Conc. to use	Application
1	HRP-Swine anti Rabbit	Dako Cytomation	1:500	WB
2	HRP-Rabbit anti Mouse	Dako Cytomation	1:500	WB

3	HRP-Goat anti Rabbit	Dako Cytomation	1:500	WB
4	Biotinatyed-Rabbit anti Goat	Dako Cytomation	1:250	IHC
5	FITC-Rabbit anti Goat	Dako Cytomation	1:250	IF
6	FITC-Swine anti Rabbit	Dako Cytomation	1:250	IF
7	TRITC-Goat anti Mouse	Dako Cytomation	1:250	IF
8	TRITC-Rabbit anti Goat	Sigma	1:250	IF

Table 2.9 List of primary and secondary antibodies used and their concentrations for Western Blotting.
Concentrations for other experimental purposes are specified where appropriate.

2.5.2 Immunoprecipitation

i Conventional co-immunoprecipitation

Cells were seeded onto 90 mm dishes and cultured until a confluency of approximately 60-80% was reached. Cells were then harvested and pelleted by centrifugation. 1 ml of immunoprecipitation buffer (50 mM Tris, pH 7.5, 150 mM NaCl, 0.2 mM Na_3VO_4, 0.5% Nonidet P-40, 1 mM phenylmethylsulfonyl fluoride in methanol (PMSF), and protease inhibitor cocktail tablets (Roche, 1 tablet/10ml)) was added to each sample pellet, mixed, and incubated on ice for 30 mins with occasional inversion to allow efficient cell lysis. 20 μl of protein G-Sepharose (PGS), pre-washed three times in immunoprecipitation buffer was added to each sample and incubated for an additional 4 hs at 4 °C with rotation to remove any proteins that interacted nonspecifically with PGS. PGS was removed by centrifugation at 14,000 rpm for 3 mins at RT. The supernatant was taken and each one was incubated with 2 μg of antibodies overnight at 4 °C with rotation. The following day, 20 ml of PGS were added to each sample and incubated at 4 °C for an additional 60 mins. PGS- antibody conjugates were recovered by centrifugation at 14,000 rpm for 3 mins. After removal of supernatant, pellets were washed with buffers in the following order: 1 ml of buffer A (PBS, 0.2% Triton X-100, and 350 mM NaCl) once, 1ml of buffer B (PBS and 0.2% Triton X-100) for 2 times. Samples were finally resuspended in SDS sample buffer, resolved on polyacrylamide gels for electrophoresis and followed by immunoblotting using desired antibodies (all antibodies used can be found in the antibody list above, Table 2.9). In some cases, 150 mm dishes were used for experimental purpose, 1.2-1.5 ml of lysis buffer was added and followed by same procedure described above.

ii Flag resin immunoprecipitation

For FLAG-resin based immunoprecipitation, 150mm dishes were routinely used. Cultured cells were washed twice with room temperature PBS, left on ice for 2 mins and lysed in 1.2 ml of lysis buffer (50 mM Tris, pH 7.5, 150 mM NaCl, 1mM EDTA, 1% Triton X-100, and protease inhibitor cocktail tablets (Roche, 1 tablet/10 ml)). Lysis was performed by incubating on ice for 30 min with occasional inversion to allow efficient cell lysis. Cell debris was removed by centrifugation at 12,000rpm for 10 mins at 4 °C and supernatant was kept for immunoprecipitation. 40 µl of FLAG-M2 resin (Sigma) was usually included for each sample (representing 20 µl of the packed gel volume). To prepare, 1 ml of TBS was added to resin to wash and a second repeat was performed. Resin was then resuspended to the original volume and added to the samples individually. FLAG-M2 resin binding was performed at 4 °C overnight with constant rotation. The following day, resin was settled by centrifugation at 12,000 rpm for 30 s. Resultant resin pellets were washed with TBS for three times. To elute the protein complexes from the resin, elution buffer was prepared (3□l peptide/100ul Flag-wash buffer (TBS), 100ul elution buffer per sample). Elution was carried out at 4 °C for 30-60 min with rotation and followed by centrifugation at 12,000 rpm for 30 s. Resultant supernatant was transferred into fresh tubes and subject to SDS-PAGE electrophoresis and western blotting analysis.

2.5.3 (Colloidal) Coomassie brilliant blue stain

Coomassie brilliant blue G250 solution (Invitrogen) was microwaved for 10 s and then polyacrylamide gels were immersed in the pre-heated solution. Staining was carried out for 30 mins with shaking. Coomassie blue was replace with Destain (20% methanol, 5% glacial acetic acid in ddH_2O) for 30-60 mins to remove unbound Coomassie blue. Stained bands were visualized using a light box and gels were then stored for later experimental purpose or dried under vacuum for long term storage.

For Colloidal Coomassie, polyacrylamide gels were stained with Colloidal Coomassie (Ammonium sulfate 10%, G250 0.1%, Ortho-phosphoric 3%, Ethanol 20%) for 1-4 hours and then destained in water for 1 hour up to overnight. Stained bands were visualized on the light box and gels were then stored for later experimental purpose or dried for long term storage.

2.5.4 Immunofluorescence analysis

i Indirect immunofluorescence

Cells were seeded out on 8-well chamber slides at 8×10^3-1×10^4/well and cultured until 60-80% confluency was reached. Cells were then washed in room temperature PBS once and subsequently fixed with ice-cold methanol at 20 °C for 10 mins. After fixation, cells were washed three times with PBS on a shaker for 5 mins each. Blocking serum was prepared at 1 in 10 dilution in PBS (the species of serum were chosen according to the species from which the secondary antibodies were raised). Cells were then incubated with blocking serum for 1 hour at RT on shaker and washed twice with PBS on shaker for 5 mins each. Antibodies were diluted in PBS at appropriate concentration according to manufacturer's recommendations normally ranging from 1:50-1:200 and added to cells. Primary antibody incubation was conducted overnight at 4 °C with constant low-speed shaking. The next day, cells were washed twice with PBS on a shaker for 5 mins each before the addition of secondary fluorescent conjugated antibodies. Secondary antibody solution was prepared at a dilution of 1 in 250 in PBS and incubation was carried out at RT on shaker for 1 hour in the dark (wrapped in aluminum foil). Cells were then washed twice in PBS on a shaker for 5 mins each and dried at 37 °C on a hot block. Chamber dividers were removed from the slides and one droplet of Vectashield Hard Set with DAPI (Vector laboratories) was added to each well to stain cell nuclei. Finally, cover-slips were then mounted on top of the slide and sealed with nail varnish. Resultant samples were ready for analysis by Leica fluorescent microscopy at Northern Institute for Cancer Research or Leica confocal microscopy at the core facility laboratory (Dr. Trevor Booth) at Medical School, Newcastle University.

ii Direct immunofluorescence

In the case of fluorescent proteins imaging such as GFP microscopy, immunodetection treatment steps were omitted. Cells were normally grown on 6-well plates with inserted coverslips. During experimental procedure, cells were washed with RT PBS and fixed with ice cold methanol for 10 mins at -20 °C. Subsequently, fixed cells were dried at 42 °C on a hot block and stained with DAPI before analysis by Leica fluorescent microscopy. In the case of combination with immune-based fluorescence experiments, cells underwent indirect immunofluorescence procedure in the dark (wrapped in aliminium foil) for all stages of the procedure and finally subject to analysis by fluorescent microscopy.

2.5.5 Nuclear/Cytoplasmic extraction

Nuclear/Cytoplasmic extraction was performed using the NE-PER Nuclear and Cytoplasmic Extraction Reagents (Pierce). Generally, appropriate volumes of CER I buffer were added to cell pellets according to manufacturer's instruction. Samples were vortexed vigorously on the highest setting for 15 seconds to fully suspend the cell pellet and incubated on ice for 10 mins. Ice-cold CER II was then applied to samples and followed by vigorous vortexing twice each for 5 s with a 1 min incubation on ice between vortexing. Samples were centrifuged at 16,000 rcf for 5 mins and supernatants (cytoplasmic fractions) were transferred to fresh pre-chilled tubes. For the remaining pellets which contained nuclei compartment, ice-cold NER buffer was applied at relevant volume according to manufacturer's recommendation. Samples were then subjected to 4 periods of repetitive vortexing on the highest setting for 15 seconds and incubation on ice for 10 mins in between vortexing. Samples were then spun down at 16,000 rcf for 10 mins and the final resultant supernatants (nuclear fractions) were transferred into fresh tubes for subsequent experimental use.

2.6 Fluorescent Activated Cell Sorting (FACS) analysis

2.6.1 Propidium Iodide (PI) DNA analysis

Cell cycle profiles were performed using propidium Iodide (PI) from Sigma, a DNA and RNA incorporating fluorescent biomolecule, which binds preferentially to cells permeabilized by Triton detergent. Adherent and floating cells were harvested into individual tubes and spun down at 2,000 rpm for 5 mins at room temperature (RT). Cells were then washed with warm PBS once, spun down and resuspended in PBS under the same conditions. Cells were then stained immediately with PI (final concentration approximately 0.25 mg/ml) in Triton-X 100 and incubated for 10 mins at RT with freshly prepared RNase A at a final concentration of 300 µg/ml. Cell cycle profiles and distributions were determined by flow cytometric analysis of 10,000 events using the FACScan flow cytometer (Becton-Dickinson). Debris and clumped cells were excluded from cell cycle distribution analysis by gating. For the calculation of cell population per cycle phase WinMDI 2.8 and FlowJo softwares at the core facility laboratory (Dr. Brain Shenton) at Medical School, Newcastle University were used.

2.6.2 BrdU proliferation assay

72 hours after SET9 knockdown in LNCaP cells, BrdU (10mg/ml) from BD was added to culture medium at a dilution of 1 in 100 and cells were incubated with BrdU for 2 hours (optimized for LNCaP cells) to allow the cooperation of BrdU during DNA synthesis. Cells were then harvested in tubes and washed twice with cold PBS. Cells were subsequently resuspended in 100 µl of BD Cytofix/Cytoperm buffer per tube and incubated on ice for 20 mins to allow the fixation and permeabilization of cells. 1 ml of Perm/Wash buffer was then added to each tube and cells were spun down and resuspended in Cytoperm Plus buffer, incubated for 10 mins on ice and subsequently washed in 1 ml of Perm/Wash buffer. Cells were then pelleted by centrifugation and re-fixed in 100 µl of Cytofix/Cytoperm buffer for 5 mins on ice. After another wash using Perm/Wash buffer, cells were treated with 100 µl of DNase (diluted to 300 µg/ml in PBS (BD)) and incubated for 1 hour at 37 °C to expose incorporated BrdU. After incubation, cells were washed again in Perm/Wash buffer and spun down before antibody staining. 1:50 dilution of FITC-fluorescent anti-BrdU antibody in Perm/Wash buffer was prepared and added to cell pellets at 50 µl for each tube. Antibody incubation was performed for 20 mins at RT. Staining cells were again

washed in Perm/Wash buffer and centrifuged. After removal of supernatant, cells were staining with 7-AAD to measure the total DNA levels. Finally, 500 µl of staining buffer was added to each tube and samples were ready for flow cytometer analysis using the FACScan flow cytometer (Becton-Dickinson) at a total count of 10,000 events per sample.

2.6.3 Apoptosis Assays

Annexin-V apoptosis analyses were performed using FITC-conjugated Annexin-V antibody highly specific for phosphatidylserine which presents on the outer surface of the plasma membrane during early apoptosis. Cells were prepared under the same condition as the cell cycle profile and after PBS wash, cells were resuspended in Annexin-V binding buffer (10ml 1.5M NaCl, 100µl 5M KCl, 100µl 1M $MgCl_2$, 100µl 1.8M $CaCl_2$, 88.7 ml H_20) with the final antibody concentration of 0.1 µg/ml (Sigma) and left at RT for 30 mins before the addition of appropriate PI and Annexin-V binding buffer. Annexin-V analyses were measured by FACScan flow cytometer (Becton-Dickinson) and data were analyzed using WinMDI 2.8.

Caspase-3 assays were carried out using active caspase-3 kits (Becton Dickinson), the detection of activated form of the enzyme which has been implicated as an “effector” caspase associated with the initiation of the “death cascade” and is therefore an important marker of the cell’s entry point into the apoptotic signaling pathway. Cells were harvested, washed with PBS twice and resuspended in Cytofix/Cytoperm solution. Cells were then stored at 4 ℃ for 20 mins to allow simultaneous fixation and permeabilization of cells. Incubated cells were then washed with PBS twice, spun down and subjected to caspase-3 FITC antibody cocktail pre-diluted in *Perm/Wash* buffer at a ratio of 1 to 4 in appropriate volume. Cells were then incubated at RT for 30 mins, PBS washed and following final wash in *Perm/Wash* buffer, pelleted, resuspended in appropriate volume of *Perm/Wash* and then ready for FACS analysis. Data were evaluated by WinMDI 2.8.

2.7 Repeat of experiments

Unless otherwise indicated, the experimental results shown as protein immunoblot (western blot) are representative of at least two repeats. All other experimental results are either representative or statistical summarisation of three repeats.

Repeat is defined as experiments at the same condition separated by both space and time. Same condition is defined as humanely achievable replication of all known parameters in the experiment being repeated, which typically include time span, temperature, cell type, cell density, medium type, chemical compound type and concentration, equipment parameters and condition, all human manoeuvre procedures and so on.

2.8 Special note

For treatment using androgenic stimulation, we were unable to acquire a continous supply of R1881 and hence had to switch to using DHT mid-way through the project.

Chapter 3

Analysis of SET9 activity in the LNCaP prostate cancer cell line

3.1 Introduction

The identification of SET9 has led to a dramatic increase in the research field aiming to establish the relationship between this histone methyltransferase (HMT) and transcriptional regulation. Due to the discovery of many chromatin modifying enzymes, these epigenetic regulators have become the hotspot of current biological research to elucidate their functionality in normal and cancerous cell states.

SET9 was initially isolated from HeLa cells and was shown to catalyse specific mono-methylation of histone H3 lysine 4 (H3-K4me1), a modification that is associated with transcriptional up-regulation via mechanisms involving promoter and enhancer methylation and assembly of transcriptional complexes and thus SET9 was proposed to function in transcription regulation (Francis et al., 2005; Kouskouti et al., 2004; Chakrabarti et al., 2003; Nishioka et al., 2002; Wang et al., 2001a). SET9 preferentially methylate core histone H3 lysine 4 in vitro, whereas it fails to methylate histone assembled into nucleosome in vitro suggesting its in vivo capability requires other factors and also suggesting a potential role of SET9 in non-histone protein methylation (Wang et al., 2001a). Co-transfection using Gal4-VP16 and SET9 stimulates the Gal4-TK-luciferase reporter expression suggesting the role of SET9 as a transcriptional co-activator. Immunoprecipitation of histone H3 polypeptide, methylated at H3K9 and H3K4 using H3 tail specific antibody revealed that H3K9 methylated histone peptide is associated with nucleosome remodeling and histone deacetylase complex (NuRD), whereas the transcriptional active marker methylated H3K4 shows remarkable disruption of interaction with the NuRD complex indicating the possible mechanism of SET9 involved transcriptional control. Subsequently, the role of SET9 in transcriptional regulation has been established with the demonstration that SET9 controls the function of several transcription factors including p53, estrogen receptor α (ERα) and NF-κB (Ea and Baltimore, 2009; Li et al., 2008; Subramanian et al., 2008; Chuikov et al., 2004). Those regulatory mechanisms that involve SET9 dictate its pivotal roles in cancer development. Methylation of the KSKK motif in p53 stabilizes the protein and causes p53 target gene activation and subsequent p53 dependent apoptosis and G2/M cell cycle arrest in response to DNA damaging agent (Ivanov et al.,

2007; Chuikov et al., 2004). Methylation of ER by SET9 at K302 is crucial for the recruitment of ER at the promoter of target genes (Subramanian et al., 2008). In vivo models implied that SET9 knockout mice increased the growth rate of mouse embryonic fibroblasts (MEFs) in response to Doxorubicin treatment, however it failed to develop tumours at one year of age even though p53 was partially inactivated possibly due to the detectable p21 expression in cells or the activation of compensatory pathways in the absence of SET9 even when p53 function was compromised (Kurash et al., 2008).

The relationship between SET9 and those vital players during carcinogenesis led us to interrogate the underlying role of this HMT in prostate cancer (CaP), a cancer in which the role of SET9 has yet to be investigated. Structural and catalytic analyses of SET9 identified a putative consensus substrate sequence for SET9-mediated methylation: R/T-S/T/A-K-D/K/N/Q (Couture et al., 2006) that is present in several in vitro and in vivo SET9 substrates, including p53 (KSK(me)K) and ERα (Pradhan et al., 2009; Subramanian et al., 2008; Chuikov et al., 2004). .Importantly, within the hinge domain of the androgen receptor (AR) the presence of a KLKK motif that is similar to the proposed SET9 target sequence suggested that SET9 may be involved in receptor regulation. Indeed, pilot work in our laboratory, indicated that SET9 is expressed in the androgen-dependent LNCaP CaP cell line, interacts directly with the AR in vivo and in vitro and methylates the receptor at position lysine 632 within the KLKK motif (Gaughan et al., 2010). In addition, SET9 was shown to up-regulate AR-mediated transactivation in LNCaP cells in a methyltransferase-dependent manner. However, these initial studies failed to assess the mechanisms of SET9 regulation in CaP cell lines that is a highly pertinent area of investigation. Using the LNCaP cell line model system, several characteristics of SET9 were investigated, including protein stability and SET9 expression profiling, to gain an insight into the inherent properties of the HMT that could be of important for AR regulation.

3.2 Special Materials and methods

The composition and suppliers of the majority of the reagents and materials can be found in the general materials and methods (Chapter 2.1). Otherwise, the materials and reagents are specified in individual chapters where appropriate.

3.2.1 SET9 expression analysis

In order to examine SET9's regulation at both protein and mRNA levels in response to different stimuli and agents, experimental approaches were set up as follows.

i SET9 mRNA expression analysis

To test SET9 mRNA expression in response to androgenic stimulation, LNCaP cells were seeded out at $7x10^5$ cells/well of a 6-well plate in steroid depleted RPMI 1640 medium and starved for 48 hours before treating with the androgen analogue R1881 (10nM) for 0, 2, 4, 6, 8, 9, 15 and 17 hours prior to total RNA extraction and subsequent TaqMan quantitative real-time PCR analysis (ABI). Prostate specific antigen (PSA) mRNA expression was used as positive control to ensure the effectiveness of R1881 and GAPDH was used to normalize RNA quantities across individual samples.

ii SET9 protein expression analysis

The measurement of SET9 expression under the influence of androgen was identical to the mRNA analysis except that LNCaP cells were lysed directly with SDS sample buffer and then subjected to electrophoresis and Western blot analysis. PSA immunoblotting was used to confirm the validity of the R1881 treatment.

To assay SET9 protein stability, LNCaP cells were grown at density of $7x10^5$ cells/well of a 6-well plate in steroid deleted RPMI 1640 medium for 48 hours and R1881 androgen analogue was then applied to cells at 1 hour prior to a

cyclohexmide (CHX) treatment to allow the stimulation of AR activity. A time course of 0, 1, 2, 3, 5, 6 hours after CHX treatment was chosen to harvest samples in to SDS sample buffer. Samples were then subjected to electrophoresis and Western blotting. p53 was used as a positive control of ubiquitin mediated proteolysis.

To gain an insight into SET9 protein levels at individual phases of the cell cycle, HeLa cells were seeded out onto 6-well plates in DMEM medium containing 10% foetal calf serum at low density (around 8×10^6 cells/well) and after 24 hours cells were treated with 2 mM thymidine (Sigma) for 18 hours, released into full medium for 9 hours and followed by a secondary thymidine block for 17 hours to arrest cells at the beginning of S phase. The synchronized cells were then released into fresh full medium and harvested every 2.5 hours for a 12.5 hour period of time. Samples were collected in SDS sample buffer for Western blot analysis and cyclin B1 was used as a control to monitor cell cycle progression. In parallel, the cell cycle position of the cells collected at different stages was also determined by Propidium iodide (PI) DNA staining using the FACS protocol mentioned in general materials and methods (Chapter 2.6.1).

3.2.2 Monitoring exogenous SET9 distribution using direct/indirect Immunofluorescence

U2OS cells were plated at $3x10^5$ cells/well on a 6-well plate containing 22 mm x 22 mm sterile coverslips in complete RPMI 1640 medium and the next day cells were forward transfected with 2µg/well of GFP-SET9 and GFP-HDAC1, respectively. After 48 hours, cells were treated using the direct immunofluorescence protocol mentioned in general materials and methods (Chapter 2.5.4). For a combination of direct and indirect immunofluorescence, U2OS cells were treated using the indirect immunofluorescence protocol and all experimental steps were performed in the dark. LNCaP cells were either plated in full medium or in steroid depleted medium and then forward transfection of GFP-SET9 and GFP-HDAC1 was performed. 48 hours post-transfection, cells grown in steroid depleted medium were either harvested or treated with R1881

for 30 minutes and 120 minutes before subjected to direct immunofluorescence analysis using the standard protocol (Chapter 2.5.4).

3.3 Results

3.3.1 Expression patterns and turnover of SET9 in prostate cancer cell lines

The role and function of SET9 in LNCaP cells have been primarily established in early studies carried out by Dr. Luke Gaughan in our laboratory. However, the regulation of SET9 has not yet been investigated in significant detail in prostate cancer cells and specifically for the androgen-dependent LNCaP cell line. Several lines of evidence indicated SET9 is involved in regulating AR-mediated transcription and is a co-activator of the receptor. To further analyze these initial findings, expression, stability and cellular distribution of SET9 was investigated in LNCaP cells as a means of providing important and as yet uncharacterised information on regulatory mechanisms of the HMT in CaP cells.

i SET9 expression in response to androgenic induction

From documented literature, the transcriptional activity of AR is regulated by cofactor proteins that enhance or reduce the transactivation of target genes. Thus, androgen and/or AR regulated co-regulators could potentially be important in the emergence of hormone-refractory disease. There are few AR co-regulators which are shown to be androgen regulated such as AIB1, CBP/P300, BRCA1 and GACS1/JMJD2C (Heemers et al., 2009; Urbanucci et al., 2008). Based on these facts, we started by assessing the expression of SET9 both at mRNA and protein level upon androgen stimulation. Using reverse transcription and real-time PCR analysis, we profiled SET9 mRNA level upon stimulation with the synthetic androgen analogue R1881 over a time course of 0-17hrs. As shown in Figure 3.1, unlike *PSA*, *SET9* expression was not regulated by R1881 over a 17 hour time-course. This was confirmed at the protein level, where SET9 levels remained constant during androgenic stimulation (Figure 3.2).

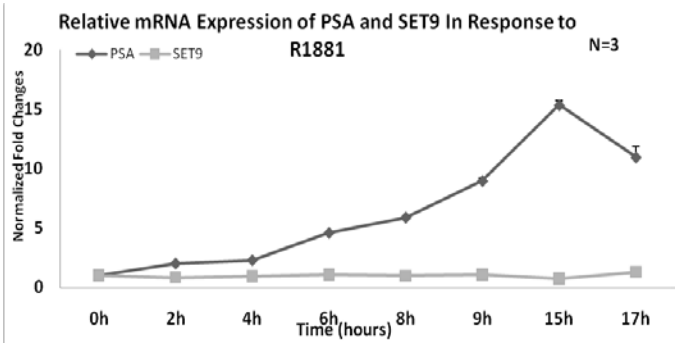

Figure 3.1 SET9 mRNA expression is not regulated by synthetic androgen R1881 in LNCaP cells. LNCaP. After another 48 hours, a 10nM R1881 time course was applied and cells were collected at various time points. mRNA was extracted and quantified using real-time PCR. PSA was used as a positive control for R1881 mediated transcription induction. All mRNA was normalized to GAPDH and cells were grown in serum-containing media and after 24 hours media replaced with androgen deprived medium experiments were performed in triplicates.

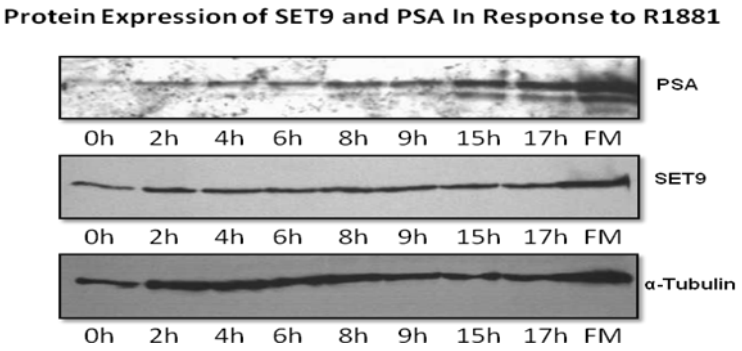

Figure 3.2 SET9 protein expression is not affected by synthetic androgen R1881 in LNCaP cells. LNCaP cells were grown in serum-containing media and 24 hours later the media was replaced with androgen deprived medium. After another 48 hours, 10nM R1881 was applied over a 17 hour time-course. Cells were lysed and subjected to western blot analysis using a SET9 antibody. PSA was used as a control for R1881 treatment and α-tubulin as a loading control.

ii SET9 expression during cell cycle progression

The protein expression of some histone methyltransferase, including SET8 and methylation of many lysine residues on histone tails is cell cycle regulated, such as methylation of histone H4K20 by SET8 and histone H3K79 by Dot1 (Fang et al., 2002; Feng et al., 2002; Rice et al., 2002). To examine a potential role for SET9 in cell cycle-dependent methylation of histone H3, we analysed SET9 protein abundance and the mono-methylation state of histone H3-K4 during the cell cycle. For this experiment, an extensively used sub-strain of HeLa cells (Hela S3) that has been used for cell cycle synchronization studies (Borun et al., 1972) was utilised as LNCaP cells proved difficult to synchronise efficiently for the study of SET9 expression. Results show that SET9 protein levels do not

change during cell cycle progression from G1/S to G2/M (Figure 3.3). As expected, cyclin B1 demonstrates increased protein expression in response to cell cycle transition with the lowest expression in G1 phase and a small increase in expression from S phase throughout G2/M phase. In the corresponding FACS cell cycle analysis, cells were synchronized as expected with more than 90 percent of the cells progressing through the cell cycle together after release into full medium (Figure 3.4).

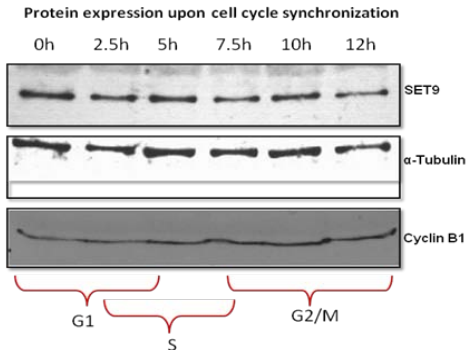

Figure 3.3 SET9 protein is not subject to change during cell cycle progression in HeLa cells.
HeLa cells were seeded onto 6-well plates in DMEM medium at low density and 24 hours later cells were treated with 2 mM thymidine for 18 hours, released into full medium for 9 hours and followed by a secondary thymidine blockade for 17 hours to arrest cells at the beginning of S phase. The synchronized cells were then released into fresh full medium and harvested every 2.5 hours for a 12.5 hour period of time. Samples were then subjected to western blot analysis. SET9 protein level was not significantly affected throughout the cell cycle. CyclinB1 acted as a positive control to monitor cell cycle progression, displaying minimal expression at G1, elevation at S and peaking at G2/M.

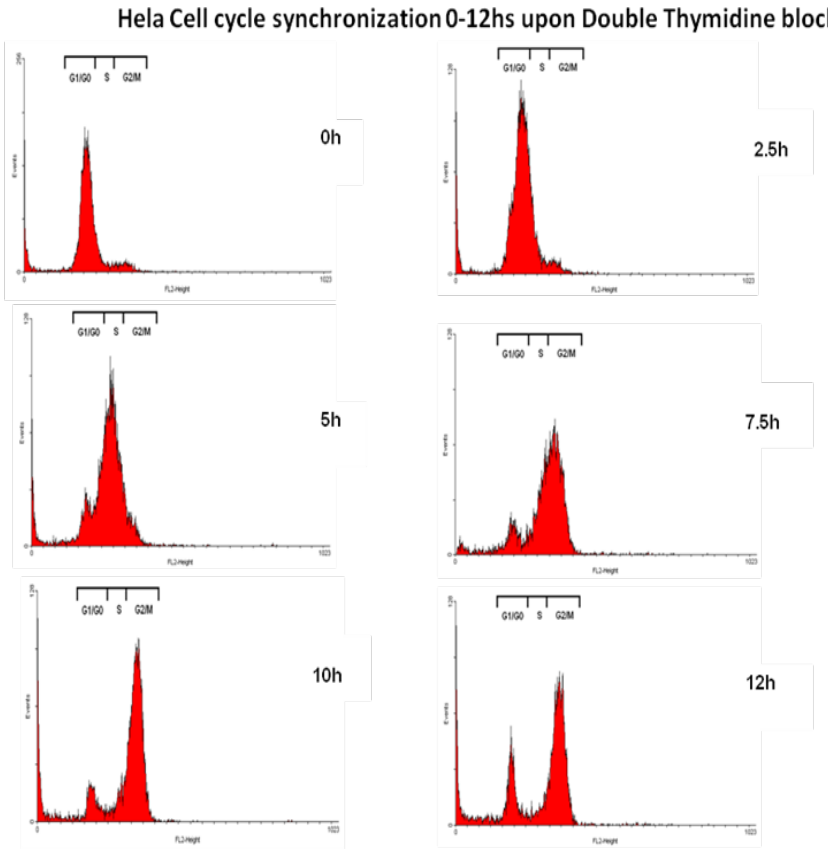

Figure 3.4 Histograms showing HeLa cell cycle synchronization and progression profile.
HeLa cells with the same double thymidine block were released into serum-containing medium and cell cycle progression was profiled using FACS-based PI staining to measure DNA content. As shown in the histograms, cells were arrested in G1 phase, upon release they progress through individual phases of the cell cycle and start to re-enter G1 after 10 hours.

iii SET9 protein stability in LNCaP cells

Protein stability represents another key mechanism of protein regulation that may be pertinent in controlling SET9 activity in LNCaP cells. To examine whether SET9 is subjected to proteolysis upon androgen stimulation, translation of SET9 was blocked using the translation inhibitor cycloheximide (CHX) in LNCaP cells to analyze the turnover of a single SET9 population within cells. In Figure 3.5, SET9 displayed a stable expression pattern during androgen stimulation in the presence of CHX demonstrating SET9 is not subject to androgen-dependent turnover as a result of proteolysis. As expected, p53 protein diminished rapidly as a consequence of protein turnover in the presence of CHX treatment.

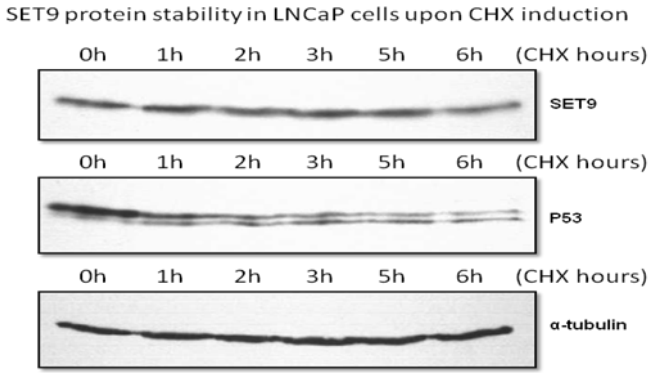

Figure 3.5 SET9 protein turnover is not affected by androgen treatment in LNCaP cells.
LNCaP cells were plated in serum-containing medium for 24 hours and then treated with 10 nM R1881 at 1 hour prior to cycloheximide (CHX) treatment. After 1, 2, 3, 5, 6, hours of CHX addition, cells were harvested and subject to Western blot analysis using antibodies to SET9, p53 and α-tubulin.

3.3.2 Localization and distribution of SET9 in cancer cell lines

SET9 was initially identified from a HeLa cell nuclear extract as a histone modifying enzyme and therefore its proposed action site was believed to be predominantly in the nucleus (Nishioka et al., 2002; Wang et al., 2001a). More recently, the majority of the studies have focused on the role of SET9 in transcriptional regulation of several nuclear transcription factors (Subramanian et al., 2008; Francis et al., 2005; Chuikov et al., 2004; Kouskouti et al., 2004)

implicating a role in the nuclear compartment of cells. In order to get a better understanding of SET9 distribution in prostate cancer cells, we applied immunofluorescence using a SET9 antibody in several cancer cell lines, including LNCaP, the osteosarcoma cell line U2OS and two androgen-independent prostate cancer cell lines, PC3 and DU145. As shown in Figure 3.6, SET9 was predominantly distributed in the cytoplasm in both LNCaP cells and U2OS cells, while in PC3 and DU145 cells (Figure 3.7), SET9 distribution was equally distributed between the nucleus and cytoplasm suggesting that the localization of this HMT is highly variable in different cancer cell types. In parallel experiments, we used a mouse monoclonal HDAC1 antibody as a control to show the well established presence of this protein predominantly in the nucleus in both LNCaP and U2OS cells (Figure 3.8).

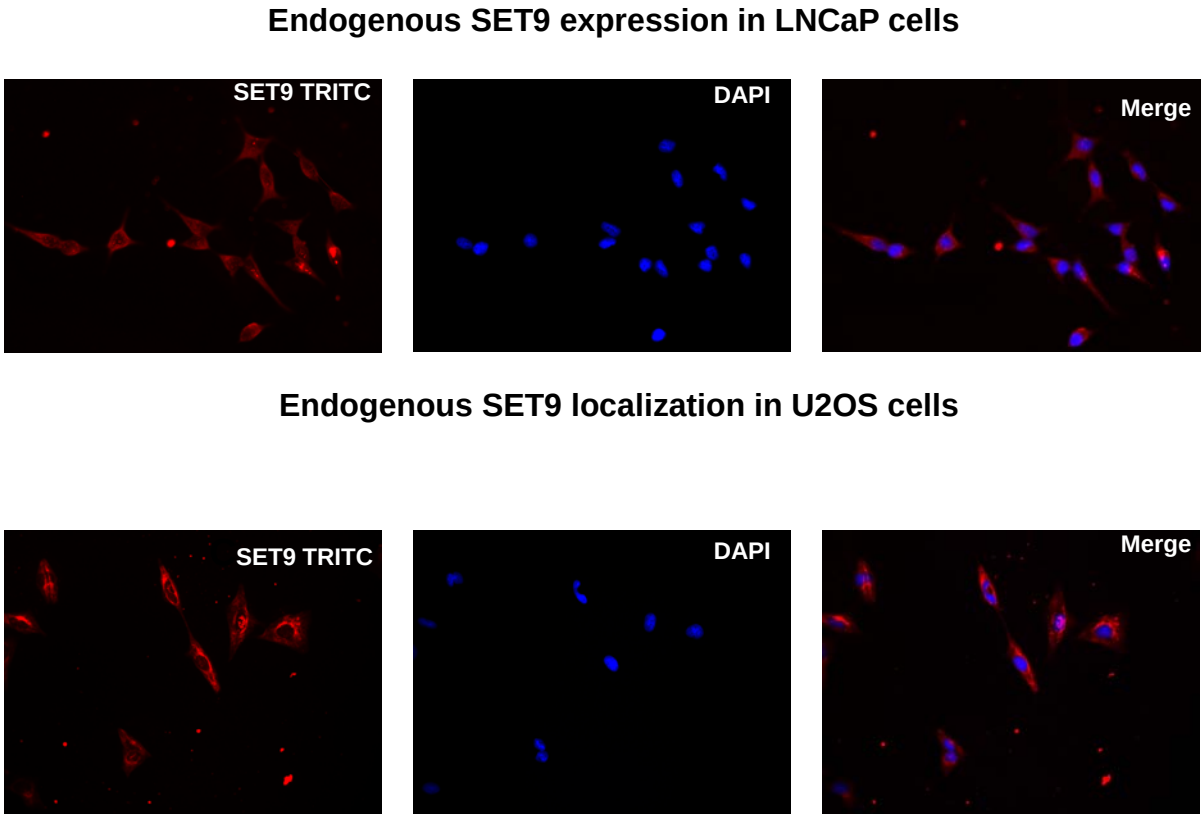

Figure 3.6 SET9 is localised predominantly in the cytoplasm in both LNCaP and U2OS cells.
LNCaP (upper) and U2OS cells (lower) were grown on chamber slides overnight in serum-containing media and then subjected to immunofluorescence analysis using a rabbit polyclonal SET9 antibody. DAPI was used for nuclear DNA staining.

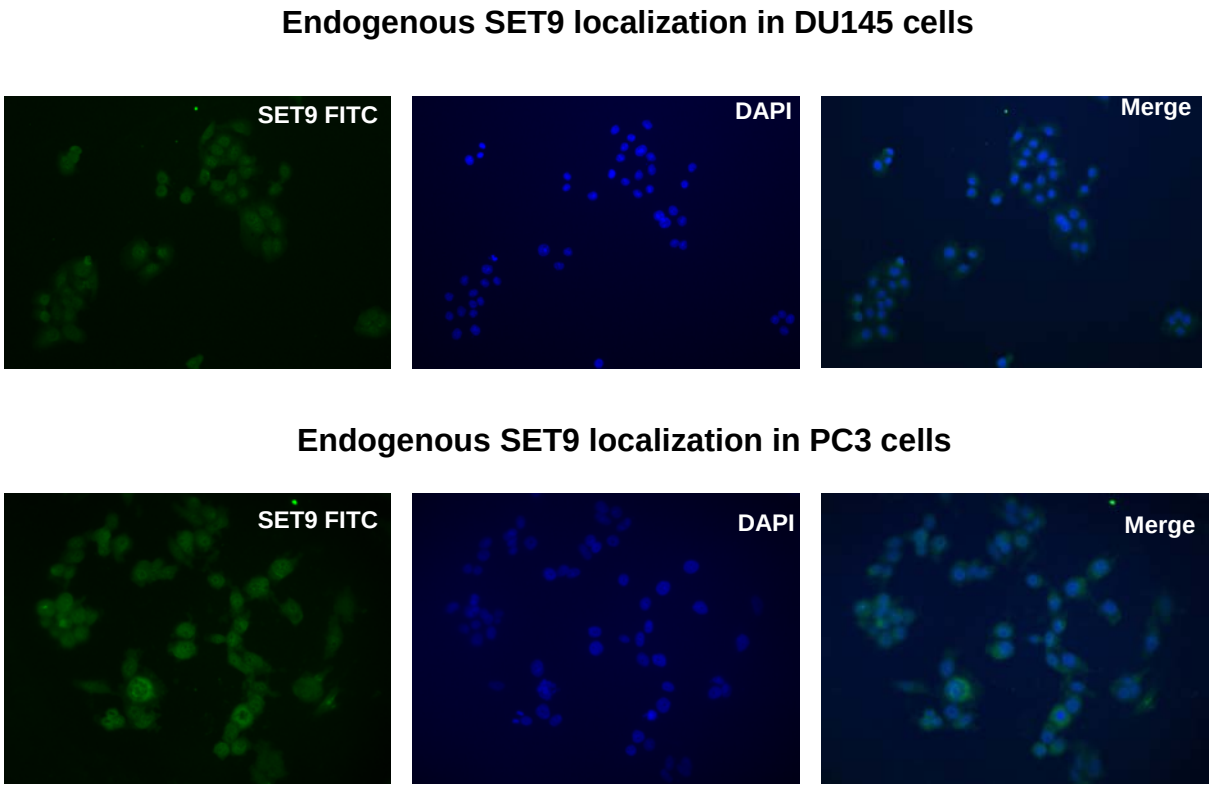

Figure 3.7 SET9 is equally distributed in the cytoplasm and nucleus of both DU145 and PC3 cells. DU145 and PC3 cells were grown on chamber slides overnight in serum-containing media and then subjected to immunofluorescence analysis using rabbit SET9 antibody. DAPI was used for nuclear DNA staining.

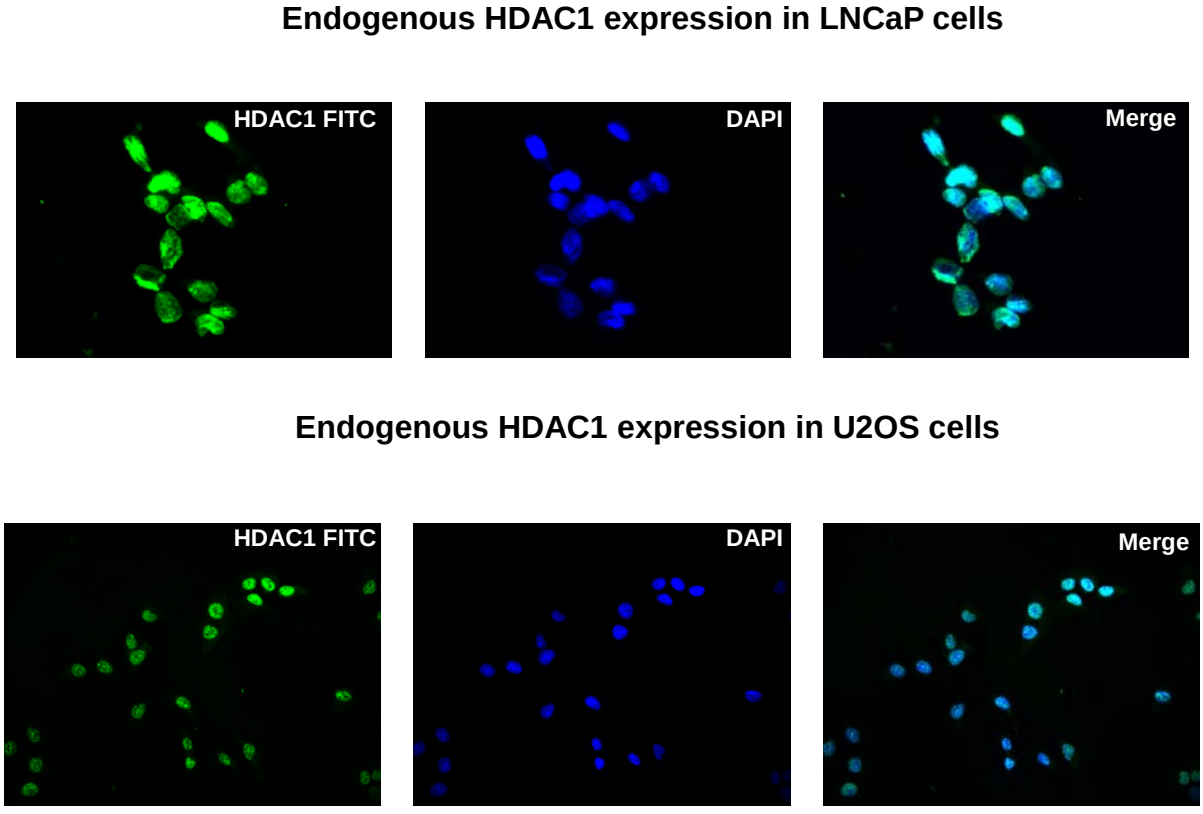

Figure 3.8 HDAC1 is predominantly nuclear in both LNCaP and U2OS cells.
LNCaP and U2OS cells were grown on chamber slides overnight in serum-containing media and then subjected to immunofluorescence analysis using a mouse HDAC1 antibody. DAPI was used for nuclear

DNA staining.

To confirm these findings, the distribution of a GFP-tagged SET9 protein was analysed in cells. The molecular cloning strategy for generating the GFP-SET9 construct is shown in Figure 3.9. The protein expression of GFP-SET9 was validated by transient transfection of the construct into U2OS cells followed by western blot using either SET9 or GFP antibody (Figure 3.10). In immunofluorescence experiments, when GFP-SET9 was transfected in U2OS

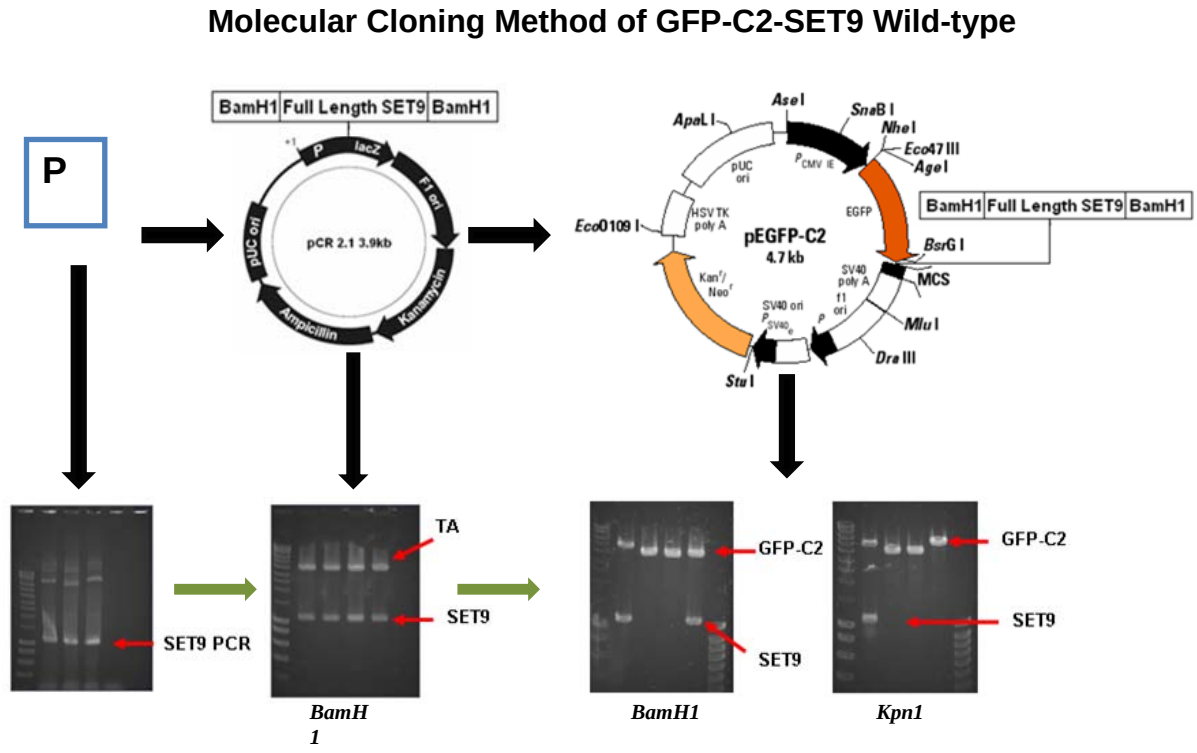

Figure 3.9 Molecular cloning strategy of GFP-C2-SET9.
Full length SET9 was amplified by PCR with two flanking BamH1 sites at 5' and 3' ends. PCR products were ligated into pCR2.1 (Invitrogen) and subcloned into GFP-C2 vector. Positive clones were selected by BamH1 and Kpn1 digestions. The sequence of the resultant clone was validated by sequencing.

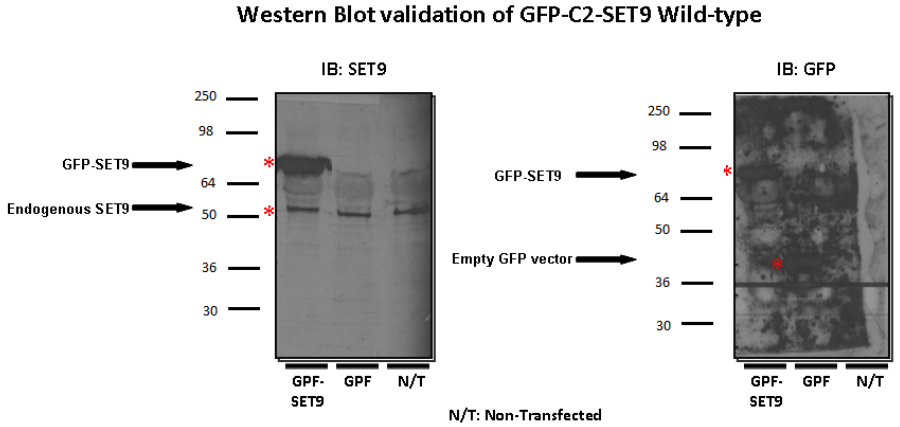

Figure 3.10 Ectopic expression of GFP-C2-SET9 in U2OS cells.
The cloned GFP-C2-SET9 was transiently transfected into U2OS cells alongside empty GFP-C2 vector. Western blotting was performed using either SET9 or GFP antibodies. SET9 antibody detected ectopically expressed SET9 (asterix) in U2OS cells as well as endogenous SET9 protein (lower band) whereas GFP

antibody detected both GFP-tagged SET9 and un-tagged GPF in cells (both denoted by asterix).

cells, as expected, SET9 showed significant distribution in the cytoplasm, but was also evident in the nuclear compartment (Figure 3.11) again confirming the results observed previously. In the parallel experiment, GFP-HDAC1 exhibited almost exclusive distribution in the nucleus, an observation which is well documented in the literature (Halkidou et al., 2004b) (Figure 3.11).

In addition, the impact of androgen on SET9 movement was tested within cells, as it has been shown that SET9 is translocated to the nucleus in response to TNFα in human vascular smooth muscle cells (HVSMC) (Li et al., 2008). Over a 2 hour R1881 treatment time-course, SET9 did not manifest a significant movement from cytoplasm to nucleus in LNCaP cells indicating that androgen may not drive the protein to go into the nucleus (Figure 3.12). Parallel experiments of AR movement in response to R1881 are found in reference (Ozanne et al., 2000). In LNCaP cells where GFP-SET9 was transfected under

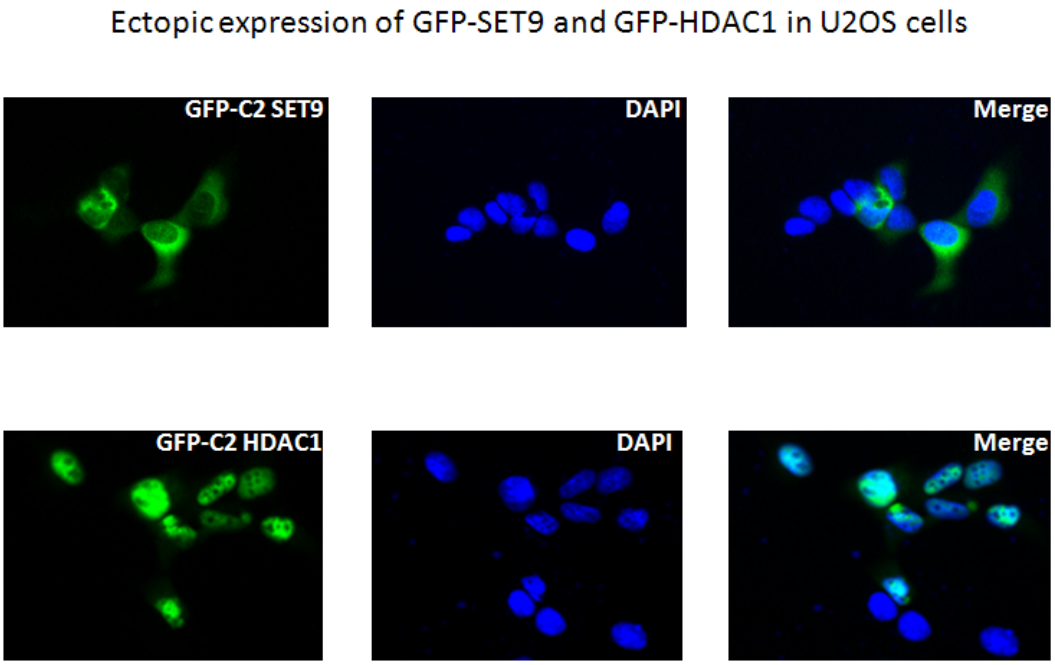

Figure 3.11 GFP-SET9 is mainly distributed in cytoplasm , but demonstrates nuclear expression in U2OS cells.
U2OS cells were seeded out in 6-well plates with cover slips and the following day cells were transfected with GFP-SET9, left for 48 hours and finally subject to immunofluorescence analysis. GFP-SET9 displayed predominant cytoplasmic expression and the control GFP-HDAC1 showed almost exclusive nuclear expression. DAPI was used for nuclear DNA staining.

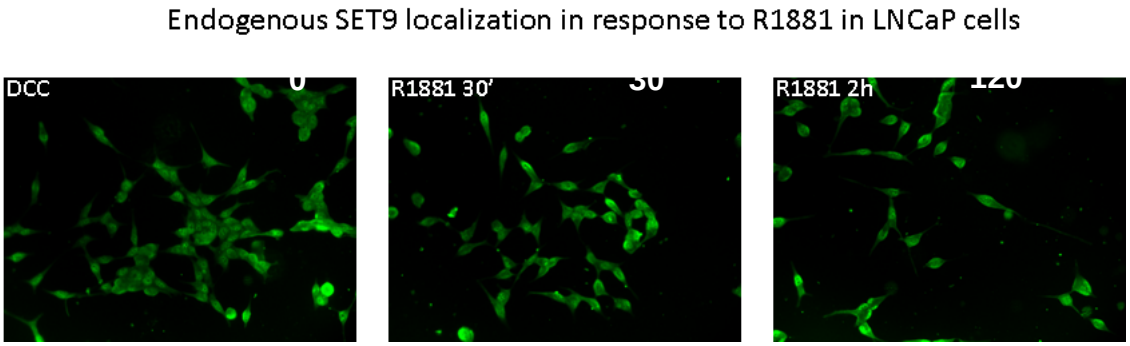

Figure 3.12 SET9 localization does not change in response to R1881 treatment in LNCaP cells.
LNCaP cells were grown in 6-well plates with cover slips and the next day cells were replaced with androgen depleted medium for 48 hours. On the day of experiment, 10 nM R881 was added and at 30 mins and 120 mins cells were washed, fixed and followed by immunofluorescence analysis. SET9 distribution was unaltered by R1881 treatment in LNCaP cells.

androgen depleted conditions, SET9 demonstrated predominant cytoplasmic distribution, although a small amount was evident in the nucleus (Figure 3.13). Switching the media to serum-containing conditions failed to impact on SET9 distribution in LNCaP cells while HDAC1 remained predominantly nuclear (Figure 3.14).

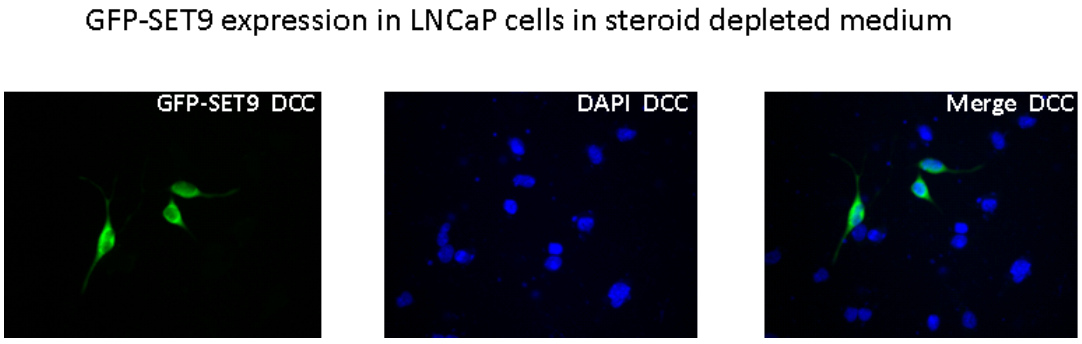

Figure 3.13 GFP-SET9 shows a major cytoplasmic distribution in LNCaP cells in androgen-depleted medium.
LNCaP cells were grown in 6-well plates containing cover slips and transfected with GFP-C2-SET9 in steroid-depleted media. Cells were incubated for 48 hours prior to immunofluorescence analysis. GFP-SET9 displayed a predominantly cytoplasmic expression in LNCaP cells with minor distribution in the nucleus under steroid depleted condition.

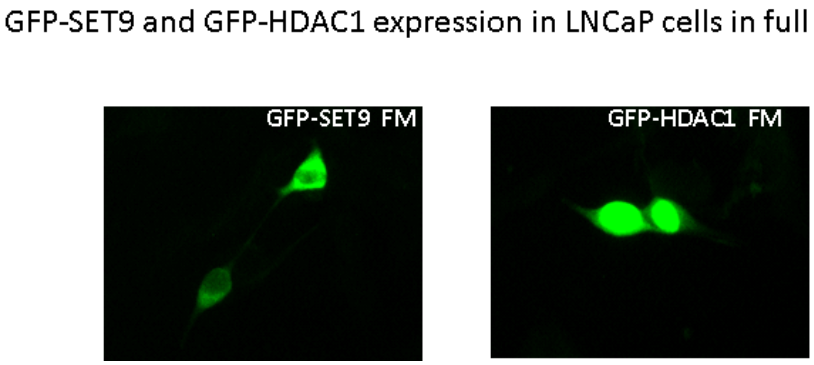

Figure 3.14 GFP-SET9 shows a major cytoplasmic distribution in LNCaP cells in steroid containing serum- medium.
LNCaP cells were grown in normal serum-containing media (androgens present) in 6-well plates containing cover slips and after 24-hours transfected with GFP-C2-SET9. Cells were incubated for 48

hours and then subject to immunofluorescence analysis. GFP-HDAC1 demonstrated exclusive nuclear distribution.

To further pursue analysis of SET9 cellular distribution, LNCaP, HeLa, PC3 and DU145 cells were subject to cytoplasmic and nuclear protein fractionation and SET9 distribution analysed by Western blotting using two different SET9 antibodies. Consistent with our immunofluorescence data, SET9 expression was limited to the cytoplasm in each of the cell lines tested, including HeLa cells (Figure 3.15). Interestingly, this data contradicts Nishioka et al., who initially identified SET9 from a HeLa cell nuclear extract. Notably, the nuclear protein PARP1 showed certain degree of cytoplasmic contamination in HeLa, PC3 and DU145 cell lines and this was probably due to the unexpected handling problem during the experimental procedure possibly at the stage of separating the nucleus and cytoplasm fractions.

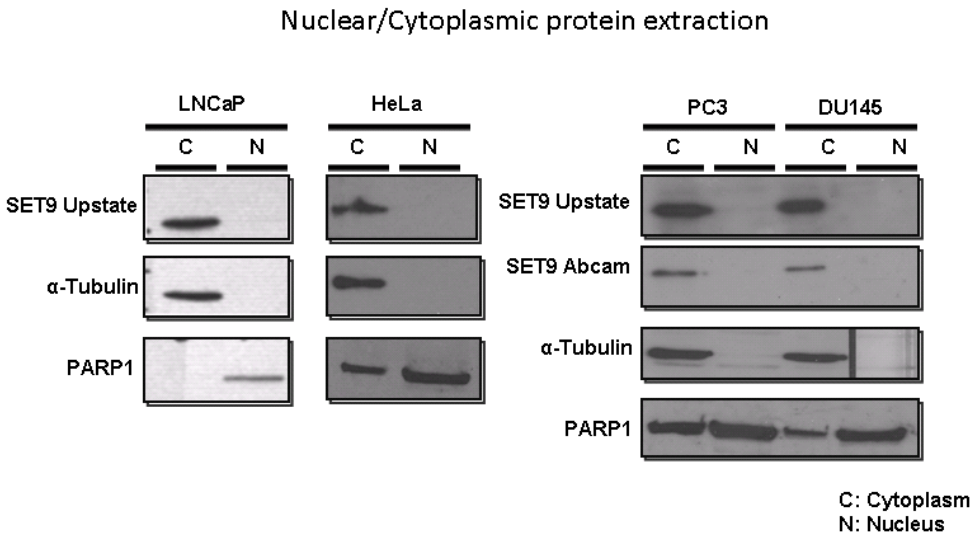

Figure 3.15 LNCaP, HeLa, PC3 and DU145 cells demonstrate cytoplasmic distribution of SET9 following nuclear/cytoplasmic fractionation.
All cells were grown in androgen containing serum media prior to cell fractionation using the NE-PER kit (Pierce). Western blots highlighted major expression of SET9 in the cytoplasmic compartment across all cell lines tested. α-tubulin and PARP1 were used as controls for cytoplasmic and nuclear compartments, respectively.

3.3.3 Assessment of the transcriptional regulation by SET9

i SET9 activity on AREIII reporter in response to androgen

SET9 is involved in transactivation of many genes either directly through the regulation of target proteins or indirectly via the regulation of histone methylation on H3-K4 (Kouskouti et al., 2004). Works from our laboratory have

demonstrated that SET9 is a co-activator for the AR in LNCaP cells (Gaughan et al., 2010), although the function of SET9 in AR regulation in other cell lines has not been tested. Thus, to provide a more thorough understanding of AR regulation by SET9 the effect of SET9 overexpression on AR activity was investigated in other cell lines especially regardingits activity on AREIII reporter in response to androgen.

As shown in Figure 3.16, ectopic expression of SET9 in LNCaP cells up-regulated endogenous AR-mediated transcription upon the androgen-responsive AREIII luciferase reporter in a methylase activity-dependent manner as the catalytically-inactive SET9 mutant ($SET9_{H297A}$) failed to enhance the reporter gene expression. These studies were subsequently extended into U2OS cells which have been used to assess the function of SET9 in regulation of p53-mediated transcription (Chuikov et al., 2004). Consistent with data from LNCaP cells, wild-type, but not the $SET9_{H297A}$ mutant, was able to enhance AR activity upon the AREIII reporter in U2OS cells grown in normal serum-containing media. (Figure 3.17).

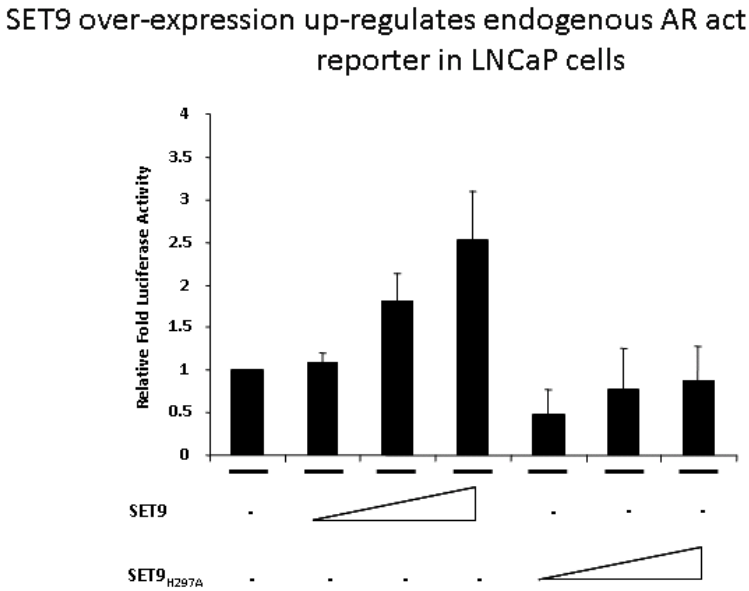

Figure 3.16 SET9 wild-type but not the catalytically-inactive $SET9_{H297A}$, mutant up-regulates AR-mediated AREIII driven gene transc ription in LNCaP cells.
LNCaP cells were transfected with AR, SET9 wild-type, SET9 mutant and the AREIII reporter in various combinations. Cells were grown for another 48 hours before subjecting to luciferase reporter assay. Data represents three independent repeats of quadruplicate samples +/- standard error.

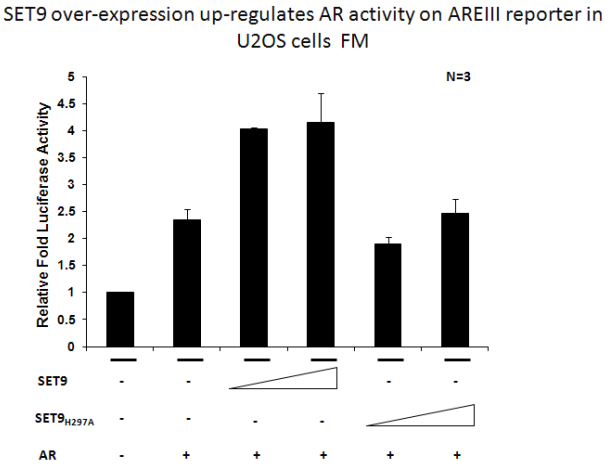

Figure 3.17 SET9 wild-type but not mutant up-regulates the AR mediated AREIII driven gene transcription in U2OS cells in serum-containing media.
U2OS cells were transfected with AR, SET9 wild-type, $SET9_{H297A}$ and the AREIII reporter in various combinations. Cells were grown for another 48 hours before subjecting to luciferase reporter assay. Data represents three independent repeats of quadruplicate samples +/- standard error.

ii The impact of SET9 knockdown on PSA production in LNCaP cells

Having established the dependency of AR on the HMT activity of SET9 for transcriptional co-activation in several cell line models, the role of SET9 in AR regulation in LNCaP cells was re-visited by examining the effect of SET9 knockdown on PSA production. As shown in Figure 3.18, siRNA mediated SET9 knockdown was optimized in LNCaP cells and the maximum knockdown was achieved 72 hours post-transfection with a concentration of 0.5µg/well on a 6-well plate format. Under this knockdown condition, mRNA expression and protein expression of the PSA gene were analysed, respectively. Upon SET9 knockdown, PSA was both down-regulated at RNA

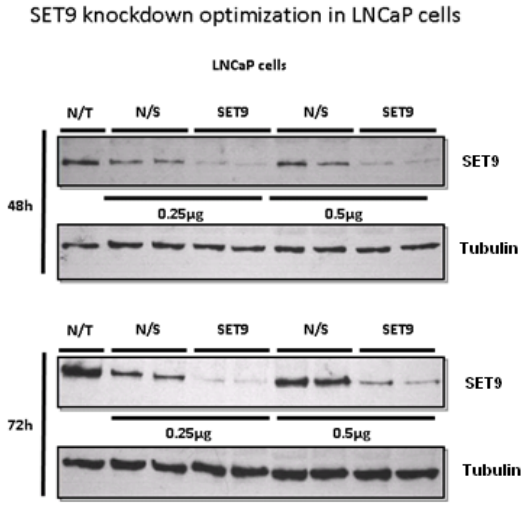

Figure 3.18 SET9 knockdown optimisation in LNCaP cells.

LNCaP cells were reverse transfected with either non-silencing (N/S) or SET9 siRNA at 0.25 µg/ml or 0.5 µg/ml for 48 or 72 hours respectively. After indicated times, transfected and non-transfected (NT) cells were lysed and subject to Western analysis using SET9 and α-tubulin antibodies. The 0.25 µg/ml for 72 hours was chosen for the following experiments.

and protein levels, which was in agreement with previous findings where SET9 up-regulated AR mediated transcription on the AREIII reporter in LNCaP cells (Figure 3.19).

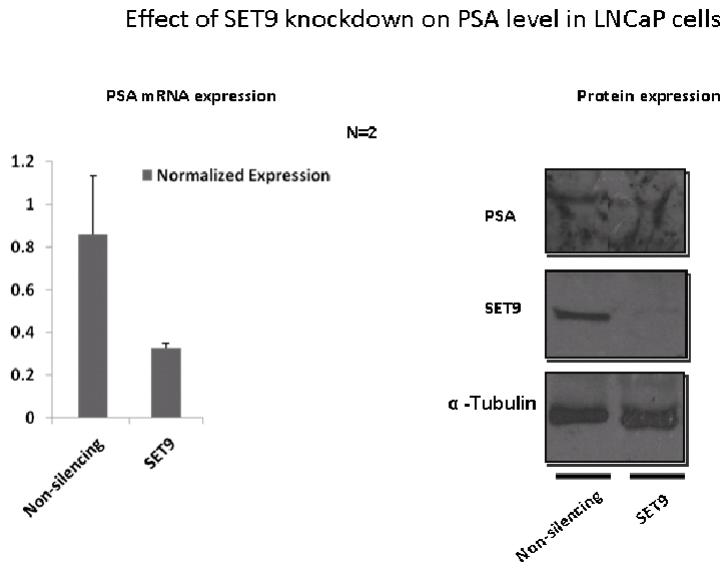

Figure 3.19 SET9 knockdown attenuates PSA gene expression in LNCaP cells.
LNCaP cells were transiently transfected with SET9 siRNA for 72 hours. Cells were lysed for western blot analysis or alternatively harvested for RNA extraction and reverse transcribed followed by real-time PCR analysis. Both mRNA quantification and western blot analysis show an evident decrease of PSA level upon SET9 knockdown compared to scrambled siRNA control.

3.3.4 Interplay between SET9 and other AR co-regulators

Regulation of AR transcriptional dynamics requires the interplay of various co-factors (Heinlein and Chang, 2002). Data from our laboratory has previously indicated that the histone deacetylase enzyme histone deacetylase 1 (HDAC1) plays a vital role in regulating AR activity. In fact, acetylation of AR is concomitantly associated with deacetylation executed by HDAC1. TIP60 and HDAC1 interact suggesting the formation of antagonistically functioning enzymes may be important for fine-tuning transcriptional rate (Gaughan et al., 2002). Whether HDAC1 is also required to remove acetyl-markers on the receptor to permit SET9-mediated methylation at the KLKK motif in AR is an interesting question, therefore, the interplay between SET9 and HDAC1 was investigated.

i SET9 and HDAC1 interact and co-localise in cells

By co-immunoprecipitation using a SET9 antibody, ectopically expressed SET9 and HDAC1 in U2OS cells grown in serum-containing media were found to interact (Figure 3.20, Left Panel). A reciprocal experiment using an anti-HDAC1 antibody for immunoprecipitation followed by immunoblotting with an anti-SET9 antibody confirmed the interaction between the two proteins although the interaction appeared very weak on the western blot (Figure 3.20, Right Panel).

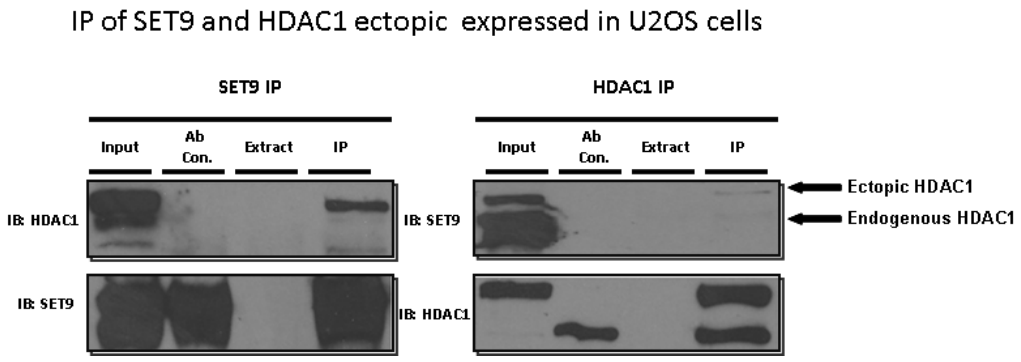

Figure 3.20 SET9 interacts with HDAC1 when over-expressed in U2OS cells.
U2OS cells were transfected with SET9 and HDAC1 and grown for 48 hours before immunoprecipitation using either SET9 or HDAC1 antibodies. Input represents 5% of total cell lysate; antibody control (Ab Con) represents IB antibody cross-reactivity with the IP antibody; Extract represents non-specific protein binding to protein G sepharose beads; IP is the immunoprecipitated sample.

To further investigate interplay between SET9 and HDAC1, immunofluorescence analysis was undertaken to examine potential co-localisation between these two proteins. In both LNCaP and U2OS cells, SET9 and HDAC1 were found to have largely disparate cellular distributions; SET9 was predominantly cytoplasmic in distribution, while HDAC1 was exclusively nuclear (Figure 3.21), consistent with our previous findings. The reason accounting for this could be that immunoprecipitation of the over-expressed proteins may have resulted in an artificial interaction due to the surplus of the proteins, which when studied using immunofluorescence under the endogenous status have minimal co-localisation.

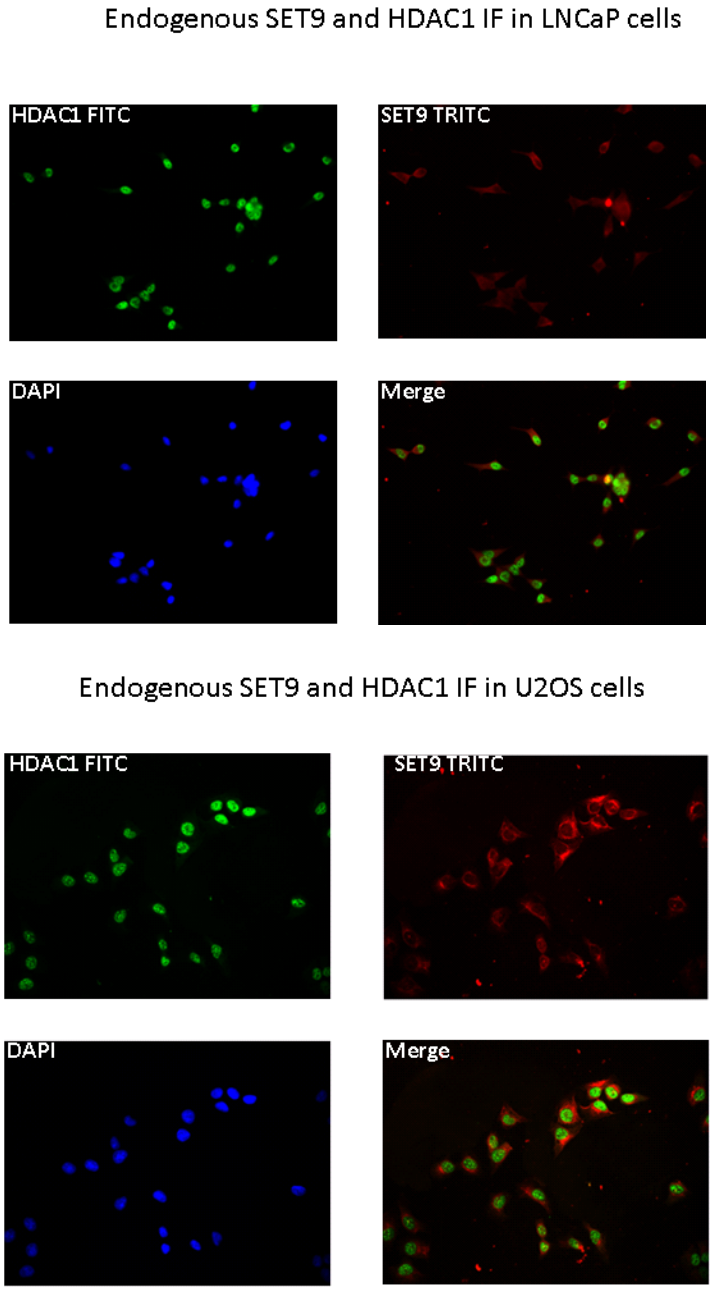

Figure 3.21 Endogenous SET9 and HDAC1 do not co-localise in LNCaP and U2OS cells.
LNCaP and U2OS cell were grown on chamber slides in normal serum-containing media for 48 hours prior to immunofluorescence using primary Anti-SET9 (rabbit) and –HDAC1 (mouse) antibodies followed by respective TRITC- and FITC-conjugated secondary antibodies. DAPI was used for DNA staining. Secondary antibody only was used as a negative control to monitor any potential non-specific staining in experiments. All secondary antibody controls showed absence of staining (data not shown).

Given that the immunoprecipitation data demonstrated an interaction between ectopically-expressed SET9 and HDAC1, it was pertinent to assess potential co-localisation of over-expressed SET9 and HDAC1 in U2OS cells. Over-expression of GFP-SET9 demonstrated both a cytoplasmic and nuclear distribution pattern, as shown previously (Figure 3.11) that overlapped with HDAC1 in the nucleus (yellow colour seen in merged image) indicating a potential interaction between these two proteins in this cell line (Figure 3.22).

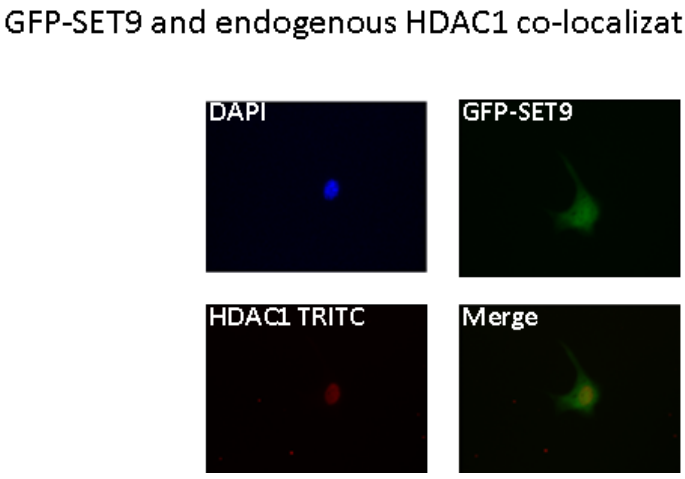

Figure 3.22 GFP-SET9 and endogenous HDAC1 show co-localization in U2OS cells.
U2OS cells growing on chamber slides were transfected with GFP-SET9 for 48 hours and then subject to immunofluorescence using an anti-HDAC1 antibody followed by addition of a TRITC secondary antibody. DAPI was used for DNA staining. Secondary antibody only was used as a negative control for experiments, where it showed no staining (data not shown).

ii SET9-mediated AR co-activation is attenuated by HDAC1

Given the interaction between SET9 and HDAC1 in both LNCaP and U2OS cells and also the fact that ectopic expression of SET9 manifested a tighter association with HDAC1 in U2OS cells, an extrapolation of this work was to address if the interaction between SET9 and HDAC1 would dictate a regulatory mechanism at the transcription level for the AR.

As shown in Figure 3.23, luciferase assays in U2OS cells transfected with the AREIII reporter, AR and increasing amounts of SET9 and/or HDAC1 showed an expected increase in AR activity upon SET9 overexpression. However, in the presence of HDAC1, AR activity was repressed, which is in-line with previous findings (Gaughan et al., 2002), and this repression was not reversed upon co-expression of increasing amounts of SET9 implying a strong antagonistic effect of HDAC1 on SET9 and AR mediated co-activation (Figure 3.23).

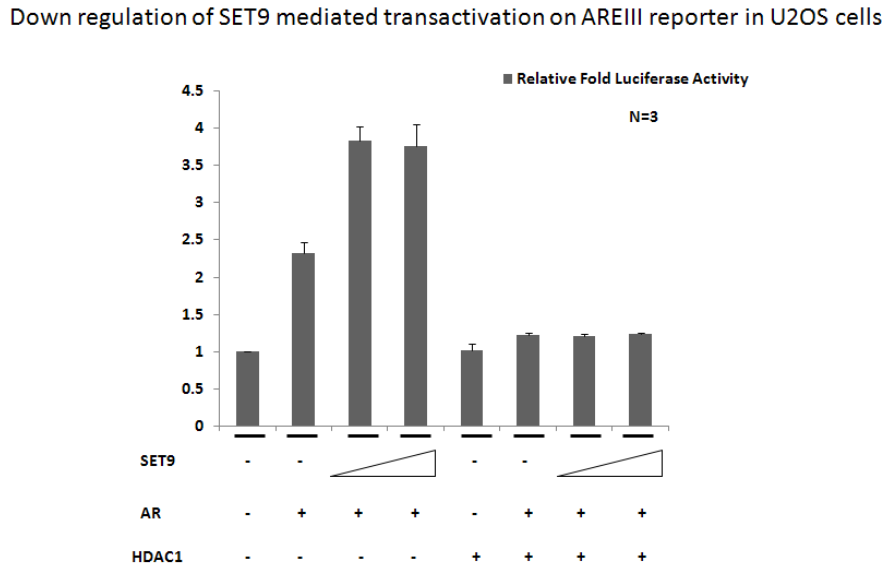

Figure 3.23 HDAC1 suppresses SET9 mediated co-activation of AR on ARE III.
U2OS cells were transfected with SET9, AR, HDAC1 and both AREIII and β-gal reporters in various combinations and left for 48 hours before luciferase reporter assay. Data represents three independent repeats of quadruplicate samples +/- standard error. All luciferase counts were normalized by β-gal assay and experiments were done in triplicates.

3.4 Discussion

The emergence of epigenetic machinery in cancer biology has led to an unforeseen discovery of numerous genes that are involved in chromatin regulation. In particular, the development and progression of prostate cancer have been linked to aberrant epigenetic regulation through different mechanisms (Nelson et al., 2009; Koeneman, 2006; Seligson et al., 2005). As a key pathway to determine the growth of prostate cancer, androgen receptor signaling is fundamentally subject to various epigenetic alterations such as phosphorylation, acetylation, ubiquitylation and methylation. More importantly, the alteration of androgen receptor signaling is inevitably accompanied by changes of elements in the surrounding environment rendering the signaling to be bypassed or adapted under particular circumstances and therein, the altered expression and activity of more than a hundred AR co-regulators constitute a substantial mechanism. Interestingly, in this context, a considerable number of AR co-regulators bear intrinsic chromatin modulating capability such as chromatin remodeling proteins BRG1 and BAF57, histone acetyltransferases SRC1, p300/CBP and PCAF and histone deacetylases HDAC1 and SIRT1 and histone methyltransferases PRMT1/5 and G9A and histone demethylases LSD1 and JMJD2C (Heemers and Tindall, 2007; Wissmann et al., 2007). In addition to that, certain histone modifications predict functional state of chromatin affecting downstream biological processes. As a well-researched histone N-terminal residue, Histone H3 lysine 4 methylation has been linked to ligand-induced androgen receptor mediated gene activation (Kim et al., 2003). SET9, as a histone methyltransferase exclusively targeting this residue, a key lysine on histone H3 that has been associated with transcription regulation, has, as yet, to be explored in prostate cancer.

Based upon previous findings on the role of SET9 in transcriptional regulation of several transcription factors, and work from our laboratory (Gaughan et al., 2010), the next line of study was to examine the regulatory processes that dictate SET9 activity within the AR signaling cascade. Experiments were designed to look at the basic properties of the protein in response to the synthetic androgen analogue R1881 and it was observed that SET9 expression

was not subject to androgenic induction suggesting that there might not be a direct feedback regulatory mechanism between SET9 and AR. However, it is not possible to fully exclude the likelihood of the regulation of SET9 by androgen as the concentration of the R1881 in use could potentially affect the gene expression in some circumstances. CBP, is one example of a well characterized AR co-activator, which showed increased expression under high concentration of DHT (10nM), but with a down-regulation of expression at lower concentrations of R1881 stimulation and this effect could also be subject to AR positivity in different cancer cell lines (Urbanucci et al., 2008; Comuzzi et al., 2004). In silico TRANSFAC based analysis might be another approach to predict putative AREs in the promoter and enhancer regions of SET9.

As ubiquitination is thought to be another key mechanism of transcriptional regulation, and also based on a previous demonstration that some AR cofactors are targeted by ubiquitination-mediated protein destruction such as HDAC1 and human PIRH2, SET9 protein half-life was measured in LNCaP cells which express functional AR and SET9 (Gaughan et al., 2005; Logan et al., 2004). Importantly, as AR mediated transactivation is induced upon androgen stimulation, the experiment was established to examine SET9 stability upon R1881 stimulation. Results showed that SET9 protein was in a steady-state during 6 hours of cycloheximide (CHX) and androgen treatment suggesting that the single SET9 population might not turn over rapidly as a result of proteosome-mediated protein degradation in the cellular environment.

The regulation of the HMT EZH2 represents notable cell cycle dependent mechanisms (Bracken et al., 2003). In addition, some histone residues are subject to periodic methylation by specific HMTs such as SET8 and Dot1. Methylation of H4K20 peaks during the S phase and starts to vanish from G2/M to G1 (Fang et al., 2002). Likewise, H3K79 methylation shows the lowest level in late S and G2 phases and starts to become hypermethylated from M and stays throughout G1 until S phase (Feng et al., 2002). Therefore a potential role for SET9 in cell cycle dependent methylation of histone H3 was investigated, SET9 protein abundance and the mono-methylation state of histone H3 K4 during cell cycle progression was analysed using the HeLa S3 cell line which is extensively used in cell cycle synchronization study and has been used in other

histone modification alteration analysis during cell cycle (Fang et al., 2002; Feng et al., 2002). The data showed that SET9 protein level did not change when cells progressed from G1/S to G2/M. However, as SET9 is a stable protein over a period of 6 hours shown by the protein stability assay, it may be difficult to detect subtle changes of SET9 protein during the cell cycle. Moreover, the fact that not all cells were synchronized during cell cycle progression may also be a disadvantage of this experiment. The corresponding methylation state analysis of histone H3-K4 was also performed by western analysis, but the anti-H3-K4me1 antibody did not provide a clear result as no visible bands were seen on the western blots (data not shown). One possibility is that samples collected for western blot analysis may not be suitable for downstream applications (large portion of cytoplasmic content) and require additional procedures such as nuclear extraction or acid extraction of histones to achieve refined samples for western blot analysis.

The cellular distribution of SET9 had not been previously investigated in detail, particularly in prostate cancer cell lines. Here immunofluorescence based assays were applied to gain an insight into the SET9 protein distribution in cells. Using either antibody based indirect immunofluorescence in LNCaP, DU145 and PC3 prostate cancer cell lines or a GFP-tagged SET9 vector in transient transfected U2OS and LNCaP cells, it was confirmed that although SET9 was expressed in both the cytoplasm and nucleus, it showed a dominant distribution in cytoplasm with a perinuclear pattern especially in LNCaP and U2OS cells. This is not surprising as it has been found before that SET9 is mainly expressed in cytoplasm of cells, although it was initially suggested as a nuclear functioning protein (Li et al., 2008). In two more advanced AR negative prostate cancer cell lines, PC3 and DU145, SET9 presented a more equal distribution between the cytoplasm and nucleus. Therefore it was important to address whether androgen could affect SET9 distribution via the AR pathway given the difference in SET9 distribution between androgen-dependent and –independent cell lines. In both the presence and absence of androgen in LNCaP cells, there was almost no difference in SET9 distribution, suggesting that activation of the AR signaling cascade fails to impact on SET9 movement. In parallel experiments, SET9 distribution in GFP-SET9-expressing LNCaP cells was analysed under androgen plus/minus conditions. As with the indirect immunofluorescence study,

there was no dramatic change in SET9 localisation in the presence and absence of androgen. One notable point was that according to the literature, Myc-tagged SET9 in U2OS cells showed more nuclear localization than cytoplasm, which conflicts with the findings in U2OS cells when GFP-SET9 was transfected (Masatsugu and Yamamoto, 2009). We argue that this might be due to the Myc antibody detecting non-specific proteins in the nucleus as opposed to direct protein-detection by GFP-SET9 that is performed herein. Interestingly, it was documented that SET9 has a particular recruitment pattern in response to certain external stimuli. TNF-α is able to drive SET9 recruitment into the nucleus to co-localize with p65 subunit of NF-kappa B in HVSMC cells within 2 hours (Li et al., 2008). Therefore, as a control for our experiments, it would be pertinent to apply TNF-α to cells expressing the GFP-SET9 protein to completely validate that the protein responds to stimuli in a similar fashion as the endogenous protein.

Data from the nuclear/cytoplasmic extractions showed that SET9 was exclusively expressed in the cytoplasmic compartment of almost all cell lines tested. Considering the SET9 antibody used for immunofluorescence was the same as that for the immunoblotting of SET9 in the cell extracts, it was interesting that no nuclear SET9 was detected by Western analysis compared to some expression in the nucleus by immunofluorescence. Moreover, given that SET9 was originally identified from a HeLa cell nuclear extract SET9 in this study was completely absent in the nucleus of HeLa cells, but instead demonstrated exclusive cytoplasmic distribution (Nishioka et al., 2002). It is intriguing to speculate that the antibody may not be sensitive enough to detect trace amounts of SET9 in the nucleus, which could be detected by the potentially more sensitive immunofluorescence technique. The other argument would be the specificity of the rabbit polyclonal SET9 antibody, however, as this specific antibody is extensively detailed in the literature and by comparing to other monoclonal SET9 antibodies that we also used for immunofluorescence and nuclear/cytoplasmic extraction purposes, we believed that this is more likely to be a variation between experimental strategies applied. Regardless of the differences observed, one statement ascertained was that although SET9 is a nuclear functioning protein, it is likely to play other extra-nuclear roles in cells and this would be an interesting avenue to explore in the future.

The finding that SET9 interacts with androgen receptor and is involved in up-regulating AR-mediated transcription in LNCaP cells indicated a co-activator role for SET9 (Gaughan et al., 2010). However, the function of SET9 within the AR signaling cascade had not been tested in other cell lines. Luciferase reporter assays performed in U2OS cells with transfected wild type SET9 and the functionally dead mutant $SET9_{H297A}$ in normal serum-containing media suggested that SET9 was able to co-activate AR mediated transcription in a methylation-dependent manner. This data is in agreement with the previous findings in LNCaP cells indicating that the enzymatic activity is required for SET9 to exert its function as a transcription co-activator (Gaughan et al., 2010). Using an alternative approach, the activity of the same AREIII luciferase reporter was assessed by inducible knocking down of SET9 in 293 cells.

As a final validation, PSA expression in LNCaP cells was measured upon SET9 knockdown. In line with the findings described above, depletion of SET9 attenuated PSA gene expression as demonstrated at both mRNA and protein level confirming the role of SET9 as an AR co-activator.

Androgen receptor co-factor interplay is another driving force of prostate cancer development from hormone sensitive to refractory state (Brooke et al., 2008; Heinlein and Chang, 2002). HDAC1 is an AR co-repressor that is co-existed in an AR containing trimeric complex with TIP60 and functions to reduce TIP60 mediated AR activity (Gaughan et al., 2002). Evidence also suggested that this regulatory mechanism might be via mdm2 mediated AR ubiquitylation and disruption (Gaughan et al., 2005). TIP60 has also been shown to be over-expressed in pre-malignant and malignant lesions of CaP, especially up-regulated in hormone refractory CaP (Halkidou et al., 2004b). Preliminary data suggested that SET9 interacts with the histone deacetylase HDAC1 (Gaughan and Robson, unpublished) and thus this was further explored. In the U2OS cell model when SET9 and HDAC1 were ectopically expressed, an interaction between these two proteins was observed. However, the ectopically expressed proteins showed much stronger association than the endogenous proteins which were observed on the same western blot (Figure 3.23). This might be due to abundant protein expression that alters the normal physiological distribution

of proteins, which causes an aberrant interaction between those two proteins, as we have demonstrated that HDAC1 and SET9 are by and large expressed in the nucleus and cytoplasm, respectively. This may also explain why endogenous SET9 and HDAC1 showed a low level interaction in cells as only small portions of those two proteins overlap together in the same cellular compartment. To further confirm this assumption, immunofluorescence was applied. As expected, in both LNCaP and U2OS cells, endogenous SET9 and HDAC1 were exclusively localized in different cellular compartments with respective cytoplasmic and nuclear distributions. In comparison, over-expression of SET9 in U2OS cells demonstrated weak to moderate staining in the nucleus where it overlapped with endogenous HDAC1, which was consistent with the immunoprecipitation data. Due to the physical interplay between SET9 and HDAC1, the impact of HDAC1 on SET9-induced AR co-activation was assessed. Intriguingly in the presence of overexpressed HDAC1, SET9-mediated co-activation of the receptor was attenuated suggesting that HDAC1 may counteract the co-activating role of SET9, in this preliminary experiment. Due to the time limitation, it was not possible to investigate this further. However, it would be particularly interesting to alternatively explore an inhibitory role for HDAC1 in SET9 mediated co-activation by including HDAC inhibitors (eg. Trichostatin A (TSA) or using siRNA specific for HDAC1 in experiments. Additionally, further immunoprecipitation and chromatin immunoprecipitation experiments could be included to certify the interaction between SET9 and HDAC1 in the nuclear compartment and to determine the recruitment partners at the androgen responsive promoters of target genes. This may help determine the mechanism whereby HDAC1 negatively regulates SET9 mediated co-activation of AR during transcription.

Chapter 4

Phenotypic importance of SET9 in LNCaP cells

4.1 Introduction

Several androgen receptor co-regulators not only play key roles in the molecular characterization of the cancer cells but also affect the biological properties determining the fate of cancer cells via various mechanisms. ARA70, a well characterised AR co-activator has been found to suppress LNCaP cell proliferation and colony formation suggesting that it may be a tissue differentiation factor or a potential tumor suppressor (Li et al., 2002). More importantly, it is believed that acetylation status of the AR is a strong determinant of prostate cellular growth and apoptosis (Fu et al., 2004). In DU145 metastatic prostate cancer cell line and prostate cancer mouse models, AR acetylation-mimic mutants K630Q and K630T, that mimic constitutive acetylation, showed elevated proliferation and colony forming efficiency compared to the wild type AR. Moreover, apoptosis of DU145 cells expressing the acetylation-mimic mutant AR proteins indicates the importance of acetylation of the receptor in driving androgen-dependent cellular phenotypes. The mechanism of this phenotypic effect is via the regulation of cell cycle control genes, cyclin D1 and cyclin E, and possibly the regulation of a subset of p21 regulated growth related genes (Fu et al., 2003). The histone arginine methyltransferase CARM1 which is an AR co-activator plays positive roles in inducing cell proliferation and prohibiting apoptosis in LNCaP cells (Majumder et al., 2006). On the other hand, JMJD2C a histone demethylase functions as an AR co-activator to induce LNCaP cell proliferation (Wissmann et al., 2007). All evidence described above suggests that AR co-regulators have a remarkable effect on regulating the cell phenotypes in the development/progression of prostate cancer.

Several reports have established a role of SET9 in the regulation of cell phenotypes. Chuikov and colleagues found that over-expression of SET9 leads to elevated apoptosis in U2OS cells and this effect was due to the positive regulation of p53 by SET9 in response to DNA damage (Chuikov et al., 2004). In a follow-up study, the same authors showed that the regulation of p53 activity by SET9-mediated methylation also induced G2/M arrest via the p53 activation pathway suggesting that SET9 has potent roles in cell proliferation and apoptosis via the regulation of the key tumour suppressor, p53 (Ivanov et al.,

2007). Further study also suggested that SET9 mediated methylation of pRb is a key post-translational modification which regulates the interaction of pRb with heterochromatin protein HP1 and is required for pRb dependent cell cycle arrest and transcriptional repression (Munro et al., 2010). In addition, SET9 has been found to be responsible for the maintenance of monocyte HVSMC-THP-1 and HUVEC-THP-1 adhesion both in the presence of absence of TNF-α treatment, suggesting involvement of SET9 in other biological processes in cells (Li et al., 2008). Although those lines of evidence support the notion that SET9 activity is associated with cell phenotype determination, there remains a lack of such evidence in prostate cancer phenotypes.

Preliminary evidence indicated that knockdown of SET9 decreased LNCaP cell proliferation suggesting a novel role for SET9 in controlling the cell fate of prostate cancer phenotypes. Following from this finding and also due to the transcriptional co-regulation by SET9 of the AR in LNCaP cells, the aim of the current study was to explore the role of SET9 in regulating the phenotype of the androgen-dependent LNCaP cell-line.

4.2 Specific materials and methods

The composition and suppliers of the majority of the reagents and materials can be found in the general materials and methods. Otherwise, the materials and reagents are specified in individual chapters where appropriate.

4.2.1 Caspase-3 assay with dual knockdown of SET9 and p53 in LNCaP cells

To assess the effect of p53 knockdown on SET9 knockdown-induced apoptosis, co-transfection of p53 and SET9 oligonucleotides in LNCaP cells was performed. A final concentration of 20nM of p53 siRNA and 25nM of SET9 was used. The concentration of the scrambled siRNA was standardized to 45nM. All subsequent experimental procedures are described in Chapter 2.6.3. For the purpose of all FACS based caspase-3 assays, 12-well plates were routinely used.

4.2.2 Caspase-3 assay with SET9 overexpression in U2OS cells

To examine the effect of SET9 on U2OS cell apoptosis, cells were seeded out at a density of $2x10^5$ cells/well of 12-well plates. The following day, cells were forward transfected with 0.5µg of wild-type and mutant $SET9_{H297A}$ per well, respectively. 48 hours post-transfection, cells were treated with 0.5µM Doxorubicin for 24 hours and then subjected to FACS caspase-3 apoptosis analysis.

4.2.3 Analysis of p21, Mdm2 and Bax expression upon Doxorubicin treatment

Both mRNA and protein analysis were based around a 6-well plate format with the plating cell number around $8x10^4$ cell/well. SET9 knockdown was performed using the before-mentioned protocol (Chapter 4.2.2) at a final concentration of 25nM. After 72 hours of transfection, cells were treated with 200nM Doxorubicin and collected in Trizol-RNA lysis buffer (Invitrogen) at 0, 3, 4, 6, 12 and 24 hour time points for real-time PCR analysis or in SDS sample buffer at 0, 1, 2, 3, 4, 6

and 22 hour time points for western blot analysis. Primer sequences for individual gene detections are stated in general materials and methods (Chapter 2.3.2). The range of time points was chosen according to similar experiments performed on SET9 which were documented in the literature (Kurash et al., 2008; Ivanov et al., 2007).

4.2.4 Statistical analysis

All FACS based experiments were analyzed using two-sample paired t-test and a p-value cut-off of 0.05 was used to evaluate the significance of data compared.

4.3 Results

4.3.1 Influence of SET9 on proliferation and cell cycle

The preliminary observation that SET9 knockdown reduced LNCaP cell proliferation (Gaughan et al., 2010) prompted a more detailed examination of the effect of SET9 on cell-cycle regulation of the LNCaP cell line.

i LNCaP PI cell cycle analysis

In an effort to address whether LNCaP cell cycle is regulated by SET9, a series of fluorescence activated cell sorting (FACS) based approaches were used, including application of propidium iodide (PI) and bromodeoxyuridine (BrdU) staining to address cell proliferation in more detail. PI is an intercalating agent and a fluorescent molecule that can bind to DNA. Due to its emission range between 562-588nm, it can used to evaluate DNA content and cell viability in flow cytometry based cell cycle analysis. BrdU is a synthetic nucleoside which is analogous to thymidine and thus it can be incorporated into the newly synthesised DNA as a substitution for thymidine during DNA replication. In conjunction with antibodies specific for BrdU, the cell proliferation can be measured. Using PI for DNA staining in combination with FACS analysis, the profile of the LNCaP cell cycle was analysed under optimized SET9 knockdown conditions. Interestingly, upon SET9 knockdown there was a 20% decrease in S phase (Figure 4.1.A (p-value=0.0049)) and reciprocal increase of the G1/G0 population in LNCaP cells (Figure 4.1.B), which was indicative of cell cycle inhibition at the G1/S transition and subsequent suppression of proliferation of the cells.

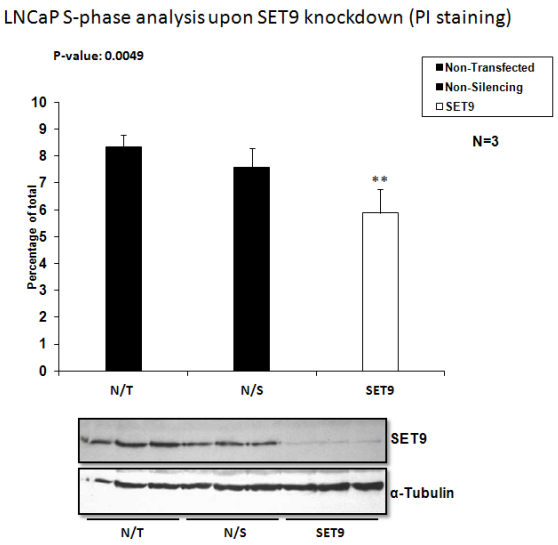

A

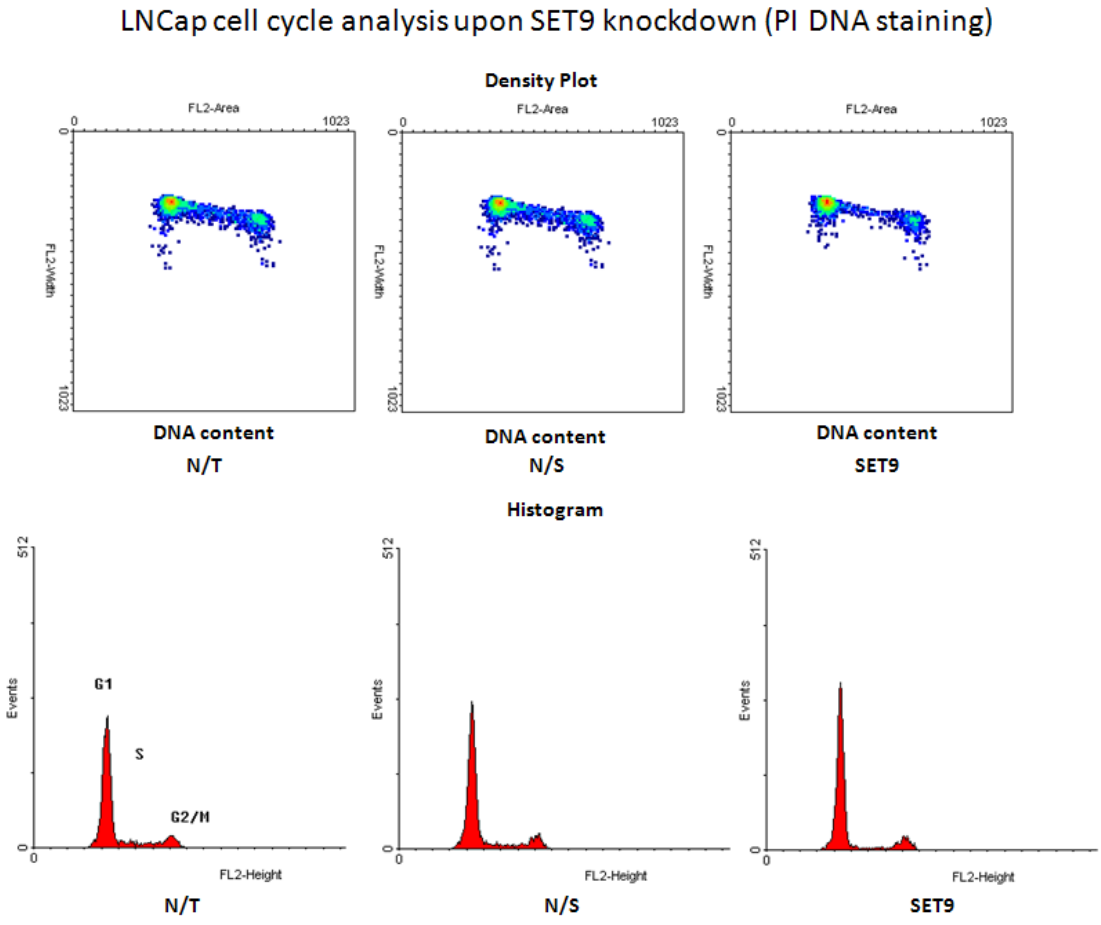

B

Figure 4.1 SET9 knockdown inhibits LNCaP cell proliferation via G1/S arrest.
(A/B) LNCaP cell cycle analysis was carried out using FACS based PI DNA staining. LNCaP cells were reverse transfected with siRNA targeting SET9 and scrambled control. Cells were left for 72 hours and then subject to FACS analysis. Upon SET9 knockdown there was a 20% decrease of S phase cells due to the partial cell cycle arrest in G1 as indicated by the dot plots and histogram. Knockdown was verified by corresponding western blot using SET9 antibody. Experiments were performed in triplicates with p-value < 0.05 indicating significance.

ii LNCaP BrdU proliferation assay

As knockdown of SET9 caused a retarded G1/S progression, the next step was to further address the S-phase reduction in response to SET9 knockdown in LNCaP cells. BrdU proliferation based FACS analysis was applied. Consistent with the previous findings, BrdU showed a 20% decrease in incorporation into the S phase in SET9-depleted cells compared to the non-silencing control cells indicating that SET9 is responsible for proliferation of LNCaP cells possibly by regulating the cellular G1/S transition (p-value=0.0076) (Figure 4.2).

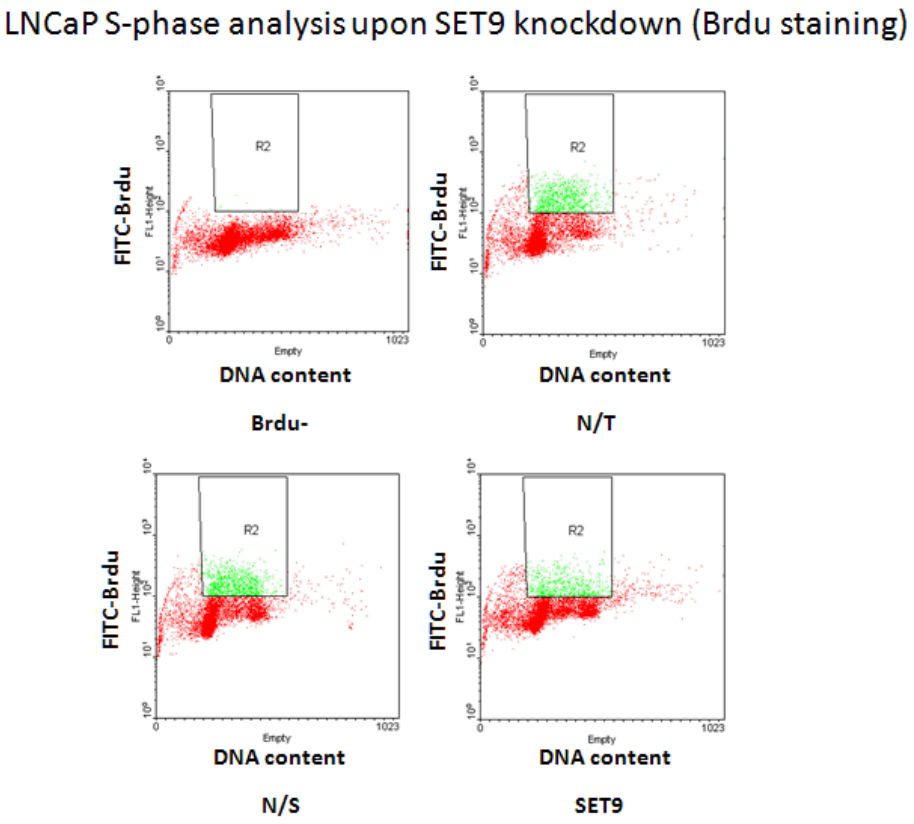

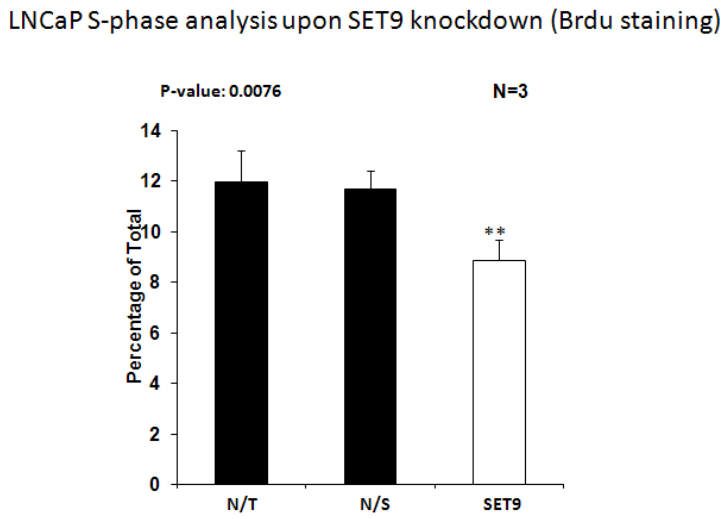

Figure 4.2 BrdU proliferation assays in LNCaP cells demonstrate SET9 is pro-proliferative.
LNCaP cells were reverse transfected with either non-silencing (N/S) or SET9 siRNA for 72 hours followed by a FACS based BrdU proliferation assay incorporating transfected and non-transfected (N/T) cells. The green dots in the dot plots represent the Brdu incorporation into the S phase cells. The bar chart represents calculated decrease in S-phase cells as a percentage of total cell number and is the average of three independent experiments performed in triplicate +/- standard error (** p-value<0.05).

4.3.2 Influence of SET9 on LNCaP cell apoptosis

i Annexin V apoptosis assay

Having established a possible mechanism of SET9 mediated LNCaP cell cycle regulation, the identification of other phenotypic influences governed by SET9 were investigated. Since SET9 has been linked to regulating cell death via p53-mediated activity, the effect of SET9 knockdown on apoptosis of the p53 wild-type cell line LNCaP was examined by an Annexin V based FACS analysis. This assay takes advantage of the fact that phosphatidylserine (PS) is translocated from the inner (cytoplasmic) leaflet of the plasma membrane to the outer (cell surface) leaflet soon after the induction of apoptosis. Annexin V protein has a strong, specific affinity for PS (4–6). PS on the outer leaflet is available to bind labeled Annexin V, providing the basis for a simple staining assay. By combining with PI DNA staining, the profile of early apoptosis (Annexin V+/PI-) is feasible and is distinguishable from late apoptosis/necrotic cells (Annexin V+/PI+). After cells were gated with PI only staining, the addition of Annexin V revealed the basal level of staining in non-transfected cells and introduction of scrambled siRNA as expected had negligible effect on apoptosis

and cell death. This level of apoptosis was acceptable and in line with previous work conducted with LNCaP cells (Thirugnanam et al., 2008). Interestingly, SET9 knockdown in LNCaP cells exhibited a shift from Annexin V negative (bottom left) to Annexin V positive (bottom right) which indicated a higher positivity of apoptotic staining compared to the non-silencing control implicating a potential involvement of SET9 in apoptosis regulation. Regardless of this, the total number of cells undergoing apoptosis was not abundant, SET9 knockdown induced 1.8 fold apoptosis over the non-silencing siRNA control (p-value=0.00047) (Figure 4.3). This data conflicts with the previous finding in U2OS cells where the over-expression of SET9 triggers apoptosis only in the presence of a DNA damaging agent Doxorubicin. This finding may constitute an alternative mechanism or an opposing regulatory role of SET9 in the context of LNCaP cells.

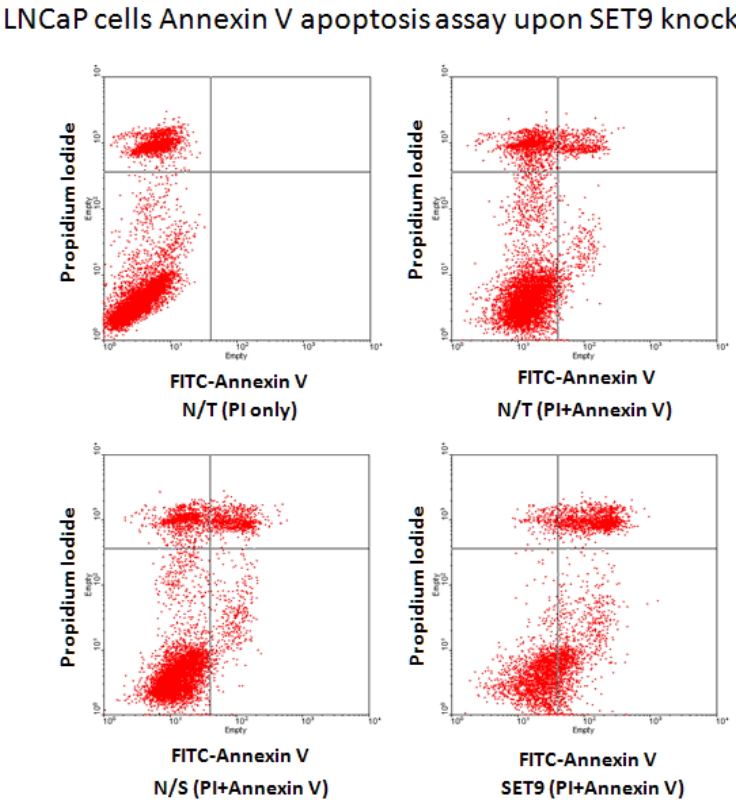

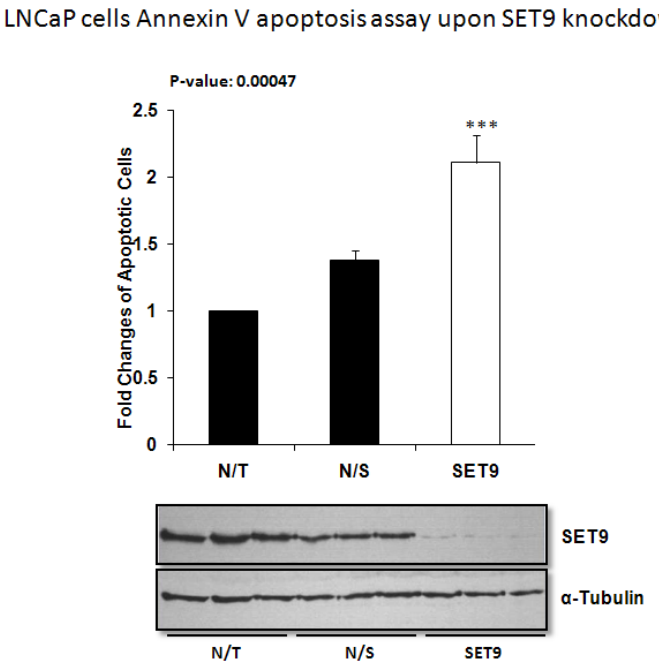

Figure 4.3 SET9 knockdown induces a small, but significant increase in LNCaP cell apoptosis using an Annexin V assay.
LNCaP cells were reverse transfected with SET9 and non-silencing (N/S) siRNA and left for 72 hours before Annexin V apoptosis assay of both transfected and non-transfected (NT) cells. In the dot plot where SET9 is depleted, there was a shift of cell population from Annexin negative to positive quadrant suggesting an increase in apoptosis in response to SET9 knockdown. The bar chart represents the fold increase of apoptotic cells upon SET9 knockdown compared to scrambled control and western blot shows the corresponding SET9 knockdown levels. Experiments were performed in triplicates and repeated three times +/- standard error (***p-value<0.05).

ii Caspase-3 apoptosis assay

In order to confirm the involvement of SET9 in LNCaP cell apoptosis, active caspase-3 assays were performed. This assay takes advantage of the caspase-3 as a convergent mediator in different signaling pathways especially in apoptosis. As a member of caspase family, it is an implicated “effector” caspase associated with the “death cascade” and thus is an important marker of the cell’s entry point into the apoptotic signaling pathway. In is also noted that in contrast to the Annexin V assay, which is mainly designed for detection of early and late apoptotic events, caspase-3 assay captures extrinsic and intrinsic apoptosis pathways. As expected, in keeping with the Annexin-V assay, cells depleted of SET9 demonstrated more positive caspase-3 staining compared with the non-silencing control cells, which again illustrates its function as a negative regulator of LNCaP cell apoptosis (Figure 4.4). It was also noted that when comparing the fold-change between the caspase-3 and Annexin V assays,

that the Annexin V assay represented more apoptotic cells (1.8 fold) than that detected by caspase-3 assay (1.3 fold, p-value=0.026). This was possibly due to the detection of both early and late apoptotic events by Annexin V, whereas the detection of caspase-3 relies upon the activation of effector caspase-3 which requires the upstream caspase activator activation via either intrinsic or extrinsic pathways.

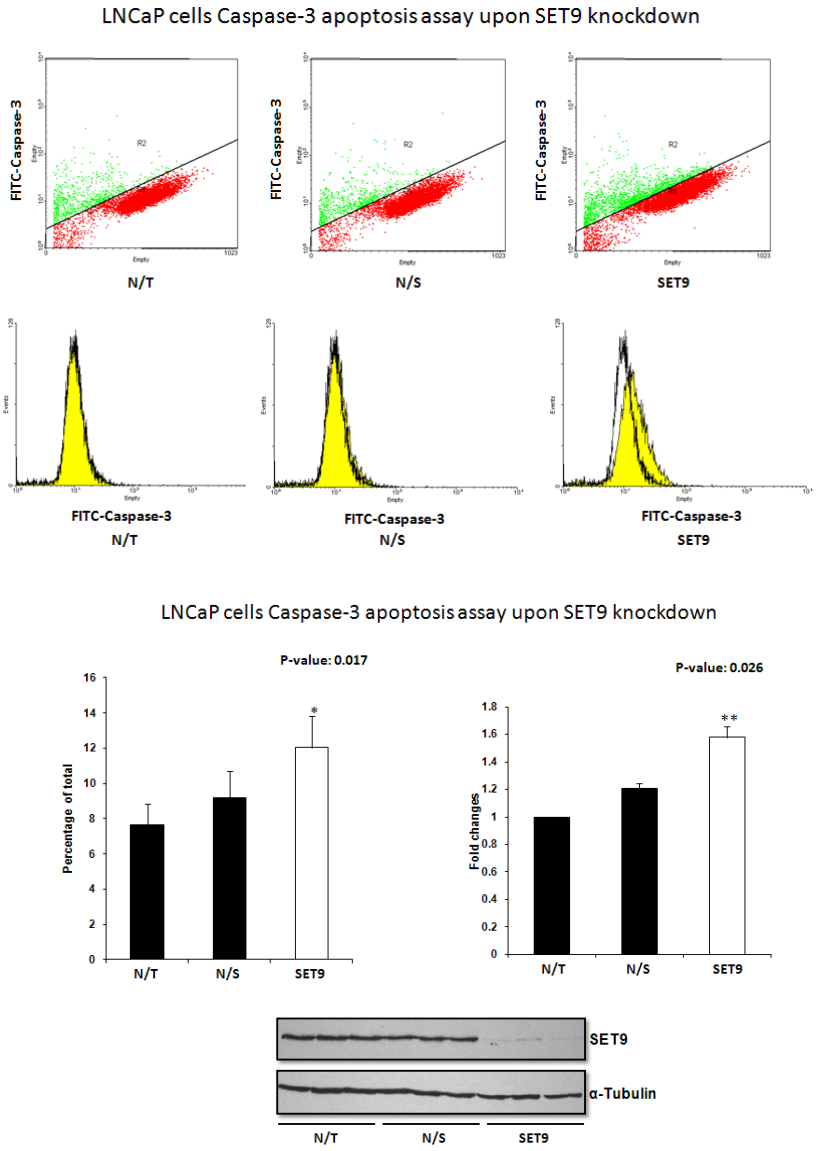

Figure 4.4 SET9 knockdown induces LNCaP cell apoptosis using caspase-3 apoptosis assay. LNCaP cells were reverse transfected with SET9 and non-silencing (N/S) siRNA and left for 72 hours before caspase-3 apoptosis assay in both transfected and non-transfected (NT) cells. The dot plots and histograms show the increased apoptosis upon SET9 knockdown as indicated by the shift from caspase-3 negative to positive. The bar charts represent the percentage of total and fold increase of apoptotic cells upon SET9 knockdown respectively compared to scrambled control. Corresponding western blots are displayed for SET9 and α-tubulin. Experiments were performed three times in triplicate +/- standard error.

4.3.3 Synergistic effect between SET9 knockdown and chemotherapeutic intervention

Evidence from U2OS cells suggested that p53-induced apoptosis is dependent upon the stabilization of p53 after DNA damage via SET9-mediated methylation and thus SET9 is required to facilitate programmed cell death in response to DNA damaging agents such as Doxorubicin, which generates double-stranded DNA breaks (Chuikov et al., 2004). A combination of SET9 knockdown and 200 nM Doxorubicin treatment in LNCaP cells, was utilized to see if this would facilitate the apoptosis events observed by SET9 knockdown alone. As expected, the percentage of total apoptotic cells was dramatically increased to 40% when 200 nM concentration of Doxorubicin was applied for 24 hours (Figure 4.5) which is an approximate 4-fold increase in apoptosis over non-treated cells (Figure 4.4). Interestingly, combining Doxorubicin treatment with SET9 knockdown further enhanced the rate of apoptosis by 20% suggesting a synergistic effect between depletion of the methyltransferase and chemotherapeutic intervention (p-value=0.013) (Figure 4.5). Poly (ADP-ribose) polymerase 1 (PARP1) is a direct downstream target of caspase-3 during activation of apoptosis and it is cleaved to two fragment by caspase-3. The 24 kDa N-terminal peptide retains the DNA binding domains of PARP1 and a C-terminal 89 kDa fragment has reduced catalytic activity and its detection is usually taken as a sensitive assay for apoptosis. As a confirmation of caspase-3 activity, western blot using PARP1 antibody showed increased cleavage (89 KDa larger fragment) with SET9 siRNA knockdown compared to the non-silencing siRNA control (Figure 4.5). Moreover, the fold change in the presence of Doxorubicin also showed a further increase compared to the siRNA treatment alone (Figure 4.5).

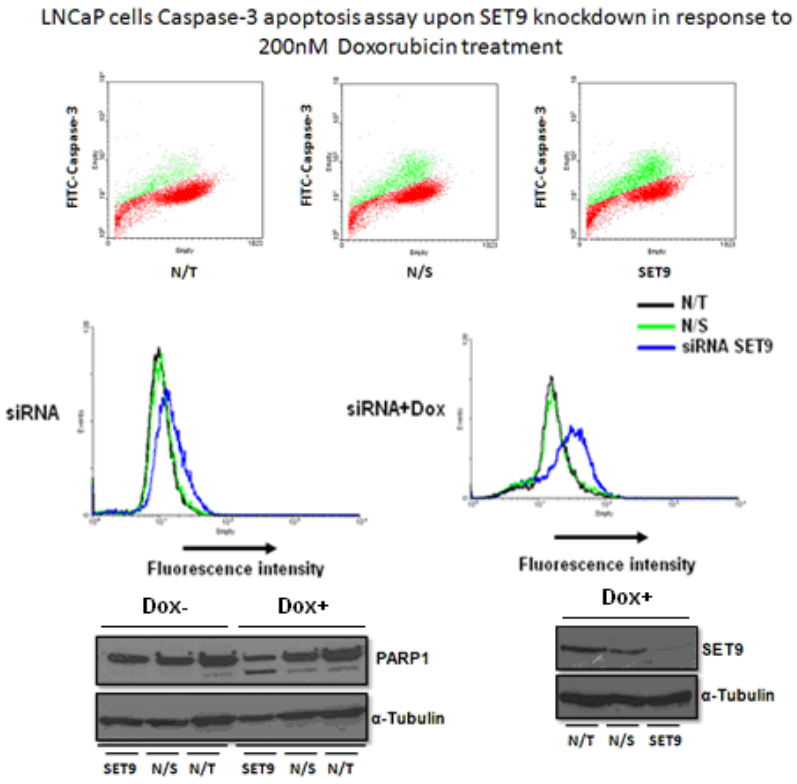

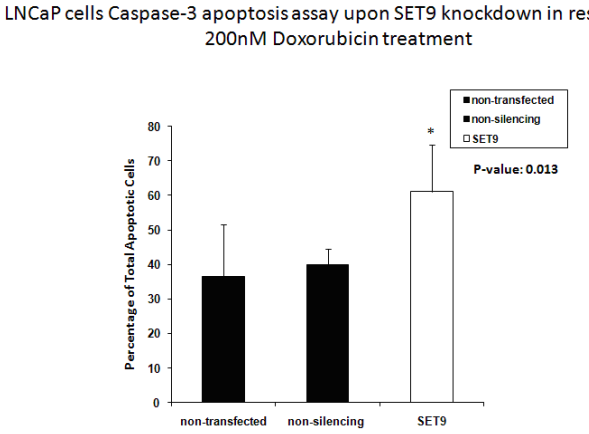

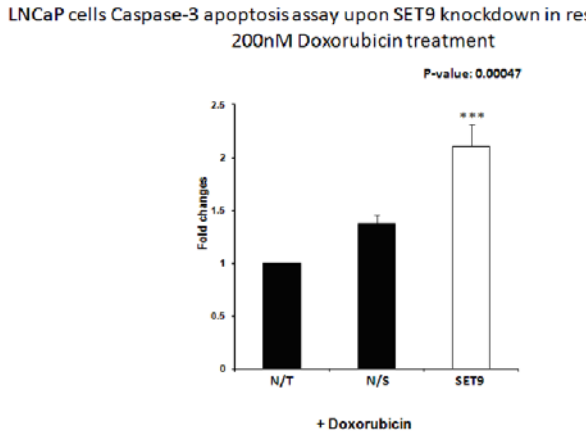

Figure 4.5 Effect of combining SET9 knockdown and Doxorubicin treatment on LNCaP cell apoptosis.

LNCaP cells were reverse transfected with SET9 and non-silencing (N/S) siRNA and left for 72 hours before Doxorubicin treatment for 24 hours prior to caspase-3 apoptosis assay using both transfected and non-transfected (NT) cells. Dot plots and histograms represent the increase of caspase-3 positivity. The

bar charts demonstrate approximately 60% apoptotic cells when SET9 knockdown is combined with Doxorubicin. The fold increase in apoptosis is also shown. The PARP1 western blot supports the caspase-3 assay data and SET9 knockdown was verified by western blot. Experiments were performed in triplicates with p-value<0.05.

4.3.4 Determining the mechanisms of SET9-mediated anti-apoptotic effect in LNCaP cells

The data suggest that SET9 is a negative regulator of apoptosis in LNCaP cells, however in U2OS cells SET9 appears to play a pro-apoptotic role as over-expression of SET9 synergizes with Doxorubicin to induce apoptosis and this mechanism is p53 dependent (Chuikov et al., 2004). In an attempt to firstly confirm these findings, the effect of SET9 over-expression on U2OS cell apoptosis in response to Doxorubicin was examined to address if the pro-apoptotic role of SET9 is reproducible in this cell line. Transient expression of wild-type SET9 enhanced apoptosis over basal, non-transfected levels by approximately 3-fold, whereas the methylation dead $SET9_{H297A}$ mutant had less pronounced effect on apoptosis (Figure 4.6). This data is consistent with published work and demonstrates that in U2OS cells, p53 plays a pro-apoptotic role (Chuikov et al., 2004).

Since the effect of SET9 knockdown on LNCaP cell apoptosis was more pronounced in the presence of Doxorubicin, a compound that has been shown to enhance p53-mediated apoptosis, it was hypothesized that this effect might be through a p53-dependent mechanism. Therefore, to address this, the first experiment in LNCaP cells was to assess a potential interaction between SET9 and p53. As hypothesised, using immunoprecipitation, it was demonstrated that SET9 interacts with p53 suggesting a potential interplay between SET9 and p53 in LNCaP cells (Figure 4.7).

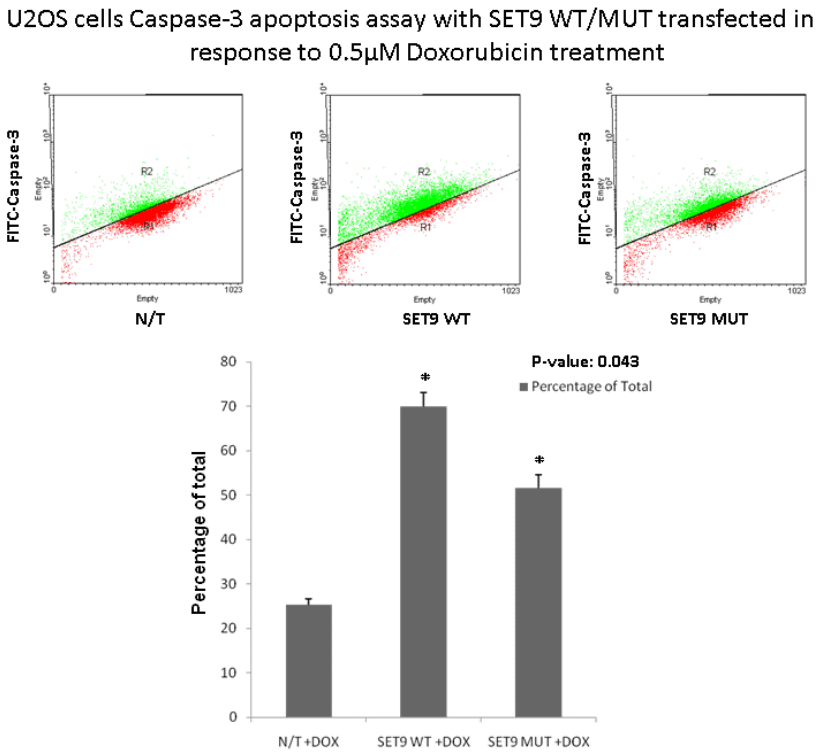

Figure 4.6 Wild type SET9 but not mutant SET9 induces apoptosis in U2OS cells.
U2OS cells were grown in complete medium and transiently transfected with wild-type SET9 and the catalytically-inactive $SET9_{H297A}$ mutant for 48 hours. Cells were then treated with 0.5 µM Doxorubicin for 24 hours and subjected to caspase-3 apoptosis assay. Dot plots represent the increase of apoptosis when wild-type SET9 is expressed. The mutant SET9 also affected apoptosis to a small degree but much less than the wild-type SET9,.The bar chart shows the change in apoptosis mediated by wild type and mutant SET9. The empty vector plasmid was included as a control in these experiments. All experiments were performedin triplicates with p-value<0.05.

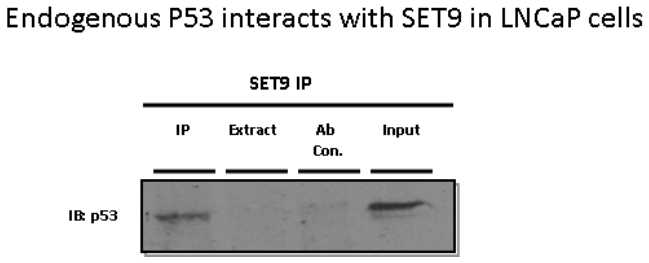

Figure 4.7 SET9 interacts with p53 in LNCaP cells.
LNCaP cells were used for immunoprecipitation using SET9 antibody. Subsequent Western blot using p53 antibody demonstrated the interaction between SET9 and p53 in LNCaP cells.

In U2OS cells, SET9-mediated methylation of p53 stabilizes the protein which consequently up-regulates p53 responsive gene expression, including p21, MDM2 and BAX (Chuikov et al., 2004). Therefore, the expression of these genes in response to SET9 knockdown incorporating a time course of Doxorubicin treatment was examined. As hypothesized, treatment with Doxorubicin in conjunction with silencing SET9 in LNCaP cells caused an earlier up-regulation (from 0-6 hours) of p21 and MDM2, when compared to the

non-silencing control siRNA, However, this effect did occur to BAX dramatically, suggesting that in contrast to the mechanisms in U2OS cells, knockdown of SET9 might selectively cause disruption and delay of p53 mediated transcription (Figure 4.8). The corresponding p21 protein synthesis in response to Doxorubicin treatment was also measured, however the protein levels did not change as dramatically as the mRNA levels when comparing the SET9 knockdown and non-silencing siRNA treated samples (Figure 4.9).

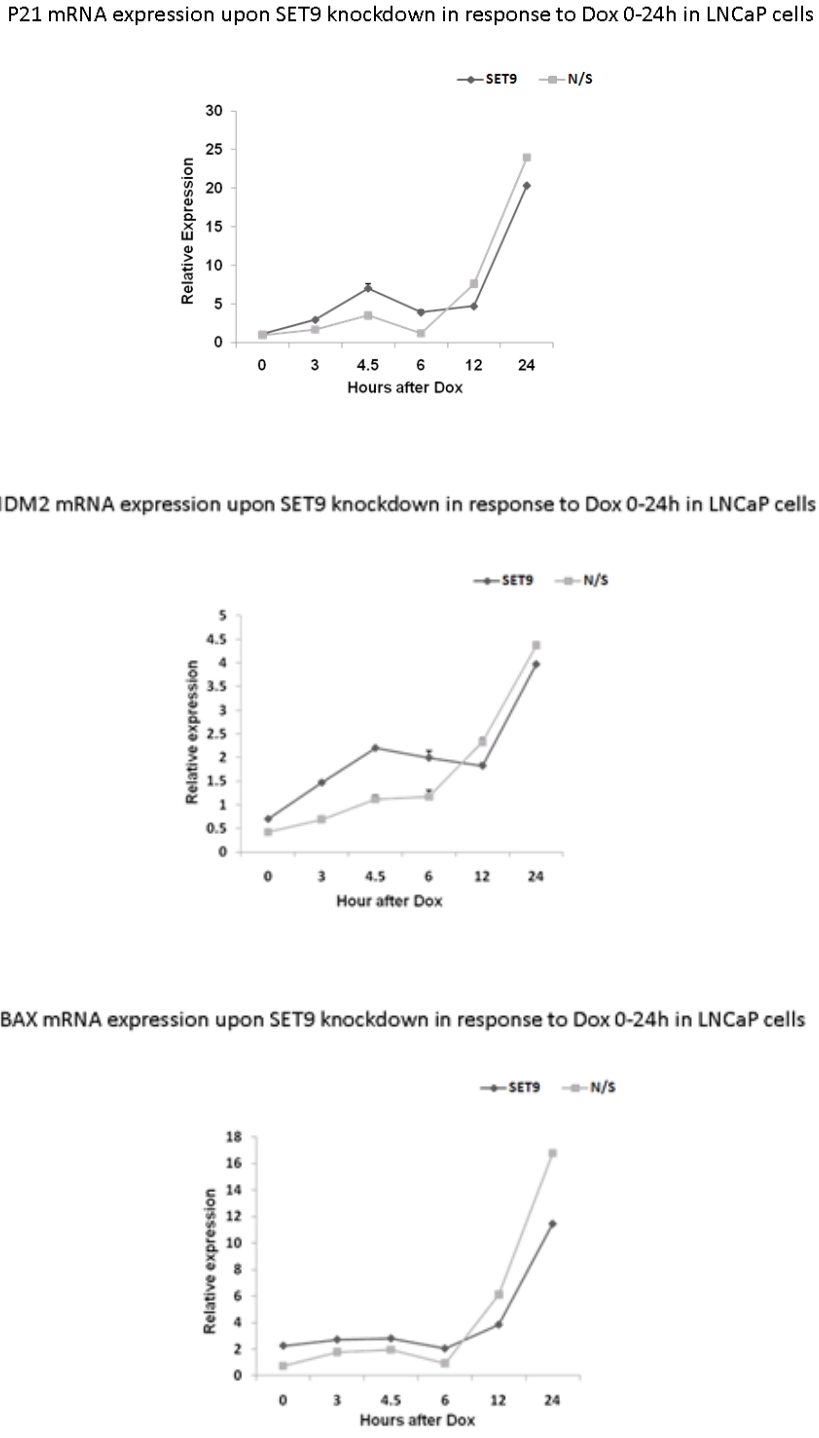

Figure 4.8 SET9 knockdown facilitates the expression of p53 regulated p21 and MDM2 in LNCaP cells in response to Doxorubicin.

LNCaP cells were reverse transfected with SET9 siRNA for 72 hours and then treated with Doxorubicin in a time course of 0, 3, 4.5, 6, 12 and 24 hours. mRNA was collected, reverse transcribed and subjected to real-time PCR analysis using specifically designed primers for p21, MDM2 and BAX. Figure shows the elevated earlier expression of p21 and MDM2 between 0-6 hours of Doxorubicin treatment compared to the scrambled control and to a lesser extent with MDM2. SET9 expression was measured at protein level (data not shown) and all related expression was normalized against GAPDH. Experiments were done in triplicates.

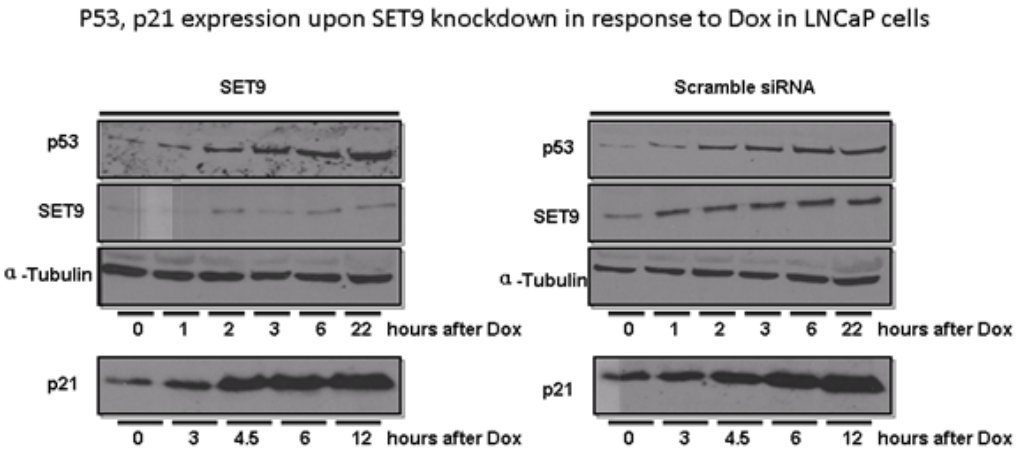

Figure 4.9 SET9 knockdown does not affect the protein stability of p53 and the corresponding expression of p21 within the 22 hours of Doxorubicin treatment.
LNCaP cells were reverse transfected with SET9 siRNA for 72 hours and then treated with Doxorubicin. Cells were harvested over the time course of either 0, 1, 2, 3, 6 and 22 hours or 1, 3, 4.5, 6 and 12 hours post-treatment and subjected to western blot analysis using p53 and p21 antibodies. p53 showed limited alteration upon SET9 knockdown and the p21 also showed no dramatic change over time.

To further analyse interplay between SET9 and p53 in the LNCaP apoptosis response, SET9 knockdown was combined with p53 knockdown to assess the requirement of p53 for LNCaP apoptosis in response to SET9 depletion. To perform those experiments, optimization of p53 knockdown was performed in the absence and presence of Doxorubicin and dual p53 and SET9 knockdown conditions in LNCaP cells were also optimized. As shown in Figure 4.10, 24, 48 and 72 hours of the knockdown efficiencies were compared each with p53 oligo concentration of 10, 25, 40 nM, respectively. In the presence of Doxorubicin, p53 expression was partially recovered due to stabilization of the protein via deregulation from mdm2 (Burns and El-Deiry, 1999). Upon optimization, the 25 nM concentration for a period of 72 hours was selected as the experimental condition and was combined with 25 nM concentration of SET9 in dual knockdown assays. Figure 4.10 also shows the combined knockdown of SET9 and p53 in the presence and absence of Doxorubicin. In line with the previous observation in caspase-3 apoptosis assays, SET9 knockdown induced 40 to 50 percent apoptosis in response to Doxorubicin treatment after 24 hours. p53 knockdown alone had little effect on Doxorubicin induced LNCaP cell apoptosis.

This finding is seemingly not consistent with previous finding where p53 has been shown as a prerequisite for the Doxorubicin induced LNCaP apoptosis (Rokhlin et al., 2008). However, this was possibly due to the treatment time with Doxorubicin, where 48 hours rather than 24 hours was used. This might lead to a more pronounced apoptosis compared to the condition herein. Alternatively, a more efficient p53 knockdown in LNCaP cells may have been achieved, compared to our transient p53 knockdown. Regardless of this discrepancy, strikingly, when p53 was knocked down in LNCaP cells under SET9 depleted condition, SET9 knockdown-induced apoptosis was completely abolished. (Figure 4.11). All above data suggests that SET9 mediated apoptosis is dependent upon p53 activation which subsequently leads to the activation of the caspase cascade. However, instead of regulating p53 in a positive manner in U2OS cells, the situation for p53 regulation by SET9 in LNCaP cells might be the opposite and the regulation of apoptosis and p53 target genes might also involve SET9 mediated AR regulation which is key to determine the fate of LNCaP cells.

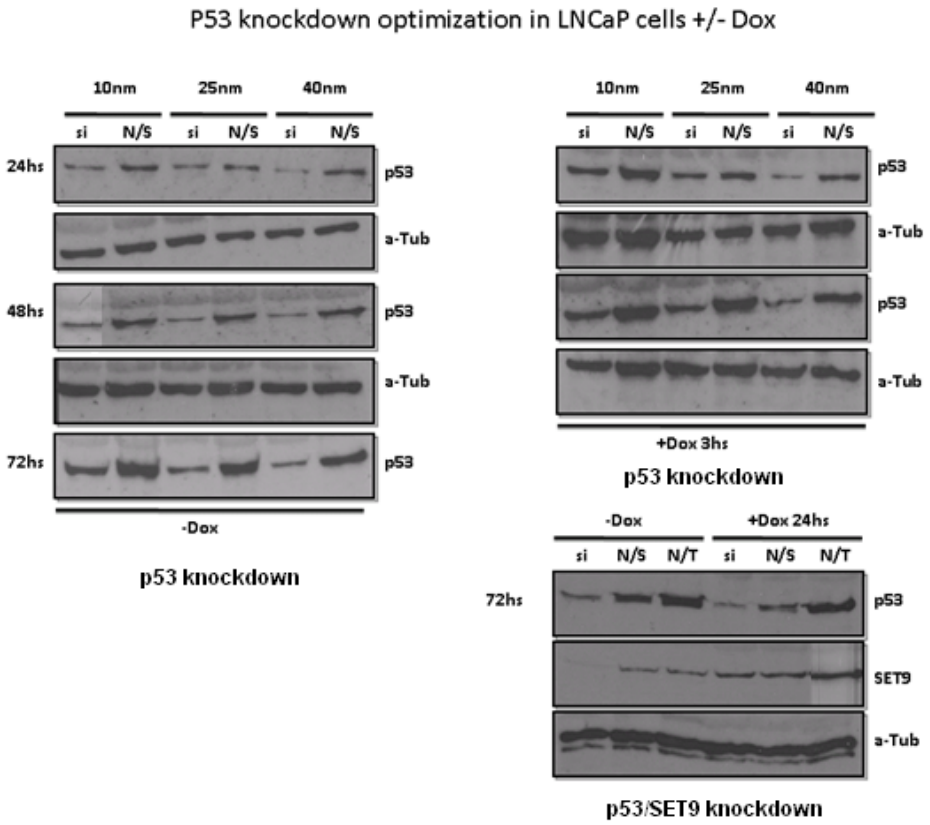

Figure 4.10 p53 knockdown optimization in LNCaP cells and dual knockdown assessment of p53/SET9.
p53 knockdown was optimized using 10, 25 and 40nM concentration in a time course of 24, 48 and 72 hours post-transfection. The 72 hours post-transfection was also extended to incorporate 24 hours Doxorubicin treatment to assess p53 level after induction. Upon optimization, 20nM p53 was combined

with 25nM SET9 siRNA to measure the dual knockdown efficiency and both proteins were depleted accordingly.

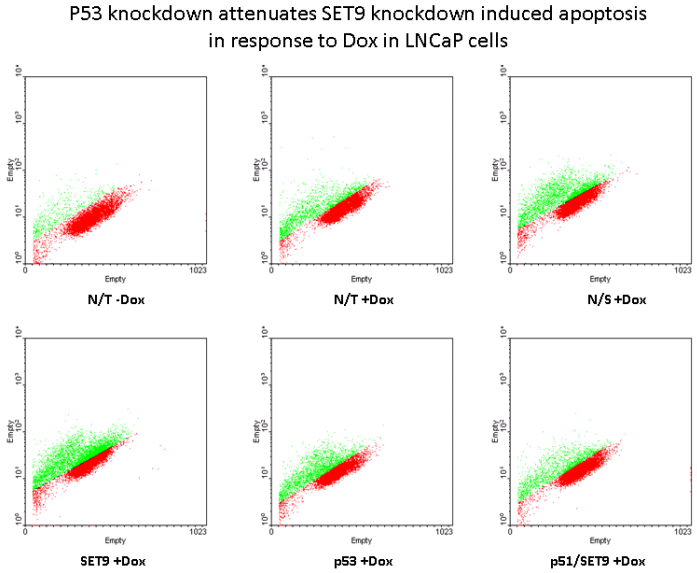

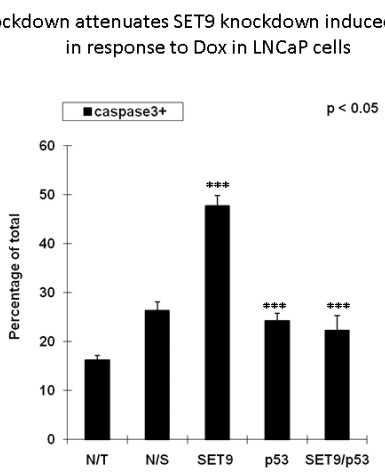

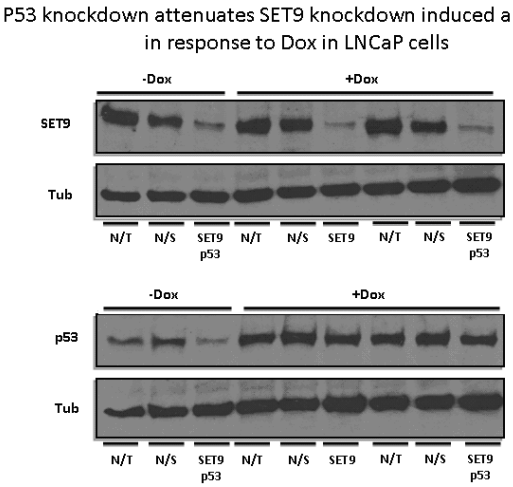

Figure 4.11 p53 knockdown attenuates SET9 knockdown mediated apoptosis in LNCaP cells in the presence of Doxorubicin (200nM).
LNCaP cells were reverse transfected with SET9, p53 and SET9/p53 combination. All siRNA concentrations were standardized to control. After 72 hours of knockdown followed by 24 hours Doxorubicin treatment, cells were harvested for caspase-3 apoptosis assay. The dot plots indicate the

lowered apoptosis when p53 is present in SET9 knockdown cells (shown by the green dots). SET9 alone caused dramatic apoptosis, whereas p53 alone had no effect on LNCaP cell apoptosis. The bar chart shows a complete inhibition of apoptosis when p53 is depleted in cells compared to SET9 knockdown alone. Knockdown was assessed by western blot. Experiments were performed in triplicates with p-value<0.05.

Finally, another prostate cancer cell line, DU145 which expresses wild-type SET9 and non-functional p53 was evaluated to assess whether SET9 can still induce apoptosis without p53 activation. Using FACS based Annexin V apoptosis assay, it was found that SET9 knockdown did not affect DU145 cell apoptosis indicating that functional p53 might be a key requirement for SET9 knockdown activated apoptosis (Figure 4.12).

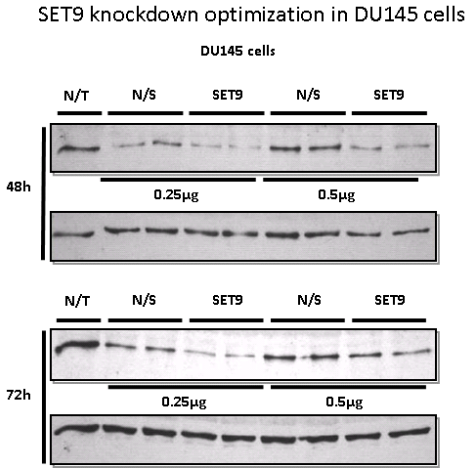

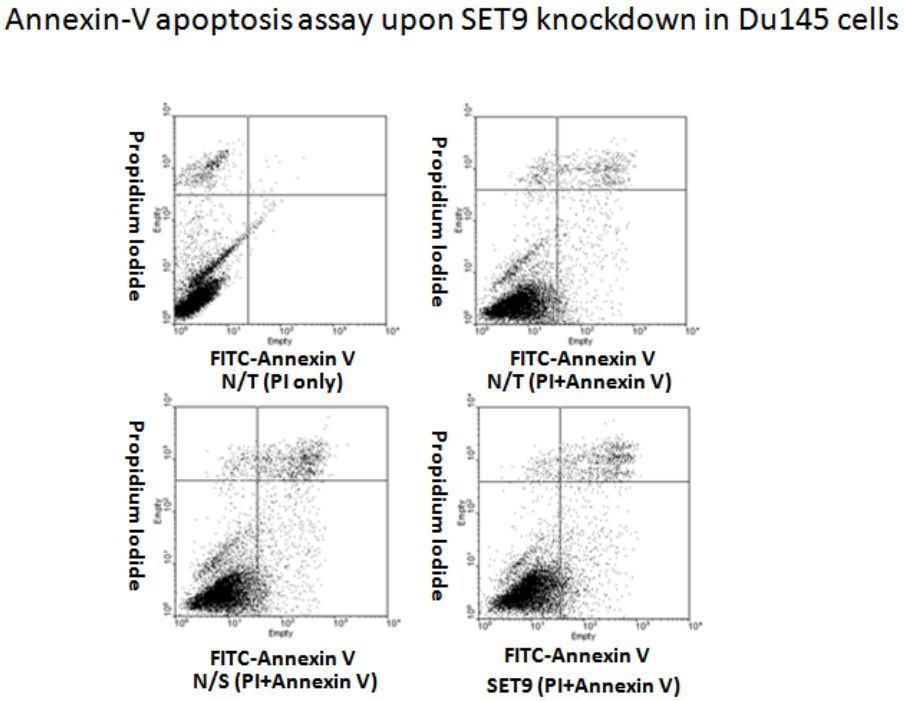

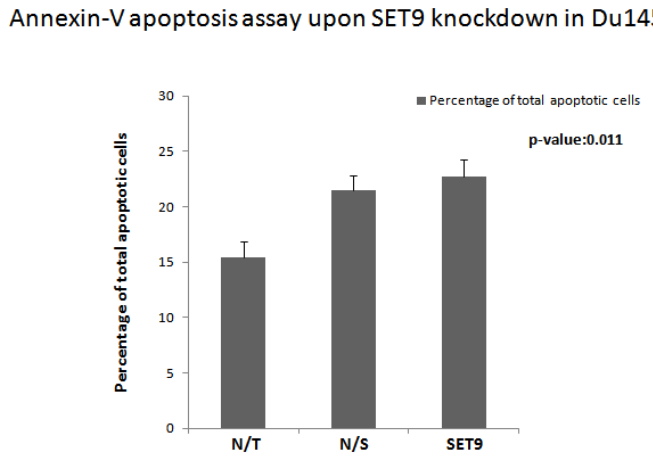

Figure 4.12 SET9 knockdown does not impact on apoptosis in DU145 cells bearing inactive p53. SET9 knockdown was first optimized in DU145 cells and a chosen 0.25µg/ml concentration was applied in subsequent experiments. DU145 cells were reverse transfected with SET9 and non-silencing (N/S) siRNAs and left for 72 hours prior to FACS Annexin V apoptosis assay using transfected and non-transfected (NT) cells. Dot plots demonstrated no significant change occurring in response to SET9 depletion compared to scrambled siRNA control, which is also evident in the bar chart. Experiments were performed in triplicates and repeated three times+/- standard error (p-value<0.05).

4.4 Discussion

In addition to members of the histone acetyltransferase and deacetylase families, the emerging members of the histone methyltransferase family may provide a series of additional potential therapeutic targets for cancer treatment. Indeed, many histone lysine methyltransferases have been linked to the pathogenesis and development of cancer, including EZH2, a H3 lysine 9 and 27 methyltransferase, which is shown to be up-regulated in aggressive prostate cancer (Varambally et al., 2002). Two other histone H3 lysine 9 methyltransferases, SUV39H1 and G9a have also been shown to be required to perpetuate the malignant phenotype of PC3 prostate cancer cell line (Kondo et al., 2008). These described examples suggest that individual histone methyltransferases have discernible roles in manipulating the cell phenotypes through different mechanisms.

Several lines of evidence suggest that SET9 is actively involved in regulation of p53 stability through the methylation of p53 at lysine 372 and this modification results in the p53-dependent apoptotic response induced by DNA damage (Chuikov et al., 2004). Early data in the laboratory showed that knockdown of SET9 decreased the proliferation of LNCaP cells suggesting an involvement of the HMT in regulating cell fate. Therefore, it was pertinent to decipher the mechanism of SET9 in regulating LNCaP cell proliferation. Cell cycle analysis using PI DNA content profiling was firstly utilized and interestingly showed that knockdown of SET9 caused G1/S arrest as reflected by the decrease of S phase and corresponding increase in G1 phase cells indicating that SET9 may facilitate cell cycle progression in LNCaP cells. This finding was also supported by the BrdU proliferation assay where a decrease of BrdU incorporated into S phase cells was observed in cells depleted of SET9. AR has been shown to stimulate G1/S transition via the cyclin D-Rb axis in prostate cancer cells and thus the G1/S arrest upon SET9 knockdown could be a result of deregulation of AR activity, by removal of receptor methylation for example, via knockdown of SET9 (Xu et al., 2006). On the other hand, androgen stimulation diminishes cyclin A levels, a mechanism due to Rb-mediated transcription repression (Balk and Knudsen, 2008). In line with this observation, recent findings have suggested that SET9 is capable of methylating Rb and blocking methylation

caused a reduced G1 accumulation compared to the wild type Rb when over-expressed in SAOS2 cells (Munro et al., 2010). Speculatively, it seems that the role of SET9 in LNCaP cell proliferation may not be via Rb, but could possibly be that dynamic methylation on AR, mediated by SET9 acts to drive AR-mediated cell turnover.

It was also noted that silencing of SET9 in both assays caused a consistent 20% decrease in S phase cells in comparison to the non-silencing siRNA control. However, the proliferation assay showed an almost 30% decrease in cell growth. Therefore, it was speculated that there might be other mechanisms responsible for the overall reduction of proliferating cells. Considering SET9 is involved in facilitating p53-driven apoptosis in U2OS cells, it was decided to address whether the overall proliferation change is partially contributed by apoptosis in LNCaP cells (Chuikov et al., 2004). Interestingly in agreement with the hypothesis, data from both Annexin V and caspase-3 assays showed increased apoptotic cells in the presence of SET9 knockdown compared to the non-silencing siRNA control, which is indicative of an anti-apoptotic role of SET9 in LNCaP cells. To further assess the role of SET9 in apoptosis regulation, treatment of SET9-depleted LNCaP cells with the DNA damage agent Doxorubicin was performed to determine whether this could alter the apoptosis induced by the knockdown alone. Strikingly, addition of Doxorubicin to cells synergized with SET9 knockdown to significantly enhance cellular apoptosis to 60%, compared to 12% without DNA-damage induction. In all, these data suggest that the DNA damaging agent Doxorubicin sensitizes LNCaP cells to apoptosis in the absence of SET9. In contrast, previous findings suggest that SET9 plays a pro-apoptotic role in U2OS cells when treated with Doxorubicin, which is contradictory with our findings. Therefore, a control experiment was performed incorporating U2OS cells transiently expressing either wild-type SET9 or the catalytically-inactive mutant $SET9_{H297A}$. Consistent with previous findings, wild-type SET9 induced significant apoptosis when cells were treated with Doxorubicin, whereas the mutant induced relatively less apoptosis confirming our previous observation in LNCaP cells where depletion of SET9 caused significant increase of apoptosis in the presence of Doxorubicin. In U2OS cells the mechanism of apoptosis involves the stabilization and nuclear activation of p53 via the methylation of its lysine residue 372 by SET9 and this

physiological impact consequently modulates p53 target gene expression, including p21 and Bax that are both pro-apoptotic (Chuikov et al., 2004) Additional supporting evidence suggests that LNCaP apoptosis can be triggered via p53 activation pathway (Jiang et al., 2004). Given that LNCaP cells express wild-type p53, it is possible to speculate that SET9 might be a determinant of p53 function in LNCaP cells that affects apoptosis induced by Doxorubicin. To begin with, co-immunoprecipitation was used as an assessment of interaction between p53 and SET9 in LNCaP cells. Under both androgen-depleted and -stimulated conditions, there was an interaction demonstrated between those two proteins (data shown in Chapter 6 Figure 4.7) suggesting a direct involvement of SET9 in regulating p53. To follow up on this finding, expression of selected p53 target genes p21, MDM2 and BAX was analysed. Unlike the phenomenon observed in U2OS cells, SET9 knockdown in LNCaP cells combined with Doxorubicin treatment raised expression of p21 and MDM2 at early time points up to 6 hours post-treatment and to a lesser extent with Bax, although between 6 and 24 hours, the expression patterns had no significant change over time. Although the trends observed were not significant for BAX, the altered expressions of p21 and MDM2 in response to SET9 knockdown were apparent and significant. This finding implies that rather than to trigger p53 activity by methylating the protein, SET9 might play a negative role in regulating p53 activity in synergy with Doxorubicin in LNCaP cells. On the other hand, in parallel experiments where the protein expressions of p53 and p21 were measured, there was no significant changes of p21 and p53 protein expression possibly due to slower response of protein translation than the production of mRNA in cells. Since our data imply that SET9 may regulate p53 and its target gene expression, we then went on to see if the apoptosis induced by SET9 with Doxorubicin treatment is potentially via the p53 dependent pathway. Interestingly, as SET9 depletion alone facilitated the apoptosis with Doxorubicin treatment, silencing p53 together with SET9 in LNCaP cells completely abrogated the apoptosis induced by SET9 knockdown alone, which was indicative of the participation of p53 activation in SET9 knockdown mediated apoptosis. Notably, induction of Doxorubicin caused an increase in p53 expression measured after 24 hours post-treatment. However, it could be argued that this sudden restoration of p53 level would not skew the interpretation of our data as the occurrence of apoptosis mediated by p53

responsive genes such as BAX would not be affected by rapid recovery of p53 level in the cells and on the contrary would be affected due to the massive reduction of p53 prior to the Doxorubicin induction. In an attempt to verify the hypothesis that SET9 knockdown mediated apoptosis is via p53 dependent pathway, the DU145 prostate cancer cell line with functionally inactive p53 was used to examine whether SET9 knockdown had the potential to induce apoptosis in the absence of functional p53. As expected, SET9 knockdown was unable to induce apoptosis in DU145 cells suggesting that this apoptosis pathway is potentially dependent upon p53 activation.

Of particular interest was the combination of SET9 knockdown with the therapeutic agent Doxorubicin, which combined together significantly augmented apoptosis and the mechanism was through a p53-dependent process. This observation seemingly contradicts the mechanism in U2OS cells where SET9 stabilizes p53 to trigger apoptosis (Chuikov et al., 2004). There are several possible reasons to explain this: 1) different cell lines bear distinct biological properties which would impact on the function of certain proteins. 2) post-translational modification patterns may affect the outcome of the impact of SET9 on p53. So far, although we established direct interaction between SET9 and p53 and this would possibly impact on the activity of the protein and subsequent gene expression, we still lack the direct evidence of p53 methylation by SET9 in LNCaP cells. Furthermore, another line of evidence suggests that the methylation of p53 K372 by SET9 may affect the subsequent acetylation status and possibly the ubiquitylation of p53, a procedure which would dictate the turnover of the protein (Ivanov et al., 2007). Moreover, the C-terminal region in p53 is a hot spot of various post-translational modifications such as acetylation, ubiquitylation, phosphorylation and methylation and individual modifications may play agonistic or antagonistic effect depending on the settings in various cellular environments. In the context of SET9 involved regulatory mechanism, it has been shown that pre-methylation of K372 assists the loading of acetylation by p300 at lysine residue 382 and the reciprocal pre-acetylation on the protein however prohibits the methylation of K372 by SET9 (Ivanov et al., 2007). Further supporting this, in addition to affecting p53 acetylation, methylation at K372 may impact other p53 modifications such as the adjacent K370 which is a target of methylation by Smyd2 (Huang et al.,

2006). Thus it is reasonable to argue that SET9 mediated apoptosis via the regulation of p53 is a combinational effect of substantial modifications on the protein with dynamic interplay between individual modulators and it is possible that in LNCaP cells there is a pre-existing p53 state distinct from the model in U2OS cells, which when SET9 is introduced would lead to a dissociation of the protein via aberrant post-translational modifications. To prove that, we need to design experiments to knockdown other major p53 modifiers such as p300, Smyd2 and MDM2 in combinations with depletion of SET9 in the LNCaP cells to see their impact on K372 methylation. 3) Another possible explanation is that in U2OS cells K372 methylation of p53 is predominantly catalyzed by SET9, whereas in the LNCaP cells it can also be catalyzed by other methyltransferases or maybe influenced by other proteins. In a recent publication, SET9 has been shown to negatively regulate E2F1 by methylating the protein at lysine 185, which prevents E2F1 accumulation during DNA damage and activation of its pro-apoptotic target gene p73. Of equal interest, this methyl mark is removed by LSD1, which is required for E2F1 stabilization and apoptotic function (Kontaki and Talianidis). Notably, this observation was achieved in p53-deficient cell line H1299, whereas in an earlier publication, H1299 cells transfected with exogenous wild-type p53 and SET9 still showed a crosstalk between those two protein suggesting that depending on the intrinsic properties of various target proteins, the function of SET9 might be altered dramatically (Chuikov et al., 2004; Kontaki and Talianidis). Thus far, whether SET9 is the major player of K372 methylation on p53 in LNCaP cells and whether there are other mechanisms involved in this regulation procedure is still awaiting to be addressed.

Chapter 5

Identification of novel SET9 interacting partners

5.1 Introduction

The identification of SET9 subsequently has led to the discovery of many non-histone protein substrates of the enzyme, including p53, Estrogen Receptor α, NF-kB and pRb all of which play prominent roles in cancer development. Likewise, some other HMT containing complexes have been identified in mammalian cells such as the EZH2 containing complex EED-EZH2 that plays significant roles in cancer cell proliferation (Cao and Zhang, 2004). Importantly, the majority of SET9 substrates have been identified via candidate-based approaches in which proteins containing a consensus or near-consensus SET9-targeting methylation motif have been assessed for interaction and modification by the methyltransferase enzyme. To date, however, no study has been conducted to identify novel SET9-interacting partners in an unbiased whole cell system, an approach that has the potential to build up mechanistic links between SET9 and other potential interacting and methylation targets in a cellular context.

The incorporation of fusion-tagged proteins in immunoprecipitation/purification and subsequent analysis of the complexes by tandem mass spectrometry (MS), termed MS/MS, is a sophisticated and well established technique that has been utilized extensively to identify novel interacting partners of a protein of interest. Indeed, the identification of several transcriptional co-regulatory complexes has been the result of combining immunoprecipitation with MS/MS analysis demonstrating the validity of using this approach. For example, immunoprecipitation and MS/MS analysis of the FLAG-tagged histone demethylase enzyme LSD1 complex resulted in the identification of the histone deacetylase (HDAC)-containing co-repressor complex CoREST which promotes the demethylation of histone H3 K4 (Lee et al., 2006b; Lee et al., 2005b). In addition, the identification of linker histone H1 associated factors and histone H3 tail associated proteins have both been the result of this approach; purification of the H1 subtype H1.2 from a stably expressing HeLa S3 clone resulted in the identification of YB1 and PURα as H1.2-interacting proteins that repress p53 dependent, p300-mediated chromatin acetylation (Kim et al., 2008). Furthermore, G9a, JMJD2C, CARM1 ASH1, MLL3 and HDACs were all found

to interact with an immunoprecipitated H3 tail peptide, purified from a HeLa S3 clone using the FLAG-M2 resin (Heo et al., 2007). A more relevant example to the study of SET9 is the identification of PTIP (Pax transcription activation domain/interacting protein)-interacting proteins including ALR, ASH2, WDR5, RBBP5 and NCOA6, which together co-exist in a histone H3 lysine 4 methyltransferase complex and PTIP has been found to be essential for the assembly of this methyltransferase complex (Patel et al., 2007). The molecular mechanisms which bridge the methylation complex of histone H3 lysine 4 and the DNA binding transcriptional regulation by PAX2 established the theoretic basis of discovering novel protein interacting partners as a way to uncover molecular basis of various cellular events.

In chapters 3, SET9 was shown to interact with HDAC1, suggesting a novel mode of regulation for the methyltransferase. However, this finding was the result of a candidate-based study that simply predicted that SET9 and HDAC1 may interact due to the existence of cross-talk between p53 acetylation and methylation during p53-mediated transcription (Kurash et al., 2008). Therefore, to gain a better and unbiased understanding of the protein interaction network that exists for SET9 in CaP cells, a combined immunoprecipitation and MS/MS approach was utilized in LNCaP cells to identify SET9-interacting proteins. It was hypothesized that by identifying novel interacting partners of SET9 in CaP cells, an insight into the function and regulation of SET9 within the AR signaling cascade and beyond would be provided and hence potentiate the definition of new therapeutic targets for prostate malignancy.

5.2 Specific materials and methods

The composition and suppliers of the majority of the reagents and materials can be found in the general materials and methods (Chapter 2.1) Otherwise, the materials and reagents are specified in individual chapters where appropriate.

5.2.1 Immunoprecipitation of SET9 containing complex from HeLa cells stably expressing 3×FLAG-SET9 or LNCaP cells expressing endogenous SET9

The molecular cloning of p3XFLAG-CMV-10 expressing full length wild-type SET9 and the generation of stable HeLa SET9 expressing cells are described in Chapter 2.2 and 2.4.2. Both SET9 over-expressing and control empty vector clone cells from 5×150mm plates (1×10^8 cells) were harvested and subjected to Immunoprecipitation using anti-FLAG-M2 affinity resin as described in detail in Chapter 2.5.2. The sample preparation steps and endogenous SET9 immunoprecipitation from LNCaP cells was the same as described in Chapter 2.5.2 except it was scaled up 40-fold to reflect the larger number of cells (4×10^8). In parallel with SET9 pull-down, rabbit IgG was used as a standard negative control to filter out non-specific bindings of target proteins to IgG and/or PGS beads during the experimental procedure.

5.2.2 Acetone precipitation prior to tandem mass spectrometry (MS/MS) analysis

For immunoprecipitated crude protein mixtures from LNCaP cell lysates, acetone precipitation was performed prior to being subjected to in-solution digestion using endoproteinase Lys-C and trypsin. Briefly, cold cell lysates were mixed with six volumes of pre-chilled 100% acetone and incubated at -20℃ until precipitates were well formed (usually overnight). Acetone was then decanted and the remaining protein pellets were then used for In-solution digestion using endoproteinase Lys-C and trypsin. Trypsin and endoproteinase Lys-C specifically hydrolyze peptide bonds at the carboxyl-terminal of arginine and lysine residues and the inclusion of endoproteinase Lys-C acts to increase the

digestion efficiency at high urea condition in the protein mixture to endure a complete digestion reaction.

5.2.3 Performing In-solution digests using endoproteinase Lys-C and trypsin

All reagents were prepared fresh. Acetone precipitated samples were re-dissolved in 50 µl 6M urea (Sigma), 100 mM Tris/50mM N_4HCO_3 by vortexing thoroughly. Then 2.5µl of reducing agent (194 mM DTT from Sigma in 0.1M Tris/HCl pH8) was added to samples, mixed and left for 1 hour at room temperature prior to the addition of 10µl alkylating reagent (195mM iodoacetamide (Sigma) in 0.1M Tris/HCl pH8) in the dark at room temperature (RT) for 1 hour to allow alkylation of the iodoacetamide. After incubation, 10µl of reducing agent was added, mixed and incubated at RT for 1 hour to consume unreacted iodoacetamide. Endo Lys C (stock concentration 0.1µg/µl (Sigma)) was then added to samples at an enzyme: substrate ratio of 1/100 and samples were vortexed and placed in a Thermomixer at 37℃, 1000rpm for overnight. After digestion with Endo Lys C, 240µl of 50mM NH4CO3 was added in order to decrease the urea concentration to approximately 1M which was suitable for efficient trypsin digestion. A protease: substrate ratio of either 1/20 or 1/100 of the stock protease (0.2µg/µl (Promega)) was applied to samples and then placed in the Thermomixer under same condition as the Endo Lys C for overnight. The reaction was finally stopped by adding 100µl of Trifluoroacetic acid (TFA) and samples were then stored at -20℃ before proceeding to the next step.

5.2.4 Performing peptide fractionation using the Agilent 3100 OFFGEL fractionator

The OFFGEL fractionator is an item of equipment that can prefractionate proteins and peptides prior to LC/MS analysis. It uses a novel isoelectrical focusing technique to ensure the high quality protein isoelectrical point-based fractionation in order to achieve high standard and reproducible MS data. For peptide isoelectrofocusing (IEF), an OFFGEL stock solution was firstly made

(8.4 M Urea, 2.4 M Thiourea, 0.08 M DTT, 50% Glycerol (Sigma) and 1.2% IPG buffer (GE Healthcare)). Immobiline DryStrip pH 3-10 24cm IPG strips were used to fractionate digested peptides. Strips were placed in an OFFGEL Tray and rehydrated using rehydration solution (0.96 ml OFFGEL stock solution to 0.24 ml dH_2O with Bromophenol Blue in). Then, 0.72 ml of each peptide sample was mixed with 2.88 ml OFFGEL stock solution (1.25×) to ensure that the salt concentration was lower than 10 mM (This is essential to ensure that IPG strips are not overheated or burned due to high salt concentration during electrophoresis). After the OFFGEL frame set was placed on top of the IPG strips, equal amounts of each sample were loaded into individual wells of the frame. The OFFGEL fractionation was performed under the OFFGEL mode (OG24PE00). After fractionation, samples in each frame well were collected in tubes using a pipette.

5.2.5 Liquid chromatography based tandem mass spectrometry analysis and data processing

Acquired samples from OFFGEL fractionation were then subjected to liquid chromatography MS/MS (LC-MS/MS) using the LTC OrbiTrap XL mass spectrometer (ThermoFisher). Raw data files were interpreted using the ThermoFisher Xcalibur software and converted to Mascot generic file (mgf) format using the ThermoFisher Proteome Discoverer software. The mgf files were then submitted automatically to X!Tandem database through the Global Protein Machine (GPM) interface. The local GPM database was also always used for large mgf files that may timeout on the global database. After all protein IDs were acquired through the GPM database, SET9 immunoprecipitation pull-down samples were compared with the control IgG pull-down and positive peptide hits were identified using Excel based data sorting.

5.3 Results

5.3.1 Construction of the 3×FLAG-SET9 wild type vector

The 3×FLAG CMV-10 construct was chosen to generate 3×FLAG-SET9 to be used for stable transfection into HeLa cells. The FLAG tag mediated fusion protein purification strategy has been documented and is compatible with the following tandem mass spectrometry (see introduction above). The detailed strategy of generation of the 3×FLAG-SET9 plasmid was described in Chapter 2.2. All individual steps and their relevant results are shown below (Figure 5.1) The amplified SET9 PCR fragment was ligated into the pre-digested Bam H1 site of the pCR2.1 vector (Invitrogen) and recombinant plasmids were identified via Bam H1 digestion. SET9 cDNA was then subcloned into the 3×FLAG CMV 10 vector (Sigma) via the Bam H1 site and recombinant p3xFlag-SET9 clones with the correct orientation were identified using individual digests with Bam H1 and Kpn 1. The recombinant vector was verified by sequencing and transient expression in U2OS cells followed by Western blot analysis using either SET9 or FLAG antibodies (Figure 5.2).

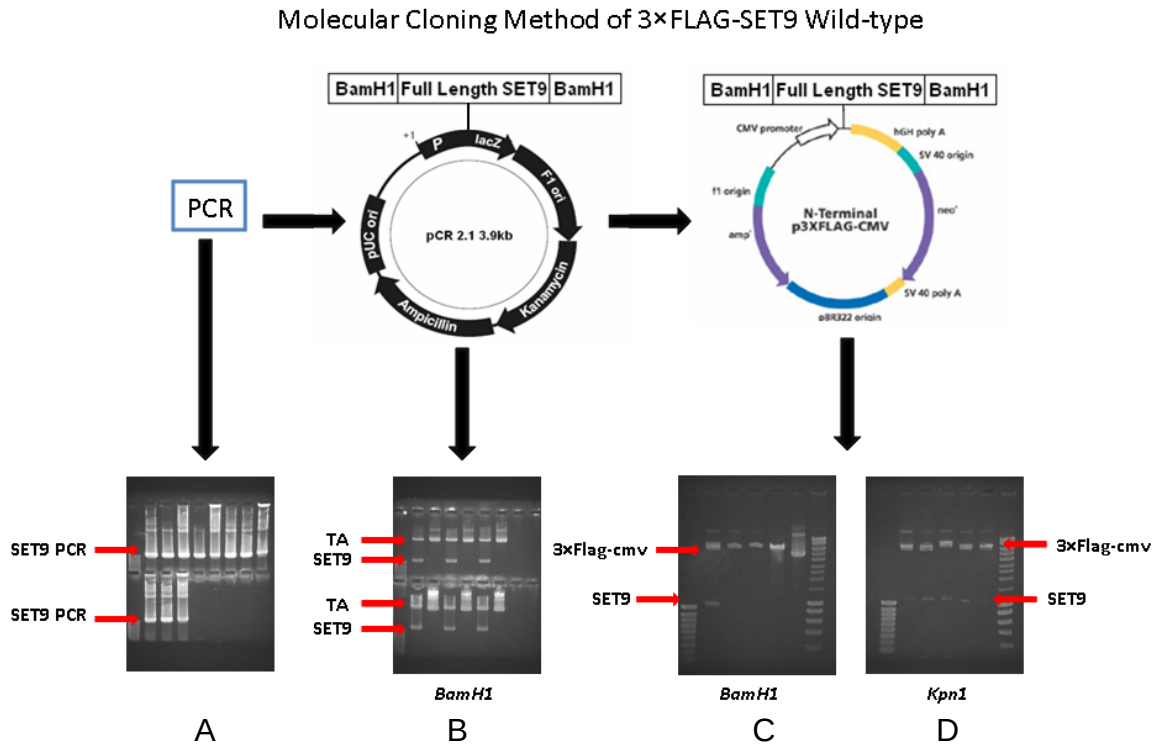

Figure 5.1 Molecular cloning strategy of 3×FLAG-SET9 wild type.
Full length SET9 fragments were amplified by PCR with two primers containing flanking BamH1 sites. The single PCR product (A) was subsequently ligated into pCR2.1 vector and then subject to *Bam* H1 digestion

to identify positive recombinant vectors (B). SET9 fragments were subcloned into 3×FLAG CMV-10 vector via *Bam* H1 sites and positive recombinant clones were selected by *Bam* H1 digestion (C). As 3×FLAG CMV-10 bears the Multiple Cloning Site (MCS) with a single *kpn1* after the BamH1 site and correctly orientated inserted SET9 contains a *Kpn1* site near the 5' end of the gene, Kpn1 restriction enzyme was used to ensure the orientation of clones and the resultant 1kb insert was released after digestion (D). The positive clone was finally validated by sequencing.

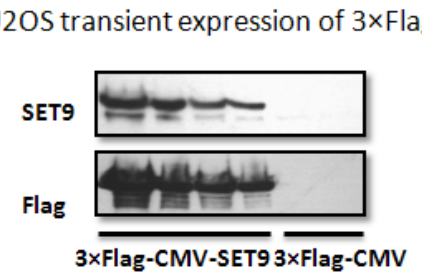

Figure 5.2 Ectopic expression of 3×FLAG-SET9 in U2OS cells.
The p3×FLAG-SET9 was transiently transfected into U2OS cells at two different concentrations alongside empty p3×FLAG-CMV-10 vector. Western blotting was carried out using either SET9 or FLAG antibody. SET9 antibody detected both endogenous and exogenous SET9 in transfected U2OS cells.

5.3.2 Generation of 3×FLAG-SET9 stable HeLa expressing clone and FLAG-M2 resin affinity purification

To generate the stable SET9 expressing HeLa clone, Lipofectamine LTX/ Plus reagent was used to forward transfect HeLa cells with 3×FLAG-SET9 vector using the standard protocol (Chapter 2.4.3). This construct takes the advantage of the neomycin resistance gene which is used for the positive clone selection. G418 was utilised for selecting stable 3xFLAG-SET9 expressing HeLa cell clones at a concentration of 500 µg/ml (Dart et al., 2009). All generation procedures are described in Chapter 2. 4.2. An empty 3xFLAG-CMV10 vector clone was also generated as a control in pull-down assay to identify potential non-specific interaction of proteins with FLAG tags. After G418 selection for 2 weeks, resistant colonies emerged and single clones were transferred into 24-well plates to continue growing until they were ready to be lysed and subjected to Western analysis, using both SET9 and FLAG antibodies to assess ectopic SET9 expression. As shown in Figure 5.3, only one out of the nine selected clones expressed FLAG-SET9 that was detected with the FLAG antibody, but not the SET9 antibody (Clone 4) (Figure 5.3). This was possibly due to the low expression level of 3×FLAG-SET9 in HeLa cells and hence was only identified using the very efficient FLAG antibody, but not the weaker-binding SET9 antibody. An additional validation experiment for Clone 4 was performed in

which SET9 levels were depleted by siRNA oligonucleotide and cell lysates subjected to anti-Flag immunoblotting. As shown in Figure 5.3 (Right Panel) transient transfection of the FLAG-SET9-expressing Clone 4 with SET9 siRNA resulted in reduced FLAG-SET9 expression confirming that the stable HeLa cell clone was indeed expressing the desired fusion protein (Figure 5.3). This cell line, termed HeLa$_{\text{-FLAG-SET9}}$ was subsequently used for SET9 immunoprecipitation procedures.

Notably, one of the clones (clone No. 3) expressed comparably high level of SET9 which could be detected by both FLAG and SET9 antibodies, however this clone did not grow properly and underwent severe morphological changes (Figure 5.4). Therefore, this cell line was not used for subsequent experiments primarily due to a failure to bulk up sufficient cells for downstream protein purification procedures.

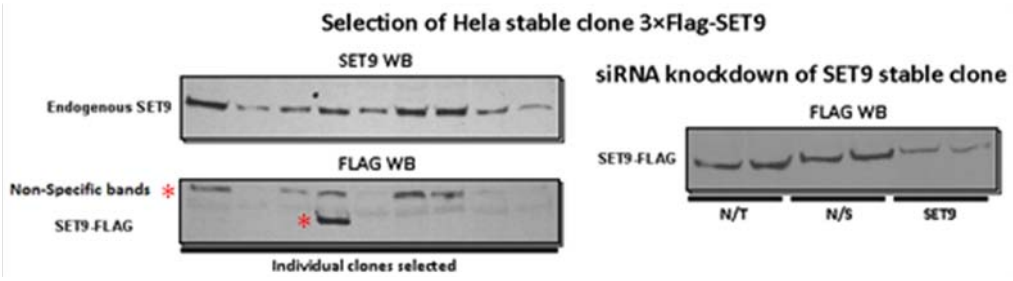

Figure 5.3 Screening of stable HeLa SET9 clone.
After G418 selection, surviving colonies were expanded and tested for SET9 positivity using western blot. As shown above, one out of nine colonies expresses FLAG-tagged SET9 as detected by FLAG antibody. This positive clone was then verified using the siRNA against SET9 and western blot using FLAG antibody showed the depletion of 3×FLAG-SET9 by siRNA knockdown.

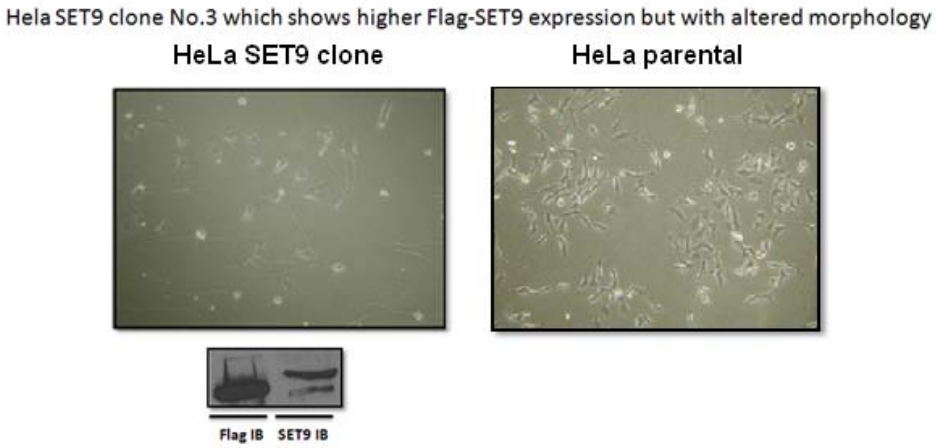

Figure 5.4 High level expression of 3×FLAG-SET9 in one HeLa clone showing significant morphological changes in culture.
The expression of FLAG-tagged SET9 were both detected by FLAG and SET9 antibodies using western blot. This clone displayed strong growth inhibition and remarkable morphological changes in culture.

5.3.3 Optimization of FLAG-SET9 immunoprecipitation using FLAG M2 resin affinity purification

Having established the FLAG-SET9-overexpressing cell line, HeLa-$_{FLAG\text{-}SET9}$, the next step was to optimize the FLAG-M2 resin for immunoprecipitating the SET9 fusion protein. The initial purification of FLAG-SET9 from HeLa$_{-FLAG\text{-}SET9}$ and the control HeLa-$_{3\times FLAG\ CMV\text{-}10}$ was performed using FLAG-M2 resin based immunoprecipitation method. Importantly, as shown in Figure 5.5, the empty vector HeLa cell clone showed no expression of exogenous SET9, while HeLa$_{-FLAG\text{-}SET9}$ demonstrated expression and immunoprecipitation of the fusion protein, as detected by Western analysis using an anti-SET9 antibody, indicating the validity of the method for separating and enriching proteins of interest (Figure 5.5, upper panel)). Purified samples were then subject to SDS-PAGE followed by Coomassie brilliant blue staining. Intriguingly, no intensely stained bands were observed on the gel. When the more sensitive Colloidal Coomassie staining was applied to a second gel containing the same samples, a small number of bands appeared in the HeLa$_{-FLAG\text{-}SET9}$ SET9 clone lanes. However, it was difficult to distinguish bands specifically associated with this clone compared to the control sample (Figure 5.5, lower panel). Given that the experiment started with a large amount of cells, the expression of the FLAG-SET9 protein in the HeLa cell clone may be inadequate for the downstream experiments to identify SET9-interacting proteins.

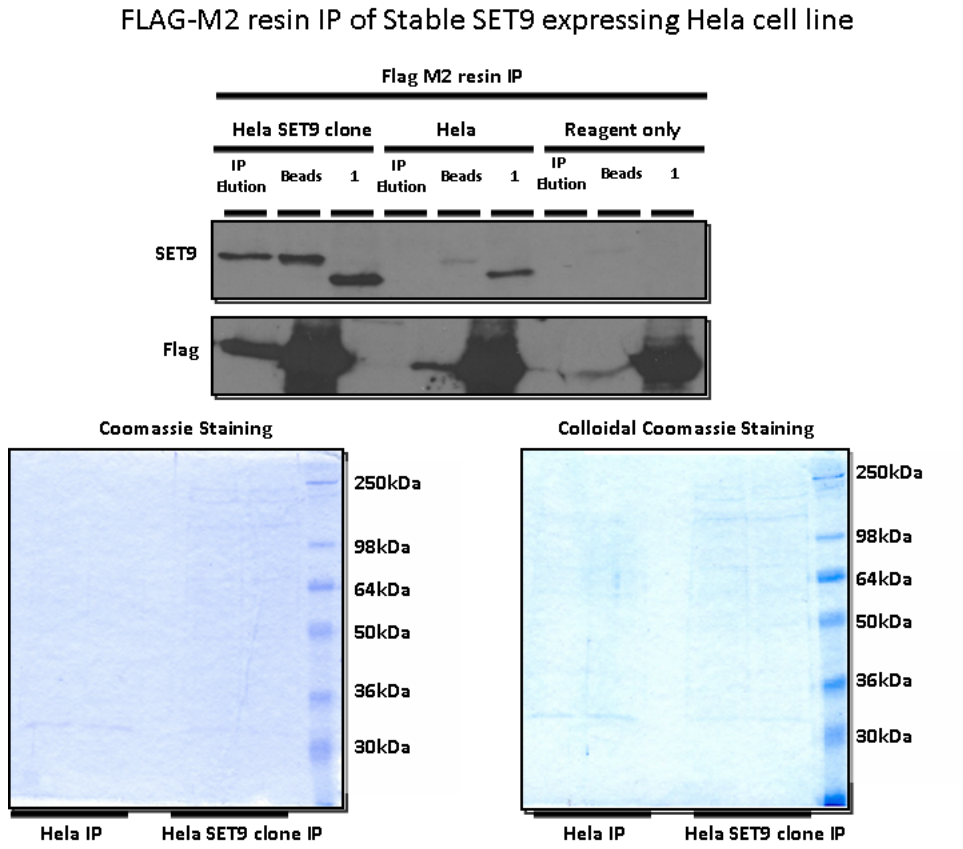

Figure 5.5 FLAG-M2 resin immunoprecipitation validation using the HeLa$_{FLAG\text{-}SET9}$ stable clone. The HeLa$_{FLAG\text{-}SET9}$ clone was used for the validation of FLAG-M2 resin based immunoprecipitation. 4×10^8 of both HeLa-$_{FLAG\text{-}SET9}$ and HeLa-$_{FLAG}$ cells were used for immunoprecipitation and control immunoprecipitation, respectively. In HeLa SET9 clone IP, the western blot shows the purified 3×FLAG-SET9 in IP elution lane. The beads lane shows the uneluted 3×FLAG-SET9 protein associated with beads. The 1 lane represents the endogenous SET9 (lower molecular weight as non-tagged by Flag) which was not co-purified with FLAG-tagged SET9. The HeLa FLAG empty clone and reagent only control showed no expression or co-purification of FLAG-tagged SET9 in this purification system. The purified FLAG-SET9 was then subjected to Coomassie and Colloidal Coomassie staining, respectively. Beads controls represent the beads after the elution steps and 1controls represent the Input samples which were cell lysate without Flag-M2 resin treatment.

5.3.4 Identification of SET9 interacting partners in LNCaP prostate cancer cells

Given that the HeLa$_{FLAG\text{-}SET9}$ clone was unsuitable for the identification of SET9-interacting proteins by immunoprecipitation, due to a low level of FLAG-SET9 expression, an alternative approach was utilised that involved immunoprecipitating endogenous SET9 from LNCaP prostate cancer cells. LNCaP cells were chosen for this purpose on two accounts; firstly, they express high level of SET9 and secondly, they are more relevant to our on-going AR and CaP studies. The work flow of the experiment is provided in Figure 5.6. In order to maximize the protein recovery to identify potential interacting partners

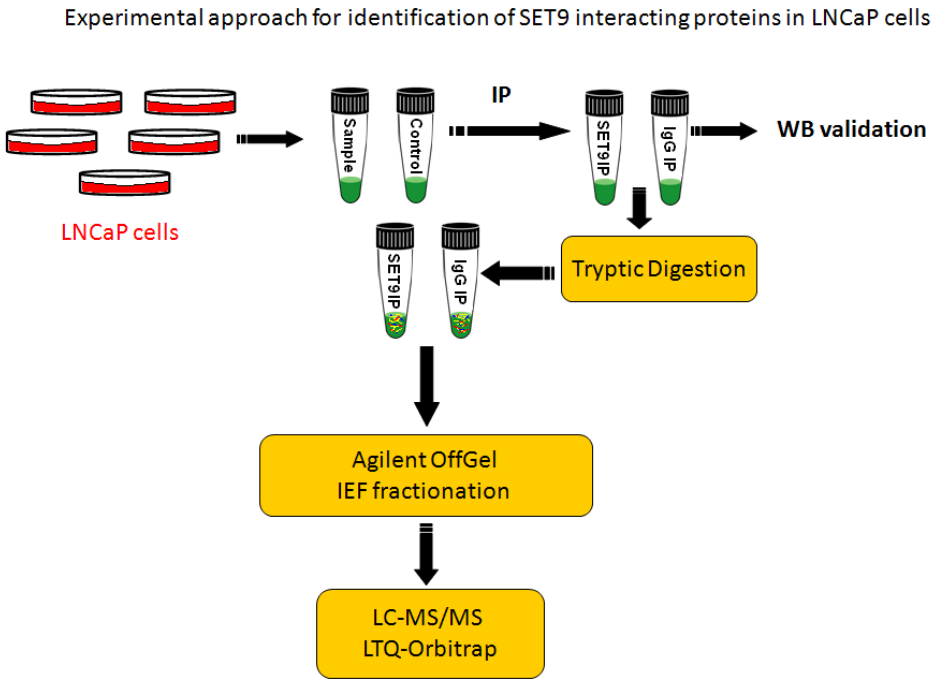

Figure 5.6 Experimental strategy for identification of SET9 interacting proteins using mass spectrometry.
Schematic representation of the experimental approach for SET9 interacting protein identification. 4×10^9 of LNCaP cells growing in full medium were subjected to immunoprecipitation using either a polyclonal SET9 antibody or a non-specific rabbit IgG antibody for control. After protein recovery, specificity of the immunoprecipitation procedure was verified by Western analysis using an anti-SET9 antibody. Immunoprecipitated proteins were then acetone precipitated and subjected to in-solution tryptic digestion. Samples were subsequently loaded onto an Agilent OffGel fractionator for separation by peptide isoelectric points. All resulting fractions were finally analyzed by LTQ-Orbitrap mass spectrometry using reverse phase liquid Chromatograghy-MS/MS. All resulting fractions were finally analyzed by LTQ-Orbitrap mass spectrometry using reverse phase liquid Chromatograghy-MS/MS.

and also as documented in the literature regarding the quantities of protein required for this type of experiment, 20×150mm plates (4×10^9 cells, roughly 200 mg protein) of LNCaP cells grown in full medium were harvested and lysed in lysis buffer (see chapter 2.5.2), prior to immunoprecipitation using either SET9 or control IgG antibodies (Heo et al., 2007; Patel et al., 2007). To assess the quality of the immunoprecipitation procedure, samples were subject to western analysis using an anti-SET9 antibody. As shown in Figure 5.7, SET9 was efficiently pulled-down by the SET9 antibody (Lane 1), but not in the control arm of the experiment (Lane 4). After samples were immunoprecipitated, in-solution digestion was applied and followed by Agilent OFFGEL IEF fractionation to separate peptides into 24 fractions for SET9 and IgG pull-down, respectively. Each fraction was then analyzed using the LC-LTQ-Orbitrap MS/MS.

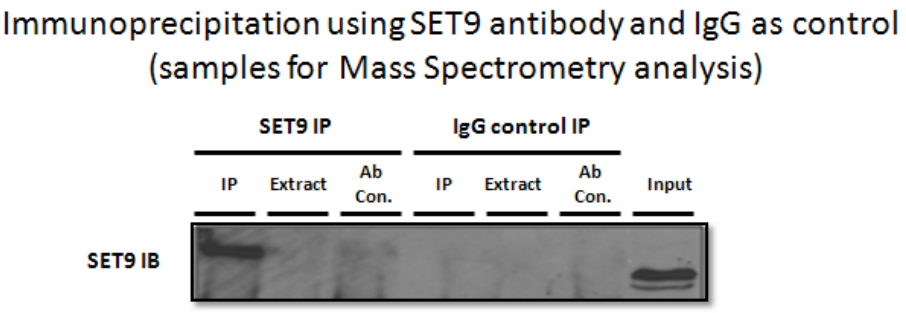

Figure 5.7 IP sample validation by immunoblotting.
The efficiency of the immunoprecipitation was assessed by Western analysis using an anti-SET9 antibody (mouse). SET9 was specifically detected n the IP sample (lane 1) only and not in the IgG control (Lane 4) confirming the pull-down of the protein. Ab con. refers to control with antibody only, with immunoprefcipitation buffer. Extract is the control with no cellular contents and antibodies in but beads only. Input refers to the control with cellular contents pre-incubated with beads but on further downstream treatments.

The summary of all identified proteins can be found in Appendix 1 and Table 5.1 lists the proteins identified by this procedure as SET9-interacting proteins in the LNCaP cell line. All identified peptide spectra of specific interacting partners are presented in Appendix 2. A valid interacting protein is defined as a protein identified specifically in SET9 immunoprecipitated sample and not being present in IgG only pull-down; having good coverage on the mass spec (rl number), and low log(e) value and their correlated molecular weight. Those protein are also not classified into the “sticky” protein category according to the previously published work (Trinkle-Mulcahy et al., 2008).

Protein ID interpretation from OffGel fractionation and LTQ-LC(MS/MS)

log(f)	rl	log(e)	pI	Mr	Description
3.74	2	-17.1	5.8	69.7	Fragile X mental retardation syndrome-related protein 1 (hFXR1p) [Source:UniProtKB/Swiss-Prot;Acc:P51114]
4.41	3	-10.8	5.8	9.7	homologuous to: Barrier-to-autointegration factor (Breakpoint cluster region protein 1). Source: Uniprot/SWISSPROT O75531
3.83	1	-10.3	5.9	36.0	PDZ domain-containing protein GIPC1 (RGS19-interacting protein 1)(GAIP C-terminus-interacting protein)(RGS-GAIP-interacting protein)(Tax interaction protein 2)(TIP-2) [Source:UniProtKB/Swiss-Prot;Acc:O14908]
4.17	2	-9.7	6.4	65.1	Lamin-A/C (70 kDa lamin)(Renal carcinoma antigen NY-REN-32) [Source:UniProtKB/Swiss-Prot;Acc:P02545]
3.81	2	-9.6	9.1	68.3	Polyadenylate-binding protein 1-like [Source:UniProtKB/Swiss-Prot;Acc:Q4VXU2]
4.29	2	-7.0	6.1	43.8	Proliferation-associated protein 2G4 (Cell cycle protein p38-2G4 homolog)(hG4-1)(ErbB3-binding protein 1) [Source:UniProtKB/Swiss-Prot;Acc:Q9UQ80]
3.38	1	-6.3	8.0	29.7	Guanine nucleotide-binding protein subunit beta-2-like 1 (Guanine nucleotide-binding protein subunit beta-like protein 12.3)(Receptor of activated protein kinase C 1)(RACK1)(Receptor for activated C kinase) [Source:UniProtKB/Swiss-Prot;Acc:P63244]
3.50	1	-5.1	7.7	38.9	Erlin-1 (Endoplasmic reticulum lipid raft-associated protein 1)(Stomatin-prohibitin-flotillin-HflC/K domain-containing protein 1)(SPFH domain-containing protein 1)(Protein KE04) [Source:UniProtKB/Swiss-Prot;Acc:O75477]
3.51	1	-5.0	4.9	104.6	AP-1 complex subunit beta-1 (Adapter-related protein complex 1 subunit beta-1)(Adaptor protein complex AP-1 subunit beta-1)(Beta-adaptin 1)(Beta1-adaptin)(Golgi adaptor HA1/AP1 adaptin beta subunit)(Clathrin assembly protein complex 1 beta large chain) [Source:UniProtKB/Swiss-Prot;Acc:Q10567]
3.54	1	-4.7	9.2	66.0	Nucleolar protein 5A (Nucleolar protein Nop56) [Source:UniProtKB/Swiss-Prot;Acc:O00567]
3.41	1	-4.5	8.5	80.2	Probable ATP-dependent RNA helicase DDX17 (EC 3.6.1.-)(DEAD box protein 17)(RNA-dependent helicase p72)(DEAD box protein p72) [Source:UniProtKB/Swiss-Prot;Acc:Q92841]
3.67	1	-3.8	6.2	77.0	Fragile X mental retardation syndrome-related protein 2 [Source:UniProtKB/Swiss-Prot;Acc:P51116]
3.27	1	-3.5	5.2	105.8	AP-2 complex subunit beta-1 (Adapter-related protein complex 2 beta-1 subunit)(Beta2-adaptin)(Beta-adaptin)(Plasma membrane adaptor HA2/AP2 adaptin beta subunit)(Clathrin assembly protein complex 2 beta large chain)(AP105B) [Source:UniProtKB/Swiss-Prot;Acc:P63010]

hFXR1p

Breakpoint cluster region protein 1

TIP-2

Lamin-A/C

Polyadenylate-binding protein 1-like

Her3-binding protein 1

RACK1

Erlin-1

AP1 complex subunit beta-1

Nucleolar protein Nop56

P72 (DDX17)

hFXR2p

AP2 complex subunit beta-1

Table5.1: Summary of proteins identified by mass spectrometry All identified proteins are listed on the table log(f) represents the sum of raw spectrum intensities, rl represents number of peptides discovered, log(e) represents expectation of finding a protein stochastically, pI represents the pI of the intact gene product and Mr represents the molecular mass of the intact gene product

5.3.5 Validation of SET9 interacting partners using immunoprecipitation

Having identified SET9 interacting proteins from the combined immunoprecipitation-mass spectrometry approach, the next step was to validate these interactions by co-immunoprecipitation experiments in LNCaP cells. The same procedure was used as above to examine the interaction of selected targets, but on a much smaller scale (4×10^8 cells). The same SET9 antibody and rabbit IgG control used in the IP above were used as described. Surprisingly, p72 a novel human member of the DEAD box family of putative

RNA-dependent ATPases and ATP-dependent RNA helicases) did not show an association with SET9 (Figure 5.8) (Lamm et al., 1996). To confirm this finding, an additional IP was performed in U2OS cells ectopically expressing SET9 and p72. Although expression of p72 was low, there was no detectable interaction between SET9 and p72 in these cells, suggesting that the two proteins may interact transiently and hence is difficult to detect by western analysis, that a particular spliced form of p72 interacts with SET9 that is not detected by western analysis or they are not binding partners (Figure 5.9).

Notably, western blot using RACK1 and Lamin A/C antibodies resulted in bands which were non-specific IgG bands and not a result of non-specific binding of the proteins to the IgG or beads. Interestingly, PARP1 western blot showed an evident interaction in the SET9 pull-down lane, however this was also the case in the IgG control pull-down, suggesting the importance of using IgG or beads as a negative control in immunoprecipitation when performing protein-protein interaction study. This finding was also in line with the previous published work in which PARP1 has been classified as a sticky protein which has the tendency to associate with beads (Trinkle-Mulcahy et al., 2008).In fact, some of identified proteins fall into the sticky protein categories including DEAD box protein p72 and Lamin A/C again supporting the rationale for using the controls (IgG/beads) in immunoprecipitation procedure in such instance.

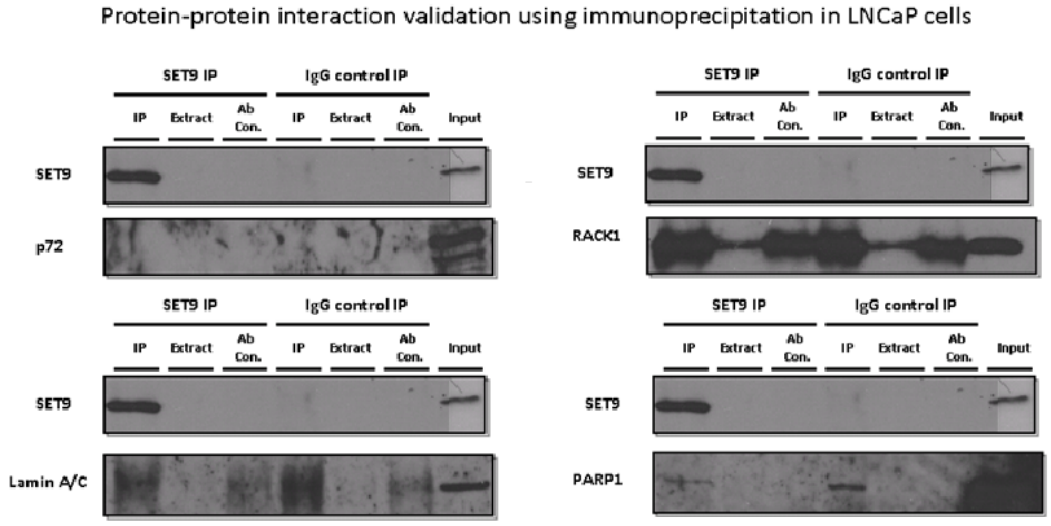

Figure 5.8 Western blot validation of selected SET9 interacting partners in LNCaP cells.
LNCaP cells were grown in complete medium and then subject to immunoprecipitation using rabbit SET9 antibody followed by individual western blot assays to detect interaction. SET9 pull-down was assessed by probing with mouse SET9 antibody. Samples were tested for interaction with p72, RACK1, Lamin A/C and

PARP1. Although Lamin A/C and PARP1 showed an interaction with SET9, the control IgG also interacted to a degree, indicating the potential non-specific binding of those two proteins with sepharose beads or random IgG. Extract is the control with no cellular contents and antibodies in but beads only. Input refers to the control with cellular contents pre-incubated with beads but on further downstream treatments.

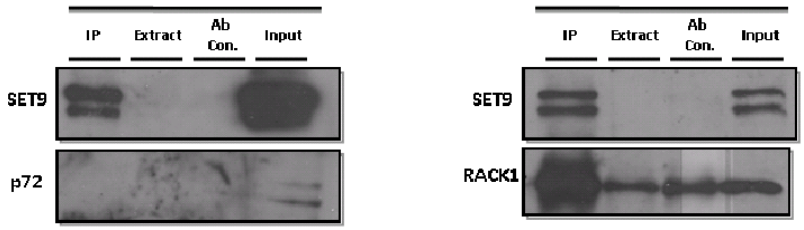

Figure 5.9 Validation of protein interaction between SET9 and p72/RACK1 in U2OS cells over-expressing SET9 and p72/RACK1.
U2OS cells were transiently transfected with the combination of SET9/p72 and SET9/RACK1, respectively. Cells were cultured for 48 hours and then subjected to immunoprecipitation using rabbit SET9 antibody. Western blot using either p72 or RACK1 showed no evident interaction between SET9 and p72/RACK1, although p72 was shown to be expressed in the Input lane. It was not possible to determine whether RACK1 was expressed, due to additional bands appearing in extract and antibody lanes. SET9 pull-down was verified using mouse SET9 antibody.

To examine the interaction of p72/SET9 and RACK1/SET9, overexpression system to test the interaction between SET9 and p72/RACK1 was used. When ectopic expression of p72 and RACK1 were induced in conjunction with ectopically expressed SET9 in U2OS cells, there was no overexpression of p72 and RACK1 observed. For p72 this might be due to the problem of the construct used and for RACK1 the postulation would be that the antibody used was not suitable or sensitive enough to detect RACK1 protein in western blot application and thus the likelihood of the interaction between these two proteins and SET9 still remains to be addressed (Figure 5.9).

Having established this system, attention was then focused on three other potential SET9 interacting proteins identified in the mass spectrometry approach, namely Fragile X Mental Retardation Syndrome-related protein 1 (FXR1), Tax interaction protein 2 (tip-2) also named PDZ domain-containing protein (GIPC1) and ErbB3 binding protein 1 (EBP1). In accordance with the mass

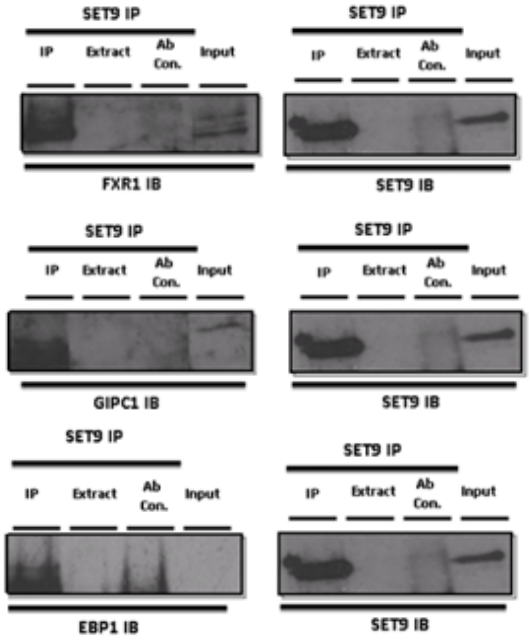

Figure 5.10 Western blot validation of interaction between SET9/FXR1, SET9/GIPC1 and SET9/EBP1 in LNCaP cells.
LNCaP cells were grown in serum-containing medium and then subject to immunoprecipitation using rabbit SET9 antibody followed by individual western blot assays to detect interaction. SET9 pull-down was assessed by probing with mouse SET9 antibody. Samples were tested for interaction with FXR1, GIPC1 and EBP1. FXR1 strongly interacted with SET9 as indicated by western blot and GIPC1 also showed a degree of interaction with SET9. Due to an antibody problem, EBP1 interaction with SET9 was not established. The reciprocal IP was also carried out using FXR1 and GIPC1 antibodies respectively under the same conditions. Western blot using SET9 antibody confirmed the association between SET9/FXR1 and to a lesser extent with SET9/GIPC1. Pull-down efficiency was verified using FXR1 and GIPC1 antibodies, respectively.

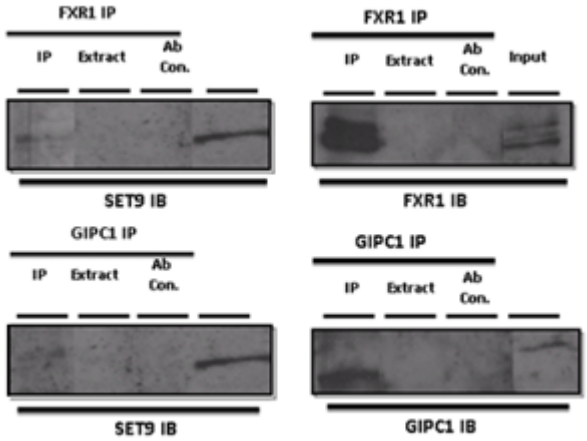

Figure 5.11 Reciprocal immunoprecipitation of SET9/FXR1 and SET9/GIPC1.
LNCaP cell lysates were prepared in the same way as mentioned above. The reciprocal IP was also carried out using FXR1 and GIPC1 antibodies respectively under the same context. Western blot using SET9 antibody confirms the association between SET9/FXR1 and to a lesser extent with SET9/GIPC1. Pull-down efficiency was verified using FXR1 and GIPC1 antibodies respectively.

spectrometry findings, using SET9 antibody to immunoprecipitate the protein complex and probing with FXR1 and GIPC1. The physical association of these two proteins with SET9 in LNCaP cells was confirmed with a particularly strong interaction between SET9 and FXR1 (Figure 5.10). The interaction between EBP1 and SET9 was also tested, however, due to the problem with the antibody (see Chapter 6) it was difficult to establish an interaction between them (Figure 5.10). Additionally, the bona fide interaction of FXR1 and GIPC1 with SET9 was tested by means of reciprocal immunoprecipitation again reconfirming the reliability of the data achieved through the mass spectrometry analysis (Figure 5.11).

5.4 Discussion

The data from previous chapters suggested two general conclusions, one was that SET9 is involved in AR-mediated transcription regulation and the second is that SET9 plays anti-apoptotic roles in LNCaP cell apoptosis in response to the DNA damaging agent Doxorubicin, in a p53-dependent manner. In order to decipher the molecular mechanisms underlying these disparate findings, a series of immunoprecipitation based approaches and mass spectrometry tools were used to identify novel SET9 interacting proteins. It was hypothesised that identifying protein interacting partners of SET9 has the potential to provide clues to the role of SET9 in these pathways.

Initially, a stable FLAG-tagged SET9 expressing HeLa cell line was generated for this purpose. However, due to the relative low expression of the exogenous FLAG-SET9 in cells, it was difficult to proceed further with this model as immunoprecipitating sufficient amounts of FLAG-SET9 for subsequent mass spectrometry analysis would not be achieved. Although difficult to explain, the failure to express large amounts of SET9 in HeLa cells may be due to an increase in apoptosis or aberrant growth such that the only surviving clones expressed very low amounts of the ectopic enzyme. Indeed, this claim is backed-up by evidence from a higher-expressing SET9 clone (Figure 5.4) that displayed severe growth inhibition and underwent severe morphological changes in culture. Importantly, although SET9 was initially identified from HeLa cells as a histone methyltransferase, the direct evidence to suggest phenotypic roles of SET9 in HeLa cells is still lacking and the only SET9 involved molecular mechanism in HeLa cell line was related to its physiological interaction with and methylation of TAF10 containing transcription initiation complex (Kouskouti et al., 2004). Interestingly, it is also noted that in some studies conducted to identify protein complexes using the same combined IP-mass spectrometry strategy, researchers used more than 100 150mm culture plates of cells in order to achieve enough material for protein identification (Patel et al., 2007; Lee et al., 2006b). Therefore, the expansion may be required to scale up samples to render the acquisition of sufficient materials for the purpose of protein identification. Furthermore, given that SET9 has significant toxicity to the growth of HeLa cells, an inducible system may be desirable to establish

regulatable expression in the cell line, which would resolve the adverse effect of ectopic expression of SET9 in HeLa cells.

Having failed using the HeLa cell-based model, LNCaP prostate cancer cells were subsequently utilized as an alternative model system for identifying SET9-associating proteins. A major advantage for this system was that it made use of the high level of endogenous SET9 in these cells that would maximize the attainability of physiologically relevant interacting proteins from a cell line that is relevant to previous studies of SET9 in the AR signaling cascade. Several proteins were discovered using this experimental approach. Upon acquisition of the data by mass spectrometry, interaction of the targets was then assessed using conventional immunoprecipitation and Western blot analysis. The limited availability of antibodies in-house did not enable an assessment of all targets on the list, including Breakpoint cluster region protein 1, Erlin-1, AP1 complex subunit beta-1, Nucleolar protein Nop56, hFXR2P and AP2 complex subunit beta-1. It was however possible to investigate p72, LaminA/C, PARP1, RACK1, FXR1, GIPC1 and EBP1. Amongst those proteins tested by immunoprecipitation the DEAD box RNA helicase p72 failed to show an interaction with SET9 and also due to the failure to over-express p72 in U2OS cells, it was difficult to confirm the interaction between SET9 and p72 (Lamm et al., 1996) . Similarly to p72, the establishment of the interaction between RACK1, a receptor for activated C kinase and SET9 failed due to antibody cross-reactivity (Chang et al., 1998). With regard to PARP1 and Lamin A/C, there appeared to be a specific interaction of these two proteins with SET9, however, the IgG control also showed similar interaction pattern with PARP1 and Lamin A/C suggesting that the interaction might not truly exist in LNCaP cells and rather possibly due to a non-specific interaction between IgG and PARP1 and Lamin A/C. Additional supporting evidence comes from the recent proteomic based analysis after immunoprecipitation which suggested that sepharose beads based protein purification would potentially co-purify many proteins that are associated with beads rather than antibodies of interest. Lamin A/C and PARP1 turned out to fall into this group of proteins (Trinkle-Mulcahy et al., 2008). Therefore, the assumption is that the interactions observed were possible artifacts rather than genuine protein-protein interactions. Towards this end, a proper explanation of why those proteins interacted with the sepharose

matrix in the mass spectrometry samples is still lacking, however it is important to highlight that many proteins found on the list were potential bead associated proteins, such as the DEAD box protein family, eukaryotic translation initiation and elongation factors, heat shock proteins, histones, hnRNP proteins, ribosomal proteins and cytoskeletal/structural/mobility proteins. Thus, the DEAD box protein p72 that was identified on the list might be a pseudo SET9 interacting protein (Trinkle-Mulcahy et al., 2008).

Subsequently, the study focused on the three proteins FXR1, GIPC1 and EBP1. FXR1 is positioned top of the list with the highest significance represented by the lowest log (e) value and the FXR2 which is firmly associated with FXR1 was also co-purified in the SET9 containing complex, therefore this is believed to be a strong candidate partner for SET9 interaction (Zhang et al., 1995). GIPC1 (TIP-2) was also chosen due to the significance of the log (e) value and its potential participation in various cell signalling pathways such as G protein-coupled receptor pathway, receptor tyrosine kinase pathway and TGF-β signalling (Blobe et al., 2001; Lou et al., 2001). EBP1 was also selected as this protein is an AR co-repressor which plays a prohibitive role in hormone resistant prostate cancer and thus its association with the AR co-activator SET9 might indicate a co-regulatory mechanism on the receptor in LNCaP cells (Zhang et al., 2008; Zhang et al., 2005b). In keeping with our assumption, the immunoprecipitation confirmed the interaction between SET9 and FXR1 and GIPC1 respectively and this was also verified by reciprocal immunoprecipitation using FXR1 and GIPC1 antibodies. Unfortunately, the association between SET9 and EBP1 could not be observed due to the antibody for Western blot analysis, which will be explained in the next chapter.

Notably, the reciprocal immunoprecipitation did not demonstrate a similarly intense interaction as that observed following pull-down by SET9 antibody and this was particularly evident with FXR1. This may be due to partial blockage of epitopes on the protein-protein interacting interface, which potentially made the FXR1 antibody binding sites inaccessible. In summary, a combination of immunoprecipitation and LC-MS/MS identified multiple protein binding partners for SET9, which were confirmed by conventional immunoprecipitation. Regardless of all problems encountered, there was a pronounced interaction

between SET9 and FXR1 in LNCaP cells and to a lesser extent with GIPC1, both proteins were further studied in the following chapter.

Chapter 6

Investigating the role of FXR1 and GIPC1 in SET9 function

6.1 Introduction

The discovery of the SET9-interacting partners FXR1 and GIPC1 may help to further our understanding of the mechanisms at play that regulate SET9 in processes such as transcription control, cell cycle regulation and apoptosis.

FXR1 (Fragile X Mental Retardation Syndrome Related protein 1) was identified as an RNA binding protein which is homologous to FMR1 (Fragile X Mental Retardation 1), a key protein whose expression is important for the development of Fragile X Mental Retardation Syndrome (Siomi et al., 1995). Similar to FMR1, the protein sequence of FXR1 contains two KH domains which mediate RNA recognition and RNA binding and an RGG box which mediates poly G and poly U containing RNA recognition and binding (Siomi et al., 1995). Early data also proved that FXR1 is predominantly distributed in the cytoplasm in various cell types and tissues implying its potential role in gene regulation at post-transcriptional level possibly through binding of 3'UTR of mRNA (Siomi et al., 1995). Subsequent findings demonstrated that FXR1 interacts with its homologues FXR2 and FMR1; each of the three proteins is capable of forming heterodimers with the others, and each can also form homodimers. All complexes have been shown to associate with ribosomal 60S subunits indicating key roles in translation and mRNA transport and metabolism (Siomi et al., 1996; Zhang et al., 1995). In addition to the KH domain, FXR1 also contains a nuclear export signal (NES) and a nuclear localization signal (NLS) which mediates the nuclear cytoplasmic shuttling of the protein and this seems to correlate with mRNA export from the nucleus (Bardoni et al., 2001; Tamanini et al., 1999). Additional studies have shown that the FXR1 transcript is alternatively spliced and in mammalian cells, there have been seven splice variants identified each with differential expression in various mammalian tissues and cells (Khandjian et al., 1998). Further characterization of FXR1 revealed that it is a human autoantigen which is re-distributed to punctuated foci in response to apoptosis suggesting a role in autoimmune response and cell death pathways (Bolivar et al., 1998). Additionally, FXR1 has also been characterized as a translation repressor of tumour necrosis factor (TNF) further supporting its role in gene regulation at the post-transcriptional level (Garnon et al., 2005). To date, there is no direct link between SET9 and FXR1 and even

the implication of FXR1 in prostate cancer has not yet been established. Therefore, the discovery of FXR1 as a binding partner of SET9 raised intriguing hypotheses which may potentially address SET9 mediated cellular and molecular mechanisms in the progression of prostate cancer.

GIPC1 (GAIP-interacting protein C terminus) is a scaffolding protein which functions in conjunction with GAIP in a G protein-coupled signalling complex to regulate cell surface receptor expression and trafficking. Like other GIPCs family members, it contains a highly conserved PDZ domain which interacts with RGS-GAIP, a GTPase-activating protein (GAP) for Gai subunits and a C-terminal acyl carrier protein domain which implies a putative function in the acylation of vesicle-bound proteins (Katoh, 2002; De Vries et al., 1998). This protein, to date has been implicated in various cell signalling pathways through the direct interaction with some key molecules. GIPC1 binds to TrkA a tyrosine kinase receptor and inhibits MAP kinase pathway activation indicating its bridging mechanism between the G protein signalling and MAP kinase pathway (Lou et al., 2001). The roles of GIPC in other signalling pathways were also suggested, such as WNT signalling, insulin-like growth factor receptor and transforming growth factor-β receptor mediated cellular communication and signal transduction, based upon various model systems (Lee et al., 2008; Katoh, 2002). Due to its comprehensive roles in signal transduction, the correlation between GIPC1 and cancer has also been established. In both cell lines and clinical samples. GIPC1 mRNA was found highly expressed in gastric, pancreatic, colorectal and lung cancers compared to bone marrow and peripheral blood leukocytes (Kirikoshi and Katoh, 2002). Additionally, in GIPC1 knock-out mice, the animals exhibited strong growth inhibition of pancreatic tumour cells through the inhibition of interaction between tyrosine kinase receptor IGF-1R and GIPC1 indicating its tumour initiating potential and a feasible therapeutic target (Muders et al., 2007). As is the case with FXR1, there is no direct link between GIPC1, SET9 and prostate cancer and thus the objective of the study was to characterise role of the FXR1 and GIPC1 in SET9 regulation of AR function and apoptosis.

6.2 Specific materials and methods

The composition and suppliers of the majority of the reagents and materials can be found in the general materials and method (Chapter 2.1). Otherwise, the materials and reagents are specified in individual chapters where appropriate.

6.2.1 Sequential immunofluorescence and confocal microscopy

LNCaP cells were grown in 8-well chamber slides in serum-containing media for 48 hours and then washed in cold PBS prior to fixation in methanol for 10 mins. Fixed cells were subsequently washed in PBS before incubating with blocking buffer for 30 mins at room temperature (1% BSA and 1% Triton-X 100 and 10% serum from the species that the secondary antibody was raised in). Cells were then washed in PBS three times for 5 mins each and then incubated with an anti-FXR1 antibody at a dilution of 1:200 in 1% BSA in Tween-PBS in a humidified chamber for 1 hr at room temperature. Cells were washed in PBS three times for 5 mins and then incubated with rabbit anti-goat TRITC secondary antibody in 1% BSA in PBS for 1 hour in the dark. After the first round of antibody labelling, cells were treated as before with the same procedure with the exception of using an anti-SET9 primary and swine anti-rabbit FITC-conjugated secondary antibodies. All steps were performed in the dark to prevent the loss of fluorescence. After the PBS wash step post secondary antibody, cells were counterstained and mounted using DAPI-containing mounting solution (Vectashield). Slides were subsequently analysed using a Leica TCS SP2UV confocal microscopy system in the Bio-Imagine Unit in the Medical School, Newcastle University. Upon data acquisition, the co-localization coefficient was analysed by ImageJ software.

6.2.2 Immunohistochemistry

To test if the FXR1 and GIPC1 antibodies were suitable for immunohistochemistry, prostate tissue sections and test Tissue Microarray (TMA) made available within the Solid Tumour Target Discovery group were initially used. Slides containing the prostate tissue sample were baked at 60 ℃ for 2 hours to prevent tissue loss during the procedure and then de-paraffinized

in two sequential xylene washes for 10 mins each. Slides were hydrated for 5 minutes each in sequential washings of 100%, 75% and 50% ethanol and water. The removal of endogenous peroxidise activity was conducted by incubating slides with hydrogen peroxide solution (3 ml of hydrogen peroxide in 180 ml methanol) for 10 mins followed by washing in running tap water and PBS wash, both for 5 mins. Antigen retrieval was subsequently performed by incubating in citrate buffer pH 6.5 in the Decloaking chamber (Biocare Medical) with the following settings: 125℃ for 3 mins and then 90℃ for 10 secs. After antigen retrieval, tissue slides were transferred to tap water for 2 mins and then PBS prior to tissue outlining with a PAP pen (DAKO) and incubation with 200-300 µl of blocking serum (PBS plus 10% serum of the species from which the secondary antibody was raised from) for 20 mins at room temperature. Subsequently, the blocking serum was drained off and appropriate strength and volume of primary antibody was added to each slide (1:250 to 1:500 dilutions of FXR1 or GIPC1 antibodies in PBS) for overnight incubation at 4 ℃. The following day, slides were washed twice in PBS for 5 mins each then incubated with biotinylated secondary antibodies at a 1: 250 dilution in PBS for 30 mins at room temperature. Slides were then washed twice in PBS for 5 mins each and incubated with ABC detection solution (Vectorlabs) for 30 mins (1% of A and 1% of B of the ABC kit in PBS). After two PBS washes for 5 mins, Diaminobenzidine tablets made (DAB) solution was prepared (1 Au tablet and 1Ag tablet (Sigma) in 5 ml of deionised water) and applied to the slides until visible colour change in the tissue was observed. Immediately after, slides were transferred to running water for 5 mins and then counterstained in fresh Harris' haematoxylin for 90 seconds followed by acid alcohol incubation (1% of concentrated HCl in 100% ethanol) for 10 seconds and subsequent running tap water for 3 mins. Slides were then dehydrated using the reverse steps to the rehydration steps and finally mounted with DPX mounting medium with appropriate sized cover slips. Slides were visualized and analysed using an in-house Aperio Imagining System.

6.2.3 Statistical analysis and other experimental tools

The protein co-localization coefficient was achieved using the ImageJ software and all FACS based experimental data were analyzed using two-sample paired

t-test and a p-value cut-off of 0.05 was used to evaluate the significance of data compared.

FACS and Western blotting were performed in this chapter, but described in detail within chapter 2. All antibody dilutions are stated in Table 2.9 in Chapter 2.

6.3 Results

6.3.1 Verifying protein-protein interaction in cells

Data presented in Chapter 5 demonstrated that endogenous FXR1 and GIPC1 interacted with SET9 in LNCaP cells (see Figure 5.10/5.11). To confirm this interaction, FXR1, GIPC1, EBP1 and SET9 were ectopically expressed in U2OS cells and subject to immunoprecipitation. Prior to this experiment, however, expression of the individual constructs including the three isoforms, -E, -F and -G of FXR1 (structures are listed below), FLAG-tagged GIPC1 and both FLAG-EBP1 and GFP-EBP1 were tested in U2OS cells. Importantly, as discussed in Chapter 5, the EBP1-SET9 interaction was unable to be confirmed in LNCaP cells due to a presumed failure of the antibody for immunoprecipitation and Western analysis. Therefore, using an over-expression system, the interaction between SET9 and EBP-1 had the potential to be confirmed. As shown in Figure 6.1, the FXR1 isoforms E, F, G and GIPC1 were all over-expressed and detected by FXR1 and either GIPC1 or Flag antibodies. Over-expression of Flag-EBP1 was only identified by Western analysis using a Flag antibody, but not the EBP1 antibody confirming our notion that the EBP1 immunoglobulin is unsuitable for protein detection by immunoblotting.

A.

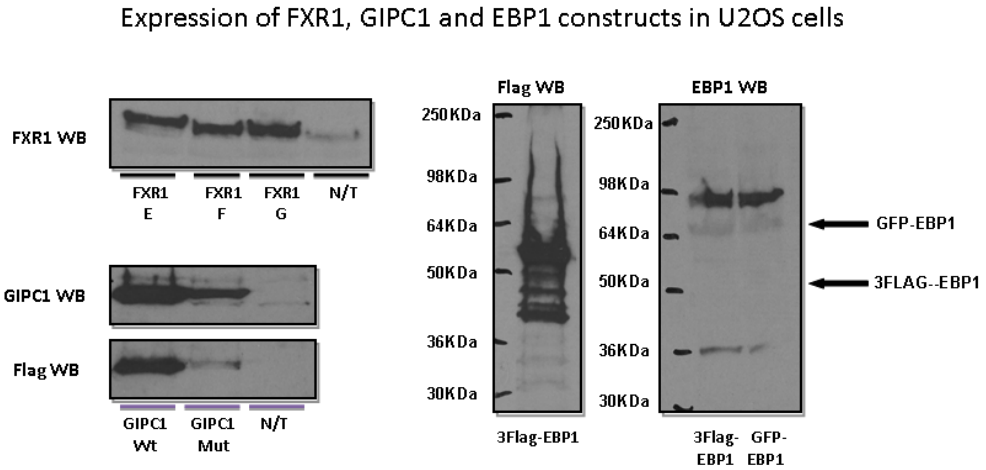

B.

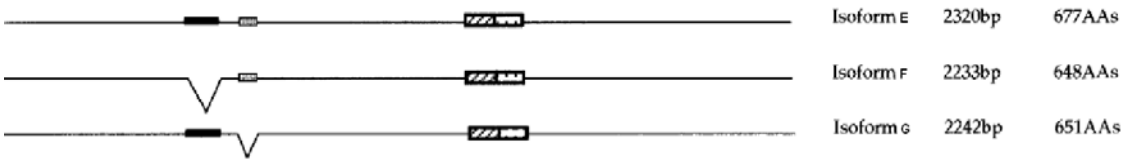

Figure 6.1 Validation of FXR1, GIPC1 and EBP1 expression in U2OS cells and schematic structures of FXR1 splicing variants E, F and G.
(A) Western blot shows the transient expression of FXR1 isoforms E, F and G, FLAG-GIPC1 wild-type and mutant, FLAG- EBP1 and GFP-EBP1 in U2OS cells detected by FXR1, GIPC1, FLAG antibody. (B) Structural representation of FXR1 E, F and G. The black box represents the 87-bp insert at position 1035 of the cDNA. The darkly striped box next to the black box represents a 78bp insert at position 1286 of the cDNA. The striped box represents 81bp insert at position 1690 of the cDNA and the lightly striped box represents a 92bp insert at position 1772 of the cDNA.

Having validated each construct by transient transfection, interactions between over-expressed SET9 and either FXR1, GIPC1 and EBP1 were examined by immunoprecipitation. Unlike the strong interaction observed in LNCaP cells between SET9 and FXR1, a weaker interaction between SET9 and the three FXR1 isoforms was observed in U2OS cells (Figure 6.2, upper left panels), even though the ectopic expression of each protein was comparable to the endogenous level in LNCaP cells (see Figure 5.10). Consistent with the findings from LNCaP cells, ectopically expressed GIPC1 interacted with SET9, confirming the interaction between these proteins (Figure 6.2, lower left panel). Unfortunately, probing SET9 immunoprecipitates with a Flag antibody failed to detect ectopically expressed Flag-EBP1 suggesting that this interaction may not be detectable using methods utilised here or might not exist naturally in U2OS cells (Figure 6.2, lower right panel).

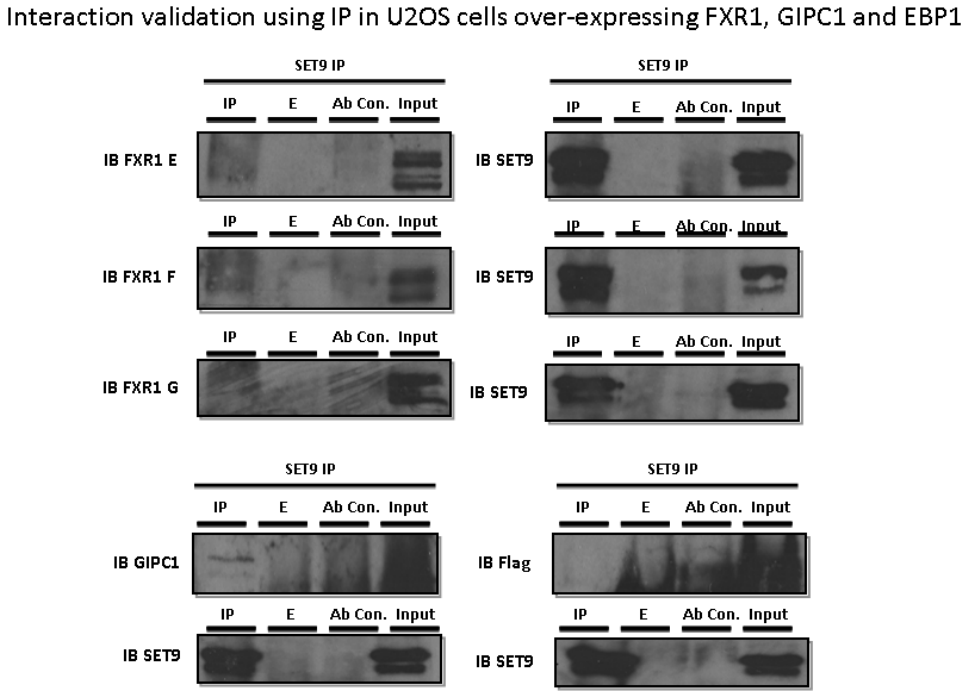

Figure 6.2: Interaction of SET9 with FXR1, GIPC1 and EBP1.
U2OS cells were transiently transfected with vectors in the following combinations (SET9/FXR1 E, F, G isoforms, SET9/GIPC1 and SET9/EBP1). Immunoprecipitation was carried out using Rabbit SET9 antibody. Western blots show the interaction of ectopically and/or trace amount of endogenously expressed FXR1 E, F, G with SET9 as well as GIPC1 with SET9.The pull-down efficiency was verified using the Mouse SET9 antibody shown above.

6.3.2 Assessment of FXR1, GIPC1 and SET9 co-localisation by confocal microscopy

The interaction between FXR1 and GIPC1 with SET9 in both LNCaP and U2OS cells confirmed the initial mass spectrometry data and subsequently led to the assumption that both newly identified proteins would co-localise with SET9 in cells. FXR1 has been shown to be predominantly cytoplasmic (Siomi et al., 1995), which is consistent with data in Chapter 3, demonstrating cytoplasmic distribution of SET9 in LNCaP cells (Figure 3.7). In keeping with the hypothesis that both FXR1 and SET9 co-localise in cells, immunofluorescence in combination with confocal microscopy demonstrated that both proteins display predominantly

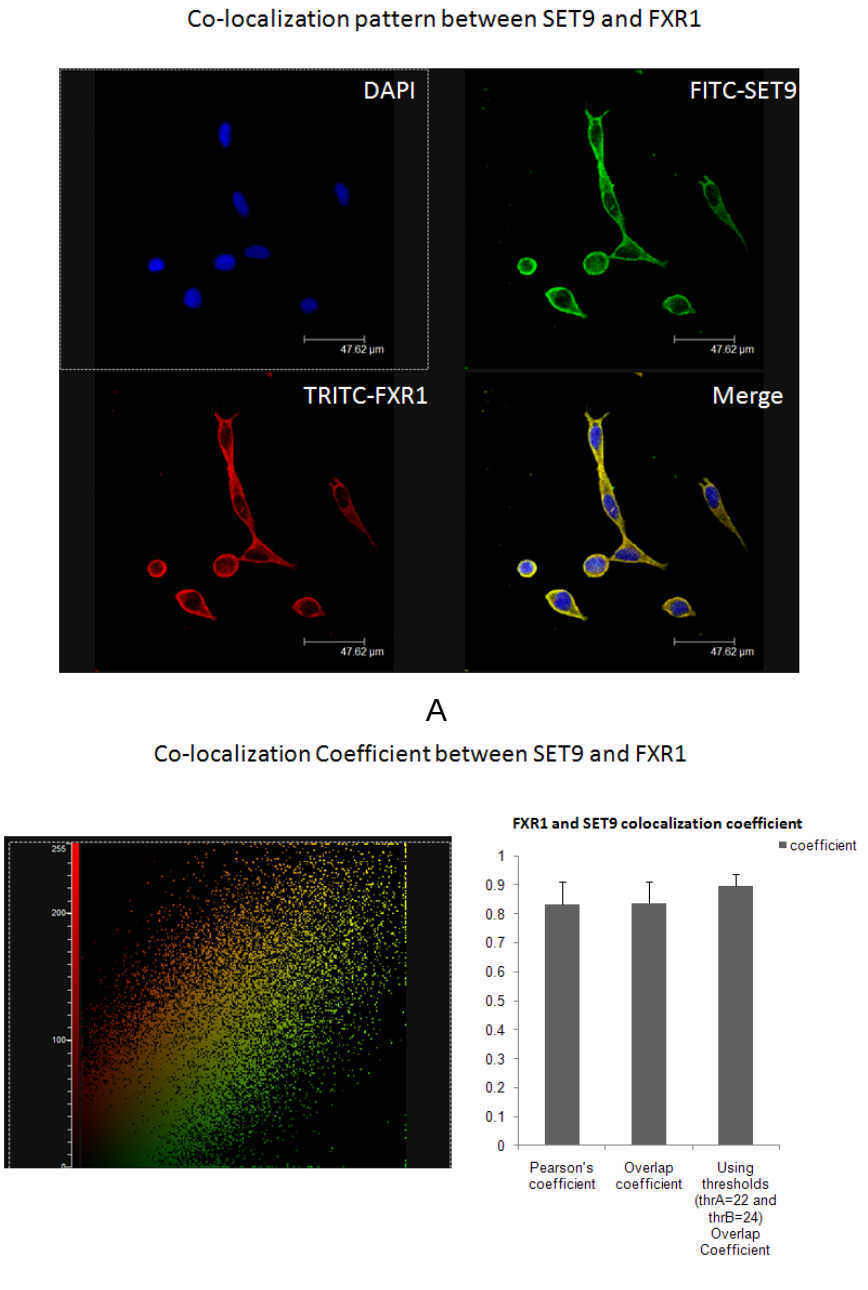

Figure 6.3 Co-localization of SET9 and FXR1 in LNCaP cells.
(A) LNCaP cells were grown in chamber slides in serum-containing medium. SET9 and FXR1 were detected by immunofluorescence staining with FXR1 (TRITC) and SET9 (FITC) antibodies and observed using confocal microscopy. (B) The scatterplot displays the intensity of co-localization between SET9 and FXR1 as shown in orange and yellow, respectively due to the merging of red and green pixels. The bar chart shows the co-localization coefficient between SET9 and FXR1, which was calculated by the ImageJ program. Experiments were performed in duplicates and repeated three times. Error bars represent the standard deviation from three independent experiments.

cytoplasmic distribution patterns in LNCaP cells (Figure 6.3, upper panel). Moreover, based upon the scattered plot and various means of coefficient analysis, approximately 80% to 90% of both proteins overlapped, which was

indicative of a strong correlation between the co-localisation of the two proteins in LNCaP cells (Figure 6.3, lower panel).

With regard to the distribution of GIPC1 and SET9, similar to the association between SET9 and FXR1, both GIPC1 and SET9 showed predominant staining in the cytoplasmic compartment (Figure 6.4, upper panel) which was confirmed

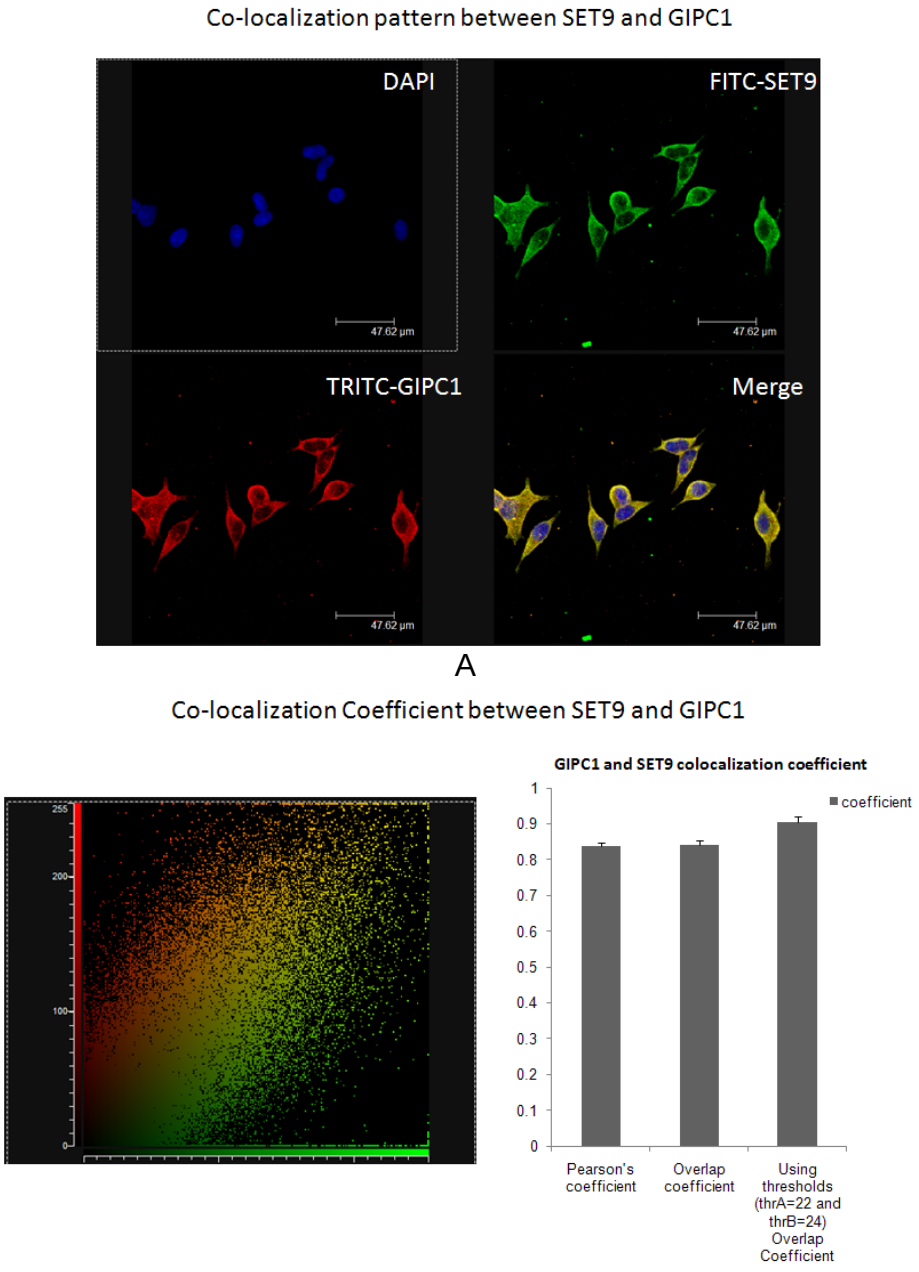

Figure 6.4 Co-localization of SET9 and GIPC1 in LNCaP cells.
(A) LNCaP cells were grown in chamber slides in complete medium. SET9 and GIPC1 were detected by immunofluorescent staining with GIPC1 (TRITC) and SET9 (FITC) antibodies consecutively and followed by confocal microscopy. (B) The scatterplot displays the intensity of co-localization between SET9 and GIPC1 as shown in orange and yellow due to the merging of red and green pixels. The bar chart shows the co-localization coefficient between SET9 and GIPC1, which was calculated by the ImageJ.Experiments were performed in duplicates.

by an 80% co-localisation efficient calculated by the ImageJ software (Figure 6.4, lower panel). Together, these data indicate a close link between SET9 and both FXR1 and GIPC1 at the cellular level.

6.3.3 Effect of silencing FXR1 and GIPC1 on SET9 knockdown induced apoptosis in LNCaP cells

In light of the interaction and co-localisation pattern between FXR1 and GIPC1 with SET9, a role for FXR1 and GIPC1 in SET9 regulation was next addressed. As described in Chapter 4, SET9 is a negative regulator of LNCaP apoptosis induced by Doxorubicin. Therefore, to begin the functional analysis of FXR1 and GIPC1 in SET9 activity, the first experiment was to determine the impact of FXR1 and GIPC1 depletion on SET9 knockdown-induced apoptosis in LNCaP cells.

Knockdown of both FXR1 and GIPC1 using siRNA was firstly optimised in LNCaP cells and Figure 6.5 below shows preliminary conditions applied to gain the optimal condition for the subsequent caspase-3 apoptosis assay with the dual knockdown of FXR1/GIPC1 and SET9. Having achieved the best conditions for the knockdown (Table 2.8 in Chapter 2), caspase-3 apoptosis assays were performed in LNCaP cells depleted of both SET9 and either FXR1 or GIPC1 and treated with 200 nM Doxorubicin. As expected, SET9 knockdown caused a significant increase in LNCaP cell apoptosis. Interestingly, although FXR1 knockdown alone had negligible effect on LNCaP cell apoptosis, depletion of both FXR1 and SET9 completely negated the effect of SET9 knockdown-induced apoptosis suggesting a role for FXR1 in driving LNCaP cell apoptosis in response to SET9 depletion (Figure 6.6).

In parallel experiments investigating the function of GIPC1 in LNCaP cell apoptosis, it was found that depleting GIPC1 alone enhanced LNCaP cell apoptosis to levels equivalent to that of SET9 knockdown (Figure 6.7, upper panel). Interestingly, dual knockdown of both proteins failed to further enhance the degree of apoptosis seen with individual protein depletions, suggesting that GIPC1

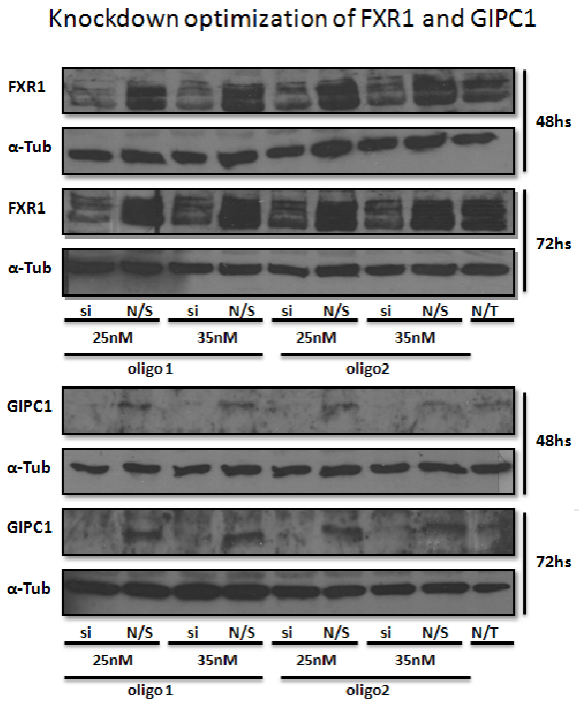

Figure 6.5 Optimization of FXR1 and GIPC1 knockdown in LNCaP cells.
LNCaP cells were reverse transfected with oligonucleaotides specifically designed against FXR1 and GIPC1 at concentrations of 25 nM. Cells were left for 48 or 72 hours post-transfection. Assessment of knockdown efficiency was conducted using Western blot analysis using either FXR1 or GIPC1 antibodies.

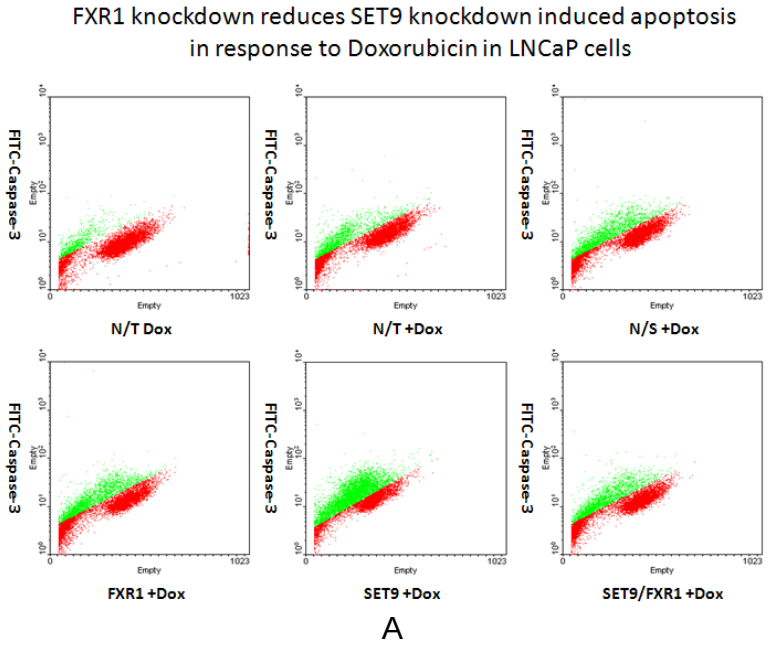

A

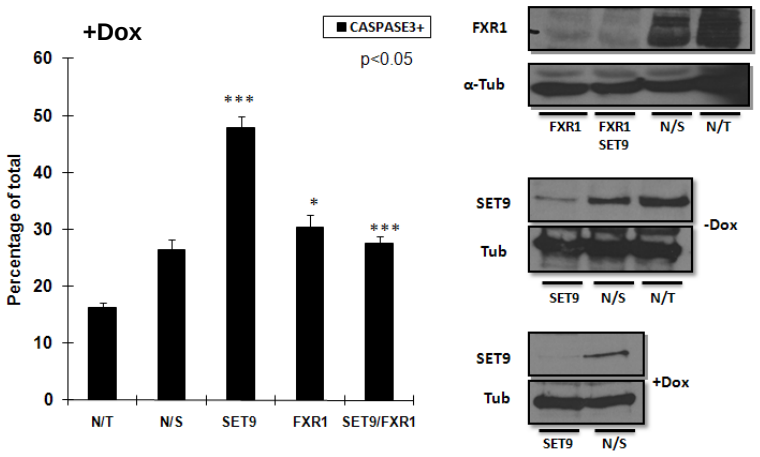

B

Figure 6.6 Ablation of FXR1 attenuates SET9 knockdown induced apoptosis in response to Doxorubicin treatment in LNCaP cells.

(A) LNCaP cells were transfected with SET9, FXR1 and FXR1/SET9 siRNA, then incubated for 72 hours and followed by Doxorubicin treatment (200nM) for 24 hours. Cells were then collected for FACS based caspase-3 apoptosis assay. The dot plots represent the dramatic decrease of SET9 silencing mediated apoptosis upon the additional knockdown of FXR1. The effect of Doxorubicin was demonstrated by the control LNCaP cells with or without Doxorubicin treatment. (B) Bar chart represents the complete inhibition of apoptosis with the dual knockdown of SET9 and FXR1 compared to SET9 knockdown only ($p<0.05$). All knockdown was checked correspondingly by western blot and experiments were performed in triplicates. (-Dox: cells without Doxorubicin treatment, +Dox: cells with Doxorubicin). The number of asterix indicate the statistical significance of the T-test analysis with one representing the significance under 0.05, two for under 0.005 and three for under 0.0005.

may function in the same pathway as SET9 to regulate apoptosis in LNCaP cells.

Considering the observation that FXR1 knockdown attenuates up-regulation of LNCaP cell apoptosis in response to SET9 depletion, combined with the fact that FXR1 directly interacts with SET9 which is a p53-interacting protein, it was hypothesised that FXR1 interacts with p53. In agreement with this assumption, immunoprecipitation experiments performed in LNCaP cells using an FXR1

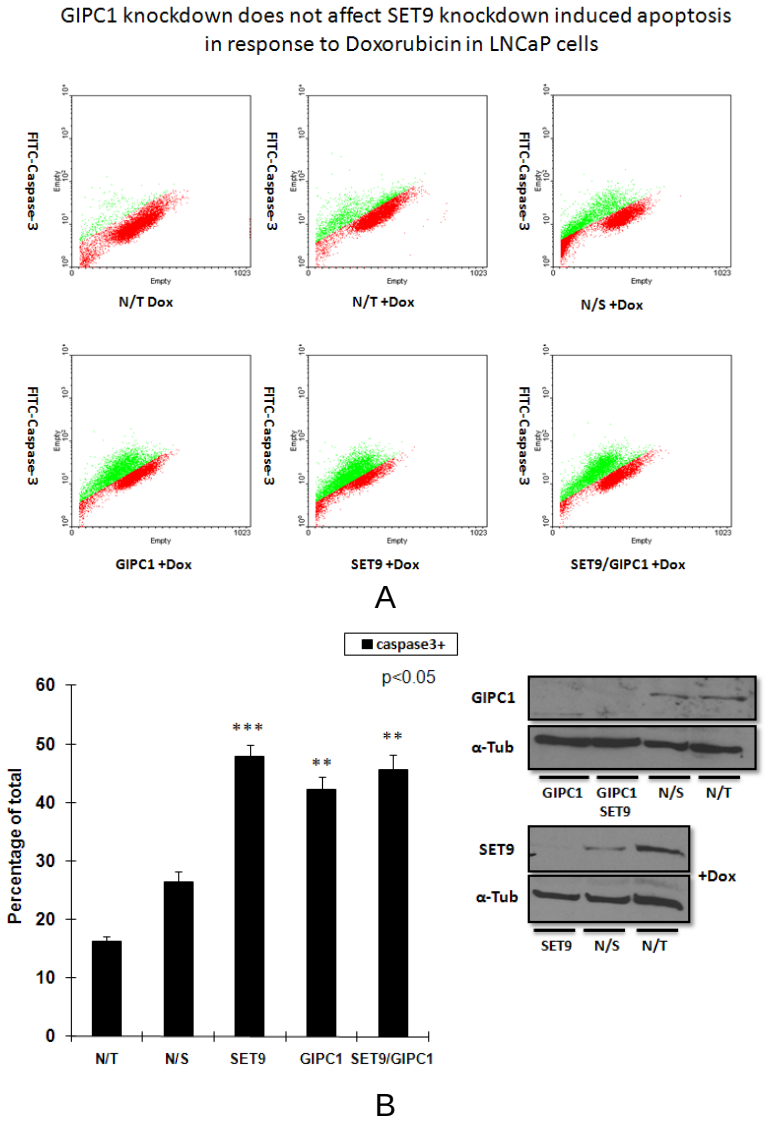

Figure 6.7 Ablation of GIPC1 has no additive effect on SET9 knockdown induced apoptosis in response to Doxorubicin treatment in LNCaP cells.
(A) LNCaP cells were transfected with SET9, GIPC1 and GIPC1/SET9 siRNA, incubated for 72 hours followed by Doxorubicin treatment (200nM) for 24 hours. Cells were then collected for FACS-based caspase-3 apoptosis assays. The dot plots represent an increase of apoptosis induced by GIPC1 silencing, whereas the dual knockdown of SET9 and GIPC1 showed no additional effect compared to SET9 knockdown alone. (B) Bar chart represents the impact of individual or combinational knockdown on LNCaP apoptosis ($p<0.05$). All knockdown was checked correspondingly by western blot and experiments were performed in triplicates.

antibody followed by p53 Western blotting showed an interaction between FXR1 and p53, both in the presence and absence of 200 nM Doxorubicin (Figure 6.8). Notably, when Doxorubicin was induced, there was a stabilization of FXR1 observed, which can be seen in Figure 6.8 and other experiments (data not shown) suggesting a possible DNA damage induced regulation of FXR1 turnover, which might be of potential research interests.

It is also worth mentioning that although FXR1 knockdown alone did not affect LNCaP cell apoptosis, when FXR1 was silenced, LNCaP cells exhibited neural extension and migration growth pattern compared to the scrambled siRNA control, indicating a potential role of FXR1 controlling LNCaP cell morphology (Figure 6.9). This resembles the neuroendocine LNCaP cell differentiation effect induced by some other proteins such as Snail transcription factor and IL-6 and Cyclic-AMP dependant kinase co-treatment (Deeble et al., 2001; McKeithen et al.).

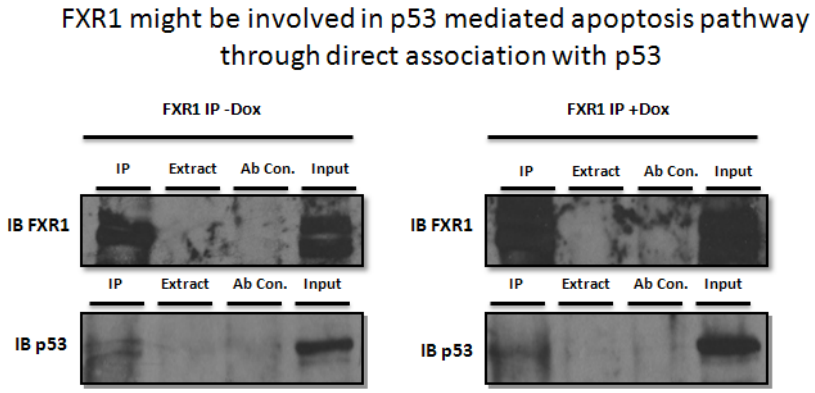

Figure 6.8 FXR1 interacts with p53 in the presence and absence of Doxorubicin in LNCaP cells.
Immunoprecipitation in LNCaP cells was carried out using FXR1 antibody and western blot using a p53 antibody showed the interaction between endogenous FXR1 and p53 both in the presence and absence of Doxorubicin induction.

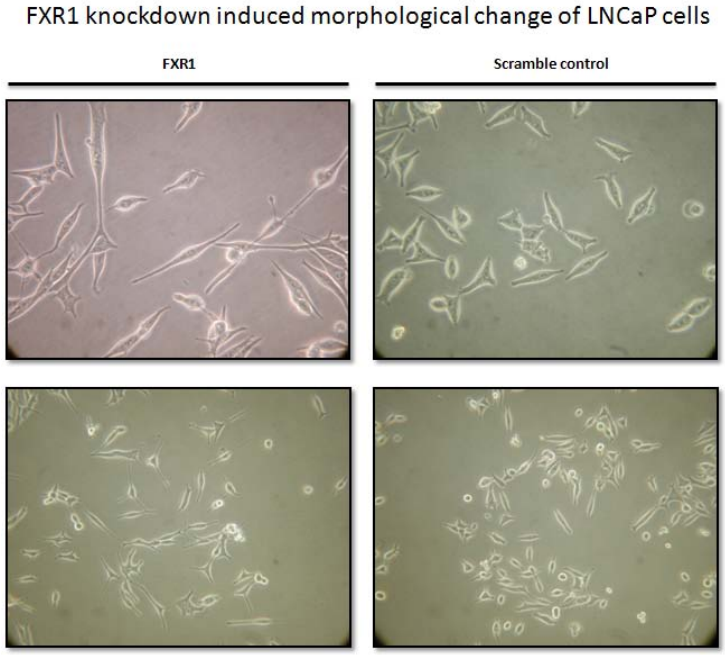

Figure 6.9 FXR1 affects LNCaP cell morphology.
LNCaP cells were transfected with FXR1 or scrambled siRNA in complete medium and after 48 hours of transfection, neuroendocrine like growth patterns were observed in FXR1 knockdown cells. The upper panels are x20 magnification and lower panels are x10 magnification.

6.3.4 Effect of FXR1, GIPC1 and EBP1 on AR mediated transcription regulation

Given that SET9 is an AR co-regulator, a potential role for FXR1 and GIPC1 in SET9-mediated AR co-activation was then addressed as a means of furthering our understanding of these proteins in SET9 regulation. In this series of experiments, HEK293T cells were transiently transfected with AR, SET9 and increasing amounts of GIPC1 and the three splicing variants of FXR1. Using the androgen-responsive AREIII luciferase reporter, it was found that SET9-mediated AR transactivation was attenuated by GIPC1, while GIPC1 itself partially co-activated AR mediated transcription in the absence of SET9, although this change was not significant (Figure 6.10).

Surprisingly, unlike what has been found previously in the literature (Zhang et al., 2005a), the known androgen receptor co-repressor EBP1 had no pronounced impact on the luciferase reporter activity either in the presence or absence of SET9 regardless of the negligible co-activating impact on AR mediated transactivation (Figure 6.10).

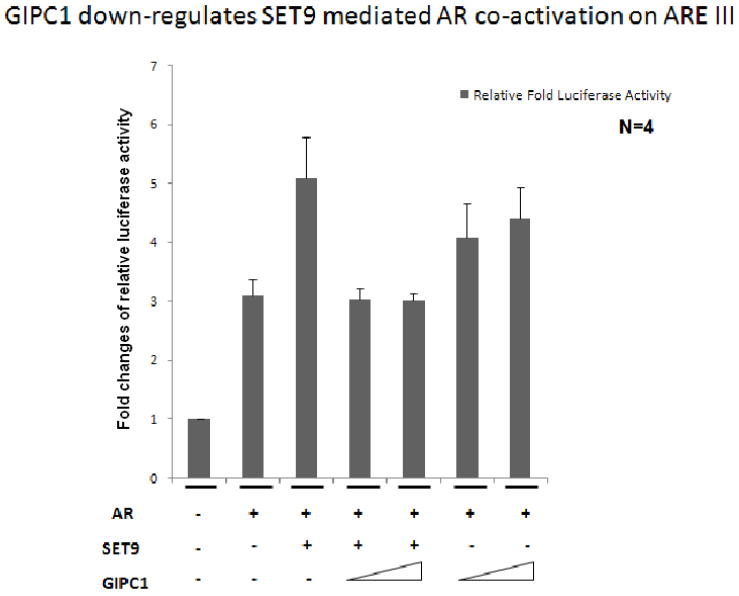

A

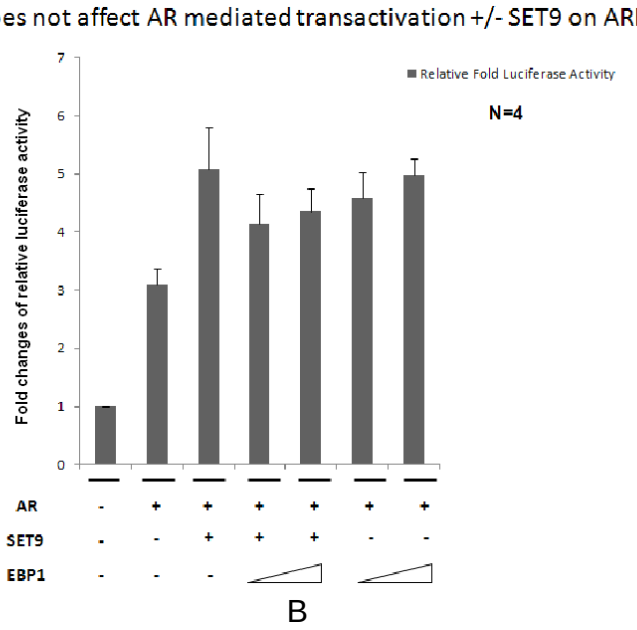

B

Figure 6.10 GIPC1 attenuates SET9-mediated AR coactivation in HEK293T cells
(A) H293 cells were transiently transfected with β-gal and AREIII reporters, AR, and combinations of SET9 and GIPC1 in androgen deprived medium for 48 hours. Cells were then stimulated with DHT (10nM) for 24 hours and subject to luciferase reporter assay. Luciferase counts were normalized using β-gal assay. Addition of GIPC1caused a reduction of SET9 mediated AR co-activation, whereas GIPC1 had little effect on AREIII without SET9 being present. (B) H293 cells were transiently transfected with β-gal AREIII reporter, AR, SET9 and EBP1 with various combinations in androgen deprived medium for 48 hours and cells were treated using the same procedure as mentioned before. EBP1 did not have significant impact on the reporter activity no matter whether SET9 was present or absent regardless of the negligible co-activating effect on the basal reporter activity. Experiments were performed in quadruplicates and repeated three times. Error bars represent +/- SE.

More striking observations were made upon analysis of the three FXR1 isoforms E, F and G in the AR-dependent reporter analysis. Each of the three FXR1 isoforms were titrated into reporter assays as described above to assess the dose-dependency of these proteins on AR-mediated transcription. Interestingly and in line with previous data, FXR1 E, F and G all suppressed SET9 co-activated AR regulated gene transcription and in particular, the F isoform seemed to reduce the reporter activity in a dose-responsive manner (Figure 6.11). Further characterization was carried out to address the antagonistic effect of FXR1 E, F and G on AR mediated transactivation by titrating increasing FXR1 amounts on the reporter. Here results showed that all three FXR1 isoforms showed individual degrees of co-repression in response to the increasing does of transfected plasmids, with FXR1 F representing the most apparent dose-dependent suppressive effect on AR driven transcription on AREIII reporter. This data was in agreement with the early on finding in this figure that FXR1 F exhibits a dose-dependent response in the presence of AR and its co-activator SET9.

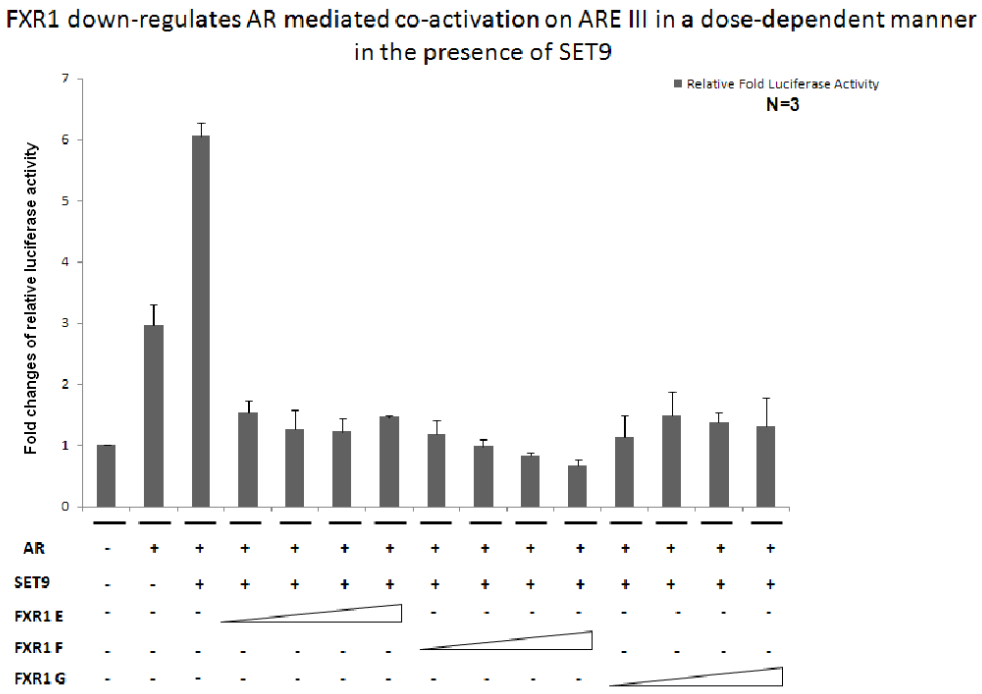

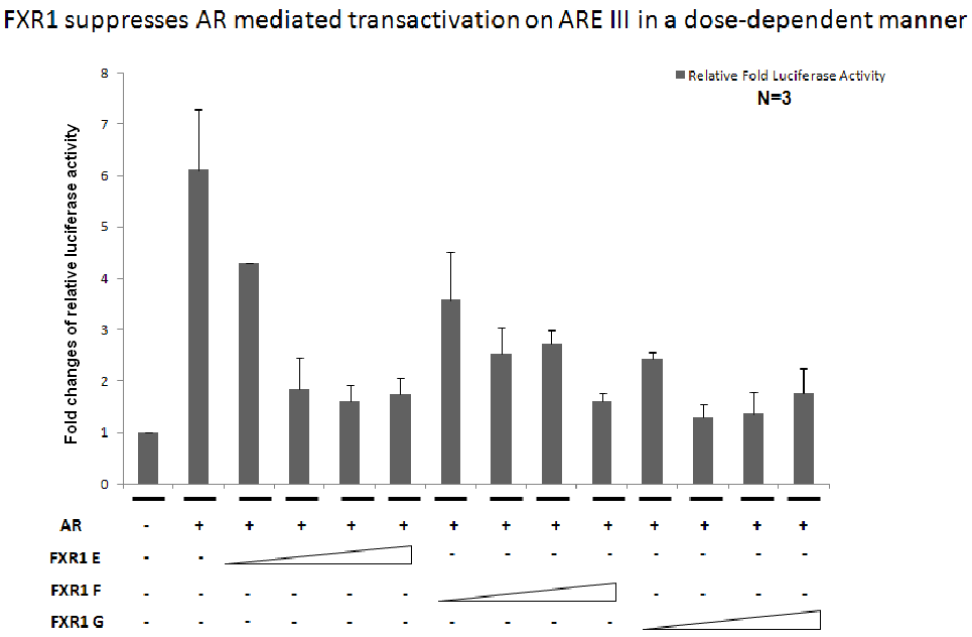

Figure 6.11 FXR1 abolishes SET9 mediated AR transcriptional activity in HEK293T cells.
H293 cells were transiently transfected with β-gal AREIII reporter, AR, SET9 and FXR1 E, F, G with various combinations in androgen deprived medium for 48 hours. Cells were then stimulated with DHT (10nM) for 24 hours and subject to luciferase reporter assay. Luciferase counts were normalized using β-gal assay. All three FXR1 isoforms repressed SET9 mediated AR co-activation and in particular the E isoform showed the strongest inhibition capability even lower than the level induced by AR alone. Experiments were performed in triplicates.

6.3.5 Regulation of SET9 by FXR1 in LNCaP cells

Having gained an insight into the antagonistic regulation of SET9-mediated AR transactivation by FXR1, a logical assumption for the effect of FXR1 on SET9 activity was that SET9 protein levels may be affected by FXR1 manipulation. To this end, siRNA mediated knockdown of FXR1 in LNCaP cells was used to determine the role of FXR1 in regulating SET9 protein levels. Consistent with this assumption, depletion of FXR1 stabilised SET9 indicating that FXR1 is a negative regulator of SET9 (Figure 6.12) and this might help explain the down-regulation of SET9 mediated transcriptional co-activating function due to the destabilization of SET9 in the excessive level of FXR1 in the reporter assays performed. In addition, the influence of GIPC1 silencing on SET9 protein level in LNCaP cells was also analysed. Consistent with the data for FXR1 knockdown, and with the findings from luciferase reporter assays, knockdown of GIPC1

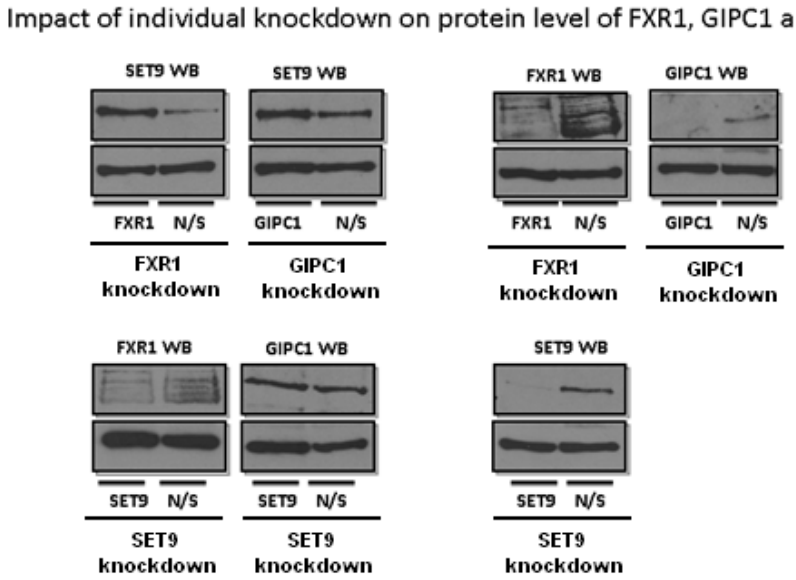

Figure 6.12 Knockdown of either FXR1or GIPC1 stabilizes SET9 protein in LNCaP cells.
LNCaP cells were reverse transfected with FXR1 and GIPC1 individually, grown for 72 hours post-transfection and lysed in SDS sample buffer for immunoblotting analysis using antibodies including SET9, FXR1 and GIPC1. A-Tubulin was used as loading control. Depletion of FXR1 dramatically stabilized SET9 protein level and to a lesser extent SET9 was stabilized following knockdown of GIPC1.

reduced SET9 protein level indicating that GIPC1 may also act as a negative regulator of SET9 in LNCaP cells (Figure 6.12).

Interestingly, it was also noted that knockdown of SET9 appeared to have a feedback regulatory role on FXR1 as depletion of SET9 caused a reduction in

FXR1 level. Nevertheless, this mutual regulatory mechanism did not seem to exist between GIPC1 and SET9 (Figure 6.12).

6.3.6 Evaluating FXR1 and GIPC1 expression in prostate clinical tissue specimens

To obtain further support for a potential involvement of FXR1 in CaP, an Oncomine database was carried out for differential FXR1 expression in normal versus tumour tissue and as expected certain degree of differential expression was observed which made the rationale of investigating the expression further in clinical specimens. To begin to analyse expression of FXR1 in both benign and cancerous prostate tissue, the suitability of the FXR1 antibody for immunohistochemistry (IHC) analysis was determined on a small cohort of benign paraffin-embedded formalin-fixed prostate tissue. In addition, staining for GIPC1 was also conducted on the same cohort of prostate tissue samples to optimise the antibody for future analysis. Figure 6.13 shows that both antibodies worked for IHC on clinical specimens and consistent with the findings in cell line work, both proteins demonstrated cytoplasmic distribution (Figure 6.13). An additional step was taken to further optimise the FXR1 antibody for protein expression analysis in the Urology Research Group's tissue microarray (TMA). Using a test TMA available as a resource for antibody optimisation, it was found that suitable staining of FXR1 was demonstrated using an antibody dilution of 1:250 (Figure 6.14). These optimisation experiments have provided a good platform to build for the analysis of FXR1 expression in benign and malignant prostate tissue specimens as a means of determining a role for FXR1 in cancer development. Given that FXR1 is shown to reduce AR activity in reporter experiments, a hypothesis to test in future studies would be that FXR1 levels are reduced during the transition from normal to malignant prostate tissue.

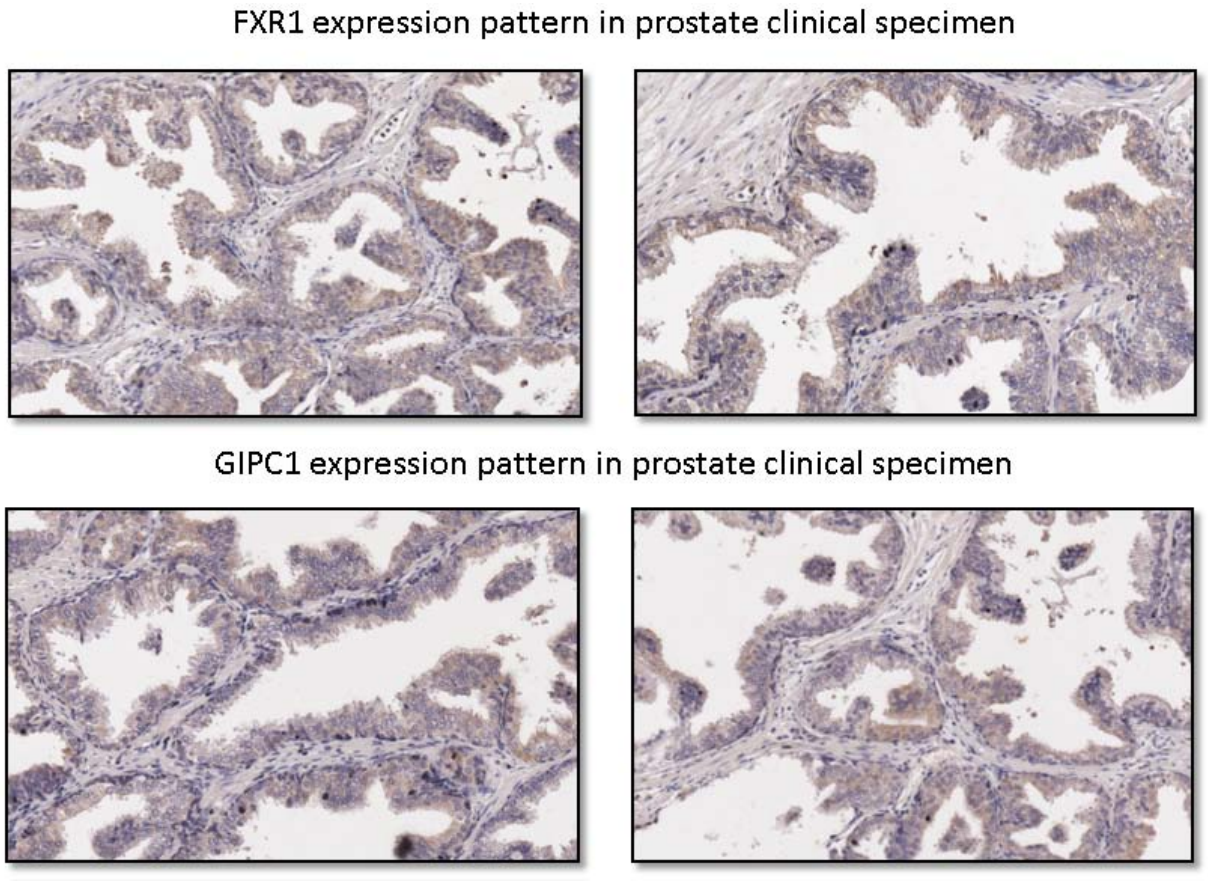

Figure 6.13 Expression and localization pattern of FXR1 and GIPC1 in prostate tissue specimens. Benign prostate clinical tissue samples were used to enable the validation and optimization of FXR1 and GIPC1 antibodies for IHC and after IHC procedure. Samples were analysed using the Aperio ScanScope Digital Scanner. A 1 in 500 antibody dilution for both FXR1 and GIPC1 was applied on the following test TMA analysis. Both FXR1 and GIPC1 displayed predominant cytoplasmic distribution with minor expression in the nucleus.

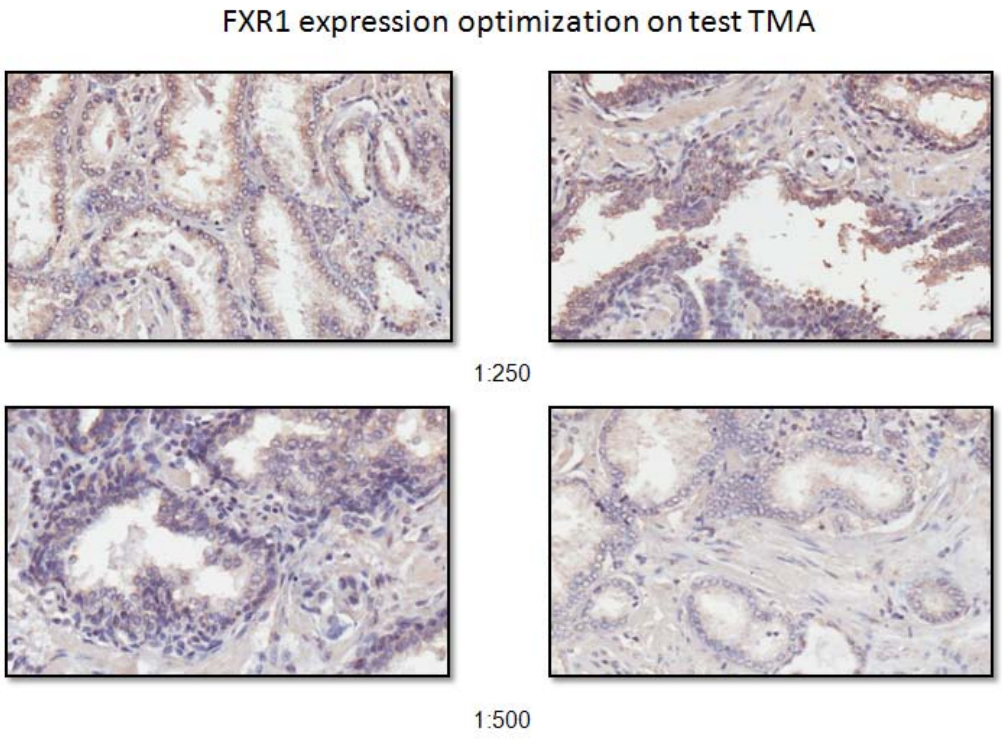

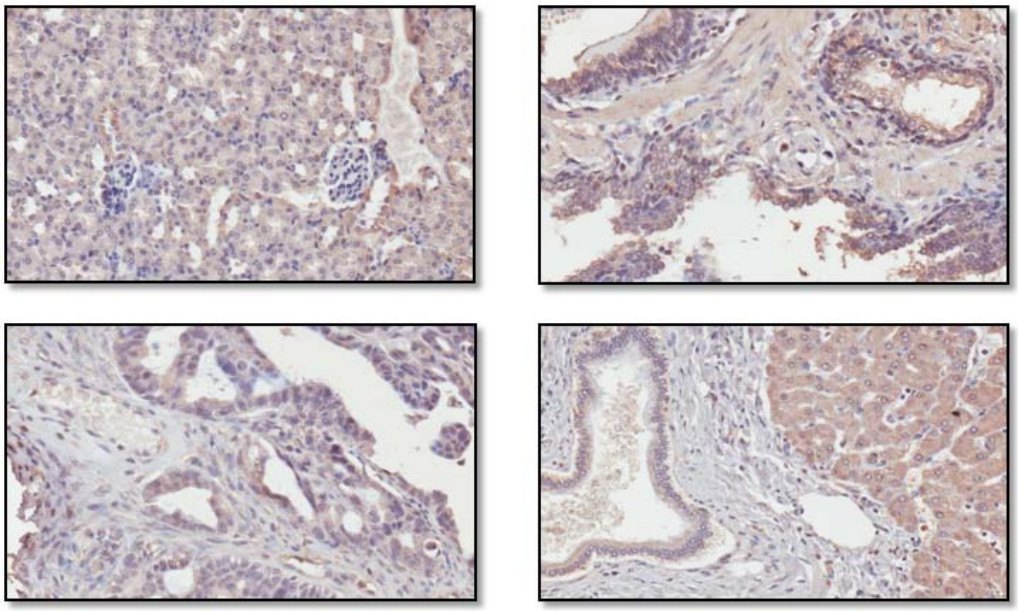

1:250

B

Figure 6.14 Optimization of FXR1 on test TMA samples.

FXR1 antibody was applied to test TMA slides consisting of major prostate tissues including 6 × BPH, 6 × prostate cancer (Gleason grade 3-8) and other tissues including liver, overy, breast and kidney at 1:250 and 1:500 dilution for IHC. Following IHC procedure, samples were analysed using the Aperio ScanScope Digital Scanner. FXR1 protein was displayed predominantly cytoplasmic distribution mainly in epithelial cells. (A) 1:250 dilution showed a clearer visualization of FXR1 distribution in cells compared to 1:500 dilution. (B) The staining patterns of other tissue cores on the test TMA are also presented at antibody concentration of 1:250.

6.4 Discussion

Mass spectrometry analysis of the purified SET9-containing complex from LNCaP prostate cancer cells identified several potential SET9-interacting proteins, including FXR1, GIPC1 and EBP1. In an attempt to further determine the interaction between FXR1, GIPC1 and EBP1 with SET9, U2OS cells were transiently transfected with mammalian expression vectors to drive over-expression of each protein and hence facilitate the detection of SET9-FXR1/GIPC1/EBP1 interactions. Using a rabbit SET9 antibody to pull down both endogenous and exogenous SET9 containing complexes, it was found that three FXR1 isoforms E, F and G were all associated with SET9 protein, although the interaction was not as strong as that observed in LNCaP cells. One explanation for these findings could be that U2OS cells have very low level of endogenous FXR1 expression and the interaction between FXR1 and SET9 under native condition in this cell line is relatively weak compared to that of LNCaP cells. The results in untransfected U2OS cells supported this notion as FXR1 antibody could only weakly detect one or possibly two isoforms of FXR1 and these isoforms as indicated by their molecular weight relative to all three un-tagged FXR1 isoforms are shorter isoforms than depicted in the literature (Figure 6.2) (Kirkpatrick et al., 1999). Another possible reason is that the interaction in LNCaP cells may require an additional factor that is lacking or is at lower levels in U2OS cells and hence the interaction is not as robust as that seen in LNCaP cells. With the same intention to look for interaction, the association between GIPC1 and SET9 was also tested when ectopically expressed in U2OS cells. In line with the data from LNCaP cells, the GIPC1 and SET9 interaction was also confirmed by immunoprecipitation of ectopically expressed proteins in U2OS cells. Notably, although the endogenous GIPC1 expression was relatively low in this cell line, it was shown to interact with over-expressed SET9 further indicating a positive interaction between the two proteins. In parallel experiments, the question of whether EBP1 and SET9 interacted was addressed. Unfortunately, no interaction was demonstrated using the anti-FLAG antibody to detect ectopic EBP1 after pull-down of the SET9 containing complex. Several reasons may explain this observation. 1) U2OS cells may not be a suitable model for the interaction study between EBP1

and SET9. 2) The interaction between EBP1 and SET9 in U2OS cells may need additional factors that are absent in this cell line. 3) Despite the low false-positive rate (6%) in the protein ID search using GPM, the LC-Orbitrap mass spectrometry protein identification has far more sensitive detection potency than the western blotting and thus some of the weak or transient interaction could not be visualized on conventional western blot analysis. Given these findings and the fact that the EBP1-SET9 interaction could not be confirmed using the current methodologies, additional experimentation focussed primarily on the interplay between SET9 and the proteins FXR1 and GIPC1.

Work described in Chapters 3 and 4 and the data published from other groups (Li et al., 2008; Siomi et al., 1995) indicated that SET9 and FXR1 are predominantly cytoplasmic proteins. Considering the observation that SET9 and FXR1/GIPC1 associate in LNCaP and U2OS cells, immunofluorecence was performed to examine potential co-localisation between the proteins in question. Using confocal microscopy to scan TRITC-labelled FXR1 and FITC-conjugated SET9 in LNCaP cells, the appearance of large spectral overlap shown in orange was apparent (Figure 6.3), a consequence of protein co-localization and this double stained pattern was calculated as approximately 80% of these two proteins co-localizing in the same cellular compartment with the majority being present in the cytoplasm. The data is consistent with the tight interaction between FXR1 and SET9 in LNCaP cells on the basis of previous immunoprecipitation and mass spectrometry analysis. Notably, although FXR1 was largely retained in the cytoplasm, there were a number of speckles dotted in the nucleus, which was in support of the previous data that FXR1 shuttles between cytoplasm and nucleus, possibly in a regulated manner (Tamanini et al., 1999). As for GIPC1, GIPC1 exhibited intensive co-localization with SET9 as reflected by double fluorescence staining and this overlap was determined statistically to be over 80%. The cytoplasmic observation for GIPC1 coincided with the location of GIPC1 and the previously documented literature stating that it is a cytoplasmic protein involved in the trafficking process of G protein coupled signalling network and other networks (Katoh, 2002; De Vries et al., 1998). Similarly to FXR1, it was postulated that the association of GIPC1 and SET9 in LNCaP cells may predict novel regulatory mechanisms of SET9 function. Taken together, the data confirmed the association between

FXR1/GIPC1 and SET9. However, it might be necessary as a further step to conduct nuclear/cytoplasmic immunoprecipitation to determine which compartment displays the stronger interaction as the dual staining of the proteins suggested a potential interaction not only in the cytoplasm but also in the nucleus and therefore this would enable a focus on the nuclear function of these proteins.

The intention to discover novel regulatory mechanisms contributed by FXR1 and GIPC1 on SET9 initiated from the investigation regarding the role of SET9 as an anti-apoptotic agent in LNCaP cells. This is a vital mechanism governed by SET9, and it was thought would perhaps reveal a link between SET9 and FXR1/GIPC1. It was shown that ablation of FXR1 by siRNA approach resulted in a substantial reduction of apoptosis initiated by SET9 knockdown solely in response to Doxorubicin treatment. This suggested a pro-apoptotic role of FXR1 in SET9 knockdown induced apoptosis in response to Doxorubicin administration. As SET9 depletion mediated apoptosis is via the retardation of p53 mediated gene transcription and knockdown of p53 completely blocks SET9 silencing mediated LNCaP cell apoptosis, the FXR1 story was taken one step forward by assessing the interaction between FXR1 and p53. It was found that FXR1 interacted with p53 both in the absence and presence of DNA damaging agent treatment. One notable observation was the presence of a doublet band appearing in the immunoprecipitation sample lane without Doxorubicin treatment. The speculation was that there might be either different splicing variants or covalently modified forms of the protein detected by the p53 antibody in LNCaP cells. The early finding supports this hypothesis as in the cyclohexmide treatment experiment investigating SET9 protein stability at least two forms of p53 co-existed. Furthermore, when comparing to the DNA damage induced immunoprecipitation sample, it seemed that one of the double bands disappeared and thus it was speculated that the other form of p53 was a potential dephosphorylated form of p53. In LNCaP cells, there are different p53 phosphorylation sites identified, including serines 9 and 15. Notably these two residues are phosphorylated to a certain degree even without external stimuli (Jiang et al., 2004). On the other hand, supporting evidence also indicates that p53 is dephosphorylated on serine 376 in response to irradiation induced DNA damage (Lakin and Jackson, 1999; Waterman et al., 1998). Therefore, it was

postulated that there might be phosphorylation or other post-translational modifications occurring on p53 in normal LNCaP cells. However, following Doxorubicin treatment, dysregulated phosphorylation may change the overall status of p53, which is reflected in the western blot results with the disappearance of one band. One conclusion from this experiment is that FXR1 plays a role as a potent regulator which in conjunction with p53 controls SET9 knockdown mediated apoptosis. As FXR1, SET9 and p53 interact with each other, there might be a ternary complex existing in LNCaP. cells Since the induction of apoptosis by SET9 knockdown relies upon p53 via its aberrant regulation as proposed earlier, one possible argument is that FXR1 may influence p53s involvement in LNCaP cell apoptosis. Considering that depletion of FXR1 alone did not cause a dramatic change in LNCaP cell apoptosis and neither did p53 alone, it is possible that FXR1 regulated p53 alteration is SET9 dependent. A further speculation is that FXR1 might impact on the combinational interplay of post-translational modifications occurring on p53 which is predominantly modulated by the dynamics of SET9 in LNCaP cells. Thus, the mechanism of apoptotic event could be established as follows: SET9 knockdown alters p53 post-translational modification dynamics which stabilizes the protein to induce apoptosis in the presence of Doxorubicin. FXR1 at some point facilitates this p53 stabilization under such a modified status generated in response to ablation of SET9. This assistant role by FXR1 is indispensable for p53 to execute its downstream function. Although FXR1 knockdown alone has limited effect on apoptosis of LNCaP cells, evident morphological change was observed, which resembled a neuroendocrine (NE) differentiation pattern when FXR1. Therefore, FXR1 knockdown might potentially drive the trans-differentiation of LNCaP cells to allow the production of neuroendocrine-like cell growth pattern, which resembles the effect observed during androgen-deprived conditions in LNCaP cells. This warrants further investigation to get a clearer understanding of the relationship between FXR1 regulatory machinery and neuroendocrine differentiation markers. Particular focus could be on signalling pathways linked with neuroendocrine differentiation, including protein kinase A and MAP kinase pathways, activated through cyclic AMP and the PI3 Kinase and STAT3 pathways, activated through the induction of cytokines such as interleukin-6 and interleukin-1β (Yuan et al., 2007; Culig et al., 2005; Hoosein, 1998).

In parallel experiments where the effect of GIPC1 on SET9 knockdown mediated apoptosis was assessed, GIPC1 seemed incapable of affecting the apoptosis induced by SET9 ablation. Although, depletion of GIPC1 alone enabled LNCaP cells to undergo apoptosis to a similar extent to that of SET9 in the presence of Doxorubicin. As this GIPC1 induced phenotypic effect was seemingly not correlated with SET9 knockdown, no further studies were conducted. Nevertheless, GIPC1 mediated apoptosis may occur via the regulation of signalling transduction possibly through MAP Kinase (Erk1/2) mediated apoptosis pathway where GIPC1 seems to function as a negative regulator through binding with TrkA (Lou et al., 2001). Moreover, as this effect occured following exposure to DNA damaging agent (Doxorubicin) which activates p53, it is possible that MAP Kinase pathway acts in association with p53 to induce apoptosis in LNCaP cells, since it is documented that p53 activation by 5-aza-2'-deoxycytidine induces pro-apoptotic gene expression and mitogen-activated protein kinases in LNCaP cells (Pulukuri and Rao, 2005).

Having established a role for FXR1 and GIPC1 in SET9 induced LNCaP cell apoptosis, the next question was to address whether they have an impact on SET9-mediated co-activation of androgen receptor-driven transcription. To this end, luciferase reporter assays were performed in HEK293T cells. Using the ARE III driven reporter, it was found that induction of FXR1 suppressed SET9 mediated co-activation of AR to levels lower than that induced by AR alone. Importantly, all three isoforms of FXR1 exerted a similar effect by down-regulating reporter activity. In parallel experiments, the effect of GIPC1 and EBP1 was tested under the same experimental conditions. Although addition of GIPC1 reduced SET9-mediated co-activation, it failed to impact on transcriptional activity of the receptor in the absence of SET9 indicating a potentially different mechanism of function to that of FXR1. In contrast to FXR1 and GIPC1, EBP1 failed to affect AR activity irrespective of the presence of SET9. This finding is inconsistent with the previous findings that demonstrated EBP1 functions as an AR co-repressor through the association with the Sin3A complex containing histone deacetylase activity (Zhang et al., 2005a). These authors applied the androgen-responsive MMTV reporter in LNCaP cells which

differs considerably from the ARE III reporter in HEK293T cells used in herein and may part explain different effects of EBP1 on AR-mediated transcription.

The finding that all three FXR1 isoforms down-regulated AR mediated gene activation (Figure 6.12) suggested FXR1 functions as an AR co-repressor on the AREIII reporter. To further probe the mechanism behind this co-repressive effect driven by FXR1, knockdown of FXR1 in LNCaP cells was performed in order to assess the turnover of SET9 accordingly. These results showed that depletion of FXR1 significantly up-regulated SET9 protein, which may suggest a mechanism for the reduction in SET9-mediated co-activation when FXR1 is over-expressed. However, the data remains limited as independent mechanisms of FXR1 as an intrinsic AR co-repressor have not been sufficiently addressed due to limited time available. Moreover, the observation that GIPC1 knockdown also caused SET9 levels to increase suggested that GIPC1 over-expression down-regulates SET9 mediated co-activation by reducing SET9 protein in the luciferase assays, although this has not been confirmed. Current knowledge on FXR1 indicates that it primarily functions as an RNA binding protein to influence gene expression at post-transcriptional level. It is feasible that FXR1 regulation of SET9 and possibly AR occurs at the transcript level where FXR1 negatively regulates SET9 and AR mRNA, in turn facilitating reduced AR mediated gene transcription. However, considering the observation of direct SET9 and FXR1 interaction in vivo, it is also possible that the protein-protein association would predict a co-regulatory mechanism involving FXR1. So far, the only molecular basis to support this notion is the nuclear-cytoplasmic shuttling of proteins governed by FXR1 (Tamanini et al., 1999). Whether FXR1 contributes towards SET9 and/or AR nuclear influx/efflux during transcription control still remains to be determined. In regard to the repression of AR mediated transcription by FXR1, providing the appearance of FXR1 in the nuclear compartment, whether it influences AR mediated transcription directly by either forming into an AR containing transcriptional complex at promoter regions or recruiting other repressive components such as HDACs still remains to be elucidated. Finally, due to the complexity of AR signalling cross-talk in hormone refractory prostate cancer, it might be possible that various signalling pathways responsible for the development of AR dependent prostate cancer such as AKT, MAP Kinase and PKC pathways could be potentially regulated by

FXR1 (Edwards and Bartlett, 2005b; Gnanapragasam et al., 2000; Weigel, 1996). From current knowledge and our findings so far, no further conclusion can be made on the molecular mechanisms lying behind the repressive regulation of transcriptional machinery involving SET9 and AR in the presence of FXR1 and these questions need to be addressed in the future.

Finally, the intention was to determine the expression pattern of FXR1 and GIPC1 in prostate clinical specimens. Upon validation of the antibodies, it was confirmed that both FXR1 and GIPC1 are largely expressed in the cytoplasm of prostate epithelial cells, consistent with the immunofluorescence data. The antibodies were applied to test TMA slides to allow the determination of appropriate concentration to use. Nevertheless as time was limited, experiments did not proceed to the stage to examine larger-scale prostate cancer TMAs containing clinical prostate tumours with varied Gleason scores. Interestingly, according to in silico RNA expression search against FXR1 using the Oncomine data base, FXR1 gene showed up-regulated expression during the initiation and advancement of prostate carcinoma in clinical patient samples, which supports a convincing reason to justify examining the expression of FXR1 protein in clinical specimens in future experiments (Tomlins et al., 2007; Lapointe et al., 2004; Vanaja et al., 2003).

Chapter 7

Summary and future direction

7.1 Current study

One primary driving force of prostate cancer (CaP) from organ confined state to metastasis and castrate resistant disease is the aberrant regulation of androgen receptor (AR) pathway. In the variety of mechanisms contributing towards regulation of receptor dynamics and activity, co-regulators are believed to play pivotal roles governing many biological aspects of AR (Heinlein and Chang, 2002). In this project, the attention was focussed on one important epigenetic regulator, SET9 which has previously been identified as a primary histone H3 lysine 4 mono-methyltransferase (Nishioka et al., 2002; Wang et al., 2001a). Follow-up investigation on this protein revealed that its function is not only restricted to histone proteins but also connected to other essential regulators, particularly in various cancer pathways, including p53, estrogen receptor (ER), NF-κB and components of basal transcriptional machinery such as TAF10 (Li et al., 2008; Subramanian et al., 2008; Chuikov et al., 2004; Kouskouti et al., 2004). Based on it's substrate protein methylation sites, a consensus sequence recognisable by SET9, R/K-S/T/A-K-D/K/N/Q, has been modelled and interestingly this lysine rich motif also appears within the AR sequence which is previously reported as a highly modifiable region (Couture et al., 2006; Gaughan et al., 2002; Fu et al., 2000). By analogy, a primary investigation was performed aiming to establish the role of SET9 in AR mediated biological processes. Our preliminary data showed that SET9 is capable of methylating the receptor at a single lysine residue, 632 in the KLKK motif by applying in vitro methylation assay and tandem mass spectrometry analysis. The methylation event dictated SET9 potency by facilitating AR mediated transcription, evident using reporter assays through ectopic expression or gene knockdown strategy, revealing its role as an AR co-activator (Gaughan et al., 2010 in press).

To further characterize SET9 in CaP cells, many biological properties of this protein were examined. It was demonstrated that SET9 is a stable protein whose expression is relatively unchanged during cell cycle progression. Using immunofluorescence and nuclear/cytoplasmic extraction, both endogenous and ectopically expressed SET9 showed predominant cytoplasmic distribution, an observation in agreement with one previous study but potentially contradictory

to the primary reported function of this protein as a histone modifying enzyme (Li et al., 2008; Nishioka et al., 2002) (Gaughan et al., 2010). The transcriptional co-activation role of SET9 was also confirmed in LNCaP cells and U2OS cells, again highlighting that SET9 is an AR co-activator. This co-activation mechanism can be significantly reversed by HDAC1, possibly through a direct interaction between the two proteins, evident when over-expressing both proteins together. Probing into the phenotypic role of SET9 in CaP cells, several observations have been made. Based upon siRNA mediated knockdown and FACS based assays, it was shown that SET9 enhanced the proliferative potential of LNCaP cells by accelerating the G1/S transition and inhibiting apoptosis suggesting an important role during cancer progression. Moreover, depletion of SET9 in LNCaP cells combined with Doxorubicin DNA damaging agent treatment induced massive apoptosis compared to SET9 knockdown alone. p53 knockdown attenuated SET9 knockdown mediated apoptosis in response to chemotherapeutic intervention, suggesting its potential apoptotic function through DNA damaging triggered pathway, a phenomenon which links this study with previous work for SET9 on p53 (Gaughan et al., 2010). Opposite to the effect observed in U2OS cells where SET9 stabilizes p53 to trigger apoptosis in response to Doxorubicin treatment, the justification was that SET9 might regulate p53 in the opposite way in LNCaP cells compared to U2OS cells as some of the p53 target genes MDM2 and p21 showed up-regulation pattern upon SET9 knockdown.

In order to interrogate SET9 involvement in cellular mechanisms for CaP cells, endogenous SET9 protein was extracted from LNCaP cells using immunoprecipitation and multiple proteins associated with SET9 were identified using LC-MS/MS from electrophoresis fractionated samples. Amongst 13 identified SET9 interacting proteins, based upon the confidence and quality of peptides identified for each protein and their relevance to cancer biology, FXR1, GIPC1 and EBP1 were chosen for further characterization. Although a link between EBP1 and SET9 could not be confirmed,, primary exploration of SET9/FXR1 and SET9/GIPC1 was established. The data highlighted a strong cytoplasmic co-localization between SET9/FXR1 and SET9/GIPC1 in LNCaP cells, which is in agreement with the immunofluorescence data done on SET9 previously and the literaturally documented work done on FXR1. In addition,

FACS based analysis revealed that FXR1 is important for SET9 knockdown mediated LNCaP cell apoptosis in the presence of Doxorubicin. This mechanism might involve SET9, p53 and FXR1, since FXR1 directly interacts with p53 in LNCaP cells. Further characterization from the transcriptional control aspect suggested that FXR1 is a robust co-repressor of AR which diminishes AR activity independently of SET9 expression. A further explanation comes from the expression analysis of SET9 in the presence of FXR1 knockdown, which suggests FXR1 might negatively regulate SET9 at the protein level, although the mechanism is still to be revealed. Finally, the investigation ended with the study of FXR1 and GIPC1 expression in CaP clinical tissue samples. the data was consistent with the cell line work demonstrating FXR1 and GIPC1 showed predominantly cytoplasmic expression, coincides with the distribution of SET9 in clinical TMA samples at various cancer grade (Gaughan et al., 2010).

7.2 Future direction

The data investigating the regulatory mechanism between SET9 and HDAC1 casts light on the molecular mechanism behind the regulation of SET9 by HDAC1 in the context of AR dynamics. As HDAC1 is involved in Tip60 mediated AR down-regulation and both Tip60 and SET9 target the KLKK motif within the receptor, there might be a similar scenario established between SET9 and HDAC1. Whether methylation is required for subsequent acetylation of surrounding lysines by other AR co-activator such as Tip60 or p300/PCAF, and whether HDAC1 could remove all these acetylated marks to inactivate the receptor to diminish transcription, is worthy of further investigation. The interaction observed between SET9/AR, SET9/HDAC1 and the ternary complex of Tip60, HDAC1 and AR suggests a potential cross-talk between the three proteins and thus the influence of HDAC1 on SET9 methylated KLKK motif is of interest for future study.

Although the overall mechanism of SET9 knockdown mediated apoptosis in LNCaP cells has been established, the exact molecular biology behind it is still unknown. Confirming the precise methylation of p53 by SET9 in LNCaP cells is essential and this might explain the distinct mechanism observed in LNCaP cells compared to U2OS cells in regulating p53 target genes.

Since FXR1 was identified in LNCaP cells as a strong candidate with regard to its capability for regulating SET9 mediated apoptosis and transcriptional control, it will be important to determine the underlying molecular mechanisms involved. How could FXR1 knockdown inhibit apoptosis induced by SET9 upon activation of p53? Is this through direct regulation of FXR1 on p53 or vice versa? How could FXR1 suppress SET9's co-activator function and is there a direct AR regulation by FXR? These questions remain to be addressed. To prioritise the questions, the key experiment would be to determine the repressive role of FXR1 on AR mediated transcription. A direct interaction between those two proteins might be pursued and as HDAC1 is a strong inhibitory regulator of AR activity, a link between FXR1 and HDAC1 could be sought to determine whether FXR1 mediated receptor inhibition is acting via HDAC1. Finally, the now optimized conditions for CaP tissue immunohistochemistry will allow us to characterise FXR1 protein expression in a clinical context, using CaP TMAs to obtain a clearer understanding of the correlation between FXR1 and CaP progression. This will constitute a novel area for future CaP biomarker discovery and the search for more effective therapeutic intervention.

Appendices

Appendix 1

Annotated spectra of protein peptides identified specifically in SET9 pull-down samples. Only one representative peptide spectrum for each protein is depicted here.

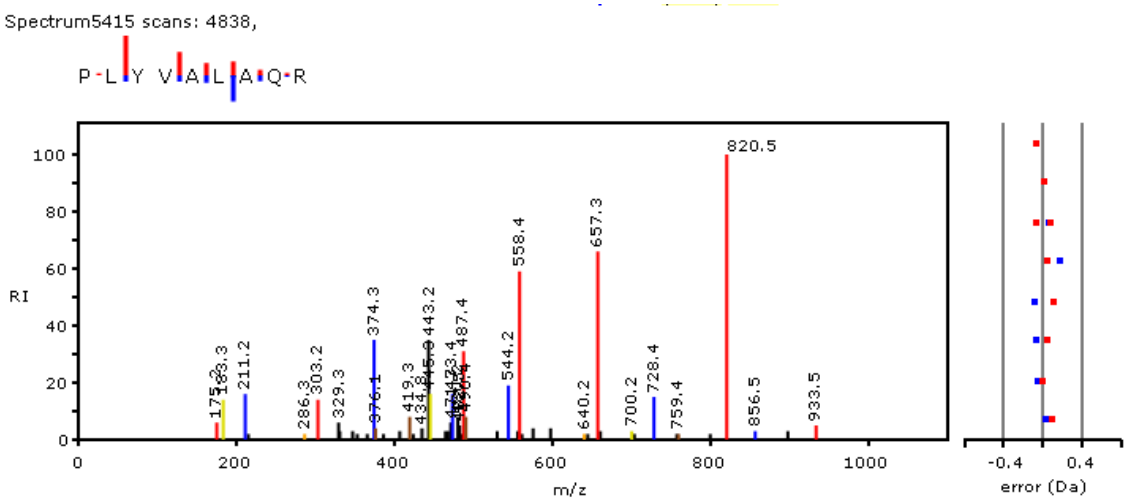

Polyadenylate-binding protein 1-like

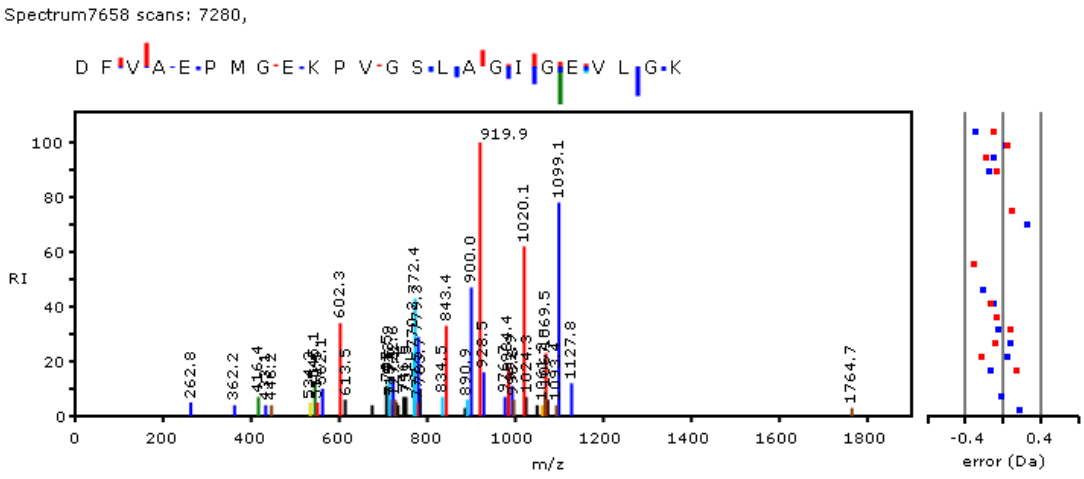

Breakpoint cluster region protein 1

Spectrum5968 scans: 5622,

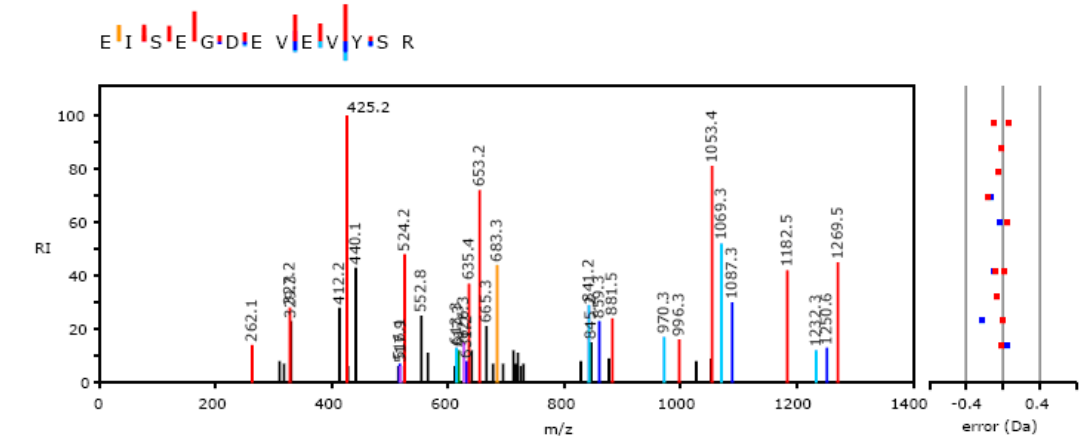

Fragile X mental retardation syndrome-related protein 1 (FXR1)

Spectrum5375 scans: 4843,

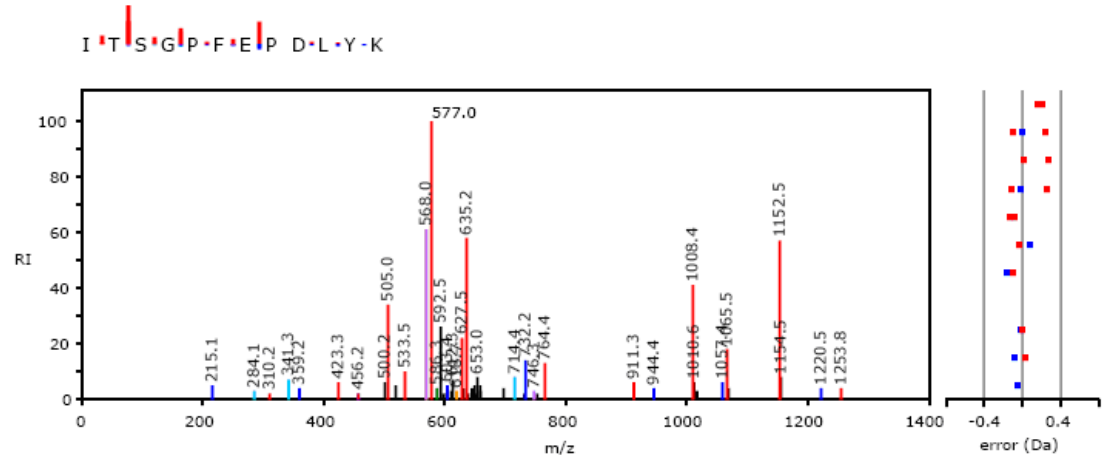

ErbB3-binding protein 1 (EBP1)

Spectrum7613 scans: 7148,

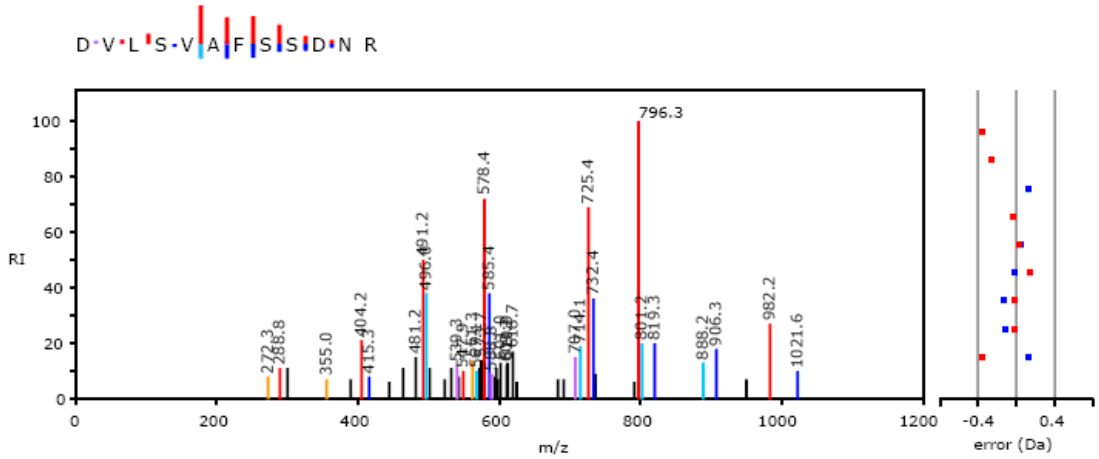

Receptor of activated protein kinase C 1

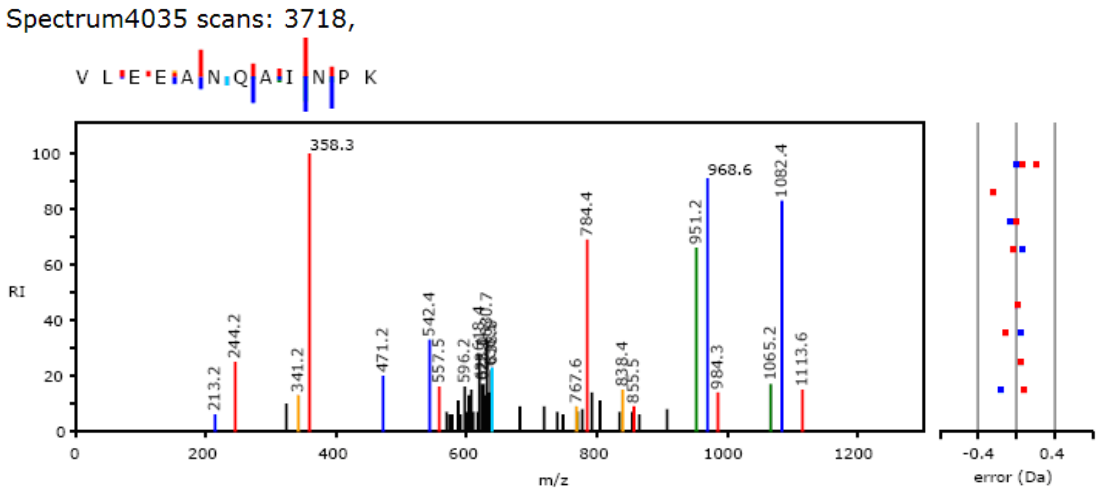

RNA-dependent helicase p72 (p72)

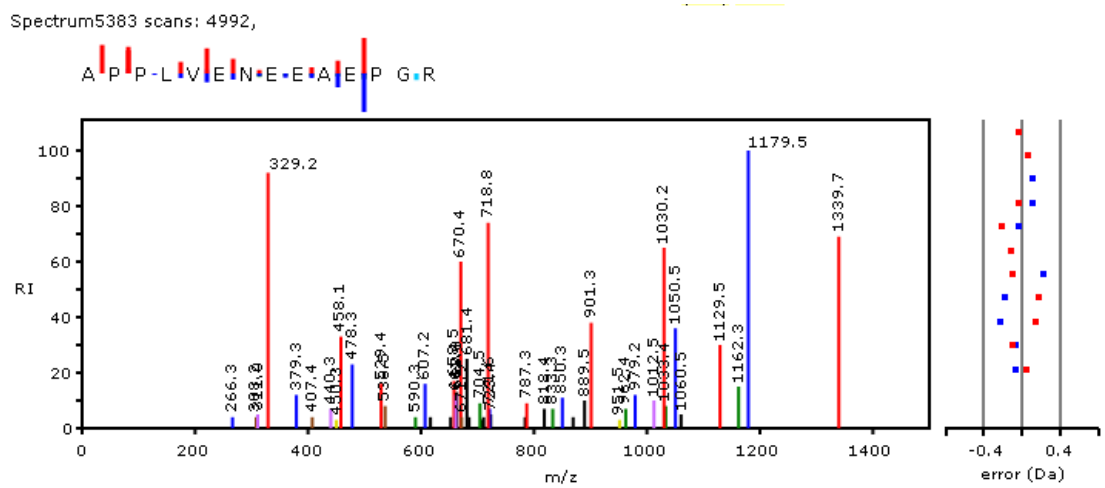

GAIP C-terminus-interacting protein (GIPC1)

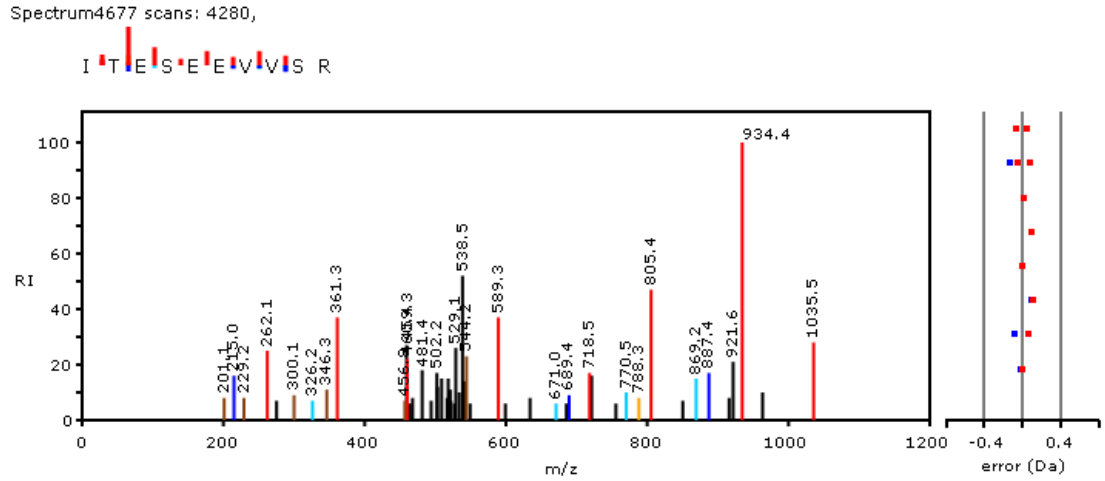

Lamin A/C

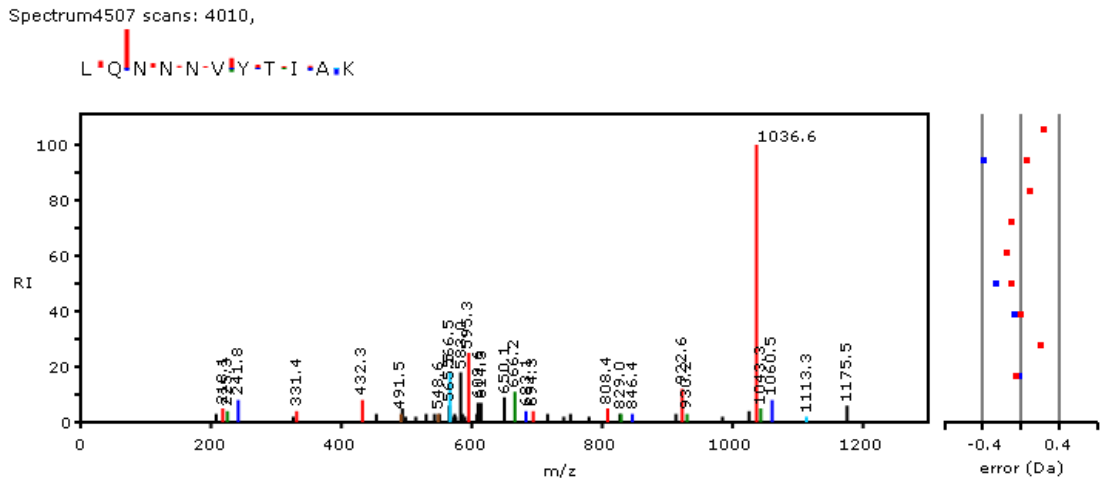

AP-2 complex subunit beta-1

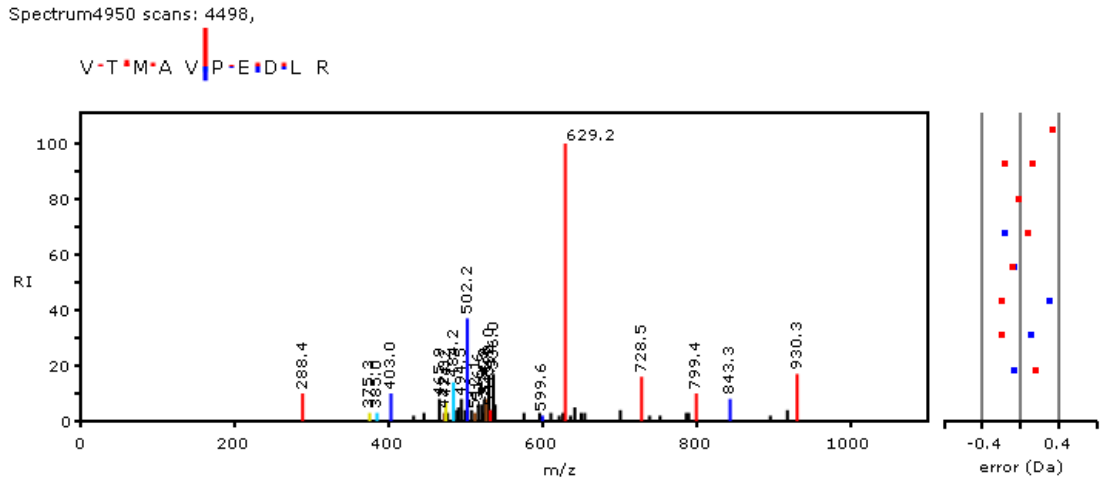

Fragile X mental retardation syndrome-related protein 2 (FXR2)

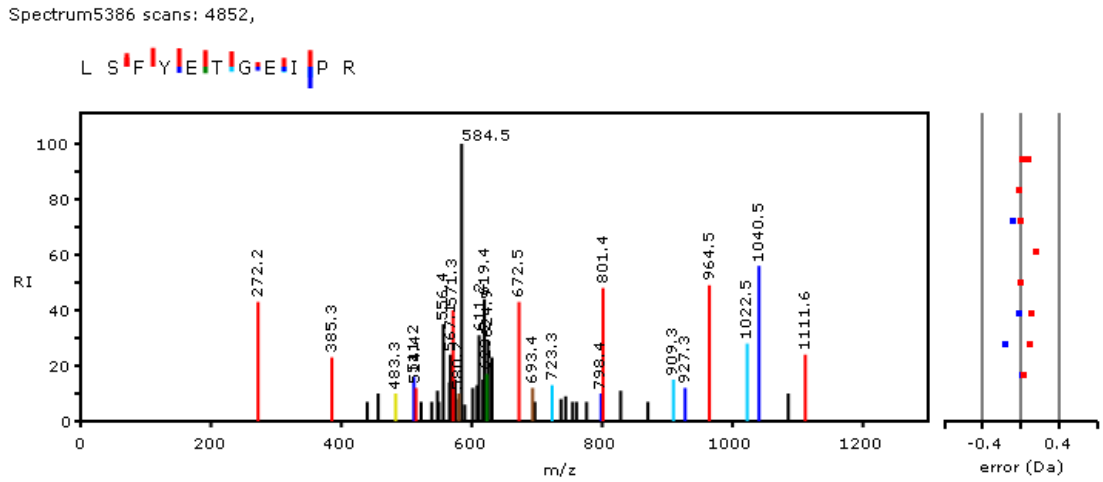

Nucleolar protein 5A

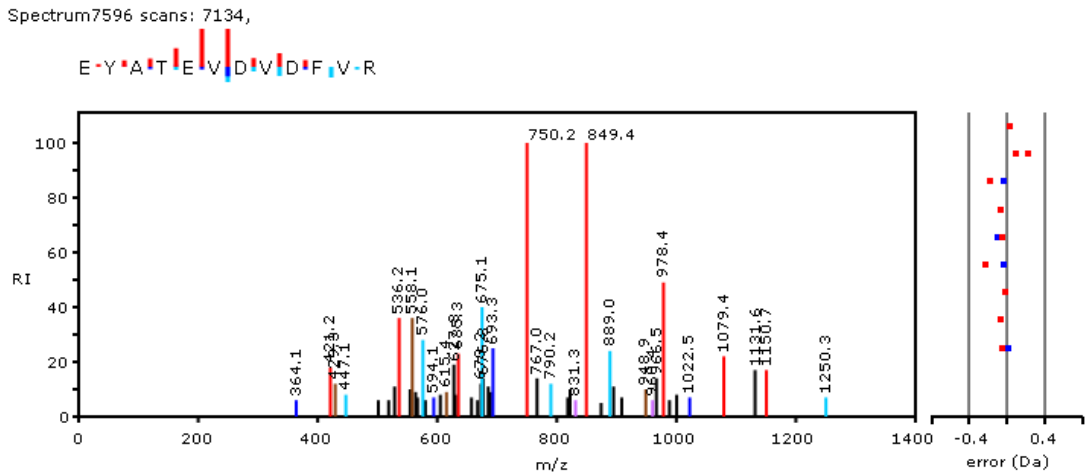

AP-1 complex subunit beta-1

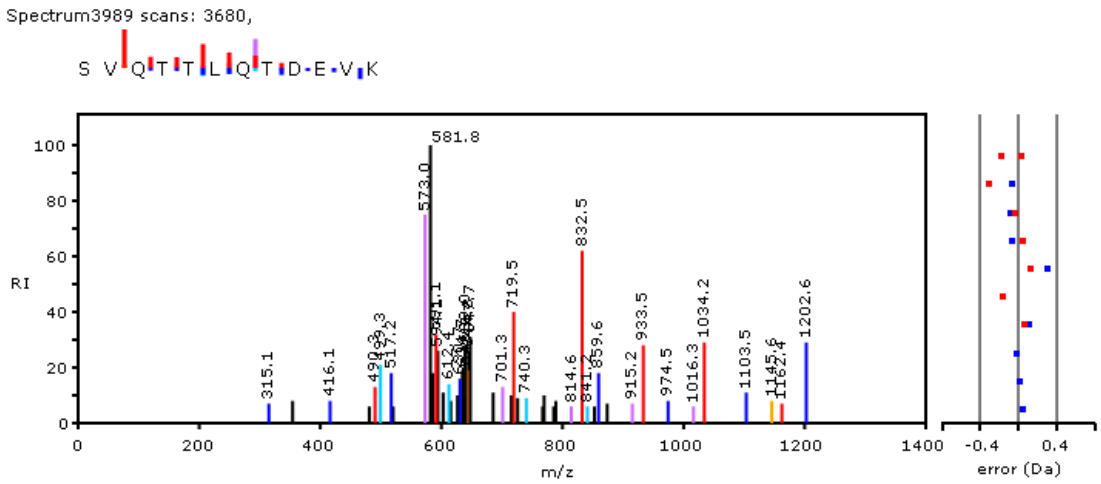

Endoplasmic reticulum lipid raft-associated protein 1 (Erlin-1)

Appendix 2

Data summary of all identified peptides in immunoprecipitated sample fractions and corresponding control fractions with their relevant information. This figure was tidied up with the exclusion of keratins and trypsins.

References

Abate-Shen, C. and Shen, M. M. (2000) 'Molecular genetics of prostate cancer', *Genes Dev,* 14, (19), pp. 2410-34.

Abrahamsson, P. A. and Lilja, H. (1990) 'Three predominant prostatic proteins', *Andrologia,* 22 Suppl 1, pp. 122-31.

Anderson, D. C. (1974) 'Sex-hormone-binding globulin', *Clin Endocrinol (Oxf),* 3, (1), pp. 69-96.

Aumuller, G. and Seitz, J. (1990) 'Protein secretion and secretory processes in male accessory sex glands', *Int Rev Cytol,* 121, pp. 127-231.

Balk, S. P. and Knudsen, K. E. (2008) 'AR, the cell cycle, and prostate cancer', *Nucl Recept Signal,* 6, pp. e001.

Ban, Y., Wang, M. C., Watt, K. W., Loor, R. and Chu, T. M. (1984) 'The proteolytic activity of human prostate-specific antigen', *Biochem Biophys Res Commun,* 123, (2), pp. 482-8.

Bardoni, B., Schenck, A. and Mandel, J. L. (2001) 'The Fragile X mental retardation protein', *Brain Res Bull,* 56, (3-4), pp. 375-82.

Berezovska, O. P., Glinskii, A. B., Yang, Z., Li, X. M., Hoffman, R. M. and Glinsky, G. V. (2006) 'Essential role for activation of the Polycomb group (PcG) protein chromatin silencing pathway in metastatic prostate cancer', *Cell Cycle,* 5, (16), pp. 1886-901.

Berman, C. G. and Clark, R. A. (1992) 'Diagnostic imaging in cancer', *Prim Care,* 19, (4), pp. 677-713.

Berquin, I. M., Min, Y., Wu, R., Wu, J., Perry, D., Cline, J. M., Thomas, M. J., Thornburg, T., Kulik, G., Smith, A., Edwards, I. J., D'Agostino, R., Zhang, H., Wu, H., Kang, J. X. and Chen, Y. Q. (2007) 'Modulation of prostate cancer genetic risk by omega-3 and omega-6 fatty acids', *J Clin Invest,* 117, (7), pp. 1866-75.

Berry, S. J. and Isaacs, J. T. (1984) 'Comparative aspects of prostatic growth and androgen metabolism with aging in the dog versus the rat', *Endocrinology,* 114, (2), pp. 511-20.

Bhatia-Gaur, R., Donjacour, A. A., Sciavolino, P. J., Kim, M., Desai, N.,

Young, P., Norton, C. R., Gridley, T., Cardiff, R. D., Cunha, G. R., Abate-Shen, C. and Shen, M. M. (1999) 'Roles for Nkx3.1 in prostate development and cancer', *Genes Dev,* 13, (8), pp. 966-77.

Birnbaum, R. S., Ware, J. L. and Plymate, S. R. (1994) 'Insulin-like growth factor-binding protein-3 expression and secretion by cultures of human prostate epithelial cells and stromal fibroblasts', *J Endocrinol,* 141, (3), pp. 535-40.

Blobe, G. C., Liu, X., Fang, S. J., How, T. and Lodish, H. F. (2001) 'A novel mechanism for regulating transforming growth factor beta (TGF-beta) signaling. Functional modulation of type III TGF-beta receptor expression through interaction with the PDZ domain protein, GIPC', *J Biol Chem,* 276, (43), pp. 39608-17.

Bolivar, J., Guelman, S., Iglesias, C., Ortiz, M. and Valdivia, M. M. (1998) 'The fragile-X-related gene FXR1 is a human autoantigen processed during apoptosis', *J Biol Chem,* 273, (27), pp. 17122-7.

Borun, T. W., Pearson, D. and Paik, W. K. (1972) 'Studies of histone methylation during the HeLa S-3 cell cycle', *J Biol Chem,* 247, (13), pp. 4288-98.

Bracken, A. P., Pasini, D., Capra, M., Prosperini, E., Colli, E. and Helin, K. (2003) 'EZH2 is downstream of the pRB-E2F pathway, essential for proliferation and amplified in cancer', *EMBO J,* 22, (20), pp. 5323-35.

Bradford, T. J., Tomlins, S. A., Wang, X. and Chinnaiyan, A. M. (2006) 'Molecular markers of prostate cancer', *Urol Oncol,* 24, (6), pp. 538-51.

Brady, M. E., Ozanne, D. M., Gaughan, L., Waite, I., Cook, S., Neal, D. E. and Robson, C. N. (1999) 'Tip60 is a nuclear hormone receptor coactivator', *J Biol Chem,* 274, (25), pp. 17599-604.

Brooke, G. N., Parker, M. G. and Bevan, C. L. (2008) 'Mechanisms of androgen receptor activation in advanced prostate cancer: differential co-activator recruitment and gene expression', *Oncogene,* 27, (21), pp. 2941-50.

Burns, T. F. and El-Deiry, W. S. (1999) 'The p53 pathway and apoptosis', *J Cell Physiol,* 181, (2), pp. 231-9.

Cao, R. and Zhang, Y. (2004) 'The functions of E(Z)/EZH2-mediated methylation of lysine 27 in histone H3', ***Curr Opin Genet Dev,*** **14, (2), pp. 155-64.**

Carling, T., Kim, K. C., Yang, X. H., Gu, J., Zhang, X. K. and Huang, S. (2004) 'A histone methyltransferase is required for maximal response to female sex hormones', ***Mol Cell Biol,*** **24, (16), pp. 7032-42.**

Carter, B. S., Ewing, C. M., Ward, W. S., Treiger, B. F., Aalders, T. W., Schalken, J. A., Epstein, J. I. and Isaacs, W. B. (1990) 'Allelic loss of chromosomes 16q and 10q in human prostate cancer', ***Proc Natl Acad Sci U S A,*** **87, (22), pp. 8751-5.**

Catalona, W. J., Richie, J. P., deKernion, J. B., Ahmann, F. R., Ratliff, T. L., Dalkin, B. L., Kavoussi, L. R., MacFarlane, M. T. and Southwick, P. C. (1994) 'Comparison of prostate specific antigen concentration versus prostate specific antigen density in the early detection of prostate cancer: receiver operating characteristic curves', ***J Urol,*** **152, (6 Pt 1), pp. 2031-6.**

Catalona, W. J., Smith, D. S., Ratliff, T. L. and Basler, J. W. (1993) 'Detection of organ-confined prostate cancer is increased through prostate-specific antigen-based screening', ***JAMA,*** **270, (8), pp. 948-54.**

Chakrabarti, S. K., Francis, J., Ziesmann, S. M., Garmey, J. C. and Mirmira, R. G. (2003) 'Covalent histone modifications underlie the developmental regulation of insulin gene transcription in pancreatic beta cells', ***J Biol Chem,*** **278, (26), pp. 23617-23.**

Chang, B. Y., Conroy, K. B., Machleder, E. M. and Cartwright, C. A. (1998) 'RACK1, a receptor for activated C kinase and a homolog of the beta subunit of G proteins, inhibits activity of src tyrosine kinases and growth of NIH 3T3 cells', ***Mol Cell Biol,*** **18, (6), pp. 3245-56.**

Chang, C. S., Kokontis, J. and Liao, S. T. (1988a) 'Molecular cloning of human and rat complementary DNA encoding androgen receptors', ***Science,*** **240, (4850), pp. 324-6.**

Chang, C. S., Kokontis, J. and Liao, S. T. (1988b) 'Structural analysis of complementary DNA and amino acid sequences of human and rat androgen receptors', ***Proc Natl Acad Sci U S A,*** **85, (19), pp.**

7211-5.

Chang, M., Tsuchiya, K., Batchelor, R. H., Rabinovitch, P. S., Kulander, B. G., Haggitt, R. C. and Burmer, G. C. (1994) 'Deletion mapping of chromosome 8p in colorectal carcinoma and dysplasia arising in ulcerative colitis, prostatic carcinoma, and malignant fibrous histiocytomas', *Am J Pathol,* 144, (1), pp. 1-6.

Chen, D., Ma, H., Hong, H., Koh, S. S., Huang, S. M., Schurter, B. T., Aswad, D. W. and Stallcup, M. R. (1999) 'Regulation of transcription by a protein methyltransferase', *Science,* 284, (5423), pp. 2174-7.

Chen, H., Tu, S. W. and Hsieh, J. T. (2005) 'Down-regulation of human DAB2IP gene expression mediated by polycomb Ezh2 complex and histone deacetylase in prostate cancer', *J Biol Chem,* 280, (23), pp. 22437-44.

Chuikov, S., Kurash, J. K., Wilson, J. R., Xiao, B., Justin, N., Ivanov, G. S., McKinney, K., Tempst, P., Prives, C., Gamblin, S. J., Barlev, N. A. and Reinberg, D. (2004) 'Regulation of p53 activity through lysine methylation', *Nature,* 432, (7015), pp. 353-60.

Cleutjens, K. B., van der Korput, H. A., van Eekelen, C. C., van Rooij, H. C., Faber, P. W. and Trapman, J. (1997) 'An androgen response element in a far upstream enhancer region is essential for high, androgen-regulated activity of the prostate-specific antigen promoter', *Mol Endocrinol,* 11, (2), pp. 148-61.

Cleutjens, K. B., van Eekelen, C. C., van der Korput, H. A., Brinkmann, A. O. and Trapman, J. (1996) 'Two androgen response regions cooperate in steroid hormone regulated activity of the prostate-specific antigen promoter', *J Biol Chem,* 271, (11), pp. 6379-88.

Cloos, P. A., Christensen, J., Agger, K., Maiolica, A., Rappsilber, J., Antal, T., Hansen, K. H. and Helin, K. (2006) 'The putative oncogene GASC1 demethylates tri- and dimethylated lysine 9 on histone H3', *Nature,* 442, (7100), pp. 307-11.

Cohen, P., Peehl, D. M. and Rosenfeld, R. G. (1994) 'The IGF axis in the prostate', *Horm Metab Res,* 26, (2), pp. 81-4.

Comuzzi, B., Nemes, C., Schmidt, S., Jasarevic, Z., Lodde, M., Pycha,

A., Bartsch, G., Offner, F., Culig, Z. and Hobisch, A. (2004) 'The androgen receptor co-activator CBP is up-regulated following androgen withdrawal and is highly expressed in advanced prostate cancer', *J Pathol,* 204, (2), pp. 159-66.

Cooney, K. A., Wetzel, J. C., Merajver, S. D., Macoska, J. A., Singleton, T. P. and Wojno, K. J. (1996) 'Distinct regions of allelic loss on 13q in prostate cancer', *Cancer Res,* 56, (5), pp. 1142-5.

Couture, J. F., Collazo, E., Hauk, G. and Trievel, R. C. (2006) 'Structural basis for the methylation site specificity of SET7/9', *Nat Struct Mol Biol,* 13, (2), pp. 140-6.

Culig, Z., Comuzzi, B., Steiner, H., Bartsch, G. and Hobisch, A. (2004) 'Expression and function of androgen receptor coactivators in prostate cancer', *J Steroid Biochem Mol Biol,* 92, (4), pp. 265-71.

Culig, Z., Steiner, H., Bartsch, G. and Hobisch, A. (2005) 'Interleukin-6 regulation of prostate cancer cell growth', *J Cell Biochem,* 95, (3), pp. 497-505.

Cunha, G. R., Donjacour, A. A., Cooke, P. S., Mee, S., Bigsby, R. M., Higgins, S. J. and Sugimura, Y. (1987) 'The endocrinology and developmental biology of the prostate', *Endocr Rev,* 8, (3), pp. 338-62.

Cunha, G. R., Ricke, W., Thomson, A., Marker, P. C., Risbridger, G., Hayward, S. W., Wang, Y. Z., Donjacour, A. A. and Kurita, T. (2004) 'Hormonal, cellular, and molecular regulation of normal and neoplastic prostatic development', *J Steroid Biochem Mol Biol,* 92, (4), pp. 221-36.

Dart, D. A., Spencer-Dene, B., Gamble, S. C., Waxman, J. and Bevan, C. L. (2009) 'Manipulating prohibitin levels provides evidence for an in vivo role in androgen regulation of prostate tumours', *Endocr Relat Cancer,* 16, (4), pp. 1157-69.

de la Cruz, X., Lois, S., Sanchez-Molina, S. and Martinez-Balbas, M. A. (2005) 'Do protein motifs read the histone code?', *Bioessays,* 27, (2), pp. 164-75.

De Vries, L., Lou, X., Zhao, G., Zheng, B. and Farquhar, M. G. (1998) 'GIPC, a PDZ domain containing protein, interacts specifically with the C terminus of RGS-GAIP', *Proc Natl Acad Sci U S A,* 95,

(21), pp. 12340-5.

Debes, J. D., Schmidt, L. J., Huang, H. and Tindall, D. J. (2002) 'p300 mediates androgen-independent transactivation of the androgen receptor by interleukin 6', ***Cancer Res,*** **62, (20), pp. 5632-6.**

Deeble, P. D., Murphy, D. J., Parsons, S. J. and Cox, M. E. (2001) 'Interleukin-6- and cyclic AMP-mediated signaling potentiates neuroendocrine differentiation of LNCaP prostate tumor cells', ***Mol Cell Biol,*** **21, (24), pp. 8471-82.**

Di Cristofano, A. and Pandolfi, P. P. (2000) 'The multiple roles of PTEN in tumor suppression', ***Cell,*** **100, (4), pp. 387-90.**

Dillon, S. C., Zhang, X., Trievel, R. C. and Cheng, X. (2005) 'The SET-domain protein superfamily: protein lysine methyltransferases', ***Genome Biol,*** **6, (8), pp. 227.**

Dobosy, J. R., Roberts, J. L., Fu, V. X. and Jarrard, D. F. (2007) 'The expanding role of epigenetics in the development, diagnosis and treatment of prostate cancer and benign prostatic hyperplasia', ***J Urol,*** **177, (3), pp. 822-31.**

Downing, S. R., Russell, P. J. and Jackson, P. (2003) 'Alterations of p53 are common in early stage prostate cancer', ***Can J Urol,*** **10, (4), pp. 1924-33.**

Dubbink, H. J., Hersmus, R., Verma, C. S., van der Korput, H. A., Berrevoets, C. A., van Tol, J., Ziel-van der Made, A. C., Brinkmann, A. O., Pike, A. C. and Trapman, J. (2004) 'Distinct recognition modes of FXXLF and LXXLL motifs by the androgen receptor', ***Mol Endocrinol,*** **18, (9), pp. 2132-50.**

Ea, C. K. and Baltimore, D. (2009) 'Regulation of NF-kappaB activity through lysine monomethylation of p65', ***Proc Natl Acad Sci U S A,*** **106, (45), pp. 18972-7.**

Edwards, J. and Bartlett, J. M. (2005a) 'The androgen receptor and signal-transduction pathways in hormone-refractory prostate cancer. Part 1: Modifications to the androgen receptor', ***BJU Int,*** **95, (9), pp. 1320-6.**

Edwards, J. and Bartlett, J. M. (2005b) 'The androgen receptor and signal-transduction pathways in hormone-refractory prostate

cancer. Part 2: Androgen-receptor cofactors and bypass pathways', *BJU Int,* 95, (9), pp. 1327-35.

Ellem, S. J. and Risbridger, G. P. (2009) 'The dual, opposing roles of estrogen in the prostate', *Ann N Y Acad Sci,* 1155, pp. 174-86.

Fang, J., Feng, Q., Ketel, C. S., Wang, H., Cao, R., Xia, L., Erdjument-Bromage, H., Tempst, P., Simon, J. A. and Zhang, Y. (2002) 'Purification and functional characterization of SET8, a nucleosomal histone H4-lysine 20-specific methyltransferase', *Curr Biol,* 12, (13), pp. 1086-99.

Farmer, G., Colgan, J., Nakatani, Y., Manley, J. L. and Prives, C. (1996) 'Functional interaction between p53, the TATA-binding protein (TBP), andTBP-associated factors in vivo', *Mol Cell Biol,* 16, (8), pp. 4295-304.

Feng, Q., Wang, H., Ng, H. H., Erdjument-Bromage, H., Tempst, P., Struhl, K. and Zhang, Y. (2002) 'Methylation of H3-lysine 79 is mediated by a new family of HMTases without a SET domain', *Curr Biol,* 12, (12), pp. 1052-8.

Francis, J., Chakrabarti, S. K., Garmey, J. C. and Mirmira, R. G. (2005) 'Pdx-1 links histone H3-Lys-4 methylation to RNA polymerase II elongation during activation of insulin transcription', *J Biol Chem,* 280, (43), pp. 36244-53.

Fronsdal, K. and Saatcioglu, F. (2005) 'Histone deacetylase inhibitors differentially mediate apoptosis in prostate cancer cells', *Prostate,* 62, (3), pp. 299-306.

Fu, M., Rao, M., Wang, C., Sakamaki, T., Wang, J., Di Vizio, D., Zhang, X., Albanese, C., Balk, S., Chang, C., Fan, S., Rosen, E., Palvimo, J. J., Janne, O. A., Muratoglu, S., Avantaggiati, M. L. and Pestell, R. G. (2003) 'Acetylation of androgen receptor enhances coactivator binding and promotes prostate cancer cell growth', *Mol Cell Biol,* 23, (23), pp. 8563-75.

Fu, M., Wang, C., Reutens, A. T., Wang, J., Angeletti, R. H., Siconolfi-Baez, L., Ogryzko, V., Avantaggiati, M. L. and Pestell, R. G. (2000) 'p300 and p300/cAMP-response element-binding protein-associated factor acetylate the androgen receptor at sites governing hormone-dependent transactivation', *J Biol Chem,* 275, (27), pp. 20853-60.

Fu, M., Wang, C., Zhang, X. and Pestell, R. G. (2004) 'Acetylation of nuclear receptors in cellular growth and apoptosis', *Biochem Pharmacol,* 68, (6), pp. 1199-208.

Fujimoto, N., Mizokami, A., Harada, S. and Matsumoto, T. (2001) 'Different expression of androgen receptor coactivators in human prostate', *Urology,* 58, (2), pp. 289-94.

Furr, B. J. (1996) 'The development of Casodex (bicalutamide): preclinical studies', *Eur Urol,* 29 Suppl 2, pp. 83-95.

Garnon, J., Lachance, C., Di Marco, S., Hel, Z., Marion, D., Ruiz, M. C., Newkirk, M. M., Khandjian, E. W. and Radzioch, D. (2005) 'Fragile X-related protein FXR1P regulates proinflammatory cytokine tumor necrosis factor expression at the post-transcriptional level', *J Biol Chem,* 280, (7), pp. 5750-63.

Gaughan, L., Logan, I. R., Cook, S., Neal, D. E. and Robson, C. N. (2002) 'Tip60 and histone deacetylase 1 regulate androgen receptor activity through changes to the acetylation status of the receptor', *J Biol Chem,* 277, (29), pp. 25904-13.

Gaughan, L., Logan, I. R., Neal, D. E. and Robson, C. N. (2005) 'Regulation of androgen receptor and histone deacetylase 1 by Mdm2-mediated ubiquitylation', *Nucleic Acids Res,* 33, (1), pp. 13-26.

Gelmann, E. P. (2002) 'Molecular biology of the androgen receptor', *J Clin Oncol,* 20, (13), pp. 3001-15.

Gnanapragasam, V. J., Leung, H. Y., Pulimood, A. S., Neal, D. E. and Robson, C. N. (2001) 'Expression of RAC 3, a steroid hormone receptor co-activator in prostate cancer', *Br J Cancer,* 85, (12), pp. 1928-36.

Gnanapragasam, V. J., Robson, C. N., Leung, H. Y. and Neal, D. E. (2000) 'Androgen receptor signalling in the prostate', *BJU Int,* 86, (9), pp. 1001-13.

Gong, J., Zhu, J., Goodman, O. B., Jr., Pestell, R. G., Schlegel, P. N., Nanus, D. M. and Shen, R. (2006) 'Activation of p300 histone acetyltransferase activity and acetylation of the androgen receptor by bombesin in prostate cancer cells', *Oncogene,* 25,

(14), pp. 2011-21.

Gronberg, H. (2003) 'Prostate cancer epidemiology', *Lancet,* 361, (9360), pp. 859-64.

Gu, W. and Roeder, R. G. (1997) 'Activation of p53 sequence-specific DNA binding by acetylation of the p53 C-terminal domain', *Cell,* 90, (4), pp. 595-606.

Halkidou, K., Cook, S., Leung, H. Y., Neal, D. E. and Robson, C. N. (2004a) 'Nuclear accumulation of histone deacetylase 4 (HDAC4) coincides with the loss of androgen sensitivity in hormone refractory cancer of the prostate', *Eur Urol,* 45, (3), pp. 382-9; author reply 389.

Halkidou, K., Gaughan, L., Cook, S., Leung, H. Y., Neal, D. E. and Robson, C. N. (2004b) 'Upregulation and nuclear recruitment of HDAC1 in hormone refractory prostate cancer', *Prostate,* 59, (2), pp. 177-89.

Halkidou, K., Gnanapragasam, V. J., Mehta, P. B., Logan, I. R., Brady, M. E., Cook, S., Leung, H. Y., Neal, D. E. and Robson, C. N. (2003) 'Expression of Tip60, an androgen receptor coactivator, and its role in prostate cancer development', *Oncogene,* 22, (16), pp. 2466-77.

Hankey, B. F., Feuer, E. J., Clegg, L. X., Hayes, R. B., Legler, J. M., Prorok, P. C., Ries, L. A., Merrill, R. M. and Kaplan, R. S. (1999) 'Cancer surveillance series: interpreting trends in prostate cancer--part I: Evidence of the effects of screening in recent prostate cancer incidence, mortality, and survival rates', *J Natl Cancer Inst,* 91, (12), pp. 1017-24.

Heemers, H. V., Regan, K. M., Schmidt, L. J., Anderson, S. K., Ballman, K. V. and Tindall, D. J. (2009) 'Androgen modulation of coregulator expression in prostate cancer cells', *Mol Endocrinol,* 23, (4), pp. 572-83.

Heemers, H. V. and Tindall, D. J. (2007) 'Androgen receptor (AR) coregulators: a diversity of functions converging on and regulating the AR transcriptional complex', *Endocr Rev,* 28, (7), pp. 778-808.

Heery, D. M., Kalkhoven, E., Hoare, S. and Parker, M. G. (1997) 'A

signature motif in transcriptional co-activators mediates binding to nuclear receptors', *Nature,* 387, (6634), pp. 733-6.

Heinlein, C. A. and Chang, C. (2002) 'Androgen receptor (AR) coregulators: an overview', *Endocr Rev,* 23, (2), pp. 175-200.

Heldin, C. H., Johnsson, A., Wennergren, S., Wernstedt, C., Betsholtz, C. and Westermark, B. (1986) 'A human osteosarcoma cell line secretes a growth factor structurally related to a homodimer of PDGF A-chains', *Nature,* 319, (6053), pp. 511-4.

Heo, K., Kim, B., Kim, K., Choi, J., Kim, H., Zhan, Y., Ranish, J. A. and An, W. (2007) 'Isolation and characterization of proteins associated with histone H3 tails in vivo', *J Biol Chem,* 282, (21), pp. 15476-83.

Holbert, M. A. and Marmorstein, R. (2005) 'Structure and activity of enzymes that remove histone modifications', *Curr Opin Struct Biol,* 15, (6), pp. 673-80.

Hong, C. Y., Suh, J. H., Kim, K., Gong, E. Y., Jeon, S. H., Ko, M., Seong, R. H., Kwon, H. B. and Lee, K. (2005) 'Modulation of androgen receptor transactivation by the SWI3-related gene product (SRG3) in multiple ways', *Mol Cell Biol,* 25, (12), pp. 4841-52.

Hoosein, N. M. (1998) 'Neuroendocrine and immune mediators in prostate cancer progression', *Front Biosci,* 3, pp. D1274-9.

Horie-Inoue, K., Bono, H., Okazaki, Y. and Inoue, S. (2004) 'Identification and functional analysis of consensus androgen response elements in human prostate cancer cells', *Biochem Biophys Res Commun,* 325, (4), pp. 1312-7.

Horoszewicz, J. S., Leong, S. S., Kawinski, E., Karr, J. P., Rosenthal, H., Chu, T. M., Mirand, E. A. and Murphy, G. P. (1983) 'LNCaP model of human prostatic carcinoma', *Cancer Res,* 43, (4), pp. 1809-18.

Hsing, A. W. and Chokkalingam, A. P. (2006) 'Prostate cancer epidemiology', *Front Biosci,* 11, pp. 1388-413.

Hsing, A. W. and Comstock, G. W. (1993) 'Serological precursors of cancer: serum hormones and risk of subsequent prostate cancer',

Cancer Epidemiol Biomarkers Prev, **2, (1), pp. 27-32.**

Hu, P. and Zhang, Y. (2006) 'Catalytic mechanism and product specificity of the histone lysine methyltransferase SET7/9: an ab initio QM/MM-FE study with multiple initial structures', ***J Am Chem Soc,*** **128, (4), pp. 1272-8.**

Huang, J., Perez-Burgos, L., Placek, B. J., Sengupta, R., Richter, M., Dorsey, J. A., Kubicek, S., Opravil, S., Jenuwein, T. and Berger, S. L. (2006) 'Repression of p53 activity by Smyd2-mediated methylation', ***Nature,*** **444, (7119), pp. 629-32.**

Huang, N., vom Baur, E., Garnier, J. M., Lerouge, T., Vonesch, J. L., Lutz, Y., Chambon, P. and Losson, R. (1998) 'Two distinct nuclear receptor interaction domains in NSD1, a novel SET protein that exhibits characteristics of both corepressors and coactivators', ***EMBO J,*** **17, (12), pp. 3398-412.**

Ingber, D. E. (2002) 'Cancer as a disease of epithelial-mesenchymal interactions and extracellular matrix regulation', ***Differentiation,*** **70, (9-10), pp. 547-60.**

Ivanov, G. S., Ivanova, T., Kurash, J., Ivanov, A., Chuikov, S., Gizatullin, F., Herrera-Medina, E. M., Rauscher, F., 3rd, Reinberg, D. and Barlev, N. A. (2007) 'Methylation-acetylation interplay activates p53 in response to DNA damage', ***Mol Cell Biol,*** **27, (19), pp. 6756-69.**

Jacobson, R. H., Ladurner, A. G., King, D. S. and Tjian, R. (2000) 'Structure and function of a human TAFII250 double bromodomain module', ***Science,*** **288, (5470), pp. 1422-5.**

Jacobson, S. and Pillus, L. (1999) 'Modifying chromatin and concepts of cancer', ***Curr Opin Genet Dev,*** **9, (2), pp. 175-84.**

Jenuwein, T. and Allis, C. D. (2001) 'Translating the histone code', ***Science,*** **293, (5532), pp. 1074-80.**

Jiang, C., Hu, H., Malewicz, B., Wang, Z. and Lu, J. (2004) 'Selenite-induced p53 Ser-15 phosphorylation and caspase-mediated apoptosis in LNCaP human prostate cancer cells', ***Mol Cancer Ther,*** **3, (7), pp. 877-84.**

Kahl, P., Gullotti, L., Heukamp, L. C., Wolf, S., Friedrichs, N.,

Vorreuther, R., Solleder, G., Bastian, P. J., Ellinger, J., Metzger, E., Schule, R. and Buettner, R. (2006) 'Androgen receptor coactivators lysine-specific histone demethylase 1 and four and a half LIM domain protein 2 predict risk of prostate cancer recurrence', *Cancer Res,* 66, (23), pp. 11341-7.

Kaighn, M. E., Narayan, K. S., Ohnuki, Y., Lechner, J. F. and Jones, L. W. (1979) 'Establishment and characterization of a human prostatic carcinoma cell line (PC-3)', *Invest Urol,* 17, (1), pp. 16-23.

Kantoff, P. W., Halabi, S., Conaway, M., Picus, J., Kirshner, J., Hars, V., Trump, D., Winer, E. P. and Vogelzang, N. J. (1999) 'Hydrocortisone with or without mitoxantrone in men with hormone-refractory prostate cancer: results of the cancer and leukemia group B 9182 study', *J Clin Oncol,* 17, (8), pp. 2506-13.

Karan, D., Kelly, D. L., Rizzino, A., Lin, M. F. and Batra, S. K. (2002) 'Expression profile of differentially-regulated genes during progression of androgen-independent growth in human prostate cancer cells', *Carcinogenesis,* 23, (6), pp. 967-75.

Katoh, M. (2002) 'GIPC gene family (Review)', *Int J Mol Med,* 9, (6), pp. 585-9.

Kellokumpu-Lehtinen, P. (1985) 'Development of sexual dimorphism in human urogenital sinus complex', *Biol Neonate,* 48, (3), pp. 157-67.

Kellokumpu-Lehtinen, P., Santti, R. and Pelliniemi, L. J. (1980) 'Correlation of early cytodifferentiation of the human fetal prostate and Leydig cells', *Anat Rec,* 196, (3), pp. 263-73.

Khandjian, E. W., Bardoni, B., Corbin, F., Sittler, A., Giroux, S., Heitz, D., Tremblay, S., Pinset, C., Montarras, D., Rousseau, F. and Mandel, J. (1998) 'Novel isoforms of the fragile X related protein FXR1P are expressed during myogenesis', *Hum Mol Genet,* 7, (13), pp. 2121-8.

Kim, J., Jia, L., Tilley, W. D. and Coetzee, G. A. (2003) 'Dynamic methylation of histone H3 at lysine 4 in transcriptional regulation by the androgen receptor', *Nucleic Acids Res,* 31, (23), pp. 6741-7.

Kim, K., Choi, J., Heo, K., Kim, H., Levens, D., Kohno, K., Johnson, E. M., Brock, H. W. and An, W. (2008) 'Isolation and characterization of a novel H1.2 complex that acts as a repressor of p53-mediated transcription', ***J Biol Chem,*** **283, (14), pp. 9113-26.**

Kirikoshi, H. and Katoh, M. (2002) 'Expression of human GIPC1 in normal tissues, cancer cell lines, and primary tumors', ***Int J Mol Med,*** **9, (5), pp. 509-13.**

Kirkpatrick, L. L., McIlwain, K. A. and Nelson, D. L. (1999) 'Alternative splicing in the murine and human FXR1 genes', ***Genomics,*** **59, (2), pp. 193-202.**

Koeneman, K. S. (2006) 'Prostate cancer stem cells, telomerase biology, epigenetic modifiers, and molecular systemic therapy for the androgen-independent lethal phenotype', ***Urol Oncol,*** **24, (2), pp. 119-21.**

Koh, S. S., Chen, D., Lee, Y. H. and Stallcup, M. R. (2001) 'Synergistic enhancement of nuclear receptor function by p160 coactivators and two coactivators with protein methyltransferase activities', ***J Biol Chem,*** **276, (2), pp. 1089-98.**

Kondo, Y., Shen, L., Ahmed, S., Boumber, Y., Sekido, Y., Haddad, B. R. and Issa, J. P. (2008) 'Downregulation of histone H3 lysine 9 methyltransferase G9a induces centrosome disruption and chromosome instability in cancer cells', ***PLoS One,*** **3, (4), pp. e2037.**

Kontaki, H. and Talianidis, I. 'Lysine methylation regulates E2F1-induced cell death', ***Mol Cell,*** **39, (1), pp. 152-60.**

Kouskouti, A., Scheer, E., Staub, A., Tora, L. and Talianidis, I. (2004) 'Gene-specific modulation of TAF10 function by SET9-mediated methylation', ***Mol Cell,*** **14, (2), pp. 175-82.**

Kramer, B. S., Hagerty, K. L., Justman, S., Somerfield, M. R., Albertsen, P. C., Blot, W. J., Ballentine Carter, H., Costantino, J. P., Epstein, J. I., Godley, P. A., Harris, R. P., Wilt, T. J., Wittes, J., Zon, R. and Schellhammer, P. (2009) 'Use of 5-alpha-reductase inhibitors for prostate cancer chemoprevention: American Society of Clinical Oncology/American Urological Association 2008 Clinical Practice Guideline', ***J Clin Oncol,*** **27, (9), pp. 1502-**

16.

Krongrad, A., Wilson, C. M., Wilson, J. D., Allman, D. R. and McPhaul, M. J. (1991) 'Androgen increases androgen receptor protein while decreasing receptor mRNA in LNCaP cells', *Mol Cell Endocrinol*, 76, (1-3), pp. 79-88.

Kulp, S. K., Chen, C. S., Wang, D. S., Chen, C. Y. and Chen, C. S. (2006) 'Antitumor effects of a novel phenylbutyrate-based histone deacetylase inhibitor, (S)-HDAC-42, in prostate cancer', *Clin Cancer Res*, 12, (17), pp. 5199-206.

Kumar, R., Betney, R., Li, J., Thompson, E. B. and McEwan, I. J. (2004) 'Induced alpha-helix structure in AF1 of the androgen receptor upon binding transcription factor TFIIF', *Biochemistry*, 43, (11), pp. 3008-13.

Kurash, J. K., Lei, H., Shen, Q., Marston, W. L., Granda, B. W., Fan, H., Wall, D., Li, E. and Gaudet, F. (2008) 'Methylation of p53 by Set7/9 mediates p53 acetylation and activity in vivo', *Mol Cell*, 29, (3), pp. 392-400.

Lachner, M. and Jenuwein, T. (2002) 'The many faces of histone lysine methylation', *Curr Opin Cell Biol*, 14, (3), pp. 286-98.

Lachner, M., O'Carroll, D., Rea, S., Mechtler, K. and Jenuwein, T. (2001) 'Methylation of histone H3 lysine 9 creates a binding site for HP1 proteins', *Nature*, 410, (6824), pp. 116-20.

Lakin, N. D. and Jackson, S. P. (1999) 'Regulation of p53 in response to DNA damage', *Oncogene*, 18, (53), pp. 7644-55.

Lamm, G. M., Nicol, S. M., Fuller-Pace, F. V. and Lamond, A. I. (1996) 'p72: a human nuclear DEAD box protein highly related to p68', *Nucleic Acids Res*, 24, (19), pp. 3739-47.

Lapointe, J., Li, C., Higgins, J. P., van de Rijn, M., Bair, E., Montgomery, K., Ferrari, M., Egevad, L., Rayford, W., Bergerheim, U., Ekman, P., DeMarzo, A. M., Tibshirani, R., Botstein, D., Brown, P. O., Brooks, J. D. and Pollack, J. R. (2004) 'Gene expression profiling identifies clinically relevant subtypes of prostate cancer', *Proc Natl Acad Sci U S A*, 101, (3), pp. 811-6.

Lawson, K. A., Wright, M. E., Subar, A., Mouw, T., Hollenbeck, A.,

Schatzkin, A. and Leitzmann, M. F. (2007) 'Multivitamin use and risk of prostate cancer in the National Institutes of Health-AARP Diet and Health Study', *J Natl Cancer Inst,* 99, (10), pp. 754-64.

Lee, C., Keefer, M., Zhao, Z. W., Kroes, R., Berg, L., Liu, X. X. and Sensibar, J. (1989) 'Demonstration of the role of prostate-specific antigen in semen liquefaction by two-dimensional electrophoresis', *J Androl,* 10, (6), pp. 432-8.

Lee, D. K. and Chang, C. (2003a) 'Molecular communication between androgen receptor and general transcription machinery', *J Steroid Biochem Mol Biol,* 84, (1), pp. 41-9.

Lee, D. Y., Northrop, J. P., Kuo, M. H. and Stallcup, M. R. (2006a) 'Histone H3 lysine 9 methyltransferase G9a is a transcriptional coactivator for nuclear receptors', *J Biol Chem,* 281, (13), pp. 8476-85.

Lee, D. Y., Teyssier, C., Strahl, B. D. and Stallcup, M. R. (2005a) 'Role of protein methylation in regulation of transcription', *Endocr Rev,* 26, (2), pp. 147-70.

Lee, H. J. and Chang, C. (2003b) 'Recent advances in androgen receptor action', *Cell Mol Life Sci,* 60, (8), pp. 1613-22.

Lee, M. G., Wynder, C., Cooch, N. and Shiekhattar, R. (2005b) 'An essential role for CoREST in nucleosomal histone 3 lysine 4 demethylation', *Nature,* 437, (7057), pp. 432-5.

Lee, M. G., Wynder, C., Norman, J. and Shiekhattar, R. (2006b) 'Isolation and characterization of histone H3 lysine 4 demethylase-containing complexes', *Methods,* 40, (4), pp. 327-30.

Lee, N. Y., Ray, B., How, T. and Blobe, G. C. (2008) 'Endoglin promotes transforming growth factor beta-mediated Smad 1/5/8 signaling and inhibits endothelial cell migration through its association with GIPC', *J Biol Chem,* 283, (47), pp. 32527-33.

Lemaitre, L., Villers, A., Mouton, D. and Puech, P. (2006) '[Transrectal ultrasound and biopsy of the prostate]', *J Radiol,* 87, (2 Pt 2), pp. 201-9.

Li, P., Yu, X., Ge, K., Melamed, J., Roeder, R. G. and Wang, Z. (2002) 'Heterogeneous expression and functions of androgen receptor

co-factors in primary prostate cancer', *Am J Pathol,* 161, (4), pp. 1467-74.

Li, Y., Reddy, M. A., Miao, F., Shanmugam, N., Yee, J. K., Hawkins, D., Ren, B. and Natarajan, R. (2008) 'Role of the histone H3 lysine 4 methyltransferase, SET7/9, in the regulation of NF-kappaB-dependent inflammatory genes. Relevance to diabetes and inflammation', *J Biol Chem,* 283, (39), pp. 26771-81.

Lichtenstein, P., Holm, N. V., Verkasalo, P. K., Iliadou, A., Kaprio, J., Koskenvuo, M., Pukkala, E., Skytthe, A. and Hemminki, K. (2000) 'Environmental and heritable factors in the causation of cancer--analyses of cohorts of twins from Sweden, Denmark, and Finland', *N Engl J Med,* 343, (2), pp. 78-85.

Lilja, H. (1985) 'A kallikrein-like serine protease in prostatic fluid cleaves the predominant seminal vesicle protein', *J Clin Invest,* 76, (5), pp. 1899-903.

Lilja, H., Ulmert, D. and Vickers, A. J. (2008) 'Prostate-specific antigen and prostate cancer: prediction, detection and monitoring', *Nat Rev Cancer,* 8, (4), pp. 268-78.

Lindholmer, C. (1974) 'The importance of seminal plasma for human sperm motility', *Biol Reprod,* 10, (5), pp. 533-42.

Link, K. A., Burd, C. J., Williams, E., Marshall, T., Rosson, G., Henry, E., Weissman, B. and Knudsen, K. E. (2005) 'BAF57 governs androgen receptor action and androgen-dependent proliferation through SWI/SNF', *Mol Cell Biol,* 25, (6), pp. 2200-15.

Liu, A. Y., True, L. D., LaTray, L., Nelson, P. S., Ellis, W. J., Vessella, R. L., Lange, P. H., Hood, L. and van den Engh, G. (1997) 'Cell-cell interaction in prostate gene regulation and cytodifferentiation', *Proc Natl Acad Sci U S A,* 94, (20), pp. 10705-10.

Logan, I. R., Sapountzi, V., Gaughan, L., Neal, D. E. and Robson, C. N. (2004) 'Control of human PIRH2 protein stability: involvement of TIP60 and the proteosome', *J Biol Chem,* 279, (12), pp. 11696-704.

Lonard, D. M. and O'Malley, B. W. (2005) 'Expanding functional diversity of the coactivators', *Trends Biochem Sci,* 30, (3), pp. 126-32.

Lou, X., Yano, H., Lee, F., Chao, M. V. and Farquhar, M. G. (2001) 'GIPC and GAIP form a complex with TrkA: a putative link between G protein and receptor tyrosine kinase pathways', ***Mol Biol Cell,*** **12, (3), pp. 615-27.**

Lu, S., Liu, M., Epner, D. E., Tsai, S. Y. and Tsai, M. J. (1999) 'Androgen regulation of the cyclin-dependent kinase inhibitor p21 gene through an androgen response element in the proximal promoter', ***Mol Endocrinol,*** **13, (3), pp. 376-84.**

Luger, K., Mader, A. W., Richmond, R. K., Sargent, D. F. and Richmond, T. J. (1997) 'Crystal structure of the nucleosome core particle at 2.8 A resolution', ***Nature,*** **389, (6648), pp. 251-60.**

Majumder, S., Liu, Y., Ford, O. H., 3rd, Mohler, J. L. and Whang, Y. E. (2006) 'Involvement of arginine methyltransferase CARM1 in androgen receptor function and prostate cancer cell viability', ***Prostate,*** **66, (12), pp. 1292-301.**

Mangelsdorf, D. J., Thummel, C., Beato, M., Herrlich, P., Schutz, G., Umesono, K., Blumberg, B., Kastner, P., Mark, M., Chambon, P. and Evans, R. M. (1995) 'The nuclear receptor superfamily: the second decade', ***Cell,*** **83, (6), pp. 835-9.**

Marshall, T. W., Link, K. A., Petre-Draviam, C. E. and Knudsen, K. E. (2003) 'Differential requirement of SWI/SNF for androgen receptor activity', ***J Biol Chem,*** **278, (33), pp. 30605-13.**

Martens, J. H., Verlaan, M., Kalkhoven, E. and Zantema, A. (2003) 'Cascade of distinct histone modifications during collagenase gene activation', ***Mol Cell Biol,*** **23, (5), pp. 1808-16.**

Martinez de Hurtado, J., Chechile Toniolo, G. and Villavicencio Mavrich, H. (1995) '[The digital rectal exam, prostate-specific antigen and transrectal echography in the diagnosis of prostatic cancer]', ***Arch Esp Urol,*** **48, (3), pp. 247-59.**

Masatsugu, T. and Yamamoto, K. (2009) 'Multiple lysine methylation of PCAF by Set9 methyltransferase', ***Biochem Biophys Res Commun,*** **381, (1), pp. 22-6.**

Massie, C. E., Adryan, B., Barbosa-Morais, N. L., Lynch, A. G., Tran, M. G., Neal, D. E. and Mills, I. G. (2007) 'New androgen receptor

genomic targets show an interaction with the ETS1 transcription factor', *EMBO Rep,* 8, (9), pp. 871-8.

Masters, J. R. (2002) 'HeLa cells 50 years on: the good, the bad and the ugly', *Nat Rev Cancer,* 2, (4), pp. 315-9.

McEwan, I. J. (2009) 'Nuclear receptors: one big family', *Methods Mol Biol,* 505, pp. 3-18.

McKeithen, D., Graham, T., Chung, L. W. and Odero-Marah, V. 'Snail transcription factor regulates neuroendocrine differentiation in LNCaP prostate cancer cells', *Prostate,* 70, (9), pp. 982-92.

McKenna, N. J., Lanz, R. B. and O'Malley, B. W. (1999) 'Nuclear receptor coregulators: cellular and molecular biology', *Endocr Rev,* 20, (3), pp. 321-44.

McKenna, N. J. and O'Malley, B. W. (2002) 'Minireview: nuclear receptor coactivators--an update', *Endocrinology,* 143, (7), pp. 2461-5.

McNeal, J. E. (1968) 'Regional morphology and pathology of the prostate', *Am J Clin Pathol,* 49, (3), pp. 347-57.

McNeal, J. E. (1969) 'Origin and development of carcinoma in the prostate', *Cancer,* 23, (1), pp. 24-34.

McNeal, J. E. (1978) 'Origin and evolution of benign prostatic enlargement', *Invest Urol,* 15, (4), pp. 340-5.

McNeal, J. E. and Bostwick, D. G. (1986) 'Intraductal dysplasia: a premalignant lesion of the prostate', *Hum Pathol,* 17, (1), pp. 64-71.

McNeal, J. E., Leav, I., Alroy, J. and Skutelsky, E. (1988) 'Differential lectin staining of central and peripheral zones of the prostate and alterations in dysplasia', *Am J Clin Pathol,* 89, (1), pp. 41-8.

Mehra, R., Tomlins, S. A., Yu, J., Cao, X., Wang, L., Menon, A., Rubin, M. A., Pienta, K. J., Shah, R. B. and Chinnaiyan, A. M. (2008) 'Characterization of TMPRSS2-ETS gene aberrations in androgen-independent metastatic prostate cancer', *Cancer Res,* 68, (10), pp. 3584-90.

Mersfelder, E. L. and Parthun, M. R. (2006) 'The tale beyond the tail: histone core domain modifications and the regulation of chromatin structure', ***Nucleic Acids Res,*** **34, (9), pp. 2653-62.**

Metzger, E., Wissmann, M., Yin, N., Muller, J. M., Schneider, R., Peters, A. H., Gunther, T., Buettner, R. and Schule, R. (2005) 'LSD1 demethylates repressive histone marks to promote androgen-receptor-dependent transcription', ***Nature,*** **437, (7057), pp. 436-9.**

Monroe, K. R., Yu, M. C., Kolonel, L. N., Coetzee, G. A., Wilkens, L. R., Ross, R. K. and Henderson, B. E. (1995) 'Evidence of an X-linked or recessive genetic component to prostate cancer risk', ***Nat Med,*** **1, (8), pp. 827-9.**

Montironi, R., Mazzucchelli, R., Lopez-Beltran, A., Cheng, L. and Scarpelli, M. (2007) 'Mechanisms of disease: high-grade prostatic intraepithelial neoplasia and other proposed preneoplastic lesions in the prostate', ***Nat Clin Pract Urol,*** **4, (6), pp. 321-32.**

Muders, M. H., Baretton, G. B., Aust, D. E., Dutta, S. K., Wang, E., Ikeda, Y., Spaller, M. R., Datta, K. and Mukhopadhyay, D. (2007) '[GIPC: a new target for therapy in pancreatic adenocarcinoma?]', ***Verh Dtsch Ges Pathol,*** **91, pp. 286-93.**

Muir, C. S., Nectoux, J. and Staszewski, J. (1991) 'The epidemiology of prostatic cancer. Geographical distribution and time-trends', ***Acta Oncol,*** **30, (2), pp. 133-40.**

Munro, S., Khaire, N., Inche, A., Carr, S. and La Thangue, N. B. (2010) 'Lysine methylation regulates the pRb tumour suppressor protein', ***Oncogene*****.**

Myers, F. A., Chong, W., Evans, D. R., Thorne, A. W. and Crane-Robinson, C. (2003) 'Acetylation of histone H2B mirrors that of H4 and H3 at the chicken beta-globin locus but not at housekeeping genes', ***J Biol Chem,*** **278, (38), pp. 36315-22.**

Nam, R. K., Sugar, L., Yang, W., Srivastava, S., Klotz, L. H., Yang, L. Y., Stanimirovic, A., Encioiu, E., Neill, M., Loblaw, D. A., Trachtenberg, J., Narod, S. A. and Seth, A. (2007) 'Expression of the TMPRSS2:ERG fusion gene predicts cancer recurrence after surgery for localised prostate cancer', ***Br J Cancer,*** **97, (12), pp. 1690-5.**

Narain, V., Cher, M. L. and Wood, D. P., Jr. (2002) 'Prostate cancer diagnosis, staging and survival', *Cancer Metastasis Rev,* 21, (1), pp. 17-27.

Narayana, A. S., Loening, S. A. and Culp, D. A. (1981) 'Flutamide in the treatment of metastatic carcinoma of the prostate', *Br J Urol,* 53, (2), pp. 152-3.

Nelson, P. S., Clegg, N., Arnold, H., Ferguson, C., Bonham, M., White, J., Hood, L. and Lin, B. (2002) 'The program of androgen-responsive genes in neoplastic prostate epithelium', *Proc Natl Acad Sci U S A,* 99, (18), pp. 11890-5.

Nelson, W. G., De Marzo, A. M. and Yegnasubramanian, S. (2009) 'Epigenetic alterations in human prostate cancers', *Endocrinology,* 150, (9), pp. 3991-4002.

Nielsen, S. J., Schneider, R., Bauer, U. M., Bannister, A. J., Morrison, A., O'Carroll, D., Firestein, R., Cleary, M., Jenuwein, T., Herrera, R. E. and Kouzarides, T. (2001) 'Rb targets histone H3 methylation and HP1 to promoters', *Nature,* 412, (6846), pp. 561-5.

Nishioka, K., Chuikov, S., Sarma, K., Erdjument-Bromage, H., Allis, C. D., Tempst, P. and Reinberg, D. (2002) 'Set9, a novel histone H3 methyltransferase that facilitates transcription by precluding histone tail modifications required for heterochromatin formation', *Genes Dev,* 16, (4), pp. 479-89.

Novac, N. and Heinzel, T. (2004) 'Nuclear receptors: overview and classification', *Curr Drug Targets Inflamm Allergy,* 3, (4), pp. 335-46.

Oesterling, J. E. (1991) 'Prostate specific antigen: a critical assessment of the most useful tumor marker for adenocarcinoma of the prostate', *J Urol,* 145, (5), pp. 907-23.

Ozanne, D. M., Brady, M. E., Cook, S., Gaughan, L., Neal, D. E. and Robson, C. N. (2000) 'Androgen receptor nuclear translocation is facilitated by the f-actin cross-linking protein filamin', *Mol Endocrinol,* 14, (10), pp. 1618-26.

Pang, S. T., Weng, W. H., Flores-Morales, A., Johansson, B., Pourian,

M. R., Nilsson, P., Pousette, A., Larsson, C. and Norstedt, G. (2006) 'Cytogenetic and expression profiles associated with transformation to androgen-resistant prostate cancer', *Prostate,* 66, (2), pp. 157-72.

Parkin, D. M., Bray, F., Ferlay, J. and Pisani, P. (2001) 'Estimating the world cancer burden: Globocan 2000', *Int J Cancer,* 94, (2), pp. 153-6.

Patel, S. R., Kim, D., Levitan, I. and Dressler, G. R. (2007) 'The BRCT-domain containing protein PTIP links PAX2 to a histone H3, lysine 4 methyltransferase complex', *Dev Cell,* 13, (4), pp. 580-92.

Patra, S. K., Patra, A. and Dahiya, R. (2001) 'Histone deacetylase and DNA methyltransferase in human prostate cancer', *Biochem Biophys Res Commun,* 287, (3), pp. 705-13.

Patra, S. K., Patra, A., Zhao, H. and Dahiya, R. (2002) 'DNA methyltransferase and demethylase in human prostate cancer', *Mol Carcinog,* 33, (3), pp. 163-71.

Pear, W. S., Nolan, G. P., Scott, M. L. and Baltimore, D. (1993) 'Production of high-titer helper-free retroviruses by transient transfection', *Proc Natl Acad Sci U S A,* 90, (18), pp. 8392-6.

Peterson, C. L. and Laniel, M. A. (2004) 'Histones and histone modifications', *Curr Biol,* 14, (14), pp. R546-51.

Petrylak, D. P., Tangen, C. M., Hussain, M. H., Lara, P. N., Jr., Jones, J. A., Taplin, M. E., Burch, P. A., Berry, D., Moinpour, C., Kohli, M., Benson, M. C., Small, E. J., Raghavan, D. and Crawford, E. D. (2004) 'Docetaxel and estramustine compared with mitoxantrone and prednisone for advanced refractory prostate cancer', *N Engl J Med,* 351, (15), pp. 1513-20.

Powell, S. M., Christiaens, V., Voulgaraki, D., Waxman, J., Claessens, F. and Bevan, C. L. (2004) 'Mechanisms of androgen receptor signalling via steroid receptor coactivator-1 in prostate', *Endocr Relat Cancer,* 11, (1), pp. 117-30.

Pradhan, S., Chin, H. G., Esteve, P. O. and Jacobsen, S. E. (2009) 'SET7/9 mediated methylation of non-histone proteins in mammalian cells', *Epigenetics,* 4, (6), pp. 383-7.

Pulukuri, S. M. and Rao, J. S. (2005) 'Activation of p53/p21Waf1/Cip1 pathway by 5-aza-2'-deoxycytidine inhibits cell proliferation, induces pro-apoptotic genes and mitogen-activated protein kinases in human prostate cancer cells', *Int J Oncol,* 26, (4), pp. 863-71.

Putzi, M. J. and De Marzo, A. M. (2000) 'Morphologic transitions between proliferative inflammatory atrophy and high-grade prostatic intraepithelial neoplasia', *Urology,* 56, (5), pp. 828-32.

Reid, J., Betney, R., Watt, K. and McEwan, I. J. (2003) 'The androgen receptor transactivation domain: the interplay between protein conformation and protein-protein interactions', *Biochem Soc Trans,* 31, (Pt 5), pp. 1042-6.

Reisman, D., Glaros, S. and Thompson, E. A. (2009) 'The SWI/SNF complex and cancer', *Oncogene,* 28, (14), pp. 1653-68.

Reissmann, T., Schally, A. V., Bouchard, P., Riethmiiller, H. and Engel, J. (2000) 'The LHRH antagonist cetrorelix: a review', *Hum Reprod Update,* 6, (4), pp. 322-31.

Rice, J. C., Nishioka, K., Sarma, K., Steward, R., Reinberg, D. and Allis, C. D. (2002) 'Mitotic-specific methylation of histone H4 Lys 20 follows increased PR-Set7 expression and its localization to mitotic chromosomes', *Genes Dev,* 16, (17), pp. 2225-30.

Richiardi, L., Fiano, V., Vizzini, L., De Marco, L., Delsedime, L., Akre, O., Tos, A. G. and Merletti, F. (2009) 'Promoter methylation in APC, RUNX3, and GSTP1 and mortality in prostate cancer patients', *J Clin Oncol,* 27, (19), pp. 3161-8.

Riley, T., Sontag, E., Chen, P. and Levine, A. (2008) 'Transcriptional control of human p53-regulated genes', *Nat Rev Mol Cell Biol,* 9, (5), pp. 402-12.

Robinson-Rechavi, M., Carpentier, A. S., Duffraisse, M. and Laudet, V. (2001) 'How many nuclear hormone receptors are there in the human genome?', *Trends Genet,* 17, (10), pp. 554-6.

Rokhlin, O. W., Scheinker, V. S., Taghiyev, A. F., Bumcrot, D., Glover, R. A. and Cohen, M. B. (2008) 'MicroRNA-34 mediates AR-dependent p53-induced apoptosis in prostate cancer', *Cancer Biol Ther,* 7, (8), pp. 1288-96.

Rubin, M. A. and De Marzo, A. M. (2004) 'Molecular genetics of human prostate cancer', *Mod Pathol,* 17, (3), pp. 380-8.

Sakr, W. A., Haas, G. P., Cassin, B. F., Pontes, J. E. and Crissman, J. D. (1993) 'The frequency of carcinoma and intraepithelial neoplasia of the prostate in young male patients', *J Urol,* 150, (2 Pt 1), pp. 379-85.

Schmidt, D. M. and McCafferty, D. G. (2007) 'trans-2-Phenylcyclopropylamine is a mechanism-based inactivator of the histone demethylase LSD1', *Biochemistry,* 46, (14), pp. 4408-16.

Schuettengruber, B., Chourrout, D., Vervoort, M., Leblanc, B. and Cavalli, G. (2007) 'Genome regulation by polycomb and trithorax proteins', *Cell,* 128, (4), pp. 735-45.

Schulz, W. A. and Hoffmann, M. J. (2009) 'Epigenetic mechanisms in the biology of prostate cancer', *Semin Cancer Biol,* 19, (3), pp. 172-80.

Seligson, D. B., Horvath, S., Shi, T., Yu, H., Tze, S., Grunstein, M. and Kurdistani, S. K. (2005) 'Global histone modification patterns predict risk of prostate cancer recurrence', *Nature,* 435, (7046), pp. 1262-6.

Sellers, W. R. and Loda, M. (2002) 'The EZH2 polycomb transcriptional repressor--a marker or mover of metastatic prostate cancer?', *Cancer Cell,* 2, (5), pp. 349-50.

Shaffer, P. L., Jivan, A., Dollins, D. E., Claessens, F. and Gewirth, D. T. (2004) 'Structural basis of androgen receptor binding to selective androgen response elements', *Proc Natl Acad Sci U S A,* 101, (14), pp. 4758-63.

Shah, U. S. and Getzenberg, R. H. (2004) 'Fingerprinting the diseased prostate: associations between BPH and prostate cancer', *J Cell Biochem,* 91, (1), pp. 161-9.

Shang, Y., Myers, M. and Brown, M. (2002) 'Formation of the androgen receptor transcription complex', *Mol Cell,* 9, (3), pp. 601-10.

Shannon, J., Phoutrides, E., Palma, A., Farris, P., Peters, L., Forester,

A., Tillotson, C. J. and Garzotto, M. (2009) 'Folate intake and prostate cancer risk: a case-control study', *Nutr Cancer,* 61, (5), pp. 617-28.

Shi, X. B., Xue, L., Yang, J., Ma, A. H., Zhao, J., Xu, M., Tepper, C. G., Evans, C. P., Kung, H. J. and deVere White, R. W. (2007) 'An androgen-regulated miRNA suppresses Bak1 expression and induces androgen-independent growth of prostate cancer cells', *Proc Natl Acad Sci U S A,* 104, (50), pp. 19983-8.

Siiteri, P. K. and Wilson, J. D. (1974) 'Testosterone formation and metabolism during male sexual differentiation in the human embryo', *J Clin Endocrinol Metab,* 38, (1), pp. 113-25.

Simard, J., Dumont, M., Soucy, P. and Labrie, F. (2002) 'Perspective: prostate cancer susceptibility genes', *Endocrinology,* 143, (6), pp. 2029-40.

Siomi, M. C., Siomi, H., Sauer, W. H., Srinivasan, S., Nussbaum, R. L. and Dreyfuss, G. (1995) 'FXR1, an autosomal homolog of the fragile X mental retardation gene', *EMBO J,* 14, (11), pp. 2401-8.

Siomi, M. C., Zhang, Y., Siomi, H. and Dreyfuss, G. (1996) 'Specific sequences in the fragile X syndrome protein FMR1 and the FXR proteins mediate their binding to 60S ribosomal subunits and the interactions among them', *Mol Cell Biol,* 16, (7), pp. 3825-32.

Smith, D. C., Chay, C. H., Dunn, R. L., Fardig, J., Esper, P., Olson, K. and Pienta, K. J. (2003) 'Phase II trial of paclitaxel, estramustine, etoposide, and carboplatin in the treatment of patients with hormone-refractory prostate carcinoma', *Cancer,* 98, (2), pp. 269-76.

Smith, R. A., Cokkinides, V. and Eyre, H. J. (2005) 'American Cancer Society Guidelines for the Early Detection of Cancer, 2005', *CA Cancer J Clin,* 55, (1), pp. 31-44; quiz 55-6.

Song, C. S., Jung, M. H., Supakar, P. C., Chatterjee, B. and Roy, A. K. (1999) 'Negative regulation of the androgen receptor gene promoter by NFI and an adjacently located multiprotein-binding site', *Mol Endocrinol,* 13, (9), pp. 1487-96.

Spitz, M. R., Currier, R. D., Fueger, J. J., Babaian, R. J. and Newell, G. R. (1991) 'Familial patterns of prostate cancer: a case-control

analysis', *J Urol,* 146, (5), pp. 1305-7.

Stone, K. R., Mickey, D. D., Wunderli, H., Mickey, G. H. and Paulson, D. F. (1978) 'Isolation of a human prostate carcinoma cell line (DU 145)', *Int J Cancer,* 21, (3), pp. 274-81.

Strahl, B. D. and Allis, C. D. (2000) 'The language of covalent histone modifications', *Nature,* 403, (6765), pp. 41-5.

Struewing, J. P., Hartge, P., Wacholder, S., Baker, S. M., Berlin, M., McAdams, M., Timmerman, M. M., Brody, L. C. and Tucker, M. A. (1997) 'The risk of cancer associated with specific mutations of BRCA1 and BRCA2 among Ashkenazi Jews', *N Engl J Med,* 336, (20), pp. 1401-8.

Subramanian, K., Jia, D., Kapoor-Vazirani, P., Powell, D. R., Collins, R. E., Sharma, D., Peng, J., Cheng, X. and Vertino, P. M. (2008) 'Regulation of estrogen receptor alpha by the SET7 lysine methyltransferase', *Mol Cell,* 30, (3), pp. 336-47.

Sun, C., Dobi, A., Mohamed, A., Li, H., Thangapazham, R. L., Furusato, B., Shaheduzzaman, S., Tan, S. H., Vaidyanathan, G., Whitman, E., Hawksworth, D. J., Chen, Y., Nau, M., Patel, V., Vahey, M., Gutkind, J. S., Sreenath, T., Petrovics, G., Sesterhenn, I. A., McLeod, D. G. and Srivastava, S. (2008) 'TMPRSS2-ERG fusion, a common genomic alteration in prostate cancer activates C-MYC and abrogates prostate epithelial differentiation', *Oncogene,* 27, (40), pp. 5348-53.

Sun, H., Lesche, R., Li, D. M., Liliental, J., Zhang, H., Gao, J., Gavrilova, N., Mueller, B., Liu, X. and Wu, H. (1999) 'PTEN modulates cell cycle progression and cell survival by regulating phosphatidylinositol 3,4,5,-trisphosphate and Akt/protein kinase B signaling pathway', *Proc Natl Acad Sci U S A,* 96, (11), pp. 6199-204.

Suzuki, H., Ueda, T., Ichikawa, T. and Ito, H. (2003) 'Androgen receptor involvement in the progression of prostate cancer', *Endocr Relat Cancer,* 10, (2), pp. 209-16.

Suzuki, M., Shigematsu, H., Shivapurkar, N., Reddy, J., Miyajima, K., Takahashi, T., Gazdar, A. F. and Frenkel, E. P. (2006) 'Methylation of apoptosis related genes in the pathogenesis and prognosis of prostate cancer', *Cancer Lett,* 242, (2), pp. 222-30.

Tamanini, F., Bontekoe, C., Bakker, C. E., van Unen, L., Anar, B., Willemsen, R., Yoshida, M., Galjaard, H., Oostra, B. A. and Hoogeveen, A. T. (1999) 'Different targets for the fragile X-related proteins revealed by their distinct nuclear localizations', ***Hum Mol Genet,*** **8, (5), pp. 863-9.**

Tannock, I. F., Osoba, D., Stockler, M. R., Ernst, D. S., Neville, A. J., Moore, M. J., Armitage, G. R., Wilson, J. J., Venner, P. M., Coppin, C. M. and Murphy, K. C. (1996) 'Chemotherapy with mitoxantrone plus prednisone or prednisone alone for symptomatic hormone-resistant prostate cancer: a Canadian randomized trial with palliative end points', ***J Clin Oncol,*** **14, (6), pp. 1756-64.**

Taplin, M. E. and Balk, S. P. (2004) 'Androgen receptor: a key molecule in the progression of prostate cancer to hormone independence', ***J Cell Biochem,*** **91, (3), pp. 483-90.**

Tenbaum, S. and Baniahmad, A. (1997) 'Nuclear receptors: structure, function and involvement in disease', ***Int J Biochem Cell Biol,*** **29, (12), pp. 1325-41.**

Thirugnanam, S., Xu, L., Ramaswamy, K. and Gnanasekar, M. (2008) 'Glycyrrhizin induces apoptosis in prostate cancer cell lines DU-145 and LNCaP', ***Oncol Rep,*** **20, (6), pp. 1387-92.**

Thornton, J. W. and Kelley, D. B. (1998) 'Evolution of the androgen receptor: structure-function implications', ***Bioessays,*** **20, (10), pp. 860-9.**

Tilley, W. D., Marcelli, M. and McPhaul, M. J. (1990) 'Expression of the human androgen receptor gene utilizes a common promoter in diverse human tissues and cell lines', ***J Biol Chem,*** **265, (23), pp. 13776-81.**

Tomlins, S. A., Mehra, R., Rhodes, D. R., Cao, X., Wang, L., Dhanasekaran, S. M., Kalyana-Sundaram, S., Wei, J. T., Rubin, M. A., Pienta, K. J., Shah, R. B. and Chinnaiyan, A. M. (2007) 'Integrative molecular concept modeling of prostate cancer progression', ***Nat Genet,*** **39, (1), pp. 41-51.**

Tomlins, S. A., Rhodes, D. R., Perner, S., Dhanasekaran, S. M., Mehra, R., Sun, X. W., Varambally, S., Cao, X., Tchinda, J., Kuefer, R.,

Lee, C., Montie, J. E., Shah, R. B., Pienta, K. J., Rubin, M. A. and Chinnaiyan, A. M. (2005) 'Recurrent fusion of TMPRSS2 and ETS transcription factor genes in prostate cancer', *Science,* 310, (5748), pp. 644-8.

Tonini, T., Bagella, L., D'Andrilli, G., Claudio, P. P. and Giordano, A. (2004) 'Ezh2 reduces the ability of HDAC1-dependent pRb2/p130 transcriptional repression of cyclin A', *Oncogene,* 23, (28), pp. 4930-7.

Toyama, Y., Kazama, T., Fuse, H. and Katayama, T. (1995) 'A case of decapitated spermatozoa in an infertile man', *Andrologia,* 27, (3), pp. 165-70.

Trinkle-Mulcahy, L., Boulon, S., Lam, Y. W., Urcia, R., Boisvert, F. M., Vandermoere, F., Morrice, N. A., Swift, S., Rothbauer, U., Leonhardt, H. and Lamond, A. (2008) 'Identifying specific protein interaction partners using quantitative mass spectrometry and bead proteomes', *J Cell Biol,* 183, (2), pp. 223-39.

Turner, B. M. (2000) 'Histone acetylation and an epigenetic code', *Bioessays,* 22, (9), pp. 836-45.

Urbanucci, A., Waltering, K. K., Suikki, H. E., Helenius, M. A. and Visakorpi, T. (2008) 'Androgen regulation of the androgen receptor coregulators', *BMC Cancer,* 8, pp. 219.

Vacher, P. (1995) 'Gn-RH agonists in the treatment of prostatic carcinoma', *Biomed Pharmacother,* 49, (7-8), pp. 325-31.

Vanaja, D. K., Cheville, J. C., Iturria, S. J. and Young, C. Y. (2003) 'Transcriptional silencing of zinc finger protein 185 identified by expression profiling is associated with prostate cancer progression', *Cancer Res,* 63, (14), pp. 3877-82.

Varambally, S., Dhanasekaran, S. M., Zhou, M., Barrette, T. R., Kumar-Sinha, C., Sanda, M. G., Ghosh, D., Pienta, K. J., Sewalt, R. G., Otte, A. P., Rubin, M. A. and Chinnaiyan, A. M. (2002) 'The polycomb group protein EZH2 is involved in progression of prostate cancer', *Nature,* 419, (6907), pp. 624-9.

Velasco, A. M., Gillis, K. A., Li, Y., Brown, E. L., Sadler, T. M., Achilleos, M., Greenberger, L. M., Frost, P., Bai, W. and Zhang,

Y. (2004) 'Identification and validation of novel androgen-regulated genes in prostate cancer', *Endocrinology,* 145, (8), pp. 3913-24.

Wang, H., Cao, R., Xia, L., Erdjument-Bromage, H., Borchers, C., Tempst, P. and Zhang, Y. (2001a) 'Purification and functional characterization of a histone H3-lysine 4-specific methyltransferase', *Mol Cell,* 8, (6), pp. 1207-17.

Wang, H., Huang, Z. Q., Xia, L., Feng, Q., Erdjument-Bromage, H., Strahl, B. D., Briggs, S. D., Allis, C. D., Wong, J., Tempst, P. and Zhang, Y. (2001b) 'Methylation of histone H4 at arginine 3 facilitating transcriptional activation by nuclear hormone receptor', *Science,* 293, (5531), pp. 853-7.

Wang, H., Wang, L., Erdjument-Bromage, H., Vidal, M., Tempst, P., Jones, R. S. and Zhang, Y. (2004) 'Role of histone H2A ubiquitination in Polycomb silencing', *Nature,* 431, (7010), pp. 873-8.

Wang, J., Scully, K., Zhu, X., Cai, L., Zhang, J., Prefontaine, G. G., Krones, A., Ohgi, K. A., Zhu, P., Garcia-Bassets, I., Liu, F., Taylor, H., Lozach, J., Jayes, F. L., Korach, K. S., Glass, C. K., Fu, X. D. and Rosenfeld, M. G. (2007) 'Opposing LSD1 complexes function in developmental gene activation and repression programmes', *Nature,* 446, (7138), pp. 882-7.

Wang, M. C., Valenzuela, L. A., Murphy, G. P. and Chu, T. M. (1979) 'Purification of a human prostate specific antigen', *Invest Urol,* 17, (2), pp. 159-63.

Waterman, M. J., Stavridi, E. S., Waterman, J. L. and Halazonetis, T. D. (1998) 'ATM-dependent activation of p53 involves dephosphorylation and association with 14-3-3 proteins', *Nat Genet,* 19, (2), pp. 175-8.

Weigel, N. L. (1996) 'Steroid hormone receptors and their regulation by phosphorylation', *Biochem J,* 319 (Pt 3), pp. 657-67.

Weinstein, S. J., Wright, M. E., Lawson, K. A., Snyder, K., Mannisto, S., Taylor, P. R., Virtamo, J. and Albanes, D. (2007) 'Serum and dietary vitamin E in relation to prostate cancer risk', *Cancer Epidemiol Biomarkers Prev,* 16, (6), pp. 1253-9.

Wissmann, M., Yin, N., Muller, J. M., Greschik, H., Fodor, B. D., Jenuwein, T., Vogler, C., Schneider, R., Gunther, T., Buettner, R., Metzger, E. and Schule, R. (2007) 'Cooperative demethylation by JMJD2C and LSD1 promotes androgen receptor-dependent gene expression', *Nat Cell Biol,* 9, (3), pp. 347-53.

Wozniak, R. J., Klimecki, W. T., Lau, S. S., Feinstein, Y. and Futscher, B. W. (2006) '5-Aza-2'-deoxycytidine-mediated reductions in G9A histone methyltransferase and histone H3 K9 di-methylation levels are linked to tumor suppressor gene reactivation', *Oncogene*.

Wright, M. E., Eng, J., Sherman, J., Hockenbery, D. M., Nelson, P. S., Galitski, T. and Aebersold, R. (2003) 'Identification of androgen-coregulated protein networks from the microsomes of human prostate cancer cells', *Genome Biol,* 5, (1), pp. R4.

Xia, T., Blackburn, W. R. and Gardner, W. A., Jr. (1990) 'Fetal prostate growth and development', *Pediatr Pathol,* 10, (4), pp. 527-37.

Xiao, B., Jing, C., Wilson, J. R., Walker, P. A., Vasisht, N., Kelly, G., Howell, S., Taylor, I. A., Blackburn, G. M. and Gamblin, S. J. (2003) 'Structure and catalytic mechanism of the human histone methyltransferase SET7/9', *Nature,* 421, (6923), pp. 652-6.

Xu, Y., Chen, S. Y., Ross, K. N. and Balk, S. P. (2006) 'Androgens induce prostate cancer cell proliferation through mammalian target of rapamycin activation and post-transcriptional increases in cyclin D proteins', *Cancer Res,* 66, (15), pp. 7783-92.

Yamane, K., Toumazou, C., Tsukada, Y., Erdjument-Bromage, H., Tempst, P., Wong, J. and Zhang, Y. (2006) 'JHDM2A, a JmjC-containing H3K9 demethylase, facilitates transcription activation by androgen receptor', *Cell,* 125, (3), pp. 483-95.

Yang, X. D., Huang, B., Li, M., Lamb, A., Kelleher, N. L. and Chen, L. F. (2009) 'Negative regulation of NF-kappaB action by Set9-mediated lysine methylation of the RelA subunit', *EMBO J,* 28, (8), pp. 1055-66.

Yuan, T. C., Veeramani, S. and Lin, M. F. (2007) 'Neuroendocrine-like prostate cancer cells: neuroendocrine transdifferentiation of prostate adenocarcinoma cells', *Endocr Relat Cancer,* 14, (3), pp. 531-47.

Zhang, Y., Akinmade, D. and Hamburger, A. W. (2005a) 'The ErbB3 binding protein Ebp1 interacts with Sin3A to repress E2F1 and AR-mediated transcription', *Nucleic Acids Res,* 33, (18), pp. 6024-33.

Zhang, Y., Linn, D., Liu, Z., Melamed, J., Tavora, F., Young, C. Y., Burger, A. M. and Hamburger, A. W. (2008) 'EBP1, an ErbB3-binding protein, is decreased in prostate cancer and implicated in hormone resistance', *Mol Cancer Ther,* 7, (10), pp. 3176-86.

Zhang, Y., O'Connor, J. P., Siomi, M. C., Srinivasan, S., Dutra, A., Nussbaum, R. L. and Dreyfuss, G. (1995) 'The fragile X mental retardation syndrome protein interacts with novel homologs FXR1 and FXR2', *EMBO J,* 14, (21), pp. 5358-66.

Zhang, Y., Wang, X. W., Jelovac, D., Nakanishi, T., Yu, M. H., Akinmade, D., Goloubeva, O., Ross, D. D., Brodie, A. and Hamburger, A. W. (2005b) 'The ErbB3-binding protein Ebp1 suppresses androgen receptor-mediated gene transcription and tumorigenesis of prostate cancer cells', *Proc Natl Acad Sci U S A,* 102, (28), pp. 9890-5.

Zhao, X., Gschwend, J. E., Powell, C. T., Foster, R. G., Day, K. C. and Day, M. L. (1997) 'Retinoblastoma protein-dependent growth signal conflict and caspase activity are required for protein kinase C-signaled apoptosis of prostate epithelial cells', *J Biol Chem,* 272, (36), pp. 22751-7.

Publications

Regulation of the androgen receptor by SET9-mediated methylation
Gaughan, Luke; Stockley, Jacqueline; Wang, Nan; McCracken, Stuart; Treumann, Achim; Armstrong, Kelly; Watt, Kate; McEwan, Iain; Wang, Chenguang.; Pestell, Richard; Robson, Craig
Nuclear Acid Research-01064-X-2010.R1

Band No	File Name	Identifier	log(t)	rl	log(e)	pI	Mr	Description
19	*090211_13_NW_C10.mgf*	ENSP00000009589	5.66	3	-14.1	9.9	13.4	40S ribosomal protein S20 [Source:UniProtKB/Swiss-Prot;Acc:P60866]
21	*090211_15_NW_C11.mgf*	ENSP00000009589	5.46	2	-8	9.9	13.4	40S ribosomal protein S20 [Source:UniProtKB/Swiss-Prot;Acc:P60866]
39	*090213_16_NW_C20.mgf*	ENSP00000014112	3.83	1	-1.3	9.2	57.2	Polypyrimidine tract-binding protein 1 (PTB)(Heterogeneous nuclear ribonucleoprotein I)(hnRNP I)(57 kDa RNA-binding protein PPTB-1) [Source:UniProtKB/Swiss-Prot;Acc:P26599]
40	*090213_17_NW_S20.mgf*	ENSP00000014112	3.61	1	-2.1	9.2	57.2	Polypyrimidine tract-binding protein 1 (PTB)(Heterogeneous nuclear ribonucleoprotein I)(hnRNP I)(57 kDa RNA-binding protein PPTB-1) [Source:UniProtKB/Swiss-Prot;Acc:P26599]
8	*090213_10_NW_S4.mgf*	ENSP00000084795	3.26	1	-5.6	12	21.6	60S ribosomal protein L18 [Source:UniProtKB/Swiss-Prot;Acc:Q07020]
37	090213_13_NW_C19.mgf	ENSP00000084795	3.5	1	-4.9	12	21.6	60S ribosomal protein L18 [Source:UniProtKB/Swiss-Prot;Acc:Q07020]
39	*090213_16_NW_C20.mgf*	ENSP00000084795	3.19	1	-1.4	12	21.6	60S ribosomal protein L18 [Source:UniProtKB/Swiss-Prot;Acc:Q07020]
15	*090211_08_NW_C8.mgf*	ENSP00000162391	4.06	1	-1.6	6.2	62.4	Forkhead box protein J2 (Fork head homologous X) [Source:UniProtKB/Swiss-Prot;Acc:Q9P0K8]
14	*090211_07_NW_S7.mgf*	ENSP00000172853	5.38	2	-1.3	9.1	772.5	Nebulin [Source:UniProtKB/Swiss-Prot;Acc:P20929]
15	*090211_08_NW_C8.mgf*	ENSP00000173527	3.74	1	-1.1	6.5	22.2	Isochorismatase domain-containing protein 1 [Source:UniProtKB/Swiss-Prot;Acc:Q96CN7]
37	090213_13_NW_C19.mgf	ENSP00000188376	3.31	1	-1.5	9.4	39.9	Phosphate carrier protein, mitochondrial Precursor (Phosphate transport protein)(PTP)(Solute carrier family 25 member 3) [Source:UniProtKB/Swiss-Prot;Acc:O00325]
8	*090213_10_NW_S4.mgf*	ENSP00000202773	4.48	3	-12.9	11	32.7	60S ribosomal protein L6 (TAX-responsive enhancer element-binding protein 107)(TAXREB107)(Neoplasm-related protein C140) [Source:UniProtKB/Swiss-Prot;Acc:O02878]
40	*090213_17_NW_S20.mgf*	ENSP00000202773	3.81	1	-1.6	11	32.7	60S ribosomal protein L6 (TAX-responsive enhancer element-binding protein 107)(TAXREB107)(Neoplasm-related protein C140) [Source:UniProtKB/Swiss-Prot;Acc:O02878]
9	*090213_11_NW_C5.mgf*	ENSP00000204732	4.91	3	-18.1	9.3	70.7	Polyadenylate-binding protein 4 (Poly(A)-binding protein 4) (PABP 4) (Inducible poly(A)-binding protein) (iPABP) (Activated-platelet protein 1) (APP-1). Source: Uniprot/SWISSPROT O13310
21	*090211_15_NW_C11.mgf*	ENSP00000207437	4.14	1	-3.2	5.6	22.7	Myosin light chain 6B (Smooth muscle and nonmuscle myosin light chain alkali 6B)(Myosin light chain 1 slow-twitch muscle A isoform)(MLC1sa) [Source:UniProtKB/Swiss-Prot;Acc:P14649]
23	*090211_18_NW_C12.mgf*	ENSP00000207437	4.1	1	-2.2	5.6	22.7	Myosin light chain 6B (Smooth muscle and nonmuscle myosin light chain alkali 6B)(Myosin light chain 1 slow-twitch muscle A isoform)(MLC1sa) [Source:UniProtKB/Swiss-Prot;Acc:P14649]
5	*090213_06_NW_C3.mgf*	ENSP00000211372	4.84	5	-11.3	11	17.7	40S ribosomal protein S18 (Ke-3)(Ke3) [Source:UniProtKB/Swiss-Prot;Acc:P62269]
35	*090211_32_NW_C18.mgf*	ENSP00000211372	3.17	1	-1.7	11	17.7	40S ribosomal protein S18 (Ke-3)(Ke3) [Source:UniProtKB/Swiss-Prot;Acc:P62269]
38	*090213_14_NW_S19.mgf*	ENSP00000211372	3.95	2	-2.6	11	17.7	40S ribosomal protein S18 (Ke-3)(Ke3) [Source:UniProtKB/Swiss-Prot;Acc:P62269]
39	*090213_16_NW_C20.mgf*	ENSP00000211372	3.31	1	-1.5	11	17.7	40S ribosomal protein S18 (Ke-3)(Ke3) [Source:UniProtKB/Swiss-Prot;Acc:P62269]
40	*090213_17_NW_S20.mgf*	ENSP00000211372	3.97	2	-7.7	11	17.7	40S ribosomal protein S18 (Ke-3)(Ke3) [Source:UniProtKB/Swiss-Prot;Acc:P62269]
41	*090213_18_NW_C21.mgf*	ENSP00000211372	3.46	1	-2.3	11	17.7	40S ribosomal protein S18 (Ke-3)(Ke3) [Source:UniProtKB/Swiss-Prot;Acc:P62269]
42	*090213_19_NW_S21.mgf*	ENSP00000211372	3.92	2	-1.9	11	17.7	40S ribosomal protein S18 (Ke-3)(Ke3) [Source:UniProtKB/Swiss-Prot;Acc:P62269]
48	*090213_26_NW_S24.mgf*	ENSP00000211372	3.63	1	-2.1	11	17.7	40S ribosomal protein S18 (Ke-3)(Ke3) [Source:UniProtKB/Swiss-Prot;Acc:P62269]
8	*090213_10_NW_S4.mgf*	ENSP00000215375	3.73	1	-2	5.3	17.5	ATP synthase subunit delta, mitochondrial Precursor (F-ATPase delta subunit) [Source:UniProtKB/Swiss-Prot;Acc:P30049]
10	*090213_12_NW_S5.mgf*	ENSP00000216019	3.41	1	-4.5	8.5	80.2	Probable ATP-dependent RNA helicase DDX17 (EC 3.6.1.-)(DEAD box protein 17)(RNA-dependent helicase p72)(DEAD box protein p72) [Source:UniProtKB/Swiss-Prot;Acc:Q92841]
9	*090213_11_NW_C5.mgf*	ENSP00000216038	4.23	1	-1.9	6.8	55.2	UPF0027 protein C22orf28 [Source:UniProtKB/Swiss-Prot;Acc:Q9Y3I0]
37	090213_13_NW_C19.mgf	ENSP00000216038	3.31	1	-2.5	6.8	55.2	UPF0027 protein C22orf28 [Source:UniProtKB/Swiss-Prot;Acc:Q9Y3I0]
38	*090213_14_NW_S19.mgf*	ENSP00000216038	3.34	1	-2.9	6.8	55.2	UPF0027 protein C22orf28 [Source:UniProtKB/Swiss-Prot;Acc:Q9Y3I0]
35	*090211_32_NW_C18.mgf*	ENSP00000216181	4.37	4	-27.1	5.5	226.4	Myosin-9 (Myosin heavy chain 9)(Myosin heavy chain, non-muscle IIa)(Non-muscle myosin heavy chain IIa)(NMMHC II-a)(NMMHC-IIA)(Cellular myosin heavy chain, type A)(Non-muscle myosin heavy chain-A)(NMMHC-A) [Source:UniProtKB/Swiss-Prot;Acc:P35579]
6	*090213_07_NW_S3.mgf*	ENSP00000216538	3.25	1	-1.2	12	31.2	
35	*090211_32_NW_C18.mgf*	ENSP00000217074	4.36	2	-7.7	9.3	37.7	Polyadenylate-binding protein 1-like [Source:UniProtKB/Swiss-Prot;Acc:Q4VXU2]
36	*090211_32_NW_S18.mgf*	ENSP00000217074	3.96	1	-2.3	9.3	37.7	Polyadenylate-binding protein 1-like [Source:UniProtKB/Swiss-Prot;Acc:Q4VXU2]
38	*090213_14_NW_S19.mgf*	ENSP00000217074	4.07	2	-6.6	9.3	37.7	Polyadenylate-binding protein 1-like [Source:UniProtKB/Swiss-Prot;Acc:Q4VXU2]
39	*090213_16_NW_C20.mgf*	ENSP00000217074	4.08	2	-6.6	9.3	37.7	Polyadenylate-binding protein 1-like [Source:UniProtKB/Swiss-Prot;Acc:Q4VXU2]
37	090213_13_NW_C19.mgf	ENSP00000217182	3.68	1	-2.8	9.1	50.4	Elongation factor 1-alpha 2 (EF-1-alpha-2)(Elongation factor 1 A-2)(eEF1A-2)(Statin S1) [Source:UniProtKB/Swiss-Prot;Acc:Q05639]
38	*090213_14_NW_S19.mgf*	ENSP00000217182	3.52	1	-1.7	9.1	50.4	Elongation factor 1-alpha 2 (EF-1-alpha-2)(Elongation factor 1 A-2)(eEF1A-2)(Statin S1) [Source:UniProtKB/Swiss-Prot;Acc:Q05639]
39	*090213_16_NW_C20.mgf*	ENSP00000217182	3.54	1	-2.8	9.1	50.4	Elongation factor 1-alpha 2 (EF-1-alpha-2)(Elongation factor 1 A-2)(eEF1A-2)(Statin S1) [Source:UniProtKB/Swiss-Prot;Acc:Q05639]
40	*090213_17_NW_S20.mgf*	ENSP00000217182	3.51	1	-3.9	9.1	50.4	Elongation factor 1-alpha 2 (EF-1-alpha-2)(Elongation factor 1 A-2)(eEF1A-2)(Statin S1) [Source:UniProtKB/Swiss-Prot;Acc:Q05639]
5	*090213_06_NW_C3.mgf*	ENSP00000217652	4.63	6	-17.8	4.6	19.8	Myosin regulatory light chain MRLC3 (Myosin regulatory light chain 2, nonsarcomeric)(Myosin RLC)(MLC-2B) [Source:UniProtKB/Swiss-Prot;Acc:P19105]
6	*090213_07_NW_S3.mgf*	ENSP00000217652	3.69	2	-5.5	4.6	19.8	Myosin regulatory light chain MRLC3 (Myosin regulatory light chain 2, nonsarcomeric)(Myosin RLC)(MLC-2B) [Source:UniProtKB/Swiss-Prot;Acc:P19105]
21	*090211_15_NW_C11.mgf*	ENSP00000217652	3.46	1	-5.2	4.6	19.8	Myosin regulatory light chain MRLC3 (Myosin regulatory light chain 2, nonsarcomeric)(Myosin RLC)(MLC-2B) [Source:UniProtKB/Swiss-Prot;Acc:P19105]
9	*090213_11_NW_C5.mgf*	ENSP00000218316	4.43	1	-1.7	7.6	67.3	Melatonin-related receptor (G protein-coupled receptor 50)(H9) [Source:UniProtKB/Swiss-Prot;Acc:O13585]
20	*090211_14_NW_S10.mgf*	ENSP00000219439	4.86	1	-1.5	8.9	37	Hydroxysteroid dehydrogenase-like protein 1 [Source:UniProtKB/Swiss-Prot;Acc:Q3SXM5]
10	*090213_12_NW_S5.mgf*	ENSP00000221418	3.52	1	-3.2	8.2	35.8	Delta(3,5)-Delta(2,4)-dienoyl-CoA isomerase, mitochondrial Precursor (EC 5.3.3.-) [Source:UniProtKB/Swiss-Prot;Acc:Q13011]
10	*090213_12_NW_S5.mgf*	ENSP00000221419	3.84	1	-6	8.6	64.2	Heterogeneous nuclear ribonucleoprotein L (hnRNP L) [Source:UniProtKB/Swiss-Prot;Acc:P14866]
5	*090213_06_NW_C3.mgf*	ENSP00000221975	4.91	4	-12.1	10	16.1	40S ribosomal protein S19 [Source:UniProtKB/Swiss-Prot;Acc:P39019]
8	*090213_10_NW_S4.mgf*	ENSP00000221975	5.07	6	-11.5	10	16.1	40S ribosomal protein S19 [Source:UniProtKB/Swiss-Prot;Acc:P39019]
21	*090211_15_NW_C11.mgf*	ENSP00000221975	5.31	2	-1.7	10	16.1	40S ribosomal protein S19 [Source:UniProtKB/Swiss-Prot;Acc:P39019]
24	*090211_19_NW_S12.mgf*	ENSP00000221975	4.58	1	-2	10	16.1	40S ribosomal protein S19 [Source:UniProtKB/Swiss-Prot;Acc:P39019]
5	*090213_06_NW_C3.mgf*	ENSP00000222956	4.34	1	-2.4	9.1	29.4	Uncharacterized protein ENSP00000222956 Fragment [Source:UniProtKB/TrEMBL;Acc:A6NCA2]
8	*090213_10_NW_S4.mgf*	ENSP00000222956	4.17	1	-1.7	9.1	29.4	Uncharacterized protein ENSP00000222956 Fragment [Source:UniProtKB/TrEMBL;Acc:A6NCA2]
5	*090213_06_NW_C3.mgf*	ENSP00000223129	3.52	1	-5.2	4.9	13.6	Replication protein A 14 kDa subunit (RP-A p14)(Replication factor A protein 3)(RF-A protein 3) [Source:UniProtKB/Swiss-Prot;Acc:P35244]
10	*090213_12_NW_S5.mgf*	ENSP00000223129	3.81	1	-2.7	4.9	13.6	Replication protein A 14 kDa subunit (RP-A p14)(Replication factor A protein 3)(RF-A protein 3) [Source:UniProtKB/Swiss-Prot;Acc:P35244]
2	*090213_03_NW_S1.mgf*	ENSP00000224784	3.51	1	-1.4	5.2	42	Actin, aortic smooth muscle (Alpha-actin-2)(Cell growth-inhibiting gene 46 protein) [Source:UniProtKB/Swiss-Prot;Acc:P62736]
10	*090213_12_NW_S5.mgf*	ENSP00000224784	4.38	3	-3.6	5.2	42	Actin, aortic smooth muscle (Alpha-actin-2)(Cell growth-inhibiting gene 46 protein) [Source:UniProtKB/Swiss-Prot;Acc:P62736]
17	*090211_11_NW_C9.mgf*	ENSP00000224784	5.14	1	-1.3	5.2	42	Actin, aortic smooth muscle (Alpha-actin-2)(Cell growth-inhibiting gene 46 protein) [Source:UniProtKB/Swiss-Prot;Acc:P62736]
19	*090211_13_NW_C10.mgf*	ENSP00000224784	6.28	8	-3.3	5.2	42	Actin, aortic smooth muscle (Alpha-actin-2)(Cell growth-inhibiting gene 46 protein) [Source:UniProtKB/Swiss-Prot;Acc:P62736]
20	*090211_14_NW_S10.mgf*	ENSP00000224784	5.49	4	-4.7	5.2	42	Actin, aortic smooth muscle (Alpha-actin-2)(Cell growth-inhibiting gene 46 protein) [Source:UniProtKB/Swiss-Prot;Acc:P62736]
30	*090211_26_NW_S15.mgf*	ENSP00000224784	4.86	1	-3.4	5.2	42	Actin, aortic smooth muscle (Alpha-actin-2)(Cell growth-inhibiting gene 46 protein) [Source:UniProtKB/Swiss-Prot;Acc:P62736]
33	*090211_29_NW_C17.mgf*	ENSP00000224784	4.26	2	-2.3	5.2	42	Actin, aortic smooth muscle (Alpha-actin-2)(Cell growth-inhibiting gene 46 protein) [Source:UniProtKB/Swiss-Prot;Acc:P62736]
34	*090211_30_NW_S17.mgf*	ENSP00000224784	3.84	1	-1.2	5.2	42	Actin, aortic smooth muscle (Alpha-actin-2)(Cell growth-inhibiting gene 46 protein) [Source:UniProtKB/Swiss-Prot;Acc:P62736]
38	*090213_14_NW_S19.mgf*	ENSP00000224784	4.29	3	-17.7	5.2	42	Actin, aortic smooth muscle (Alpha-actin-2)(Cell growth-inhibiting gene 46 protein) [Source:UniProtKB/Swiss-Prot;Acc:P62736]
8	*090213_10_NW_S4.mgf*	ENSP00000225430	3.46	1	-14.2	12	23.3	60S ribosomal protein L19 [Source:UniProtKB/Swiss-Prot;Acc:P84098]
5	*090213_06_NW_C3.mgf*	ENSP00000227378	3.98	2	-6.9	5.4	70.9	Heat shock cognate 71 kDa protein (Heat shock 70 kDa protein 8) [Source:UniProtKB/Swiss-Prot;Acc:P11142]
6	*090213_07_NW_S3.mgf*	ENSP00000227378	3.24	1	-5.2	5.4	70.9	Heat shock cognate 71 kDa protein (Heat shock 70 kDa protein 8) [Source:UniProtKB/Swiss-Prot;Acc:P11142]
8	*090213_10_NW_S4.mgf*	ENSP00000227378	4.3	3	-27	5.4	70.9	Heat shock cognate 71 kDa protein (Heat shock 70 kDa protein 8) [Source:UniProtKB/Swiss-Prot;Acc:P11142]
9	*090213_11_NW_C5.mgf*	ENSP00000227378	5.92	5	-15.1	5.4	70.9	Heat shock cognate 71 kDa protein (Heat shock 70 kDa protein 8) [Source:UniProtKB/Swiss-Prot;Acc:P11142]
10	*090213_12_NW_S5.mgf*	ENSP00000227378	4.72	7	-20.7	5.4	70.9	Heat shock cognate 71 kDa protein (Heat shock 70 kDa protein 8) [Source:UniProtKB/Swiss-Prot;Acc:P11142]
17	*090211_11_NW_C9.mgf*	ENSP00000227378	4.54	4	-10.2	5.4	70.9	Heat shock cognate 71 kDa protein (Heat shock 70 kDa protein 8) [Source:UniProtKB/Swiss-Prot;Acc:P11142]
20	*090211_14_NW_S10.mgf*	ENSP00000227378	3.34	1	-4.5	5.4	70.9	Heat shock cognate 71 kDa protein (Heat shock 70 kDa protein 8) [Source:UniProtKB/Swiss-Prot;Acc:P11142]
9	*090213_11_NW_C5.mgf*	ENSP00000228140	3.62	1	-6.4	11	17.2	40S ribosomal protein S13 [Source:UniProtKB/Swiss-Prot;Acc:P62277]
10	*090213_12_NW_S5.mgf*	ENSP00000228140	3.73	1	-5.1	11	17.2	40S ribosomal protein S13 [Source:UniProtKB/Swiss-Prot;Acc:P62277]
21	*090211_15_NW_C11.mgf*	ENSP00000228140	5.09	1	-4.2	11	17.2	40S ribosomal protein S13 [Source:UniProtKB/Swiss-Prot;Acc:P62277]
24	*090211_19_NW_S12.mgf*	ENSP00000228140	4.75	1	-3.9	11	17.2	40S ribosomal protein S13 [Source:UniProtKB/Swiss-Prot;Acc:P62277]
36	*090211_32_NW_S18.mgf*	ENSP00000228140	4.15	1	-2.5	11	17.2	40S ribosomal protein S13 [Source:UniProtKB/Swiss-Prot;Acc:P62277]

37	090213 13 NW C19.mgf	ENSP00000228140	4.09	2	-4	11	17.2	40S ribosomal protein S13 [Source:UniProtKB/Swiss-Prot;Acc:P62277]
38	*090213_14_NW_S19.mgf*	ENSP00000228140	3.74	1	-3.6	11	17.2	40S ribosomal protein S13 [Source:UniProtKB/Swiss-Prot;Acc:P62277]
39	*090213_16_NW_C20.mgf*	ENSP00000228140	3.38	1	-4.1	11	17.2	40S ribosomal protein S13 [Source:UniProtKB/Swiss-Prot;Acc:P62277]
40	*090213_17_NW_S20.mgf*	ENSP00000228140	4.17	2	-12.4	11	17.2	40S ribosomal protein S13 [Source:UniProtKB/Swiss-Prot;Acc:P62277]
41	*090213_18_NW_C21.mgf*	ENSP00000228140	3.3	1	-1.2	11	17.2	40S ribosomal protein S13 [Source:UniProtKB/Swiss-Prot;Acc:P62277]
42	*090213_19_NW_S21.mgf*	ENSP00000228140	3.34	1	-3.8	11	17.2	40S ribosomal protein S13 [Source:UniProtKB/Swiss-Prot;Acc:P62277]
9	*090213_11_NW_C5.mgf*	ENSP00000228251	3.5	1	-12.5	9.8	40.1	DNA-binding protein A (Cold shock domain-containing protein A)(Single-strand DNA-binding protein NF-GMB) [Source:UniProtKB/Swiss-Prot;Acc:P16989]
40	*090213_17_NW_S20.mgf*	ENSP00000229239	3.68	1	-3.8	8.6	36	Glyceraldehyde-3-phosphate dehydrogenase (GAPDH)(EC 1.2.1.12) [Source:UniProtKB/Swiss-Prot;Acc:P04406]
41	*090213_18_NW_C21.mgf*	ENSP00000229239	3.61	1	-1.7	8.6	36	Glyceraldehyde-3-phosphate dehydrogenase (GAPDH)(EC 1.2.1.12) [Source:UniProtKB/Swiss-Prot;Acc:P04406]
9	*090213_11_NW_C5.mgf*	ENSP00000236051	4.46	1	-1.4	10	34.8	Probable rRNA-processing protein EBP2 (EBNA1-binding protein 2)(Nucleolar protein p40) [Source:UniProtKB/Swiss-Prot;Acc:O99848]
5	*090213 06 NW C3.mgf*	ENSP00000240851	5.43	12	-47.8	4.9	43.4	Protein TFG (TRK-fused gene protein) [Source:UniProtKB/Swiss-Prot;Acc:O92734]
6	*090213 07 NW S3.mgf*	ENSP00000240851	4.4	5	-18.3	4.9	43.4	Protein TFG (TRK-fused gene protein) [Source:UniProtKB/Swiss-Prot;Acc:O92734]
8	*090213 10 NW S4.mgf*	ENSP00000240851	4.16	2	-3.1	4.9	43.4	Protein TFG (TRK-fused gene protein) [Source:UniProtKB/Swiss-Prot;Acc:O92734]
5	*090213 06 NW C3.mgf*	ENSP00000242284	5.17	9	-24.7	4.5	23.6	Clathrin light chain A (Lca) [Source:UniProtKB/Swiss-Prot;Acc:P09496]
6	*090213 07 NW S3.mgf*	ENSP00000242284	4.92	5	-17.2	4.5	23.6	Clathrin light chain A (Lca) [Source:UniProtKB/Swiss-Prot;Acc:P09496]
8	*090213 10 NW S4.mgf*	ENSP00000242284	4.61	1	-1.3	4.5	23.6	Clathrin light chain A (Lca) [Source:UniProtKB/Swiss-Prot;Acc:P09496]
14	*090211 07 NW S7.mgf*	ENSP00000242284	4.12	1	-2.3	4.5	23.6	Clathrin light chain A (Lca) [Source:UniProtKB/Swiss-Prot;Acc:P09496]
10	*090213_12_NW_S5.mgf*	ENSP00000244020	3.66	1	-3.2	11	39.6	Splicing factor, arginine/serine-rich 6 (Pre-mRNA-splicing factor SRP55) [Source:UniProtKB/Swiss-Prot;Acc:Q13247]
21	*090211_15_NW_C11.mgf'*	ENSP00000244534	4.74	2	-10.5	11	22.3	Histone H1.3 (Histone H1c) [Source:UniProtKB/Swiss-Prot;Acc:P16402]
9	*090213 11 NW C5.mgf*	ENSP00000244573	5.58	2	-7.8	11	21.8	Histone H1.1 [Source:UniProtKB/Swiss-Prot;Acc:Q02539]
10	*090213 12 NW S5.mgf*	ENSP00000244573	4.07	1	-6.8	11	21.8	Histone H1.1 [Source:UniProtKB/Swiss-Prot;Acc:Q02539]
14	*090211 07 NW S7.mgf*	ENSP00000246911	4.17	1	-2	5.8	31.8	Interferon-induced 35 kDa protein (IFP 35) [Source:UniProtKB/Swiss-Prot;Acc:P80217]
8	*090213_10_NW_S4.mgf*	ENSP00000247207	4.24	3	-16.3	5.6	70	Heat shock-related 70 kDa protein 2 (Heat shock 70 kDa protein 2) [Source:UniProtKB/Swiss-Prot;Acc:P54652]
19	*090211_13_NW_C10.mgf*	ENSP00000248071	4.31	1	-1.6	9.1	37.4	Krueppel-like factor 2 (Lung krueppel-like factor) [Source:UniProtKB/Swiss-Prot;Acc:Q9Y5W3]
9	*090213_11_NW_C5.mgf*	ENSP00000248553	4.98	2	-10.2	6	22.8	Heat shock protein beta-1 (HspB1)(Heat shock 27 kDa protein)(HSP 27)(Stress-responsive protein 27)(SRP27)(Estrogen-regulated 24 kDa protein)(28 kDa heat shock protein) [Source:UniProtKB/Swiss-Prot;Acc:P04792]
10	*090213_12_NW_S5.mgf*	ENSP00000248553	4.32	2	-6.9	6	22.8	Heat shock protein beta-1 (HspB1)(Heat shock 27 kDa protein)(HSP 27)(Stress-responsive protein 27)(SRP27)(Estrogen-regulated 24 kDa protein)(28 kDa heat shock protein) [Source:UniProtKB/Swiss-Prot;Acc:P04792]
19	*090211_13_NW_C10.mgf*	ENSP00000248553	4.71	1	-4.1	6	22.8	Heat shock protein beta-1 (HspB1)(Heat shock 27 kDa protein)(HSP 27)(Stress-responsive protein 27)(SRP27)(Estrogen-regulated 24 kDa protein)(28 kDa heat shock protein) [Source:UniProtKB/Swiss-Prot;Acc:P04792]
20	*090211_14_NW_S10.mgf*	ENSP00000248553	4.31	1	-3.2	6	22.8	Heat shock protein beta-1 (HspB1)(Heat shock 27 kDa protein)(HSP 27)(Stress-responsive protein 27)(SRP27)(Estrogen-regulated 24 kDa protein)(28 kDa heat shock protein) [Source:UniProtKB/Swiss-Prot;Acc:P04792]
10	*090213_12_NW_S5.mgf*	ENSP00000250113	3.67	1	-3.8	6.2	77	Fragile X mental retardation syndrome-related protein 2 [Source:UniProtKB/Swiss-Prot;Acc:P51116]
37	090213 13 NW C19.mgf	ENSP00000251453	3.97	2	-10	10	16.4	40S ribosomal protein S16 [Source:UniProtKB/Swiss-Prot;Acc:P62249]
38	*090213_14_NW_S19.mgf*	ENSP00000251453	3.97	1	-1.1	10	16.4	40S ribosomal protein S16 [Source:UniProtKB/Swiss-Prot;Acc:P62249]
38	*090213_14_NW_S19.mgf*	ENSP00000251595	3.34	1	-1.3	8.7	15.2	Hemoglobin subunit alpha (Hemoglobin alpha chain)(Alpha-globin) [Source:UniProtKB/Swiss-Prot;Acc:P69905]
37	090213 13 NW C19.mgf	ENSP00000252543	3.57	1	-2.7	12	12.2	60S ribosomal protein L36 [Source:UniProtKB/Swiss-Prot;Acc:Q9Y3U8]
38	*090213_14_NW_S19.mgf*	ENSP00000252543	3.91	1	-3.7	12	12.2	60S ribosomal protein L36 [Source:UniProtKB/Swiss-Prot;Acc:Q9Y3U8]
39	*090213_16_NW_C20.mgf*	ENSP00000252543	3.28	1	-3.3	12	12.2	60S ribosomal protein L36 [Source:UniProtKB/Swiss-Prot;Acc:Q9Y3U8]
40	*090213_17_NW_S20.mgf*	ENSP00000252543	4.01	2	-3.6	12	12.2	60S ribosomal protein L36 [Source:UniProtKB/Swiss-Prot;Acc:Q9Y3U8]
41	*090213_18_NW_C21.mgf*	ENSP00000252543	3.78	1	-2.5	12	12.2	60S ribosomal protein L36 [Source:UniProtKB/Swiss-Prot;Acc:Q9Y3U8]
42	*090213_19_NW_S21.mgf*	ENSP00000252543	3.68	2	-4	12	12.2	60S ribosomal protein L36 [Source:UniProtKB/Swiss-Prot;Acc:Q9Y3U8]
9	*090213 11 NW C5.mgf*	ENSP00000253788	4.01	1	-3.8	11	15.8	60S ribosomal protein L27 [Source:UniProtKB/Swiss-Prot;Acc:P61353]
6	*090213_07_NW_S3.mgf*	ENSP00000254108	4.21	4	-15.6	9.4	53.4	RNA-binding protein FUS (Oncogene FUS)(Oncogene TLS)(Translocated in liposarcoma protein)(POMp75)(75 kDa DNA-pairing protein) [Source:UniProtKB/Swiss-Prot;Acc:P35637]
8	*090213_10_NW_S4.mgf*	ENSP00000254108	4.41	3	-5.3	9.4	53.4	RNA-binding protein FUS (Oncogene FUS)(Oncogene TLS)(Translocated in liposarcoma protein)(POMp75)(75 kDa DNA-pairing protein) [Source:UniProtKB/Swiss-Prot;Acc:P35637]
9	*090213_11_NW_C5.mgf*	ENSP00000254108	5.26	3	-18.9	9.4	53.4	RNA-binding protein FUS (Oncogene FUS)(Oncogene TLS)(Translocated in liposarcoma protein)(POMp75)(75 kDa DNA-pairing protein) [Source:UniProtKB/Swiss-Prot;Acc:P35637]
10	*090213_12_NW_S5.mgf*	ENSP00000254108	4.48	1	-8.1	9.4	53.4	RNA-binding protein FUS (Oncogene FUS)(Oncogene TLS)(Translocated in liposarcoma protein)(POMp75)(75 kDa DNA-pairing protein) [Source:UniProtKB/Swiss-Prot;Acc:P35637]
19	*090211_13_NW_C10.mgf*	ENSP00000254108	6.11	4	-5.5	9.4	53.4	RNA-binding protein FUS (Oncogene FUS)(Oncogene TLS)(Translocated in liposarcoma protein)(POMp75)(75 kDa DNA-pairing protein) [Source:UniProtKB/Swiss-Prot;Acc:P35637]
20	*090211_14_NW_S10.mgf*	ENSP00000254108	5.53	2	-8.6	9.4	53.4	RNA-binding protein FUS (Oncogene FUS)(Oncogene TLS)(Translocated in liposarcoma protein)(POMp75)(75 kDa DNA-pairing protein) [Source:UniProtKB/Swiss-Prot;Acc:P35637]
5	*090213_06_NW_C3.mgf*	ENSP00000254436	5.79	4	-2.8	6.1	54.2	52 kDa Ro protein (Sjoegren syndrome type A antigen)(SS-A)(Ro(SS-A))(52 kDa ribonucleoprotein autoantigen Ro/SS-A)(Tripartite motif-containing protein 21)(RING finger protein 81) [Source:UniProtKB/Swiss-Prot;Acc:P19474]
6	*090213_07_NW_S3.mgf*	ENSP00000254436	5.07	2	-2	6.1	54.2	52 kDa Ro protein (Sjoegren syndrome type A antigen)(SS-A)(Ro(SS-A))(52 kDa ribonucleoprotein autoantigen Ro/SS-A)(Tripartite motif-containing protein 21)(RING finger protein 81) [Source:UniProtKB/Swiss-Prot;Acc:P19474]
8	*090213_10_NW_S4.mgf*	ENSP00000254436	5.01	7	-25.9	6.1	54.2	52 kDa Ro protein (Sjoegren syndrome type A antigen)(SS-A)(Ro(SS-A))(52 kDa ribonucleoprotein autoantigen Ro/SS-A)(Tripartite motif-containing protein 21)(RING finger protein 81) [Source:UniProtKB/Swiss-Prot;Acc:P19474]
21	*090211_15_NW_C11.mgf'*	ENSP00000254436	4.73	1	-1.9	6.1	54.2	52 kDa Ro protein (Sjoegren syndrome type A antigen)(SS-A)(Ro(SS-A))(52 kDa ribonucleoprotein autoantigen Ro/SS-A)(Tripartite motif-containing protein 21)(RING finger protein 81) [Source:UniProtKB/Swiss-Prot;Acc:P19474]
35	*090211_32_NW_C18.mgf*	ENSP00000254436	4.15	1	-1.6	6.1	54.2	52 kDa Ro protein (Sjoegren syndrome type A antigen)(SS-A)(Ro(SS-A))(52 kDa ribonucleoprotein autoantigen Ro/SS-A)(Tripartite motif-containing protein 21)(RING finger protein 81) [Source:UniProtKB/Swiss-Prot;Acc:P19474]
36	*090211_32_NW_S18.mgf*	ENSP00000254436	3.87	1	-1.4	6.1	54.2	52 kDa Ro protein (Sjoegren syndrome type A antigen)(SS-A)(Ro(SS-A))(52 kDa ribonucleoprotein autoantigen Ro/SS-A)(Tripartite motif-containing protein 21)(RING finger protein 81) [Source:UniProtKB/Swiss-Prot;Acc:P19474]
38	*090213_14_NW_S19.mgf*	ENSP00000254436	3.27	1	-2.4	6.1	54.2	52 kDa Ro protein (Sjoegren syndrome type A antigen)(SS-A)(Ro(SS-A))(52 kDa ribonucleoprotein autoantigen Ro/SS-A)(Tripartite motif-containing protein 21)(RING finger protein 81) [Source:UniProtKB/Swiss-Prot;Acc:P19474]
15	*090211_08_NW_C8.mgf*	ENSP00000254653	4.9	1	-1.4	9.4	78.9	IQ and AAA domain-containing protein [Source:UniProtKB/Swiss-Prot;Acc:Q86XH1]
40	*090213_17_NW_S20.mgf*	ENSP00000255136	3.81	2	-9.6	9.1	68.3	Polyadenylate-binding protein 1-like [Source:UniProtKB/Swiss-Prot;Acc:Q4VXU2]
8	*090213_10_NW_S4.mgf*	ENSP00000255381	3.77	1	-1.8	5.7	222.9	Myosin-4 (Myosin heavy chain 4)(Myosin heavy chain 2b)(MyHC-2b)(Myosin heavy chain IIb)(MyHC-IIb)(Myosin heavy chain, skeletal muscle, fetal) [Source:UniProtKB/Swiss-Prot;Acc:Q9Y623]
9	*090213 11 NW C5.mgf*	ENSP00000256397	5.25	1	-1.3	6	87	
9	*090213_11_NW_C5.mgf*	ENSP00000257192	4.63	2	-10.5	4.9	113.7	Desmoglein-1 Precursor (Desmosomal glycoprotein 1)(DG1)(DGI)(Pemphigus foliaceus antigen) [Source:UniProtKB/Swiss-Prot;Acc:Q02413]
10	*090213_12_NW_S5.mgf*	ENSP00000257192	3.49	1	-4.5	4.9	113.7	Desmoglein-1 Precursor (Desmosomal glycoprotein 1)(DG1)(DGI)(Pemphigus foliaceus antigen) [Source:UniProtKB/Swiss-Prot;Acc:Q02413]
8	*090213_10_NW_S4.mgf*	ENSP00000257197	4.18	1	-4.4	5.3	93.8	Desmocollin-1 Precursor (Desmosomal glycoprotein 2/3)(DG2/DG3) [Source:UniProtKB/Swiss-Prot;Acc:Q08554]
16	*'090211_09_NW_S8.mgf*	ENSP00000258383	3.53	1	-1.5	8.6	37.5	39S ribosomal protein L44, mitochondrial Precursor (L44mt)(EC 3.1.26.-)(MRP-L44) [Source:UniProtKB/Swiss-Prot;Acc:Q9H9J2]
15	*090211_08_NW_C8.mgf*	ENSP00000258599	3.77	1	-1.1	6.7	43.8	
15	*090211_08_NW_C8.mgf*	ENSP00000258886	4.97	2	-7.6	6.6	105	Iron-responsive element-binding protein 2 (IRE-BP 2)(Iron regulatory protein 2)(IRP2) [Source:UniProtKB/Swiss-Prot;Acc:P48200]
35	*090211_32_NW_C18.mgf*	ENSP00000259469	4.09	1	-3.7	11	14.5	60S ribosomal protein L35 [Source:UniProtKB/Swiss-Prot;Acc:P42766]
37	090213 13 NW C19.mgf	ENSP00000259469	3.93	1	-7.8	11	14.5	60S ribosomal protein L35 [Source:UniProtKB/Swiss-Prot;Acc:P42766]
38	*090213_14_NW_S19.mgf*	ENSP00000259469	3.59	1	-3.5	11	14.5	60S ribosomal protein L35 [Source:UniProtKB/Swiss-Prot;Acc:P42766]
40	*090213_17_NW_S20.mgf*	ENSP00000259469	3.31	1	-2.9	11	14.5	60S ribosomal protein L35 [Source:UniProtKB/Swiss-Prot;Acc:P42766]
41	*090213_18_NW_C21.mgf*	ENSP00000259469	3.97	2	-4.3	11	14.5	60S ribosomal protein L35 [Source:UniProtKB/Swiss-Prot;Acc:P42766]
42	*090213_19_NW_S21.mgf*	ENSP00000259469	3.27	1	-3.3	11	14.5	60S ribosomal protein L35 [Source:UniProtKB/Swiss-Prot;Acc:P42766]
43	*090213_20_NW_C22.mgf*	ENSP00000259469	3.22	1	-5	11	14.5	60S ribosomal protein L35 [Source:UniProtKB/Swiss-Prot;Acc:P42766]
35	*090211_32_NW_C18.mgf*	ENSP00000259791	4.67	3	-16.4	11	14.1	Histone H2A type 1-B/E (H2A/m)(H2A.2)(H2A/a) [Source:UniProtKB/Swiss-Prot;Acc:P04908]
21	*090211_15_NW_C11.mgf'*	ENSP00000259925	3.59	1	-1.6	4.8	49.6	Tubulin beta chain (Tubulin beta-5 chain) [Source:UniProtKB/Swiss-Prot;Acc:P07437]
38	*090213_14_NW_S19.mgf*	ENSP00000259925	3.2	1	-2.7	4.8	49.6	Tubulin beta chain (Tubulin beta-5 chain) [Source:UniProtKB/Swiss-Prot;Acc:P07437]
39	*090213_16_NW_C20.mgf*	ENSP00000259925	3.24	1	-6.7	4.8	49.6	Tubulin beta chain (Tubulin beta-5 chain) [Source:UniProtKB/Swiss-Prot;Acc:P07437]
40	*090213_17_NW_S20.mgf*	ENSP00000259925	4.66	6	-15.6	4.8	49.6	Tubulin beta chain (Tubulin beta-5 chain) [Source:UniProtKB/Swiss-Prot;Acc:P07437]
5	*090213 06 NW C3.mgf*	ENSP00000260968	4.62	5	-13.7	10	17.4	40S RIBOSOMAL S15

19	*090211_13_NW_C10.mgf*	ENSP00000261182	3.82	1	-6.3	4.4	45.3	Nucleosome assembly protein 1-like 1 (NAP-1-related protein)(hNRP) [Source:UniProtKB/Swiss-Prot;Acc:P55209]
37	090213_13_NW_C19.mgf	ENSP00000261210	3.72	1	-2.7	9.4	50.6	Lamina-associated polypeptide 2, isoforms beta/gamma (Thymopoietin, isoforms beta/gamma)(TP beta/gamma)(Thymopoietin-related peptide isoforms beta/gamma)(TPRP isoforms beta/gamma) [Contains Thymopoietin(TP)(Splenin);Thymopentin(TP5)] [Source:UniProtKB/Swiss-Prot;Acc:P42167]
38	*090213_14_NW_S19.mgf*	ENSP00000261210	3.82	1	-1.1	9.4	50.6	Lamina-associated polypeptide 2, isoforms beta/gamma (Thymopoietin, isoforms beta/gamma)(TP beta/gamma)(Thymopoietin-related peptide isoforms beta/gamma)(TPRP isoforms beta/gamma) [Contains Thymopoietin(TP)(Splenin);Thymopentin(TP5)] [Source:UniProtKB/Swiss-Prot;Acc:P42167]
16	*'090211_09_NW_S8.mgf*	ENSP00000261712	4.45	1	-1.1	6.1	47.4	26S proteasome non-ATPase regulatory subunit 11 (26S proteasome regulatory subunit S9)(26S proteasome regulatory subunit p44.5) [Source:UniProtKB/Swiss-Prot;Acc:O00231]
11	*090211_04_NW_C6.mgf'*	ENSP00000261868	4.8	2	-1.9	4.7	29	Eukaryotic translation initiation factor 3 subunit J (eIF3j)(Eukaryotic translation initiation factor 3 subunit 1)(eIF-3-alpha)(eIF3 p35) [Source:UniProtKB/Swiss-Prot;Acc:O75822]
31	*090211_27_NW_C16.mgf*	ENSP00000262584	4.42	1	-1.9	11	28	60S ribosomal protein L8 [Source:UniProtKB/Swiss-Prot;Acc:P62917]
32	*090211_28_NW_S16.mgf*	ENSP00000262584	4.51	1	-2.6	11	28	60S ribosomal protein L8 [Source:UniProtKB/Swiss-Prot;Acc:P62917]
33	*090211_29_NW_C17.mgf*	ENSP00000262584	4.71	2	-2.7	11	28	60S ribosomal protein L8 [Source:UniProtKB/Swiss-Prot;Acc:P62917]
34	*090211_30_NW_S17.mgf*	ENSP00000262584	5.33	4	-5.1	11	28	60S ribosomal protein L8 [Source:UniProtKB/Swiss-Prot;Acc:P62917]
37	090213 13 NW C19.mgf	ENSP00000262584	3.58	1	-4.3	11	28	60S ribosomal protein L8 [Source:UniProtKB/Swiss-Prot;Acc:P62917]
42	*090213_19_NW_S21.mgf*	ENSP00000262584	3.64	1	-3.4	11	28	60S ribosomal protein L8 [Source:UniProtKB/Swiss-Prot;Acc:P62917]
48	*090213_26_NW_S24.mgf*	ENSP00000262584	3.68	1	-3.6	11	28	60S ribosomal protein L8 [Source:UniProtKB/Swiss-Prot;Acc:P62917]
20	*090211_14_NW_S10.mgf*	ENSP00000262746	4.33	1	-1.2	8.3	22.1	Peroxiredoxin-1 (EC 1.11.1.15)(Thioredoxin peroxidase 2)(Thioredoxin-dependent peroxide reductase 2)(Proliferation-associated gene protein)(PAG)(Natural killer cell-enhancing factor A)(NKEF-A) [Source:UniProtKB/Swiss-Prot;Acc:Q06830]
23	*090211_18_NW_C12.mgf*	ENSP00000263102	4.89	1	-1.1	6.9	53.3	Coiled-coil domain-containing protein 6 (Protein H4)(Papillary thyroid carcinoma-encoded protein) [Source:UniProtKB/Swiss-Prot;Acc:Q16204]
9	*090213_11_NW_C5.mgf*	ENSP00000263200	3.7	1	-3.2	5.6	186.9	Clathrin heavy chain 2 (CLH-22) [Source:UniProtKB/Swiss-Prot;Acc:P53675]
20	*090211_14_NW_S10.mgf*	ENSP00000263200	3.51	1	-4.1	5.6	186.9	Clathrin heavy chain 2 (CLH-22) [Source:UniProtKB/Swiss-Prot;Acc:P53675]
38	*090213_14_NW_S19.mgf*	ENSP00000264051	3.84	1	-1.1	5.4	82.4	Ephexin-1 (Eph-interacting exchange protein)(Neuronal guanine nucleotide exchange factor) [Source:UniProtKB/Swiss-Prot;Acc:Q8N5V2]
9	*090213_11_NW_C5.mgf*	ENSP00000264073	3.78	1	-6.8	9.2	36.1	ELAV-like protein 1 (Hu-antigen R)(HuR) [Source:UniProtKB/Swiss-Prot;Acc:Q15717]
10	*090213_12_NW_S5.mgf*	ENSP00000264073	3.34	1	-5.3	9.2	36.1	ELAV-like protein 1 (Hu-antigen R)(HuR) [Source:UniProtKB/Swiss-Prot;Acc:Q15717]
5	*090213_06_NW_C3.mgf*	ENSP00000264198	3.75	1	-1.5	8.5	39.8	Mitochondrial ubiquitin ligase activator of NFKB 1 (EC 6.3.2.-)(E3 ubiquitin-protein ligase MUL1)(NF-kappa-B-activating protein 266)(Mitochondrial-anchored protein ligase)(RING finger protein 218) [Source:UniProtKB/Swiss-Prot;Acc:Q969V5]
6	*090213_07_NW_S3.mgf*	ENSP00000264258	4.12	2	-3.5	11	14.5	60S ribosomal protein L31 [Source:UniProtKB/Swiss-Prot;Acc:P62899]
20	*090211_14_NW_S10.mgf*	ENSP00000264258	4.2	1	-1.3	11	14.5	60S ribosomal protein L31 [Source:UniProtKB/Swiss-Prot;Acc:P62899]
21	*090211_15_NW_C11.mgf'*	ENSP00000264258	3.75	1	-1.3	11	14.5	60S ribosomal protein L31 [Source:UniProtKB/Swiss-Prot;Acc:P62899]
13	*090211_06_NW_C7.mgf*	ENSP00000264930	3.52	1	-1.3	6.2	120.2	Solute carrier family 12 member 7 (Electroneutral potassium-chloride cotransporter 4)(K-Cl cotransporter 4) [Source:UniProtKB/Swiss-Prot;Acc:Q9Y666]
17	*090211_11_NW_C9.mgf'*	ENSP00000264933	3.5	1	-2.1	5.2	21.9	Programmed cell death protein 6 (Apoptosis-linked gene 2 protein)(Probable calcium-binding protein ALG-2) [Source:UniProtKB/Swiss-Prot;Acc:O75340]
19	*090211_13_NW_C10.mgf*	ENSP00000265100	5.83	2	-1.2	11	17.2	60S ribosomal protein L26-like 1 [Source:UniProtKB/Swiss-Prot;Acc:Q9UNX3]
20	*090211_14_NW_S10.mgf*	ENSP00000265100	5.41	2	-1.7	11	17.2	60S ribosomal protein L26-like 1 [Source:UniProtKB/Swiss-Prot;Acc:Q9UNX3]
19	*090211_13_NW_C10.mgf*	ENSP00000265264	4.54	3	-7.3	11	17.8	60S ribosomal protein L24 (Ribosomal protein L30) [Source:UniProtKB/Swiss-Prot;Acc:P83731]
12	*090211_05_NW_S6.mgf*	ENSP00000266679	4.98	1	-1.6	7.3	63.4	Cleavage and polyadenylation specificity factor subunit 6 (Cleavage and polyadenylation specificity factor 68 kDa subunit)(CPSF 68 kDa subunit)(Pre-mRNA cleavage factor Im 68 kDa subunit)(Protein HPBRII-4/7) [Source:UniProtKB/Swiss-Prot;Acc:Q16630]
9	*090213_11_NW_C5.mgf*	ENSP00000266732	3.25	1	-4.9	7.6	75.4	Lamina-associated polypeptide 2, isoforms beta/gamma (Thymopoietin, isoforms beta/gamma)(TP beta/gamma)(Thymopoietin-related peptide isoforms beta/gamma)(TPRP isoforms beta/gamma) [Contains Thymopoietin(TP)(Splenin);Thymopentin(TP5)] [Source:UniProtKB/Swiss-Prot;Acc:P42167]
10	*090213_12_NW_S5.mgf*	ENSP00000266732	3.61	1	-2.6	7.6	75.4	Lamina-associated polypeptide 2, isoforms beta/gamma (Thymopoietin, isoforms beta/gamma)(TP beta/gamma)(Thymopoietin-related peptide isoforms beta/gamma)(TPRP isoforms beta/gamma) [Contains Thymopoietin(TP)(Splenin);Thymopentin(TP5)] [Source:UniProtKB/Swiss-Prot;Acc:P42167]
5	*090213_06_NW_C3.mgf*	ENSP00000269122	5.03	14	-61.8	5.5	191.5	Clathrin heavy chain 1 (CLH-17) [Source:UniProtKB/Swiss-Prot;Acc:O00610]
6	*090213_07_NW_S3.mgf*	ENSP00000269122	3.56	2	-18	5.5	191.5	Clathrin heavy chain 1 (CLH-17) [Source:UniProtKB/Swiss-Prot;Acc:O00610]
8	*090213_10_NW_S4.mgf*	ENSP00000269122	4.95	6	-37.1	5.5	191.5	Clathrin heavy chain 1 (CLH-17) [Source:UniProtKB/Swiss-Prot;Acc:O00610]
9	*090213_11_NW_C5.mgf*	ENSP00000269122	6.38	10	-25.3	5.5	191.5	Clathrin heavy chain 1 (CLH-17) [Source:UniProtKB/Swiss-Prot;Acc:O00610]
10	*090213_12_NW_S5.mgf*	ENSP00000269122	4.93	4	-13.4	5.5	191.5	Clathrin heavy chain 1 (CLH-17) [Source:UniProtKB/Swiss-Prot;Acc:O00610]
15	*090211_08_NW_C8.mgf*	ENSP00000269122	5.91	2	-1.8	5.5	191.5	Clathrin heavy chain 1 (CLH-17) [Source:UniProtKB/Swiss-Prot;Acc:O00610]
17	*090211_11_NW_C9.mgf'*	ENSP00000269122	4.95	3	-19.5	5.5	191.5	Clathrin heavy chain 1 (CLH-17) [Source:UniProtKB/Swiss-Prot;Acc:O00610]
19	*090211_13_NW_C10.mgf*	ENSP00000269122	4.85	5	-18.6	5.5	191.5	Clathrin heavy chain 1 (CLH-17) [Source:UniProtKB/Swiss-Prot;Acc:O00610]
21	*090211_15_NW_C11.mgf'*	ENSP00000269122	4.6	2	-13.5	5.5	191.5	Clathrin heavy chain 1 (CLH-17) [Source:UniProtKB/Swiss-Prot;Acc:O00610]
33	*090211_29_NW_C17.mgf*	ENSP00000269122	4.4	1	-1.1	5.5	191.5	Clathrin heavy chain 1 (CLH-17) [Source:UniProtKB/Swiss-Prot;Acc:O00610]
35	*090211_32_NW_C18.mgf*	ENSP00000269122	4.65	3	-14.1	5.5	191.5	Clathrin heavy chain 1 (CLH-17) [Source:UniProtKB/Swiss-Prot;Acc:O00610]
37	090213 13 NW C19.mgf	ENSP00000269122	3.69	2	-9.9	5.5	191.5	Clathrin heavy chain 1 (CLH-17) [Source:UniProtKB/Swiss-Prot;Acc:O00610]
38	*090213_14_NW_S19.mgf*	ENSP00000269122	4.02	1	-1.2	5.5	191.5	Clathrin heavy chain 1 (CLH-17) [Source:UniProtKB/Swiss-Prot;Acc:O00610]
9	*090213_11_NW_C5.mgf*	ENSP00000270460	4.37	1	-1.8	4.7	60.3	Epsin-1 (EPS-15-interacting protein 1)(EH domain-binding mitotic phosphoprotein) [Source:UniProtKB/Swiss-Prot;Acc:Q9Y6I3]
5	*090213_06_NW_C3.mgf*	ENSP00000270625	5.14	2	-2.1	10	18.4	40S ribosomal protein S11 [Source:UniProtKB/Swiss-Prot;Acc:P62280]
6	*090213_07_NW_S3.mgf*	ENSP00000270625	3.89	1	-2.5	10	18.4	40S ribosomal protein S11 [Source:UniProtKB/Swiss-Prot;Acc:P62280]
8	*090213_10_NW_S4.mgf*	ENSP00000270625	4.35	1	-2.9	10	18.4	40S ribosomal protein S11 [Source:UniProtKB/Swiss-Prot;Acc:P62280]
41	*090213_18_NW_C21.mgf*	ENSP00000270625	3.42	1	-1.2	10	18.4	40S ribosomal protein S11 [Source:UniProtKB/Swiss-Prot;Acc:P62280]
42	*090213_19_NW_S21.mgf*	ENSP00000270625	3.38	1	-1.2	10	18.4	40S ribosomal protein S11 [Source:UniProtKB/Swiss-Prot;Acc:P62280]
48	*090213_26_NW_S24.mgf*	ENSP00000270625	3.5	1	-2.9	10	18.4	40S ribosomal protein S11 [Source:UniProtKB/Swiss-Prot;Acc:P62280]
5	*090213_06_NW_C3.mgf*	ENSP00000272298	5.89	29	-36.5	4.1	16.8	Calmodulin (CaM) [Source:UniProtKB/Swiss-Prot;Acc:P62158]
6	*090213_07_NW_S3.mgf*	ENSP00000272298	5.26	11	-34.8	4.1	16.8	Calmodulin (CaM) [Source:UniProtKB/Swiss-Prot;Acc:P62158]
13	*090211_06_NW_C7.mgf*	ENSP00000272972	4.98	2	-1.4	6.3	106.7	Ankyrin repeat and MYND domain-containing protein 1 (Testis-specific ankyrin-like protein 1)(Zinc finger MYND domain-containing protein 13) [Source:UniProtKB/Swiss-Prot;Acc:Q9P2S6]
18	*090211_12_NW_S9.mgf*	ENSP00000273038	3.25	1	-1.5	8.5	30.9	Transcription cofactor vestigial-like protein 4 (Vgl-4) [Source:UniProtKB/Swiss-Prot;Acc:Q14135]
6	*090213_07_NW_S3.mgf*	ENSP00000274031	5.22	3	-5.7	4.5	40.7	Histone-lysine N-methyltransferase SETD7 (EC 2.1.1.43)(Histone H3-K4 methyltransferase SETD7)(H3-K4-HMTase SETD7)(SET domain-containing protein 7)(SET7/9)(Lysine N-methyltransferase 7) [Source:UniProtKB/Swiss-Prot;Acc:Q8WTS6]
8	*090213_10_NW_S4.mgf*	ENSP00000274031	5.71	13	-21.5	4.5	40.7	Histone-lysine N-methyltransferase SETD7 (EC 2.1.1.43)(Histone H3-K4 methyltransferase SETD7)(H3-K4-HMTase SETD7)(SET domain-containing protein 7)(SET7/9)(Lysine N-methyltransferase 7) [Source:UniProtKB/Swiss-Prot;Acc:Q8WTS6]
10	*090213_12_NW_S5.mgf*	ENSP00000274031	5.7	8	-44.2	4.5	40.7	Histone-lysine N-methyltransferase SETD7 (EC 2.1.1.43)(Histone H3-K4 methyltransferase SETD7)(H3-K4-HMTase SETD7)(SET domain-containing protein 7)(SET7/9)(Lysine N-methyltransferase 7) [Source:UniProtKB/Swiss-Prot;Acc:Q8WTS6]
20	*090211_14_NW_S10.mgf*	ENSP00000274031	4.85	1	-1.5	4.5	40.7	Histone-lysine N-methyltransferase SETD7 (EC 2.1.1.43)(Histone H3-K4 methyltransferase SETD7)(H3-K4-HMTase SETD7)(SET domain-containing protein 7)(SET7/9)(Lysine N-methyltransferase 7) [Source:UniProtKB/Swiss-Prot;Acc:Q8WTS6]
15	*090211_08_NW_C8.mgf*	ENSP00000274764	6.13	3	-3.6	10	14.2	Histone H2B type 1-A (Histone H2B, testis)(Testis-specific histone H2B) [Source:UniProtKB/Swiss-Prot;Acc:O96A08]
17	*090211_11_NW_C9.mgf'*	ENSP00000274764	5.05	1	-2.5	10	14.2	Histone H2B type 1-A (Histone H2B, testis)(Testis-specific histone H2B) [Source:UniProtKB/Swiss-Prot;Acc:O96A08]
18	*090211_12_NW_S9.mgf*	ENSP00000274764	4.72	1	-1.8	10	14.2	Histone H2B type 1-A (Histone H2B, testis)(Testis-specific histone H2B) [Source:UniProtKB/Swiss-Prot;Acc:O96A08]
9	*090213_11_NW_C5.mgf*	ENSP00000276079	3.38	1	-2	9	54.2	Non-POU domain-containing octamer-binding protein (NonO protein)(54 kDa nuclear RNA- and DNA-binding protein)(p54(nrb))(p54nrb)(55 kDa nuclear protein)(NMT55)(DNA-binding p52/p100 complex, 52 kDa subunit) [Source:UniProtKB/Swiss-Prot;Acc:Q15233]
10	*090213_12_NW_S5.mgf*	ENSP00000276079	3.51	1	-7.1	9	54.2	Non-POU domain-containing octamer-binding protein (NonO protein)(54 kDa nuclear RNA- and DNA-binding protein)(p54(nrb))(p54nrb)(55 kDa nuclear protein)(NMT55)(DNA-binding p52/p100 complex, 52 kDa subunit) [Source:UniProtKB/Swiss-Prot;Acc:Q15233]
10	*090213_12_NW_S5.mgf*	ENSP00000277860	3.64	1	-4.6	9.5	13.4	SMALL NUCLEAR RIBONUCLEOPROTEIN SM D2 SNRNP CORE D2 SM D2
5	*090213_06_NW_C3.mgf*	ENSP00000278572	4.8	8	-17.3	9.7	26.7	40S ribosomal protein S3 [Source:UniProtKB/Swiss-Prot;Acc:P23396]
6	*090213_07_NW_S3.mgf*	ENSP00000278572	5.08	5	-11.4	9.7	26.7	40S ribosomal protein S3 [Source:UniProtKB/Swiss-Prot;Acc:P23396]
10	*090213_12_NW_S5.mgf*	ENSP00000278572	3.96	2	-1.8	9.7	26.7	40S ribosomal protein S3 [Source:UniProtKB/Swiss-Prot;Acc:P23396]
19	*090211_13_NW_C10.mgf*	ENSP00000278572	4.02	2	-3.6	9.7	26.7	40S ribosomal protein S3 [Source:UniProtKB/Swiss-Prot;Acc:P23396]
20	*090211_14_NW_S10.mgf*	ENSP00000278572	4.07	1	-3.1	9.7	26.7	40S ribosomal protein S3 [Source:UniProtKB/Swiss-Prot;Acc:P23396]
21	*090211_15_NW_C11.mgf'*	ENSP00000278572	4.03	3	-5.1	9.7	26.7	40S ribosomal protein S3 [Source:UniProtKB/Swiss-Prot;Acc:P23396]
23	*090211_18_NW_C12.mgf*	ENSP00000278572	3.47	1	-5.2	9.7	26.7	40S ribosomal protein S3 [Source:UniProtKB/Swiss-Prot;Acc:P23396]
31	*090211_27_NW_C16.mgf*	ENSP00000278572	5.58	3	-4.8	9.7	26.7	40S ribosomal protein S3 [Source:UniProtKB/Swiss-Prot;Acc:P23396]
32	*090211_28_NW_S16.mgf*	ENSP00000278572	4.93	1	-4	9.7	26.7	40S ribosomal protein S3 [Source:UniProtKB/Swiss-Prot;Acc:P23396]

37	090213_13_NW_C19.mgf	ENSP00000278572	3.61	1	-1.8	9.7	26.7	40S ribosomal protein S3 [Source:UniProtKB/Swiss-Prot;Acc:P23396]
38	*090213_14_NW_S19.mgf*	ENSP00000278572	3.33	1	-1.6	9.7	26.7	40S ribosomal protein S3 [Source:UniProtKB/Swiss-Prot;Acc:P23396]
35	*090211_32_NW_C18.mgf*	ENSP00000279259	5.15	2	-2.8	10	14.4	Ubiquitin-like protein FUBI [Source:UniProtKB/Swiss-Prot;Acc:P35544]
36	*090211_32_NW_S18.mgf*	ENSP00000279259	4.07	1	-2.2	10	14.4	Ubiquitin-like protein FUBI [Source:UniProtKB/Swiss-Prot;Acc:P35544]
37	090213_13_NW_C19.mgf	ENSP00000279259	4.2	2	-1.7	10	14.4	Ubiquitin-like protein FUBI [Source:UniProtKB/Swiss-Prot;Acc:P35544]
38	*090213_14_NW_S19.mgf*	ENSP00000279259	4.45	3	-4.8	10	14.4	Ubiquitin-like protein FUBI [Source:UniProtKB/Swiss-Prot;Acc:P35544]
39	*090213_16_NW_C20.mgf*	ENSP00000279259	3.73	1	-2.7	10	14.4	Ubiquitin-like protein FUBI [Source:UniProtKB/Swiss-Prot;Acc:P35544]
40	*090213_17_NW_S20.mgf*	ENSP00000279259	4.56	3	-4.1	10	14.4	Ubiquitin-like protein FUBI [Source:UniProtKB/Swiss-Prot;Acc:P35544]
39	*090213_16_NW_C20.mgf*	ENSP00000281456	3.52	1	-1.5	9.8	33	ADP/ATP translocase 1 (Adenine nucleotide translocator 1)(ANT 1)(ADP,ATP carrier protein 1)(Solute carrier family 25 member 4)(ADP,ATP carrier protein, heart/skeletal muscle isoform T1) [Source:UniProtKB/Swiss-Prot;Acc:P12235]
14	*090211_07_NW_S7.mgf*	ENSP00000281513	5.18	2	-8.7	5.6	268.4	Neuroblastoma-amplified gene protein [Source:UniProtKB/Swiss-Prot;Acc:A2RRP1]
5	*090213_06_NW_C3.mgf*	ENSP00000282050	3.61	1	-7.6	9.2	59.7	ATP synthase subunit alpha, mitochondrial Precursor [Source:UniProtKB/Swiss-Prot;Acc:P25705]
8	*090213_10_NW_S4.mgf*	ENSP00000282050	4.06	1	-7.3	9.2	59.7	ATP synthase subunit alpha, mitochondrial Precursor [Source:UniProtKB/Swiss-Prot;Acc:P25705]
8	*090213_10_NW_S4.mgf*	ENSP00000283179	3.43	1	-1.9	5.6	88.9	Heterogeneous nuclear ribonucleoprotein U (hnRNP U)(Scaffold attachment factor A)(SAF-A)(p120)(pp120) [Source:UniProtKB/Swiss-Prot;Acc:O00839]
19	*090211_13_NW_C10.mgf*	ENSP00000283179	3.79	1	-4.6	5.6	88.9	Heterogeneous nuclear ribonucleoprotein U (hnRNP U)(Scaffold attachment factor A)(SAF-A)(p120)(pp120) [Source:UniProtKB/Swiss-Prot;Acc:O00839]
10	*090213_12_NW_S5.mgf*	ENSP00000287038	3.37	1	-3.8	9.7	12.8	60S ribosomal protein L30 [Source:UniProtKB/Swiss-Prot;Acc:P62888]
40	*090213_17_NW_S20.mgf*	ENSP00000287144	3.72	1	-6.1	11	18.5	60S RIBOSOMAL L29
42	*090213_19_NW_S21.mgf*	ENSP00000287144	4.16	1	-8	11	18.5	60S RIBOSOMAL L29
43	*090213_20_NW_C22.mgf*	ENSP00000287144	3.36	1	-5.5	11	18.5	60S RIBOSOMAL L29
47	*090213_25_NW_C24.mgf*	ENSP00000287144	3.4	1	-7.4	11	18.5	60S RIBOSOMAL L29
48	*090213_26_NW_S24.mgf*	ENSP00000287144	3.61	1	-8.4	11	18.5	60S RIBOSOMAL L29
23	*090211_18_NW_C12.mgf*	ENSP00000289032	4.43	3	-8.9	9.2	80.9	Zinc finger protein 782 [Source:UniProtKB/Swiss-Prot;Acc:Q6ZMW2]
24	*090211_19_NW_S12.mgf*	ENSP00000289032	3.84	1	-1.1	9.2	80.9	Zinc finger protein 782 [Source:UniProtKB/Swiss-Prot;Acc:Q6ZMW2]
38	*090213_14_NW_S19.mgf*	ENSP00000289734	3.98	1	-1.8	5.8	205.9	Ankyrin-1 (Erythrocyte ankyrin)(Ankyrin-R) [Source:UniProtKB/Swiss-Prot;Acc:P16157]
1	*090213_02_NW_C1.mgf*	ENSP00000289816	3.63	1	-3.5	8.7	59.8	Zinc finger protein 276 (Zfp-276) [Source:UniProtKB/Swiss-Prot;Acc:Q8N554]
2	*090213_03_NW_S1.mgf*	ENSP00000289816	4.36	3	-2.2	8.7	59.8	Zinc finger protein 276 (Zfp-276) [Source:UniProtKB/Swiss-Prot;Acc:Q8N554]
4	*090213_05_NW_S2.mgf*	ENSP00000289816	4.02	2	-3.3	8.7	59.8	Zinc finger protein 276 (Zfp-276) [Source:UniProtKB/Swiss-Prot;Acc:Q8N554]
8	*090213_10_NW_S4.mgf*	ENSP00000289816	4.55	2	-1.3	8.7	59.8	Zinc finger protein 276 (Zfp-276) [Source:UniProtKB/Swiss-Prot;Acc:Q8N554]
12	*090211_05_NW_S6.mgf*	ENSP00000289816	4.11	2	-1.5	8.7	59.8	Zinc finger protein 276 (Zfp-276) [Source:UniProtKB/Swiss-Prot;Acc:Q8N554]
21	*090211_15_NW_C11.mgf'*	ENSP00000289816	3.74	1	-1.2	8.7	59.8	Zinc finger protein 276 (Zfp-276) [Source:UniProtKB/Swiss-Prot;Acc:Q8N554]
29	*090211_25_NW_C15.mgf*	ENSP00000289816	4.57	1	-1.2	8.7	59.8	Zinc finger protein 276 (Zfp-276) [Source:UniProtKB/Swiss-Prot;Acc:Q8N554]
30	*090211_26_NW_S15.mgf*	ENSP00000289816	3.58	1	-2.8	8.7	59.8	Zinc finger protein 276 (Zfp-276) [Source:UniProtKB/Swiss-Prot;Acc:Q8N554]
32	*090211_28_NW_S16.mgf*	ENSP00000289816	4.49	2	-1.3	8.7	59.8	Zinc finger protein 276 (Zfp-276) [Source:UniProtKB/Swiss-Prot;Acc:Q8N554]
34	*090211_30_NW_S17.mgf*	ENSP00000289816	4.45	3	-1.5	8.7	59.8	Zinc finger protein 276 (Zfp-276) [Source:UniProtKB/Swiss-Prot;Acc:Q8N554]
36	*090211_32_NW_S18.mgf*	ENSP00000289816	4.46	2	-1.8	8.7	59.8	Zinc finger protein 276 (Zfp-276) [Source:UniProtKB/Swiss-Prot;Acc:Q8N554]
37	090213_13_NW_C19.mgf	ENSP00000289816	3.95	1	-1.8	8.7	59.8	Zinc finger protein 276 (Zfp-276) [Source:UniProtKB/Swiss-Prot;Acc:Q8N554]
40	*090213_17_NW_S20.mgf*	ENSP00000289816	3.36	1	-1.3	8.7	59.8	Zinc finger protein 276 (Zfp-276) [Source:UniProtKB/Swiss-Prot;Acc:Q8N554]
42	*090213_19_NW_S21.mgf*	ENSP00000289816	3.23	1	-1.1	8.7	59.8	Zinc finger protein 276 (Zfp-276) [Source:UniProtKB/Swiss-Prot;Acc:Q8N554]
47	*090213_25_NW_C24.mgf*	ENSP00000289816	4.2	1	-1.3	8.7	59.8	Zinc finger protein 276 (Zfp-276) [Source:UniProtKB/Swiss-Prot;Acc:Q8N554]
31	*090211_27_NW_C16.mgf*	ENSP00000289989	3.3	1	-1.1	8.5	39.6	Uncharacterized protein C8orf58 [Source:UniProtKB/Swiss-Prot;Acc:Q8NAV2]
9	*090213_11_NW_C5.mgf*	ENSP00000292309	4.95	1	-1.2	6	302.9	NBEL2_HUMAN Isoform 3 of Q6ZNJ1 - Homo sapiens (Human) [Source:UniprotKB/SpliceVariant;Acc:Q6ZNJ1-3]
5	*090213_06_NW_C3.mgf*	ENSP00000293371	6.03	10	-19	6.1	11.3	Dermcidin Precursor (Preproteolysin) [Contains Survival-promoting peptide;DCD-1] [Source:UniProtKB/Swiss-Prot;Acc:P81605]
6	*090213_07_NW_S3.mgf*	ENSP00000293371	4.98	5	-14.4	6.1	11.3	Dermcidin Precursor (Preproteolysin) [Contains Survival-promoting peptide;DCD-1] [Source:UniProtKB/Swiss-Prot;Acc:P81605]
8	*090213_10_NW_S4.mgf*	ENSP00000293371	4.16	2	-14.6	6.1	11.3	Dermcidin Precursor (Preproteolysin) [Contains Survival-promoting peptide;DCD-1] [Source:UniProtKB/Swiss-Prot;Acc:P81605]
9	*090213_11_NW_C5.mgf*	ENSP00000293618	4.8	2	-6.8	6.1	81.2	La-related protein 4 (La ribonucleoprotein domain family member 4) [Source:UniProtKB/Swiss-Prot;Acc:Q71RC2]
9	*090213_11_NW_C5.mgf*	ENSP00000293760	4.21	1	-5.1	9.2	56.9	LEM domain-containing protein 2 (hLEM2) [Source:UniProtKB/Swiss-Prot;Acc:Q8NC56]
10	*090213_12_NW_S5.mgf*	ENSP00000293760	3.7	1	-5.8	9.2	56.9	LEM domain-containing protein 2 (hLEM2) [Source:UniProtKB/Swiss-Prot;Acc:Q8NC56]
18	*090211_12_NW_S9.mgf*	ENSP00000295137	5.23	4	-9.4	5.3	41.8	Actin, gamma-enteric smooth muscle (Smooth muscle gamma-actin)(Gamma-2-actin)(Alpha-actin-3) [Source:UniProtKB/Swiss-Prot;Acc:P63267]
5	*090213_06_NW_C3.mgf*	ENSP00000295470	4.02	2	-13.8	9.6	46.4	Heterogeneous nuclear ribonucleoprotein D-like (hnRPD-like protein)(hnHNRP-DL)(JKT41-binding protein)(AU-rich element RNA-binding factor)(Protein laAUF1) [Source:UniProtKB/Swiss-Prot;Acc:O14979]
9	*090213_11_NW_C5.mgf*	ENSP00000295897	4.44	1	-1.8	5.9	69.3	Serum albumin Precursor [Source:UniProtKB/Swiss-Prot;Acc:P02768]
48	*090213_26_NW_S24.mgf*	ENSP00000295897	3.77	2	-6.5	5.9	69.3	Serum albumin Precursor [Source:UniProtKB/Swiss-Prot;Acc:P02768]
48	*090213_26_NW_S24.mgf*	ENSP00000296028	3.33	1	-1.5	9	13.9	Platelet basic protein Precursor (PBP)(C-X-C motif chemokine 7)(Small-inducible cytokine B7)(Leukocyte-derived growth factor)(LDGF)(Macrophage-derived growth factor)(MDGF) [Contains Connective tissue-activating peptide III(CTAP-III)(Low-affinity platelet factor IV)(LA-PF4);TC-2;Connective tissue-activating peptide III(1-81)(CTAP-III(1-81));Beta-thromboglobulin(Beta-TG);Neutrophil-activating peptide 2(74)(NAP-2(74));Neutrophil-activating peptide 2(73)(NAP-2(73));Neutrophil-activating peptide 2(NAP-2);TC-1;Neutrophil-activating peptide 2(1-66)(NAP-2(1-66));Neutrophil-activating peptide 2(1-63)(NAP-2(1-63))] [Source:UniProtKB/Swiss-Prot;Acc:P02775]
5	*090213_06_NW_C3.mgf*	ENSP00000296930	5.2	7	-15.4	4.6	32.6	Nucleophosmin (NPM)(Nucleolar phosphoprotein B23)(Numatrin)(Nucleolar protein NO38) [Source:UniProtKB/Swiss-Prot;Acc:P06748]
6	*090213_07_NW_S3.mgf*	ENSP00000296930	5.2	6	-24.9	4.6	32.6	Nucleophosmin (NPM)(Nucleolar phosphoprotein B23)(Numatrin)(Nucleolar protein NO38) [Source:UniProtKB/Swiss-Prot;Acc:P06748]
8	*090213_10_NW_S4.mgf*	ENSP00000296930	5.65	3	-2.3	4.6	32.6	Nucleophosmin (NPM)(Nucleolar phosphoprotein B23)(Numatrin)(Nucleolar protein NO38) [Source:UniProtKB/Swiss-Prot;Acc:P06748]
38	*090213_14_NW_S19.mgf*	ENSP00000297012	3.73	1	-1.7	11	14.2	Histone H2A type 1-A (H2A/r) [Source:UniProtKB/Swiss-Prot;Acc:Q96QV6]
39	*090213_16_NW_C20.mgf*	ENSP00000297012	4.82	4	-6	11	14.2	Histone H2A type 1-A (H2A/r) [Source:UniProtKB/Swiss-Prot;Acc:Q96QV6]
40	*090213_17_NW_S20.mgf*	ENSP00000297012	4.32	3	-7.3	11	14.2	Histone H2A type 1-A (H2A/r) [Source:UniProtKB/Swiss-Prot;Acc:Q96QV6]
41	*090213_18_NW_C21.mgf*	ENSP00000297012	4.22	2	-1.3	11	14.2	Histone H2A type 1-A (H2A/r) [Source:UniProtKB/Swiss-Prot;Acc:Q96QV6]
47	*090213_25_NW_C24.mgf*	ENSP00000297012	3.65	1	-2.1	11	14.2	Histone H2A type 1-A (H2A/r) [Source:UniProtKB/Swiss-Prot;Acc:Q96QV6]
48	*090213_26_NW_S24.mgf*	ENSP00000297012	3.74	1	-1.6	11	14.2	Histone H2A type 1-A (H2A/r) [Source:UniProtKB/Swiss-Prot;Acc:Q96QV6]
5	*090213_06_NW_C3.mgf*	ENSP00000297185	5.97	22	-37.3	5.9	73.6	Stress-70 protein, mitochondrial Precursor (75 kDa glucose-regulated protein)(GRP 75)(Heat shock 70 kDa protein 9)(Peptide-binding protein 74)(PBP74)(Mortalin)(MOT) [Source:UniProtKB/Swiss-Prot;Acc:P38646]
6	*090213_07_NW_S3.mgf*	ENSP00000297185	5.64	11	-26.9	5.9	73.6	Stress-70 protein, mitochondrial Precursor (75 kDa glucose-regulated protein)(GRP 75)(Heat shock 70 kDa protein 9)(Peptide-binding protein 74)(PBP74)(Mortalin)(MOT) [Source:UniProtKB/Swiss-Prot;Acc:P38646]
8	*090213_10_NW_S4.mgf*	ENSP00000297185	5.5	16	-74.3	5.9	73.6	Stress-70 protein, mitochondrial Precursor (75 kDa glucose-regulated protein)(GRP 75)(Heat shock 70 kDa protein 9)(Peptide-binding protein 74)(PBP74)(Mortalin)(MOT) [Source:UniProtKB/Swiss-Prot;Acc:P38646]
9	*090213_11_NW_C5.mgf*	ENSP00000297185	6.47	11	-44.8	5.9	73.6	Stress-70 protein, mitochondrial Precursor (75 kDa glucose-regulated protein)(GRP 75)(Heat shock 70 kDa protein 9)(Peptide-binding protein 74)(PBP74)(Mortalin)(MOT) [Source:UniProtKB/Swiss-Prot;Acc:P38646]
10	*090213_12_NW_S5.mgf*	ENSP00000297185	5.82	16	-28.9	5.9	73.6	Stress-70 protein, mitochondrial Precursor (75 kDa glucose-regulated protein)(GRP 75)(Heat shock 70 kDa protein 9)(Peptide-binding protein 74)(PBP74)(Mortalin)(MOT) [Source:UniProtKB/Swiss-Prot;Acc:P38646]
15	*090211_08_NW_C8.mgf*	ENSP00000297185	6.04	3	-23.5	5.9	73.6	Stress-70 protein, mitochondrial Precursor (75 kDa glucose-regulated protein)(GRP 75)(Heat shock 70 kDa protein 9)(Peptide-binding protein 74)(PBP74)(Mortalin)(MOT) [Source:UniProtKB/Swiss-Prot;Acc:P38646]
16	*'090211_09_NW_S8.mgf*	ENSP00000297185	4.27	2	-5.6	5.9	73.6	Stress-70 protein, mitochondrial Precursor (75 kDa glucose-regulated protein)(GRP 75)(Heat shock 70 kDa protein 9)(Peptide-binding protein 74)(PBP74)(Mortalin)(MOT) [Source:UniProtKB/Swiss-Prot;Acc:P38646]
17	*090211_11_NW_C9.mgf'*	ENSP00000297185	6.62	11	-41.5	5.9	73.6	Stress-70 protein, mitochondrial Precursor (75 kDa glucose-regulated protein)(GRP 75)(Heat shock 70 kDa protein 9)(Peptide-binding protein 74)(PBP74)(Mortalin)(MOT) [Source:UniProtKB/Swiss-Prot;Acc:P38646]
18	*090211_12_NW_S9.mgf*	ENSP00000297185	5.87	3	-14.7	5.9	73.6	Stress-70 protein, mitochondrial Precursor (75 kDa glucose-regulated protein)(GRP 75)(Heat shock 70 kDa protein 9)(Peptide-binding protein 74)(PBP74)(Mortalin)(MOT) [Source:UniProtKB/Swiss-Prot;Acc:P38646]
19	*090211_13_NW_C10.mgf*	ENSP00000297185	6.46	9	-43.9	5.9	73.6	Stress-70 protein, mitochondrial Precursor (75 kDa glucose-regulated protein)(GRP 75)(Heat shock 70 kDa protein 9)(Peptide-binding protein 74)(PBP74)(Mortalin)(MOT) [Source:UniProtKB/Swiss-Prot;Acc:P38646]

20	*090211_14_NW_S10.mgf*	ENSP00000297185	5.95	9	-35.7	5.9	73.6	Stress-70 protein, mitochondrial Precursor (75 kDa glucose-regulated protein)(GRP 75)(Heat shock 70 kDa protein 9)(Peptide-binding protein 74)(PBP74)(Mortalin)(MOT) [Source:UniProtKB/Swiss-Prot;Acc:P38646]	
21	*090211_15_NW_C11.mgf*	ENSP00000297185	5.93	6	-42.4	5.9	73.6	Stress-70 protein, mitochondrial Precursor (75 kDa glucose-regulated protein)(GRP 75)(Heat shock 70 kDa protein 9)(Peptide-binding protein 74)(PBP74)(Mortalin)(MOT) [Source:UniProtKB/Swiss-Prot;Acc:P38646]	
23	*090211_18_NW_C12.mgf*	ENSP00000297185	5.02	3	-11.4	5.9	73.6	Stress-70 protein, mitochondrial Precursor (75 kDa glucose-regulated protein)(GRP 75)(Heat shock 70 kDa protein 9)(Peptide-binding protein 74)(PBP74)(Mortalin)(MOT) [Source:UniProtKB/Swiss-Prot;Acc:P38646]	
24	*090211_19_NW_S12.mgf*	ENSP00000297185	5.18	5	-20.3	5.9	73.6	Stress-70 protein, mitochondrial Precursor (75 kDa glucose-regulated protein)(GRP 75)(Heat shock 70 kDa protein 9)(Peptide-binding protein 74)(PBP74)(Mortalin)(MOT) [Source:UniProtKB/Swiss-Prot;Acc:P38646]	
25	*090211_20_NW_C13.mgf*	ENSP00000297185	4.76	2	-12.7	5.9	73.6	Stress-70 protein, mitochondrial Precursor (75 kDa glucose-regulated protein)(GRP 75)(Heat shock 70 kDa protein 9)(Peptide-binding protein 74)(PBP74)(Mortalin)(MOT) [Source:UniProtKB/Swiss-Prot;Acc:P38646]	
26	*090211_21_NW_S13.mgf*	ENSP00000297185	4.06	1	-4.1	5.9	73.6	Stress-70 protein, mitochondrial Precursor (75 kDa glucose-regulated protein)(GRP 75)(Heat shock 70 kDa protein 9)(Peptide-binding protein 74)(PBP74)(Mortalin)(MOT) [Source:UniProtKB/Swiss-Prot;Acc:P38646]	
30	*090211_26_NW_S15.mgf*	ENSP00000297185	3.39	1	-3.4	5.9	73.6	Stress-70 protein, mitochondrial Precursor (75 kDa glucose-regulated protein)(GRP 75)(Heat shock 70 kDa protein 9)(Peptide-binding protein 74)(PBP74)(Mortalin)(MOT) [Source:UniProtKB/Swiss-Prot;Acc:P38646]	
32	*090211_28_NW_S16.mgf*	ENSP00000297185	4.08	3	-17.5	5.9	73.6	Stress-70 protein, mitochondrial Precursor (75 kDa glucose-regulated protein)(GRP 75)(Heat shock 70 kDa protein 9)(Peptide-binding protein 74)(PBP74)(Mortalin)(MOT) [Source:UniProtKB/Swiss-Prot;Acc:P38646]	
33	*090211_29_NW_C17.mgf*	ENSP00000297185	3.75	1	-10.6	5.9	73.6	Stress-70 protein, mitochondrial Precursor (75 kDa glucose-regulated protein)(GRP 75)(Heat shock 70 kDa protein 9)(Peptide-binding protein 74)(PBP74)(Mortalin)(MOT) [Source:UniProtKB/Swiss-Prot;Acc:P38646]	
34	*090211_30_NW_S17.mgf*	ENSP00000297185	3.55	1	-3.6	5.9	73.6	Stress-70 protein, mitochondrial Precursor (75 kDa glucose-regulated protein)(GRP 75)(Heat shock 70 kDa protein 9)(Peptide-binding protein 74)(PBP74)(Mortalin)(MOT) [Source:UniProtKB/Swiss-Prot;Acc:P38646]	
35	*090211_32_NW_C18.mgf*	ENSP00000297185	4.78	3	-6.7	5.9	73.6	Stress-70 protein, mitochondrial Precursor (75 kDa glucose-regulated protein)(GRP 75)(Heat shock 70 kDa protein 9)(Peptide-binding protein 74)(PBP74)(Mortalin)(MOT) [Source:UniProtKB/Swiss-Prot;Acc:P38646]	
36	*090211_32_NW_S18.mgf*	ENSP00000297185	4.54	3	-18.9	5.9	73.6	Stress-70 protein, mitochondrial Precursor (75 kDa glucose-regulated protein)(GRP 75)(Heat shock 70 kDa protein 9)(Peptide-binding protein 74)(PBP74)(Mortalin)(MOT) [Source:UniProtKB/Swiss-Prot;Acc:P38646]	
37	090213_13_NW_C19.mgf	ENSP00000297185	4.5	7	-39.3	5.9	73.6	Stress-70 protein, mitochondrial Precursor (75 kDa glucose-regulated protein)(GRP 75)(Heat shock 70 kDa protein 9)(Peptide-binding protein 74)(PBP74)(Mortalin)(MOT) [Source:UniProtKB/Swiss-Prot;Acc:P38646]	
38	*090213_14_NW_S19.mgf*	ENSP00000297185	4.75	9	-37.4	5.9	73.6	Stress-70 protein, mitochondrial Precursor (75 kDa glucose-regulated protein)(GRP 75)(Heat shock 70 kDa protein 9)(Peptide-binding protein 74)(PBP74)(Mortalin)(MOT) [Source:UniProtKB/Swiss-Prot;Acc:P38646]	
39	*090213_16_NW_C20.mgf*	ENSP00000297185	4.15	4	-24.2	5.9	73.6	Stress-70 protein, mitochondrial Precursor (75 kDa glucose-regulated protein)(GRP 75)(Heat shock 70 kDa protein 9)(Peptide-binding protein 74)(PBP74)(Mortalin)(MOT) [Source:UniProtKB/Swiss-Prot;Acc:P38646]	
40	*090213_17_NW_S20.mgf*	ENSP00000297185	4.58	7	-21.9	5.9	73.6	Stress-70 protein, mitochondrial Precursor (75 kDa glucose-regulated protein)(GRP 75)(Heat shock 70 kDa protein 9)(Peptide-binding protein 74)(PBP74)(Mortalin)(MOT) [Source:UniProtKB/Swiss-Prot;Acc:P38646]	
41	*090213_18_NW_C21.mgf*	ENSP00000297185	3.9	2	-7.9	5.9	73.6	Stress-70 protein, mitochondrial Precursor (75 kDa glucose-regulated protein)(GRP 75)(Heat shock 70 kDa protein 9)(Peptide-binding protein 74)(PBP74)(Mortalin)(MOT) [Source:UniProtKB/Swiss-Prot;Acc:P38646]	
42	*090213_19_NW_S21.mgf*	ENSP00000297185	4.38	4	-11.9	5.9	73.6	Stress-70 protein, mitochondrial Precursor (75 kDa glucose-regulated protein)(GRP 75)(Heat shock 70 kDa protein 9)(Peptide-binding protein 74)(PBP74)(Mortalin)(MOT) [Source:UniProtKB/Swiss-Prot;Acc:P38646]	
43	*090213_20_NW_C22.mgf*	ENSP00000297185	3.4	1	-1.7	5.9	73.6	Stress-70 protein, mitochondrial Precursor (75 kDa glucose-regulated protein)(GRP 75)(Heat shock 70 kDa protein 9)(Peptide-binding protein 74)(PBP74)(Mortalin)(MOT) [Source:UniProtKB/Swiss-Prot;Acc:P38646]	
44	*090213_21_NW_S22.mgf*	ENSP00000297185	3.58	1	-4.6	5.9	73.6	Stress-70 protein, mitochondrial Precursor (75 kDa glucose-regulated protein)(GRP 75)(Heat shock 70 kDa protein 9)(Peptide-binding protein 74)(PBP74)(Mortalin)(MOT) [Source:UniProtKB/Swiss-Prot;Acc:P38646]	ENSP00000297185
45	*090213_23_NW_C23.mgf*	ENSP00000297185	3.16	1	-3.6	5.9	73.6	Stress-70 protein, mitochondrial Precursor (75 kDa glucose-regulated protein)(GRP 75)(Heat shock 70 kDa protein 9)(Peptide-binding protein 74)(PBP74)(Mortalin)(MOT) [Source:UniProtKB/Swiss-Prot;Acc:P38646]	ENSP00000297185
47	*090213_25_NW_C24.mgf*	ENSP00000297185	4.08	2	-6.6	5.9	73.6	Stress-70 protein, mitochondrial Precursor (75 kDa glucose-regulated protein)(GRP 75)(Heat shock 70 kDa protein 9)(Peptide-binding protein 74)(PBP74)(Mortalin)(MOT) [Source:UniProtKB/Swiss-Prot;Acc:P38646]	
48	*090213_26_NW_S24.mgf*	ENSP00000297185	4.42	4	-8.1	5.9	73.6	Stress-70 protein, mitochondrial Precursor (75 kDa glucose-regulated protein)(GRP 75)(Heat shock 70 kDa protein 9)(Peptide-binding protein 74)(PBP74)(Mortalin)(MOT) [Source:UniProtKB/Swiss-Prot;Acc:P38646]	
9	*090213_11_NW_C5.mgf*	ENSP00000299198	3.77	1	-1.7	5.3	42.6	Creatine kinase B-type (EC 2.7.3.2)(Creatine kinase B chain)(B-CK) [Source:UniProtKB/Swiss-Prot;Acc:P12277]	
10	*090213_12_NW_S5.mgf*	ENSP00000299299	3.54	1	-4.3	6.3	12	Pterin-4-alpha-carbinolamine dehydratase (PHS)(EC 4.2.1.96)(4-alpha-hydroxy-tetrahydropterin dehydratase)(Phenylalanine hydroxylase-stimulating protein)(Pterin carbinolamine dehydratase)(PCD)(Dimerization cofactor of hepatocyte nuclear factor 1-alpha)(Dimerization cofactor of HNF1)(DCoH) [Source:UniProtKB/Swiss-Prot;Acc:P61457]	
23	*090211_18_NW_C12.mgf*	ENSP00000299977	4.28	1	-1.2	8.5	101	Schlafen family member 5 [Source:UniProtKB/Swiss-Prot;Acc:Q08AF3]	
10	*090213_12_NW_S5.mgf*	ENSP00000300026	3.74	1	-2.6	9.4	23.7	Peptidyl-prolyl cis-trans isomerase B Precursor (PPIase)(Rotamase)(EC 5.2.1.8)(Cyclophilin B)(S-cyclophilin)(SCYLP)(CYP-S1) [Source:UniProtKB/Swiss-Prot;Acc:P23284]	
5	*090213_06_NW_C3.mgf*	ENSP00000300291	3.42	1	-8.5	8.9	26.2	Cleavage and polyadenylation specificity factor subunit 5 (Cleavage and polyadenylation specificity factor 25 kDa subunit)(CPSF 25 kDa subunit)(Pre-mRNA cleavage factor Im 25 kDa subunit)(Nucleoside diphosphate-linked moiety X motif 21)(Nudix motif 21) [Source:UniProtKB/Swiss-Prot;Acc:O43809]	
9	*090213_11_NW_C5.mgf*	ENSP00000301740	3.51	1	-5.3	12	299.4	Serine/arginine repetitive matrix protein 2 (Serine/arginine-rich splicing factor-related nuclear matrix protein of 300 kDa)(Ser/Arg-related nuclear matrix protein)(SR-related nuclear matrix protein of 300 kDa)(Splicing coactivator subunit SRm300)(300 kDa nuclear matrix antigen) [Source:UniProtKB/Swiss-Prot;Acc:O9UQ35]	
10	*090213_12_NW_S5.mgf*	ENSP00000301740	3.53	1	-6.4	12	299.4	Serine/arginine repetitive matrix protein 2 (Serine/arginine-rich splicing factor-related nuclear matrix protein of 300 kDa)(Ser/Arg-related nuclear matrix protein)(SR-related nuclear matrix protein of 300 kDa)(Splicing coactivator subunit SRm300)(300 kDa nuclear matrix antigen) [Source:UniProtKB/Swiss-Prot;Acc:O9UQ35]	
10	*090213_12_NW_S5.mgf*	ENSP00000302886	4.29	2	-7	6.1	43.8	Proliferation-associated protein 2G4 (Cell cycle protein p38-2G4 homolog)(hG4-1)(ErbB3-binding protein 1) [Source:UniProtKB/Swiss-Prot;Acc:O9UQ80]	
8	*090213_10_NW_S4.mgf*	ENSP00000302896	4.16	1	-3	11	22.6	40S ribosomal protein S9 [Source:UniProtKB/Swiss-Prot;Acc:P46781]	
21	*090211_15_NW_C11.mgf*	ENSP00000302896	4.09	2	-9.1	11	22.6	40S ribosomal protein S9 [Source:UniProtKB/Swiss-Prot;Acc:P46781]	
35	*090211_32_NW_C18.mgf*	ENSP00000306099	3.5	1	-6.4	8.5	55.9	Fibrinogen beta chain Precursor [Contains Fibrinopeptide B] [Source:UniProtKB/Swiss-Prot;Acc:P02675]	
26	*090211_21_NW_S13.mgf*	ENSP00000306124	3.48	1	-1.1	6.7	83.6	Protein kinase C epsilon type (EC 2.7.11.13)(nPKC-epsilon) [Source:UniProtKB/Swiss-Prot;Acc:O02156]	
9	*090213_11_NW_C5.mgf*	ENSP00000306330	3.44	1	-1.5	4.8	28.3	14-3-3 protein gamma (Protein kinase C inhibitor protein 1)(KCIP-1) [Source:UniProtKB/Swiss-Prot;Acc:P61981]	
5	*090213_06_NW_C3.mgf*	ENSP00000306469	6.09	15	-22.4	5.4	42	Beta-actin-like protein 2 (Kappa-actin) [Source:UniProtKB/Swiss-Prot;Acc:Q562R1]	
6	*090213_07_NW_S3.mgf*	ENSP00000306469	5.04	6	-18	5.4	42	Beta-actin-like protein 2 (Kappa-actin) [Source:UniProtKB/Swiss-Prot;Acc:Q562R1]	
11	*090211_04_NW_C6.mgf*	ENSP00000306469	6.07	5	-12.1	5.4	42	Beta-actin-like protein 2 (Kappa-actin) [Source:UniProtKB/Swiss-Prot;Acc:Q562R1]	
9	*090213_11_NW_C5.mgf*	ENSP00000307633	3.26	1	-1.3	6.3	59.9	Fragile X mental retardation syndrome-related protein 1 (hFXR1p) [Source:UniProtKB/Swiss-Prot;Acc:P51114]	
16	*'090211_09_NW_S8.mgf*	ENSP00000307634	5.22	1	-1.3	8.2	94.4	Centaurin-gamma-2 (ARF-GAP with GTP-binding protein-like, ankyrin repeat and pleckstrin homology domains 1)(AGAP-1)(GTP-binding and GTPase-activating protein 1)(GGAP1) [Source:UniProtKB/Swiss-Prot;Acc:Q9UPQ3]	
40	*090213_17_NW_S20.mgf*	ENSP00000307699	4.67	1	-1.1	6.3	40.7	Putative homeodomain transcription factor 2 [Source:UniProtKB/Swiss-Prot;Acc:Q8N3S3]	
47	*090213_25_NW_C24.mgf*	ENSP00000307786	5.02	6	-14.7	9.6	11.7	Cytochrome c [Source:UniProtKB/Swiss-Prot;Acc:P99999]	
48	*090213_26_NW_S24.mgf*	ENSP00000307786	5.38	6	-10.9	9.6	11.7	Cytochrome c [Source:UniProtKB/Swiss-Prot;Acc:P99999]	
9	*090213_11_NW_C5.mgf*	ENSP00000307889	5.26	2	-1.9	12	24.2	60S ribosomal protein L13 (Breast basic conserved protein 1) [Source:UniProtKB/Swiss-Prot;Acc:P26373]	
10	*090213_12_NW_S5.mgf*	ENSP00000307889	4.06	1	-2	12	24.2	60S ribosomal protein L13 (Breast basic conserved protein 1) [Source:UniProtKB/Swiss-Prot;Acc:P26373]	
19	*090211_13_NW_C10.mgf*	ENSP00000307889	4.12	1	-1.1	12	24.2	60S ribosomal protein L13 (Breast basic conserved protein 1) [Source:UniProtKB/Swiss-Prot;Acc:P26373]	
35	*090211_32_NW_C18.mgf*	ENSP00000307889	4.5	2	-7.3	12	24.2	60S ribosomal protein L13 (Breast basic conserved protein 1) [Source:UniProtKB/Swiss-Prot;Acc:P26373]	
36	*090211_32_NW_S18.mgf*	ENSP00000307889	3.9	1	-4.9	12	24.2	60S ribosomal protein L13 (Breast basic conserved protein 1) [Source:UniProtKB/Swiss-Prot;Acc:P26373]	
37	090213_13_NW_C19.mgf	ENSP00000307889	4.62	7	-9.9	12	24.2	60S ribosomal protein L13 (Breast basic conserved protein 1) [Source:UniProtKB/Swiss-Prot;Acc:P26373]	
38	*090213_14_NW_S19.mgf*	ENSP00000307889	3.9	3	-4.5	12	24.2	60S ribosomal protein L13 (Breast basic conserved protein 1) [Source:UniProtKB/Swiss-Prot;Acc:P26373]	
39	*090213_16_NW_C20.mgf*	ENSP00000307889	4.16	3	-4	12	24.2	60S ribosomal protein L13 (Breast basic conserved protein 1) [Source:UniProtKB/Swiss-Prot;Acc:P26373]	
40	*090213_17_NW_S20.mgf*	ENSP00000307889	4.58	6	-9.2	12	24.2	60S ribosomal protein L13 (Breast basic conserved protein 1) [Source:UniProtKB/Swiss-Prot;Acc:P26373]	
9	*090213_11_NW_C5.mgf*	ENSP00000308753	3.42	1	-2.3	5.1	39.6	Tropomodulin-3 (Ubiquitous tropomodulin)(U-Tmod) [Source:UniProtKB/Swiss-Prot;Acc:Q9NYL9]	
6	*090213_07_NW_S3.mgf*	ENSP00000309323	3.24	1	-4.9	6	37.2	EUKARYOTIC TRANSLATION INITIATION FACTOR 2 SUBUNIT 2 EUKARYOTIC TRANSLATION INITIATION FACTOR 2 SUBUNIT BETA EIF 2 BETA	
5	*090213_06_NW_C3.mgf*	ENSP00000309415	3.53	1	-1.1	4.6	25.2	Clathrin light chain B (Lcb) [Source:UniProtKB/Swiss-Prot;Acc:P09497]	
6	*090213_07_NW_S3.mgf*	ENSP00000309415	3.98	1	-3.1	4.6	25.2	Clathrin light chain B (Lcb) [Source:UniProtKB/Swiss-Prot;Acc:P09497]	
20	*090211_14_NW_S10.mgf*	ENSP00000309431	4.57	1	-2.3	4.8	49.5	Tubulin beta-8 chain B [Source:UniProtKB/Swiss-Prot;Acc:A6NNZ2]	
5	*090213_06_NW_C3.mgf*	ENSP00000309558	4.38	5	-13	8	61.8	TATA-binding protein-associated factor 2N (RNA-binding protein 56)(TAFII68)(TAF(II)68) [Source:UniProtKB/Swiss-Prot;Acc:Q92804]	

6	*090213_07_NW_S3.mgf*	ENSP00000309558	3.67	3	-13.6	8	61.8	TATA-binding protein-associated factor 2N (RNA-binding protein 56)(TAFII68)(TAF(II)68) [Source:UniProtKB/Swiss-Prot;Acc:Q92804]
25	*090211_20_NW_C13.mgf*	ENSP00000310696	3.27	1	-1.4	9.9	34.9	Beta-1,4-galactosyltransferase 2 (Beta-1,4-GalTase 2)(Beta4Gal-T2)(b4Gal-T2)(EC 2.4.1.-)(UDP-galactose:beta-N-acetylglucosamine beta-1,4-galactosyltransferase 2)(UDP-Gal:beta-GlcNAc beta-1,4-galactosyltransferase 2) [Includes Lactose synthase A protein(EC 2.4.1.22);N-acetyllactosamine synthase(EC 2.4.1.90)(Nal synthetase);Beta-N-acetylglucosaminylglycopeptide beta-1,4-galactosyltransferase(EC 2.4.1.38);Beta-N-acetylglucosaminyl-glycolipid beta-1,4-galactosyltransferase(EC 2.4.1.-)] [Source:UniProtKB/Swiss-Prot;Acc:O60909]
5	*090213_06_NW_C3.mgf*	ENSP00000311028	6.22	13	-37.3	10	16.3	40S ribosomal protein S14 [Source:UniProtKB/Swiss-Prot;Acc:P62263]
6	*090213_07_NW_S3.mgf*	ENSP00000311028	5.72	9	-17.2	10	16.3	40S ribosomal protein S14 [Source:UniProtKB/Swiss-Prot;Acc:P62263]
8	*090213_10_NW_S4.mgf*	ENSP00000311028	5.03	14	-24.2	10	16.3	40S ribosomal protein S14 [Source:UniProtKB/Swiss-Prot;Acc:P62263]
32	*090211_28_NW_S16.mgf*	ENSP00000311028	3.84	1	-3.3	10	16.3	40S ribosomal protein S14 [Source:UniProtKB/Swiss-Prot;Acc:P62263]
33	*090211_29_NW_C17.mgf*	ENSP00000311028	3.92	1	-1.2	10	16.3	40S ribosomal protein S14 [Source:UniProtKB/Swiss-Prot;Acc:P62263]
34	*090211_30_NW_S17.mgf*	ENSP00000311028	4.25	2	-2.8	10	16.3	40S ribosomal protein S14 [Source:UniProtKB/Swiss-Prot;Acc:P62263]
40	*090213_17_NW_S20.mgf*	ENSP00000311028	3.87	2	-3.4	10	16.3	40S ribosomal protein S14 [Source:UniProtKB/Swiss-Prot;Acc:P62263]
42	*090213_19_NW_S21.mgf*	ENSP00000311028	4.24	1	-5.2	10	16.3	40S ribosomal protein S14 [Source:UniProtKB/Swiss-Prot;Acc:P62263]
47	*090213_25_NW_C24.mgf*	ENSP00000311028	3.92	1	-4.7	10	16.3	40S ribosomal protein S14 [Source:UniProtKB/Swiss-Prot;Acc:P62263]
48	*090213_26_NW_S24.mgf*	ENSP00000311028	4	1	-4.8	10	16.3	40S ribosomal protein S14 [Source:UniProtKB/Swiss-Prot;Acc:P62263]
8	*090213_10_NW_S4.mgf*	ENSP00000311113	3.58	1	-5.7	5.8	81.7	Junction plakoglobin (Desmoplakin-3)(Desmoplakin III)(Catenin gamma) [Source:UniProtKB/Swiss-Prot;Acc:P14923]
40	*090213_17_NW_S20.mgf*	ENSP00000311113	3.34	1	-1.6	5.8	81.7	Junction plakoglobin (Desmoplakin-3)(Desmoplakin III)(Catenin gamma) [Source:UniProtKB/Swiss-Prot;Acc:P14923]
5	*090213_06_NW_C3.mgf*	ENSP00000311430	6.33	10	-13.9	11	47.7	60S ribosomal protein L4 (L1) [Source:UniProtKB/Swiss-Prot;Acc:P36578]
6	*090213_07_NW_S3.mgf*	ENSP00000311430	5.9	5	-8.3	11	47.7	60S ribosomal protein L4 (L1) [Source:UniProtKB/Swiss-Prot;Acc:P36578]
10	*090213_12_NW_S5.mgf*	ENSP00000311430	3.63	1	-3	11	47.7	60S ribosomal protein L4 (L1) [Source:UniProtKB/Swiss-Prot;Acc:P36578]
38	*090213_14_NW_S19.mgf*	ENSP00000311430	3.51	1	-1.6	11	47.7	60S ribosomal protein L4 (L1) [Source:UniProtKB/Swiss-Prot;Acc:P36578]
9	*090213_11_NW_C5.mgf*	ENSP00000313007	4.63	3	-18.4	9.5	70.6	Polyadenylate-binding protein 1 (Poly(A)-binding protein 1)(PABP 1) [Source:UniProtKB/Swiss-Prot;Acc:P11940]
19	*090211_13_NW_C10.mgf*	ENSP00000313007	4.04	1	-2.7	9.5	70.6	Polyadenylate-binding protein 1 (Poly(A)-binding protein 1)(PABP 1) [Source:UniProtKB/Swiss-Prot;Acc:P11940]
20	*090211_14_NW_S10.mgf*	ENSP00000313007	3.72	1	-4.5	9.5	70.6	Polyadenylate-binding protein 1 (Poly(A)-binding protein 1)(PABP 1) [Source:UniProtKB/Swiss-Prot;Acc:P11940]
37	090213_13_NW_C19.mgf	ENSP00000313007	4.16	3	-16.4	9.5	70.6	Polyadenylate-binding protein 1 (Poly(A)-binding protein 1)(PABP 1) [Source:UniProtKB/Swiss-Prot;Acc:P11940]
8	*090213_10_NW_S4.mgf*	ENSP00000313199	4.68	2	-9.5	7.6	38.4	Heterogeneous nuclear ribonucleoprotein D0 (hnRNP D0)(AU-rich element RNA-binding protein 1) [Source:UniProtKB/Swiss-Prot;Acc:O14103]
40	*090213_17_NW_S20.mgf*	ENSP00000314414	3.27	1	-3.5	5.2	105.8	AP-2 complex subunit beta-1 (Adapter-related protein complex 2 beta-1 subunit)(Beta2-adaptin)(Beta-adaptin)(Plasma membrane adaptor HA2/AP2 adaptin beta subunit)(Clathrin assembly protein complex 2 beta large chain)(AP105B) [Source:UniProtKB/Swiss-Prot;Acc:P63010]
15	*090211_08_NW_C8.mgf*	ENSP00000314556	4.54	1	-1.9	6.6	162.4	Uveal autoantigen with coiled-coil domains and ankyrin repeats [Source:UniProtKB/Swiss-Prot;Acc:O9BZF9]
8	*090213_10_NW_S4.mgf*	ENSP00000316411	4.41	3	-10.8	5.8	9.7	No other features on this peptide
24	*090211_19_NW_S12.mgf*	ENSP00000317614	4.03	1	-1.1	9.5	119.5	Zinc finger protein 518B [Source:UniProtKB/Swiss-Prot;Acc:Q9C0D4]
5	*090213_06_NW_C3.mgf*	ENSP00000318195	4.74	7	-25.6	4.6	76.6	Nucleolin (Protein C23) [Source:UniProtKB/Swiss-Prot;Acc:P19338]
6	*090213_07_NW_S3.mgf*	ENSP00000318195	4.51	3	-13.3	4.6	76.6	Nucleolin (Protein C23) [Source:UniProtKB/Swiss-Prot;Acc:P19338]
8	*090213_10_NW_S4.mgf*	ENSP00000318195	4.18	3	-19.8	4.6	76.6	Nucleolin (Protein C23) [Source:UniProtKB/Swiss-Prot;Acc:P19338]
21	*090211_15_NW_C11.mgf*	ENSP00000318195	4.47	1	-2.4	4.6	76.6	Nucleolin (Protein C23) [Source:UniProtKB/Swiss-Prot;Acc:P19338]
5	*090213_06_NW_C3.mgf*	ENSP00000318197	4.37	3	-21.3	5	49.8	Tubulin alpha-3E chain (Alpha-tubulin 3E) [Source:UniProtKB/Swiss-Prot;Acc:Q6PEY2]
6	*090213_07_NW_S3.mgf*	ENSP00000318197	4.21	4	-27.4	5	49.8	Tubulin alpha-3E chain (Alpha-tubulin 3E) [Source:UniProtKB/Swiss-Prot;Acc:Q6PEY2]
17	*090211_11_NW_C9.mgf*	ENSP00000318197	5.14	3	-4.6	5	49.8	Tubulin alpha-3E chain (Alpha-tubulin 3E) [Source:UniProtKB/Swiss-Prot;Acc:Q6PEY2]
18	*090211_12_NW_S9.mgf*	ENSP00000318197	3.44	1	-2.3	5	49.8	Tubulin alpha-3E chain (Alpha-tubulin 3E) [Source:UniProtKB/Swiss-Prot;Acc:Q6PEY2]
11	*090211_04_NW_C6.mgf*	ENSP00000318646	4.91	1	-4.9	10	14.8	40S ribosomal protein S15a [Source:UniProtKB/Swiss-Prot;Acc:P62244]
19	*090211_13_NW_C10.mgf*	ENSP00000318646	5.03	1	-2.3	10	14.8	40S ribosomal protein S15a [Source:UniProtKB/Swiss-Prot;Acc:P62244]
20	*090211_14_NW_S10.mgf*	ENSP00000318646	4.97	2	-1.7	10	14.8	40S ribosomal protein S15a [Source:UniProtKB/Swiss-Prot;Acc:P62244]
35	*090211_32_NW_C18.mgf*	ENSP00000318646	4.53	1	-1.6	10	14.8	40S ribosomal protein S15a [Source:UniProtKB/Swiss-Prot;Acc:P62244]
36	*090211_32_NW_S18.mgf*	ENSP00000318646	4.22	1	-1.8	10	14.8	40S ribosomal protein S15a [Source:UniProtKB/Swiss-Prot;Acc:P62244]
37	090213_13_NW_C19.mgf	ENSP00000318646	4.2	2	-2.4	10	14.8	40S ribosomal protein S15a [Source:UniProtKB/Swiss-Prot;Acc:P62244]
41	*090213_18_NW_C21.mgf*	ENSP00000318646	3.97	1	-2.2	10	14.8	40S ribosomal protein S15a [Source:UniProtKB/Swiss-Prot;Acc:P62244]
5	*090213_06_NW_C3.mgf*	ENSP00000319739	4.07	2	-9.4	4.3	36.9	Reticulocalbin-2 Precursor (Calcium-binding protein ERC-55)(E6-binding protein)(E6BP) [Source:UniProtKB/Swiss-Prot;Acc:Q14257]
6	*090213_07_NW_S3.mgf*	ENSP00000319739	3.79	1	-19.1	4.3	36.9	Reticulocalbin-2 Precursor (Calcium-binding protein ERC-55)(E6-binding protein)(E6BP) [Source:UniProtKB/Swiss-Prot;Acc:Q14257]
39	*090213_16_NW_C20.mgf*	ENSP00000321744	3.78	1	-2.2	10	13.9	Histone H2B type 1-C/E/F/G/I (H2B.a/g/h/k/l)(H2B.1 A)(H2B/a)(H2B/g)(H2B/h)(H2B/k)(H2B/l) [Source:UniProtKB/Swiss-Prot;Acc:P62807]
40	*090213_17_NW_S20.mgf*	ENSP00000321744	3.8	1	-1.4	10	13.9	Histone H2B type 1-C/E/F/G/I (H2B.a/g/h/k/l)(H2B.1 A)(H2B/a)(H2B/g)(H2B/h)(H2B/k)(H2B/l) [Source:UniProtKB/Swiss-Prot;Acc:P62807]
5	*090213_06_NW_C3.mgf*	ENSP00000322419	6.42	21	-33.8	4.4	11.7	60S acidic ribosomal protein P2 (Renal carcinoma antigen NY-REN-44) [Source:UniProtKB/Swiss-Prot;Acc:P05387]
6	*090213_07_NW_S3.mgf*	ENSP00000322419	6.03	11	-34.8	4.4	11.7	60S acidic ribosomal protein P2 (Renal carcinoma antigen NY-REN-44) [Source:UniProtKB/Swiss-Prot;Acc:P05387]
8	*090213_10_NW_S4.mgf*	ENSP00000322419	4.99	4	-25.5	4.4	11.7	60S acidic ribosomal protein P2 (Renal carcinoma antigen NY-REN-44) [Source:UniProtKB/Swiss-Prot;Acc:P05387]
11	*090211_04_NW_C6.mgf*	ENSP00000322419	5.64	16	-19.9	4.4	11.7	60S acidic ribosomal protein P2 (Renal carcinoma antigen NY-REN-44) [Source:UniProtKB/Swiss-Prot;Acc:P05387]
12	*090211_05_NW_S6.mgf*	ENSP00000322419	3.47	1	-5.8	4.4	11.7	60S acidic ribosomal protein P2 (Renal carcinoma antigen NY-REN-44) [Source:UniProtKB/Swiss-Prot;Acc:P05387]
9	*090213_11_NW_C5.mgf*	ENSP00000322439	3.61	1	-1.6	7.3	49.8	Elongation factor Tu, mitochondrial Precursor (EF-Tu)(P43) [Source:UniProtKB/Swiss-Prot;Acc:P49411]
10	*090213_12_NW_S5.mgf*	ENSP00000322439	3.39	1	-4	7.3	49.8	Elongation factor Tu, mitochondrial Precursor (EF-Tu)(P43) [Source:UniProtKB/Swiss-Prot;Acc:P49411]
31	*090211_27_NW_C16.mgf*	ENSP00000322707	4.32	3	-10.9	8.5	37	Tubulin alpha-1C chain (Tubulin alpha-6 chain)(Alpha-tubulin 6) [Source:UniProtKB/Swiss-Prot;Acc:O9BQE3]
5	*090213_06_NW_C3.mgf*	ENSP00000324173	3.94	2	-18	5.1	72.3	78 kDa glucose-regulated protein Precursor (GRP 78)(Heat shock 70 kDa protein 5)(Immunoglobulin heavy chain-binding protein)(BiP)(Endoplasmic reticulum lumenal Ca(2+)-binding protein grp78) [Source:UniProtKB/Swiss-Prot;Acc:P11021]
6	*090213_07_NW_S3.mgf*	ENSP00000324173	4.27	2	-15.4	5.1	72.3	78 kDa glucose-regulated protein Precursor (GRP 78)(Heat shock 70 kDa protein 5)(Immunoglobulin heavy chain-binding protein)(BiP)(Endoplasmic reticulum lumenal Ca(2+)-binding protein grp78) [Source:UniProtKB/Swiss-Prot;Acc:P11021]
8	*090213_10_NW_S4.mgf*	ENSP00000324173	4.17	3	-15.1	5.1	72.3	78 kDa glucose-regulated protein Precursor (GRP 78)(Heat shock 70 kDa protein 5)(Immunoglobulin heavy chain-binding protein)(BiP)(Endoplasmic reticulum lumenal Ca(2+)-binding protein grp78) [Source:UniProtKB/Swiss-Prot;Acc:P11021]
9	*090213_11_NW_C5.mgf*	ENSP00000324173	4.2	2	-12.9	5.1	72.3	78 kDa glucose-regulated protein Precursor (GRP 78)(Heat shock 70 kDa protein 5)(Immunoglobulin heavy chain-binding protein)(BiP)(Endoplasmic reticulum lumenal Ca(2+)-binding protein grp78) [Source:UniProtKB/Swiss-Prot;Acc:P11021]
10	*090213_12_NW_S5.mgf*	ENSP00000324173	4.3	4	-14.3	5.1	72.3	78 kDa glucose-regulated protein Precursor (GRP 78)(Heat shock 70 kDa protein 5)(Immunoglobulin heavy chain-binding protein)(BiP)(Endoplasmic reticulum lumenal Ca(2+)-binding protein grp78) [Source:UniProtKB/Swiss-Prot;Acc:P11021]
12	*090211_05_NW_S6.mgf*	ENSP00000324173	4.01	2	-10.8	5.1	72.3	78 kDa glucose-regulated protein Precursor (GRP 78)(Heat shock 70 kDa protein 5)(Immunoglobulin heavy chain-binding protein)(BiP)(Endoplasmic reticulum lumenal Ca(2+)-binding protein grp78) [Source:UniProtKB/Swiss-Prot;Acc:P11021]
17	*090211_11_NW_C9.mgf*	ENSP00000324173	4.48	2	-9.4	5.1	72.3	78 kDa glucose-regulated protein Precursor (GRP 78)(Heat shock 70 kDa protein 5)(Immunoglobulin heavy chain-binding protein)(BiP)(Endoplasmic reticulum lumenal Ca(2+)-binding protein grp78) [Source:UniProtKB/Swiss-Prot;Acc:P11021]
18	*090211_12_NW_S9.mgf*	ENSP00000324392	4.6	1	-1.3	5.5	118.4	Protein ALO17 (ALK lymphoma oligomerization partner on chromosome 17) [Source:UniProtKB/Swiss-Prot;Acc:Q9HCF4]
5	*090213_06_NW_C3.mgf*	ENSP00000324438	5.17	5	-9.1	8.7	9.1	40S ribosomal protein S21 [Source:UniProtKB/Swiss-Prot;Acc:P63220]
6	*090213_07_NW_S3.mgf*	ENSP00000324438	4.51	3	-5.5	8.7	9.1	40S ribosomal protein S21 [Source:UniProtKB/Swiss-Prot;Acc:P63220]
9	*090213_11_NW_C5.mgf*	ENSP00000324438	3.43	1	-7.4	8.7	9.1	40S ribosomal protein S21 [Source:UniProtKB/Swiss-Prot;Acc:P63220]
10	*090213_12_NW_S5.mgf*	ENSP00000324438	4.23	2	-3.8	8.7	9.1	40S ribosomal protein S21 [Source:UniProtKB/Swiss-Prot;Acc:P63220]
21	*090211_15_NW_C11.mgf*	ENSP00000325376	4.6	2	-8	8.8	77.5	Heterogeneous nuclear ribonucleoprotein M (hnRNP M) [Source:UniProtKB/Swiss-Prot;Acc:P52272]
10	*090213_12_NW_S5.mgf*	ENSP00000326128	3.83	1	-1.2	6.6	81	La-related protein 5 (La ribonucleoprotein domain family member 5) [Source:UniProtKB/Swiss-Prot;Acc:Q92615]
14	*090211_07_NW_S7.mgf*	ENSP00000327699	4.87	1	-1.3	8.2	55.9	
5	*090213_06_NW_C3.mgf*	ENSP00000328902	3.98	2	-3.3	8.5	29.4	FBRNP. Source: Uniprot/SPTREMBL Q65ZQ3
11	*090211_04_NW_C6.mgf*	ENSP00000329646	4.98	1	-1.3	7.5	34.5	Multiple C2 and transmembrane domain-containing protein 2 [Source:UniProtKB/Swiss-Prot;Acc:Q6DN12]
9	*090213_11_NW_C5.mgf*	ENSP00000330074	4.94	3	-6.2	11	22.6	Histone H1.5 (Histone H1a) [Source:UniProtKB/Swiss-Prot;Acc:P16401]
10	*090213_12_NW_S5.mgf*	ENSP00000330074	4.15	2	-6.2	11	22.6	Histone H1.5 (Histone H1a) [Source:UniProtKB/Swiss-Prot;Acc:P16401]
6	*090213_07_NW_S3.mgf*	ENSP00000330165	3.42	1	-2.1	11	12.5	60S ribosomal protein L35a (Cell growth-inhibiting gene 33 protein) [Source:UniProtKB/Swiss-Prot;Acc:P18077]
37	090213_13_NW_C19.mgf	ENSP00000330165	3.6	1	-1.4	11	12.5	60S ribosomal protein L35a (Cell growth-inhibiting gene 33 protein) [Source:UniProtKB/Swiss-Prot;Acc:P18077]
38	*090213_14_NW_S19.mgf*	ENSP00000330165	3.49	1	-1.1	11	12.5	60S ribosomal protein L35a (Cell growth-inhibiting gene 33 protein) [Source:UniProtKB/Swiss-Prot;Acc:P18077]
41	*090213_18_NW_C21.mgf*	ENSP00000330165	3.75	1	-1.3	11	12.5	60S ribosomal protein L35a (Cell growth-inhibiting gene 33 protein) [Source:UniProtKB/Swiss-Prot;Acc:P18077]

5	*090213_06_NW_C3.mgf*	ENSP00000330516	6.06	9	-10.3	9.4	68.4	RNA-binding protein EWS (EWS oncogene)(Ewing sarcoma breakpoint region 1 protein) [Source:UniProtKB/Swiss-Prot;Acc:Q01844]
6	*090213_07_NW_S3.mgf*	ENSP00000330516	4.16	3	-4.6	9.4	68.4	RNA-binding protein EWS (EWS oncogene)(Ewing sarcoma breakpoint region 1 protein) [Source:UniProtKB/Swiss-Prot;Acc:Q01844]
8	*090213_10_NW_S4.mgf*	ENSP00000330516	4.39	2	-6.4	9.4	68.4	RNA-binding protein EWS (EWS oncogene)(Ewing sarcoma breakpoint region 1 protein) [Source:UniProtKB/Swiss-Prot;Acc:Q01844]
9	*090213_11_NW_C5.mgf*	ENSP00000330516	5.55	4	-15.4	9.4	68.4	RNA-binding protein EWS (EWS oncogene)(Ewing sarcoma breakpoint region 1 protein) [Source:UniProtKB/Swiss-Prot;Acc:Q01844]
10	*090213_12_NW_S5.mgf*	ENSP00000330516	3.78	1	-5.7	9.4	68.4	RNA-binding protein EWS (EWS oncogene)(Ewing sarcoma breakpoint region 1 protein) [Source:UniProtKB/Swiss-Prot;Acc:Q01844]
5	*090213_06_NW_C3.mgf*	ENSP00000330879	3.29	1	-6	10	21.8	60S ribosomal protein L9, Source: Uniprot/SWISSPROT P32969
6	*090213_07_NW_S3.mgf*	ENSP00000330879	3.73	1	-5.9	10	21.8	60S ribosomal protein L9, Source: Uniprot/SWISSPROT P32969
8	*090213_10_NW_S4.mgf*	ENSP00000330879	3.86	1	-3.4	10	21.8	60S ribosomal protein L9, Source: Uniprot/SWISSPROT P32969
5	*090213_06_NW_C3.mgf*	ENSP00000331275	5.79	9	-14.9	11	7.8	AMBIGUOUS
6	*090213_07_NW_S3.mgf*	ENSP00000331275	4.77	5	-12.5	11	7.8	No description available.
8	*090213_10_NW_S4.mgf*	ENSP00000331275	4.18	2	-9.1	11	7.8	No description available
10	*090213_12_NW_S5.mgf*	ENSP00000331901	3.76	1	-3.1	6.3	49.9	Elongation factor 1-gamma (EF-1-gamma)(eEF-1B gamma) [Source:UniProtKB/Swiss-Prot;Acc:P26641]
11	*090211_04_NW_C6.mgf*	ENSP00000331902	4.95	2	-7	7.7	161.5	Collagen alpha-5(IV) chain Precursor [Source:UniProtKB/Swiss-Prot;Acc:P29400]
16	*'090211_09_NW_S8.mgf*	ENSP00000331902	4.67	2	-7.3	7.7	161.5	Collagen alpha-5(IV) chain Precursor [Source:UniProtKB/Swiss-Prot;Acc:P29400]
5	*090213_06_NW_C3.mgf*	ENSP00000332117	5.4	5	-4	10	17.5	No description available
6	*090213_07_NW_S3.mgf*	ENSP00000332117	3.95	2	-3.4	10	17.5	No description available
8	*090213_10_NW_S4.mgf*	ENSP00000332117	3.63	2	-1.8	10	17.5	No description available
13	*090211_06_NW_C7.mgf*	ENSP00000333157	4.2	1	-1.3	6	29.2	Growth hormone variant Precursor (GH-V)(Placenta-specific growth hormone)(Growth hormone 2) [Source:UniProtKB/Swiss-Prot;Acc:P01242]
29	*090211_25_NW_C15.mgf*	ENSP00000337774	3.37	1	-1.4	10	8.6	
9	*090213_11_NW_C5.mgf*	ENSP00000338235	4.8	3	-11.6	9.3	63.8	Protein LYRIC (Lysine-rich CEACAM1 co-isolated protein)(3D3/LYRIC)(Metastasis adhesion protein)(Metadherin)(Astrocyte elevated gene-1 protein)(AEG-1) [Source:UniProtKB/Swiss-Prot;Acc:Q86UE4]
10	*090213_12_NW_S5.mgf*	ENSP00000338235	4.41	3	-2.3	9.3	63.8	Protein LYRIC (Lysine-rich CEACAM1 co-isolated protein)(3D3/LYRIC)(Metastasis adhesion protein)(Metadherin)(Astrocyte elevated gene-1 protein)(AEG-1) [Source:UniProtKB/Swiss-Prot;Acc:Q86UE4]
37	090213_13_NW_C19.mgf	ENSP00000338371	3.29	1	-7.7	6.6	182.5	Trinucleotide repeat-containing gene 6B protein [Source:UniProtKB/Swiss-Prot;Acc:O9UPQ9]
8	*090213_10_NW_S4.mgf*	ENSP00000338477	3.77	1	-11.9	5.4	45.6	Heterogeneous nuclear ribonucleoprotein F (hnRNP F)(Nucleolin-like protein mcs94-1) [Source:UniProtKB/Swiss-Prot;Acc:P52597]
13	*090211_06_NW_C7.mgf*	ENSP00000338788	5.32	2	-8.4	5.2	49.1	Zinc finger CCCH domain-containing protein 15 (DRG family-regulatory protein 1)(Likely ortholog of mouse immediate early response erythropoietin 4) [Source:UniProtKB/Swiss-Prot;Acc:Q8WU90]
8	*090213_10_NW_S4.mgf*	ENSP00000339027	5.12	2	-4.5	5.7	34.3	60S acidic ribosomal protein P0 (L10E) [Source:UniProtKB/Swiss-Prot;Acc:P05388]
37	090213_13_NW_C19.mgf	ENSP00000339027	3.95	2	-7.7	5.7	34.3	60S acidic ribosomal protein P0 (L10E) [Source:UniProtKB/Swiss-Prot;Acc:P05388]
38	*090213_14_NW_S19.mgf*	ENSP00000339027	3.85	2	-5.8	5.7	34.3	60S acidic ribosomal protein P0 (L10E) [Source:UniProtKB/Swiss-Prot;Acc:P05388]
39	*090213_16_NW_C20.mgf*	ENSP00000339027	4.35	2	-7.8	5.7	34.3	60S acidic ribosomal protein P0 (L10E) [Source:UniProtKB/Swiss-Prot;Acc:P05388]
40	*090213_17_NW_S20.mgf*	ENSP00000339027	4.3	2	-6.4	5.7	34.3	60S acidic ribosomal protein P0 (L10E) [Source:UniProtKB/Swiss-Prot;Acc:P05388]
42	*090213_19_NW_S21.mgf*	ENSP00000339027	3.63	1	-6.6	5.7	34.3	60S acidic ribosomal protein P0 (L10E) [Source:UniProtKB/Swiss-Prot;Acc:P05388]
19	*090211_13_NW_C10.mgf*	ENSP00000339058	5.58	2	-3.4	10	17.7	60S RIBOSOMAL
20	*090211_14_NW_S10.mgf*	ENSP00000339058	4.49	1	-1.6	10	17.7	60S RIBOSOMAL
21	*090211_15_NW_C11.mgf*	ENSP00000339058	5.61	4	-2.2	10	17.7	60S RIBOSOMAL
24	*090211_19_NW_S12.mgf*	ENSP00000339058	3.24	1	-3.2	10	17.7	60S RIBOSOMAL
35	*090211_32_NW_C18.mgf*	ENSP00000339064	3.66	1	-2.1	11	15.8	60S ribosomal protein L32 [Source:UniProtKB/Swiss-Prot;Acc:P62910]
37	090213_13_NW_C19.mgf	ENSP00000339064	3.9	3	-4.1	11	15.8	60S ribosomal protein L32 [Source:UniProtKB/Swiss-Prot;Acc:P62910]
38	*090213_14_NW_S19.mgf*	ENSP00000339064	4.15	1	-1.2	11	15.8	60S ribosomal protein L32 [Source:UniProtKB/Swiss-Prot;Acc:P62910]
39	*090213_16_NW_C20.mgf*	ENSP00000339064	3.19	1	-2.9	11	15.8	60S ribosomal protein L32 [Source:UniProtKB/Swiss-Prot;Acc:P62910]
40	*090213_17_NW_S20.mgf*	ENSP00000339064	3.62	2	-4.3	11	15.8	60S ribosomal protein L32 [Source:UniProtKB/Swiss-Prot;Acc:P62910]
5	*090213_06_NW_C3.mgf*	ENSP00000339095	4.04	2	-3.4	10	22.1	40S ribosomal protein S7 [Source:UniProtKB/Swiss-Prot;Acc:P62081]
35	*090211_32_NW_C18.mgf*	ENSP00000339095	3.96	1	-3.2	10	22.1	40S ribosomal protein S7 [Source:UniProtKB/Swiss-Prot;Acc:P62081]
38	*090213_14_NW_S19.mgf*	ENSP00000339095	3.58	1	-2.6	10	22.1	40S ribosomal protein S7 [Source:UniProtKB/Swiss-Prot;Acc:P62081]
40	*090213_17_NW_S20.mgf*	ENSP00000339095	3.52	1	-1.4	10	22.1	40S ribosomal protein S7 [Source:UniProtKB/Swiss-Prot;Acc:P62081]
21	*090211_15_NW_C11.mgf*	ENSP00000339566	4.67	2	-10.5	11	21.4	Histone H1.2 (Histone H1d) [Source:UniProtKB/Swiss-Prot;Acc:P16403]
23	*090211_18_NW_C12.mgf*	ENSP00000339566	4.23	1	-4.2	11	21.4	Histone H1.2 (Histone H1d) [Source:UniProtKB/Swiss-Prot;Acc:P16403]
5	*090213_06_NW_C3.mgf*	ENSP00000340251	4.7	3	-18.8	9.2	38.7	Lamina-associated polypeptide 2, isoforms beta/gamma (Thymopoietin, isoforms beta/gamma)(TP beta/gamma)(Thymopoietin-related peptide isoforms beta/gamma)(TPRP isoforms beta/gamma) [Contains Thymopoietin(TP)(Splenin);Thymopentin(TP5)] [Source:UniProtKB/Swiss-Prot;Acc:P42167]
19	*090211_13_NW_C10.mgf*	ENSP00000340251	4.79	2	-2.7	9.2	38.7	Lamina-associated polypeptide 2, isoforms beta/gamma (Thymopoietin, isoforms beta/gamma)(TP beta/gamma)(Thymopoietin-related peptide isoforms beta/gamma)(TPRP isoforms beta/gamma) [Contains Thymopoietin(TP)(Splenin);Thymopentin(TP5)] [Source:UniProtKB/Swiss-Prot;Acc:P42167]
20	*090211_14_NW_S10.mgf*	ENSP00000340251	3.61	2	-1.7	9.2	38.7	Lamina-associated polypeptide 2, isoforms beta/gamma (Thymopoietin, isoforms beta/gamma)(TP beta/gamma)(Thymopoietin-related peptide isoforms beta/gamma)(TPRP isoforms beta/gamma) [Contains Thymopoietin(TP)(Splenin);Thymopentin(TP5)] [Source:UniProtKB/Swiss-Prot;Acc:P42167]
39	*090213_16_NW_C20.mgf*	ENSP00000340251	4.06	2	-8.4	9.2	38.7	Lamina-associated polypeptide 2, isoforms beta/gamma (Thymopoietin, isoforms beta/gamma)(TP beta/gamma)(Thymopoietin-related peptide isoforms beta/gamma)(TPRP isoforms beta/gamma) [Contains Thymopoietin(TP)(Splenin);Thymopentin(TP5)] [Source:UniProtKB/Swiss-Prot;Acc:P42167]
5	*090213_06_NW_C3.mgf*	ENSP00000340329	4.84	3	-19.6	5.1	78.6	Caprin-1 (Cytoplasmic activation- and proliferation-associated protein 1)(GPI-anchored membrane protein 1)(GPI-anchored protein p137)(GPI-p137)(p137GPI)(Cell cycle associated protein 1)(Membrane component chromosome 11 surface marker 1) [Source:UniProtKB/Swiss-Prot;Acc:Q14444]
8	*090213_10_NW_S4.mgf*	ENSP00000340329	4.46	3	-5.5	5.1	78.6	Caprin-1 (Cytoplasmic activation- and proliferation-associated protein 1)(GPI-anchored membrane protein 1)(GPI-anchored protein p137)(GPI-p137)(p137GPI)(Cell cycle associated protein 1)(Membrane component chromosome 11 surface marker 1) [Source:UniProtKB/Swiss-Prot;Acc:Q14444]
9	*090213_11_NW_C5.mgf*	ENSP00000340329	5.42	5	-26.2	5.1	78.6	Caprin-1 (Cytoplasmic activation- and proliferation-associated protein 1)(GPI-anchored membrane protein 1)(GPI-anchored protein p137)(GPI-p137)(p137GPI)(Cell cycle associated protein 1)(Membrane component chromosome 11 surface marker 1) [Source:UniProtKB/Swiss-Prot;Acc:Q14444]
10	*090213_12_NW_S5.mgf*	ENSP00000340329	4.59	4	-21.4	5.1	78.6	Caprin-1 (Cytoplasmic activation- and proliferation-associated protein 1)(GPI-anchored membrane protein 1)(GPI-anchored protein p137)(GPI-p137)(p137GPI)(Cell cycle associated protein 1)(Membrane component chromosome 11 surface marker 1) [Source:UniProtKB/Swiss-Prot;Acc:Q14444]
17	*090211_11_NW_C9.mgf*	ENSP00000340329	5.02	3	-14.7	5.1	78.6	Caprin-1 (Cytoplasmic activation- and proliferation-associated protein 1)(GPI-anchored membrane protein 1)(GPI-anchored protein p137)(GPI-p137)(p137GPI)(Cell cycle associated protein 1)(Membrane component chromosome 11 surface marker 1) [Source:UniProtKB/Swiss-Prot;Acc:Q14444]
21	*090211_15_NW_C11.mgf*	ENSP00000340469	5.68	7	-16.9	10	13.6	40S RIBOSOMAL S25
23	*090211_18_NW_C12.mgf*	ENSP00000340469	5.57	4	-7.7	10	13.6	40S RIBOSOMAL S25
24	*090211_19_NW_S12.mgf*	ENSP00000340469	5.46	6	-16.3	10	13.6	40S RIBOSOMAL S25
25	*090211_20_NW_C13.mgf*	ENSP00000340469	4.54	1	-2.5	10	13.6	40S RIBOSOMAL S25
26	*090211_21_NW_S13.mgf*	ENSP00000340469	4.79	3	-2.2	10	13.6	40S RIBOSOMAL S25
5	*090213_06_NW_C3.mgf*	ENSP00000340510	4.29	1	-1.1	5.5	204.6	Periplakin (195 kDa cornified envelope precursor protein)(190 kDa paraneoplastic pemphigus antigen) [Source:UniProtKB/Swiss-Prot;Acc:O60437]
19	*090211_13_NW_C10.mgf*	ENSP00000340554	4.87	4	-21.7	6.2	2663	titin isoform novex-3 [Source:RefSeq peptide;Acc:NP_596870]
8	*090213_10_NW_S4.mgf*	ENSP00000340698	3.83	1	-10.3	5.9	36	PDZ domain-containing protein GIPC1 (RGS19-interacting protein 1)(GAIP C-terminus-interacting protein)(RGS-GAIP-interacting protein)(Tax interaction protein 2)(TIP-2) [Source:UniProtKB/Swiss-Prot;Acc:O14908]
17	*090211_11_NW_C9.mgf*	ENSP00000340857	3.53	1	-7.2	8.9	84.7	Heterogeneous nuclear ribonucleoprotein U-like protein 1 (Adenovirus early region 1B-associated protein 5)(E1B-55 kDa-associated protein 5)(E1B-AP5) [Source:UniProtKB/Swiss-Prot;Acc:Q9BUJ2]
19	*090211_13_NW_C10.mgf*	ENSP00000341885	6.04	4	-19.4	10	31.3	40S ribosomal protein S2 (S4)(LLRep3 protein) [Source:UniProtKB/Swiss-Prot;Acc:P15880]
15	*090211_08_NW_C8.mgf*	ENSP00000343329	5.02	2	-7.5	9.9	33.5	
9	*090213_11_NW_C5.mgf*	ENSP00000343405	3.78	1	-5.1	6.7	118.2	Protein transport protein Sec24C (SEC24-related protein C) [Source:UniProtKB/Swiss-Prot;Acc:P53992]
9	*090213_11_NW_C5.mgf*	ENSP00000343513	3.34	1	-4.5	4.9	31.2	ELONGATION FACTOR 1 EF 1
15	*090211_08_NW_C8.mgf*	ENSP00000343801	4.47	1	-2.7	10	12.2	60S RIBOSOMAL L7A
17	*090211_11_NW_C9.mgf*	ENSP00000343801	5.88	4	-3.8	10	12.2	60S RIBOSOMAL L7A
18	*090211_12_NW_S9.mgf*	ENSP00000343801	5.6	4	-4.4	10	12.2	60S RIBOSOMAL L7A
5	*090213_06_NW_C3.mgf*	ENSP00000344777	4.65	2	-1.7	10	17.8	Putative uncharacterized protein ENSP00000344777 [Source:UniProtKB/TrEMBL;Acc:A6NP00]
6	*090213_07_NW_S3.mgf*	ENSP00000344777	3.89	1	-2	10	17.8	Putative uncharacterized protein ENSP00000344777 [Source:UniProtKB/TrEMBL;Acc:A6NP00]

40	*090213_17_NW_S20.mgf*	ENSP00000344777	4.16	2	-7.9	10	17.8	Putative uncharacterized protein ENSP00000344777 [Source:UniProtKB/TrEMBL;Acc:A6NP00]		
41	*090213_18_NW_C21.mgf*	ENSP00000344777	4.34	2	-12.9	10	17.8	Putative uncharacterized protein ENSP00000344777 [Source:UniProtKB/TrEMBL;Acc:A6NP00]		
42	*090213_19_NW_S21.mgf*	ENSP00000344777	4.24	1	-5.7	10	17.8	Putative uncharacterized protein ENSP00000344777 [Source:UniProtKB/TrEMBL;Acc:A6NP00]		
46	*090213_24_NW_S23.mgf*	ENSP00000344777	3.49	1	-4.7	10	17.8	Putative uncharacterized protein ENSP00000344777 [Source:UniProtKB/TrEMBL;Acc:A6NP00]	ENSP00000344777	
13	*090211_06_NW_C7.mgf*	ENSP00000344950	4.21	1	-1.7	9.6	67.7	La-related protein 7 (La ribonucleoprotein domain family member 7)(P-TEFb-interaction protein for 7SK stability)(PIP7S) [Source:UniProtKB/Swiss-Prot;Acc:Q4G0J3]		
25	*090211_20_NW_C13.mgf*	ENSP00000345060	4.39	1	-1.1	5.5	257.1	Probable G-protein coupled receptor 179 Precursor (Probable G-protein coupled receptor 158-like 1) [Source:UniProtKB/Swiss-Prot;Acc:O6PRD1]		
8	*090213_10_NW_S4.mgf*	ENSP00000345156	3.79	1	-9.7	11	23.4	60S ribosomal protein L14 (CAG-ISL 7) [Source:UniProtKB/Swiss-Prot;Acc:P50914]		
24	*090211_19_NW_S12.mgf*	ENSP00000345157	3.78	1	-1.5	9.7	16.3			
19	*090211_13_NW_C10.mgf*	ENSP00000346018	4.15	2	-8.1	11	30	60S ribosomal protein L7a (Surfeit locus protein 3)(PLA-X polypeptide) [Source:UniProtKB/Swiss-Prot;Acc:P62424]		
5	*090213_06_NW_C3.mgf*	ENSP00000346045	4.72	6	-14.4	9.8	15.5	40S ribosomal protein S17 [Source:UniProtKB/Swiss-Prot;Acc:P08708]		
6	*090213_07_NW_S3.mgf*	ENSP00000346045	3.98	1	-2.5	9.8	15.5	40S ribosomal protein S17 [Source:UniProtKB/Swiss-Prot;Acc:P08708]		
12	*090211_05_NW_S6.mgf*	ENSP00000346051	4.8	1	-1.9	5.8	126.3	Zinc finger protein ZFPM2 (Zinc finger protein multitype 2)(Friend of GATA protein 2)(FOG-2)(hFOG-2) [Source:UniProtKB/Swiss-Prot;Acc:Q8WW38]		
11	*090211_04_NW_C6.mgf*	ENSP00000346080	4.5	1	-3.8	9.7	15.6	60S ribosomal protein L22-like 1 [Source:UniProtKB/Swiss-Prot;Acc:Q6P5R6]		
12	*090211_05_NW_S6.mgf*	ENSP00000346080	3.81	1	-2.8	9.7	15.6	60S ribosomal protein L22-like 1 [Source:UniProtKB/Swiss-Prot;Acc:Q6P5R6]		
31	*090211_27_NW_C16.mgf*	ENSP00000346080	4.93	1	-1.4	9.7	15.6	60S ribosomal protein L22-like 1 [Source:UniProtKB/Swiss-Prot;Acc:Q6P5R6]		
15	*090211_08_NW_C8.mgf*	ENSP00000346081	5.79	3	-8	9	208.8	HERV-K_7p22.1 provirus ancestral Pro protein (EC 3.4.23.-) (HERV- K(HML-2.HOM) Pro protein) (HERV-K108 Pro protein) (HERV-K(C7) Pro protein) (Protease) (Proteinase) (PR). Source: Uniprot/SWISSPROT Q9Y6I0		
40	*090213_17_NW_S20.mgf*	ENSP00000346120	3.39	1	-2.7	9.3	87.3	Nucleolar RNA helicase 2 (EC 3.6.1.-)(Nucleolar RNA helicase II)(Nucleolar RNA helicase Gu)(RH II/Gu)(Gu-alpha)(DEAD box protein 21) [Source:UniProtKB/Swiss-Prot;Acc:Q9NR30]		
42	*090213_19_NW_S21.mgf*	ENSP00000346120	3.33	1	-2	9.3	87.3	Nucleolar RNA helicase 2 (EC 3.6.1.-)(Nucleolar RNA helicase II)(Nucleolar RNA helicase Gu)(RH II/Gu)(Gu-alpha)(DEAD box protein 21) [Source:UniProtKB/Swiss-Prot;Acc:Q9NR30]		
5	*090213_06_NW_C3.mgf*	ENSP00000346598	5.54	8	-14.8	4.8	32.9	Uncharacterized protein ENSP00000346598 [Source:UniProtKB/TrEMBL;Acc:A6NE09]		
6	*090213_07_NW_S3.mgf*	ENSP00000346598	5.09	6	-13.5	4.8	32.9	Uncharacterized protein ENSP00000346598 [Source:UniProtKB/TrEMBL;Acc:A6NE09]		
8	*090213_10_NW_S4.mgf*	ENSP00000346598	4.27	1	-5.4	4.8	32.9	Uncharacterized protein ENSP00000346598 [Source:UniProtKB/TrEMBL;Acc:A6NE09]		
24	*090211_19_NW_S12.mgf*	ENSP00000346598	3.56	1	-1.1	4.8	32.9	Uncharacterized protein ENSP00000346598 [Source:UniProtKB/TrEMBL;Acc:A6NE09]		
35	*090211_32_NW_C18.mgf*	ENSP00000346598	3.97	1	-6.2	4.8	32.9	Uncharacterized protein ENSP00000346598 [Source:UniProtKB/TrEMBL;Acc:A6NE09]		
38	*090213_14_NW_S19.mgf*	ENSP00000346598	3.96	2	-12	4.8	32.9	Uncharacterized protein ENSP00000346598 [Source:UniProtKB/TrEMBL;Acc:A6NE09]		
40	*090213_17_NW_S20.mgf*	ENSP00000346598	4.03	1	-8	4.8	32.9	Uncharacterized protein ENSP00000346598 [Source:UniProtKB/TrEMBL;Acc:A6NE09]		
42	*090213_19_NW_S21.mgf*	ENSP00000346598	3.55	1	-5.8	4.8	32.9	Uncharacterized protein ENSP00000346598 [Source:UniProtKB/TrEMBL;Acc:A6NE09]		
47	*090213_25_NW_C24.mgf*	ENSP00000346598	3.5	1	-7.1	4.8	32.9	Uncharacterized protein ENSP00000346598 [Source:UniProtKB/TrEMBL;Acc:A6NE09]		
48	*090213_26_NW_S24.mgf*	ENSP00000346598	3.71	1	-7.3	4.8	32.9	Uncharacterized protein ENSP00000346598 [Source:UniProtKB/TrEMBL;Acc:A6NE09]		
8	*090213_10_NW_S4.mgf*	ENSP00000346634	4.15	1	-3.6	10	108.6	Thyroid hormone receptor-associated protein 3 (Thyroid hormone receptor-associated protein complex 150 kDa component)(Trap150) [Source:UniProtKB/Swiss-Prot;Acc:Q9Y2W1]		
19	*090211_13_NW_C10.mgf*	ENSP00000346634	3.79	1	-3.3	10	108.6	Thyroid hormone receptor-associated protein 3 (Thyroid hormone receptor-associated protein complex 150 kDa component)(Trap150) [Source:UniProtKB/Swiss-Prot;Acc:Q9Y2W1]		
37	090213_13_NW_C19.mgf	ENSP00000346634	3.6	1	-3.1	10	108.6	Thyroid hormone receptor-associated protein 3 (Thyroid hormone receptor-associated protein complex 150 kDa component)(Trap150) [Source:UniProtKB/Swiss-Prot;Acc:Q9Y2W1]		
37	090213 13 NW C19.mgf	ENSP00000346975	4.08	2	-7.6	11	29.6	similar to 60S ribosomal protein L7a (LOC401640), mRNA Source: RefSeq_dna XR_017380		
40	*090213_17_NW_S20.mgf*	ENSP00000346975	4.31	3	-9.6	11	29.6	similar to 60S ribosomal protein L7a (LOC401640), mRNA Source: RefSeq_dna XR_017380		
8	*090213_10_NW_S4.mgf*	ENSP00000347049	4.93	3	-4.8	10	21.4	KERATIN ASSOCIATED KERATIN ASSOCIATED KERATIN ASSOCIATED KERATIN ASSOCIATED KERATIN ASSOCIATED		
17	*090211_11_NW_C9.mgf*	ENSP00000347271	5.56	6	-3.4	10	18.9	40S ribosomal protein S10 [Source:UniProtKB/Swiss-Prot;Acc:P46783]		
13	*090211_06_NW_C7.mgf*	ENSP00000347325	5.33	2	-7.6	6.8	449.1	Histone-lysine N-methyltransferase MLL3 (EC 2.1.1.43)(Myeloid/lymphoid or mixed-lineage leukemia protein 3)(Homologous to ALR protein)(Lysine N-methyltransferase 2C) [Source:UniProtKB/Swiss-Prot;Acc:Q8NEZ4]		
17	*090211_11_NW_C9.mgf*	ENSP00000348031	4.75	1	-1.1	8.4	296.5	Histone-lysine N-methyltransferase, H3 lysine-36 and H4 lysine-20 specific (EC 2.1.1.43)(H3-K36-HMTase)(H4-K20-HMTase)(Nuclear receptor-binding SET domain-containing protein 1)(NR-binding SET domain-containing protein)(Androgen receptor-associated coregulator 267)(Lysine N-methyltransferase 3B) [Source:UniProtKB/Swiss-Prot;Acc:Q96L73]		
16	*'090211_09_NW_S8.mgf*	ENSP00000348531	5.57	5	-16	10	13.9	Histone H2B type 1-H (H2B j) (H2B/j). Source: Uniprot/SWISSPROT Q93079		
5	*090213_06_NW_C3.mgf*	ENSP00000348578	4.67	6	-20.5	5.4	52.1	Ras GTPase-activating protein-binding protein 1 (EC 3.6.1.-)(G3BP-1)(ATP-dependent DNA helicase VIII)(HDH-VIII)(GAP SH3 domain-binding protein 1) [Source:UniProtKB/Swiss-Prot;Acc:Q13283]		
8	*090213_10_NW_S4.mgf*	ENSP00000348578	3.9	1	-9.6	5.4	52.1	Ras GTPase-activating protein-binding protein 1 (EC 3.6.1.-)(G3BP-1)(ATP-dependent DNA helicase VIII)(HDH-VIII)(GAP SH3 domain-binding protein 1) [Source:UniProtKB/Swiss-Prot;Acc:Q13283]		
19	*090211_13_NW_C10.mgf*	ENSP00000348578	3.54	1	-2.4	5.4	52.1	Ras GTPase-activating protein-binding protein 1 (EC 3.6.1.-)(G3BP-1)(ATP-dependent DNA helicase VIII)(HDH-VIII)(GAP SH3 domain-binding protein 1) [Source:UniProtKB/Swiss-Prot;Acc:Q13283]		
37	090213 13 NW C19.mgf	ENSP00000348933	3.35	1	-2.5	6.3	24.5	Coiled-coil domain-containing protein 25 [Source:UniProtKB/Swiss-Prot;Acc:Q86WR0]		
5	*090213_06_NW_C3.mgf*	ENSP00000349101	5.95	7	-17	4.8	28.4	Heterogeneous nuclear ribonucleoproteins A2/B1 (hnRNP A2 / hnRNP B1) [Source:UniProtKB/Swiss-Prot;Acc:P22626]		
6	*090213_07_NW_S3.mgf*	ENSP00000349101	5.15	3	-4.7	4.8	28.4	Heterogeneous nuclear ribonucleoproteins A2/B1 (hnRNP A2 / hnRNP B1) [Source:UniProtKB/Swiss-Prot;Acc:P22626]		
8	*090213_10_NW_S4.mgf*	ENSP00000349101	4.34	2	-3.1	4.8	28.4	Heterogeneous nuclear ribonucleoproteins A2/B1 (hnRNP A2 / hnRNP B1) [Source:UniProtKB/Swiss-Prot;Acc:P22626]		
19	*090211_13_NW_C10.mgf*	ENSP00000349101	5.1	1	-1.5	4.8	28.4	Heterogeneous nuclear ribonucleoproteins A2/B1 (hnRNP A2 / hnRNP B1) [Source:UniProtKB/Swiss-Prot;Acc:P22626]		
20	*090211_14_NW_S10.mgf*	ENSP00000349101	4.75	1	-1.2	4.8	28.4	Heterogeneous nuclear ribonucleoproteins A2/B1 (hnRNP A2 / hnRNP B1) [Source:UniProtKB/Swiss-Prot;Acc:P22626]		
17	*090211_11_NW_C9.mgf*	ENSP00000349185	5.02	1	-2	11	29.6	60S RIBOSOMAL L7		
19	*090211_13_NW_C10.mgf*	ENSP00000349185	5.19	3	-10.9	11	29.6	60S RIBOSOMAL L7		
20	*090211_14_NW_S10.mgf*	ENSP00000349185	4.49	2	-8.3	11	29.6	60S RIBOSOMAL L7		
21	*090211_15_NW_C11.mgf*	ENSP00000349185	4.44	1	-2.1	11	29.6	60S RIBOSOMAL L7		
23	*090211_18_NW_C12.mgf*	ENSP00000349185	3.96	1	-2.5	11	29.6	60S RIBOSOMAL L7		
24	*090211_19_NW_S12.mgf*	ENSP00000349185	4.02	1	-2.6	11	29.6	60S RIBOSOMAL L7		
25	*090211_20_NW_C13.mgf*	ENSP00000349185	4.02	1	-3.1	11	29.6	60S RIBOSOMAL L7		
5	*090213_06_NW_C3.mgf*	ENSP00000349362	3.7	2	-4.9	11	12.9	Protein Family: 40S RIBOSOMAL S26		
5	*090213_06_NW_C3.mgf*	ENSP00000349435	4	3	-20.8	10	45.9	60S ribosomal protein L3 (HIV-1 TAR RNA-binding protein B) (TARBP-B). Source: Uniprot/SWISSPROT P39023		
8	*090213_10_NW_S4.mgf*	ENSP00000349435	3.42	1	-2.7	10	45.9	60S ribosomal protein L3 (HIV-1 TAR RNA-binding protein B) (TARBP-B). Source: Uniprot/SWISSPROT P39023		
38	*090213_14_NW_S19.mgf*	ENSP00000349435	3.66	1	-3.3	10	45.9	60S ribosomal protein L3 (HIV-1 TAR RNA-binding protein B) (TARBP-B). Source: Uniprot/SWISSPROT P39023		
39	*090213_16_NW_C20.mgf*	ENSP00000349435	3.16	1	-3.3	10	45.9	60S ribosomal protein L3 (HIV-1 TAR RNA-binding protein B) (TARBP-B). Source: Uniprot/SWISSPROT P39023		
40	*090213_17_NW_S20.mgf*	ENSP00000349435	3.6	1	-3.1	10	45.9	60S ribosomal protein L3 (HIV-1 TAR RNA-binding protein B) (TARBP-B). Source: Uniprot/SWISSPROT P39023		
5	*090213_06_NW_C3.mgf*	ENSP00000349748	3.72	2	-18.9	9.5	76.1	Splicing factor, proline- and glutamine-rich (Polypyrimidine tract-binding protein-associated-splicing factor)(PTB-associated-splicing factor)(PSF)(DNA-binding p52/p100 complex, 100 kDa subunit)(100 kDa DNA-pairing protein)(hPOMp100) [Source:UniProtKB/Swiss-Prot;Acc:P23246]		
5	*090213_06_NW_C3.mgf*	ENSP00000349960	6.21	34	-61.5	5.3	41.7	Actin, cytoplasmic 1 (Beta-actin) [Source:UniProtKB/Swiss-Prot;Acc:P60709]		
6	*090213_07_NW_S3.mgf*	ENSP00000349960	5.17	13	-30.3	5.3	41.7	Actin, cytoplasmic 1 (Beta-actin) [Source:UniProtKB/Swiss-Prot;Acc:P60709]		
8	*090213_10_NW_S4.mgf*	ENSP00000349960	5.42	8	-23.4	5.3	41.7	Actin, cytoplasmic 1 (Beta-actin) [Source:UniProtKB/Swiss-Prot;Acc:P60709]		
9	*090213_11_NW_C5.mgf*	ENSP00000349960	6.3	12	-25.5	5.3	41.7	Actin, cytoplasmic 1 (Beta-actin) [Source:UniProtKB/Swiss-Prot;Acc:P60709]		
11	*090211_04_NW_C6.mgf*	ENSP00000349960	7.11	21	-32.3	5.3	41.7	Actin, cytoplasmic 1 (Beta-actin) [Source:UniProtKB/Swiss-Prot;Acc:P60709]		
12	*090211_05_NW_S6.mgf*	ENSP00000349960	6.48	17	-30.4	5.3	41.7	Actin, cytoplasmic 1 (Beta-actin) [Source:UniProtKB/Swiss-Prot;Acc:P60709]		
21	*090211_15_NW_C11.mgf*	ENSP00000349960	5.53	5	-13.8	5.3	41.7	Actin, cytoplasmic 1 (Beta-actin) [Source:UniProtKB/Swiss-Prot;Acc:P60709]		
23	*090211_18_NW_C12.mgf*	ENSP00000349960	5.49	5	-12.6	5.3	41.7	Actin, cytoplasmic 1 (Beta-actin) [Source:UniProtKB/Swiss-Prot;Acc:P60709]		
24	*090211_19_NW_S12.mgf*	ENSP00000349960	5.36	8	-18	5.3	41.7	Actin, cytoplasmic 1 (Beta-actin) [Source:UniProtKB/Swiss-Prot;Acc:P60709]		
25	*090211_20_NW_C13.mgf*	ENSP00000349960	5.42	5	-11.8	5.3	41.7	Actin, cytoplasmic 1 (Beta-actin) [Source:UniProtKB/Swiss-Prot;Acc:P60709]		
26	*090211_21_NW_S13.mgf*	ENSP00000349960	5.09	3	-11.6	5.3	41.7	Actin, cytoplasmic 1 (Beta-actin) [Source:UniProtKB/Swiss-Prot;Acc:P60709]		
28	*090211_22_NW_S14.mgf*	ENSP00000349960	5.09	3	-11.8	5.3	41.7	Actin, cytoplasmic 1 (Beta-actin) [Source:UniProtKB/Swiss-Prot;Acc:P60709]		
29	*090211_25_NW_C15.mgf*	ENSP00000349960	4.83	3	-9.2	5.3	41.7	Actin, cytoplasmic 1 (Beta-actin) [Source:UniProtKB/Swiss-Prot;Acc:P60709]		
31	*090211_27_NW_C16.mgf*	ENSP00000349960	3.5	1	-2.3	5.3	41.7	Actin, cytoplasmic 1 (Beta-actin) [Source:UniProtKB/Swiss-Prot;Acc:P60709]		
32	*090211_28_NW_S16.mgf*	ENSP00000349960	4.31	2	-11.7	5.3	41.7	Actin, cytoplasmic 1 (Beta-actin) [Source:UniProtKB/Swiss-Prot;Acc:P60709]		
37	090213 13 NW C19.mgf	ENSP00000349960	4.76	4	-11	5.3	41.7	Actin, cytoplasmic 1 (Beta-actin) [Source:UniProtKB/Swiss-Prot;Acc:P60709]		
47	*090213_25_NW_C24.mgf*	ENSP00000349960	3.94	3	-16.9	5.3	41.7	Actin, cytoplasmic 1 (Beta-actin) [Source:UniProtKB/Swiss-Prot;Acc:P60709]		

48	*090213_26_NW_S24.mgf*	ENSP00000349960	4.43	4	-21.4	5.3	41.7	Actin, cytoplasmic 1 (Beta-actin) [Source:UniProtKB/Swiss-Prot;Acc:P60709]
6	*090213_07_NW_S3.mgf*	ENSP00000350170	3.74	2	-17.1	5.8	69.7	Fragile X mental retardation syndrome-related protein 1 (hFXR1p) [Source:UniProtKB/Swiss-Prot;Acc:P51114]
6	*090213_07_NW_S3.mgf*	ENSP00000350199	3.51	1	-5	4.9	104.6	AP-1 complex subunit beta-1 (Adapter-related protein complex 1 subunit beta-1)(Adaptor protein complex AP-1 subunit beta-1)(Beta-adaptin 1)(Beta1-adaptin)(Golgi adaptor HA1/AP1 adaptin beta subunit)(Clathrin assembly protein complex 1 beta large chain) [Source:UniProtKB/Swiss-Prot;Acc:Q10567]
19	*090211_13_NW_C10.mgf*	ENSP00000350494	5.04	1	-3.3	11	16.6	60S RIBOSOMAL L27A
20	*090211_14_NW_S10.mgf*	ENSP00000350494	4.3	1	-1.1	11	16.6	60S RIBOSOMAL L27A
21	*090211_15_NW_C11.mgf*	ENSP00000350494	4.35	1	-3.1	11	16.6	60S RIBOSOMAL L27A
9	*090213_11_NW_C5.mgf*	ENSP00000350580	5.25	8	-11.4	10	13.9	Histone H2B type 1-B (H2B.f)(H2B/f)(H2B.1) [Source:UniProtKB/Swiss-Prot;Acc:P33778]
10	*090213_12_NW_S5.mgf*	ENSP00000350580	3.26	1	-7.4	10	13.9	Histone H2B type 1-B (H2B.f)(H2B/f)(H2B.1) [Source:UniProtKB/Swiss-Prot;Acc:P33778]
8	*090213_10_NW_S4.mgf*	ENSP00000351108	4.3	2	-7.9	6.5	35.9	Heterogeneous nuclear ribonucleoprotein A/B (hnRNP A/B)(APOBEC1-binding protein 1)(ABBP-1) [Source:UniProtKB/Swiss-Prot;Acc:Q99729]
29	*090211_25_NW_C15.mgf*	ENSP00000351483	3.84	1	-1.4	6.9	128.6	Electroneutral sodium bicarbonate exchanger 1 (Electroneutral Na+-driven Cl-HCO3 exchanger)(Solute carrier family 4 member 8)(k-NBC3) [Source:UniProtKB/Swiss-Prot;Acc:Q2Y0W8]
5	*090213_06_NW_C3.mgf*	ENSP00000351906	4.39	3	-15.8	11	19	60S RIBOSOMAL L21
38	*090213_14_NW_S19.mgf*	ENSP00000351906	3.5	1	-3.4	11	19	60S RIBOSOMAL L21
9	*090213_11_NW_C5.mgf*	ENSP00000352402	3.23	1	-2	12	24.2	
10	*090213_12_NW_S5.mgf*	ENSP00000352402	4.38	3	-5.9	12	24.2	similar to ribosomal protein L15 (LOC402694), mRNA Source: RefSeq dna NM_001089590
14	*090211_07_NW_S7.mgf*	ENSP00000352847	3.88	1	-1.4	8.6	65.2	
9	*090213_11_NW_C5.mgf*	ENSP00000352980	5.76	5	-7.6	11	11.4	Histone H4 [Source:UniProtKB/Swiss-Prot;Acc:P62805]
10	*090213_12_NW_S5.mgf*	ENSP00000352980	4.62	2	-5.3	11	11.4	Histone H4 [Source:UniProtKB/Swiss-Prot;Acc:P62805]
16	*'090211_09_NW_S8.mgf*	ENSP00000352980	3.42	1	-1.2	11	11.4	Histone H4 [Source:UniProtKB/Swiss-Prot;Acc:P62805]
21	*090211_15_NW_C11.mgf*	ENSP00000352980	5.05	1	-2.1	11	11.4	Histone H4 [Source:UniProtKB/Swiss-Prot;Acc:P62805]
5	*090213_06_NW_C3.mgf*	ENSP00000353659	4.62	5	-11.4	10	24.4	No other features on this peptide
6	*090213_07_NW_S3.mgf*	ENSP00000353659	4.02	4	-10.9	10	24.4	No other features on this peptide
5	*090213_06_NW_C3.mgf*	ENSP00000353679	4.22	1	-1.1	5.5	85.5	Neprilysin (EC 3.4.24.11)(Neutral endopeptidase 24.11)(Neutral endopeptidase)(NEP)(Enkephalinase)(Atriopeptidase)(Common acute lymphocytic leukemia antigen)(CALLA)(CD10 antigen) [Source:UniProtKB/Swiss-Prot;Acc:P08473]
6	*090213_07_NW_S3.mgf*	ENSP00000353679	3.83	1	-1.6	5.5	85.5	Neprilysin (EC 3.4.24.11)(Neutral endopeptidase 24.11)(Neutral endopeptidase)(NEP)(Enkephalinase)(Atriopeptidase)(Common acute lymphocytic leukemia antigen)(CALLA)(CD10 antigen) [Source:UniProtKB/Swiss-Prot;Acc:P08473]
8	*090213_10_NW_S4.mgf*	ENSP00000353679	3.95	1	-10.4	5.5	85.5	Neprilysin (EC 3.4.24.11)(Neutral endopeptidase 24.11)(Neutral endopeptidase)(NEP)(Enkephalinase)(Atriopeptidase)(Common acute lymphocytic leukemia antigen)(CALLA)(CD10 antigen) [Source:UniProtKB/Swiss-Prot;Acc:P08473]
9	*090213_11_NW_C5.mgf*	ENSP00000353679	3.93	1	-2.7	5.5	85.5	Neprilysin (EC 3.4.24.11)(Neutral endopeptidase 24.11)(Neutral endopeptidase)(NEP)(Enkephalinase)(Atriopeptidase)(Common acute lymphocytic leukemia antigen)(CALLA)(CD10 antigen) [Source:UniProtKB/Swiss-Prot;Acc:P08473]
10	*090213_12_NW_S5.mgf*	ENSP00000353679	3.46	1	-4.7	5.5	85.5	Neprilysin (EC 3.4.24.11)(Neutral endopeptidase 24.11)(Neutral endopeptidase)(NEP)(Enkephalinase)(Atriopeptidase)(Common acute lymphocytic leukemia antigen)(CALLA)(CD10 antigen) [Source:UniProtKB/Swiss-Prot;Acc:P08473]
18	*090211_12_NW_S9.mgf*	ENSP00000353679	4.54	1	-2.5	5.5	85.5	Neprilysin (EC 3.4.24.11)(Neutral endopeptidase 24.11)(Neutral endopeptidase)(NEP)(Enkephalinase)(Atriopeptidase)(Common acute lymphocytic leukemia antigen)(CALLA)(CD10 antigen) [Source:UniProtKB/Swiss-Prot;Acc:P08473]
8	*090213_10_NW_S4.mgf*	ENSP00000353736	3.44	1	-1.5	11	23.6	60S RIBOSOMAL L13A
11	*090211_04_NW_C6.mgf*	ENSP00000353736	5.3	2	-4.5	11	23.6	60S RIBOSOMAL L13A
20	*090211_14_NW_S10.mgf*	ENSP00000353769	4.13	1	-1.2	9.3	139.2	Splicing factor, arginine/serine-rich 19 (Serine arginine-rich pre-mRNA splicing factor SR-A1)(SR-A1)(SR-related-CTD-associated factor)(SCAF) [Source:UniProtKB/Swiss-Prot;Acc:Q9H7N4]
9	*090213_11_NW_C5.mgf*	ENSP00000353941	4.22	2	-6.4	7.5	25.7	Ig kappa chain C region. Source: Uniprot/SWISSPROT P01834
10	*090213_12_NW_S5.mgf*	ENSP00000353941	4.13	2	-5.7	7.5	25.7	Ig kappa chain C region. Source: Uniprot/SWISSPROT P01834
38	*090213_14_NW_S19.mgf*	ENSP00000354021	4.44	2	-6.4	8.7	36	Heterogeneous nuclear ribonucleoproteins A2/B1 (hnRNP A2 / hnRNP B1) [Source:UniProtKB/Swiss-Prot;Acc:P22626]
39	*090213_16_NW_C20.mgf*	ENSP00000354021	4.18	1	-3.7	8.7	36	Heterogeneous nuclear ribonucleoproteins A2/B1 (hnRNP A2 / hnRNP B1) [Source:UniProtKB/Swiss-Prot;Acc:P22626]
5	*090213_06_NW_C3.mgf*	ENSP00000354029	4.9	3	-7.5	9.2	14.5	No other features on this peptide
15	*090211_08_NW_C8.mgf*	ENSP00000354074	3.43	1	-2.3	11	15.1	40S ribosomal protein S24 [Source:UniProtKB/Swiss-Prot;Acc:P62847]
17	*090211_11_NW_C9.mgf*	ENSP00000354074	3.92	2	-3.1	11	15.1	40S ribosomal protein S24 [Source:UniProtKB/Swiss-Prot;Acc:P62847]
20	*090211_14_NW_S10.mgf*	ENSP00000354346	4.78	1	-2.2	5.9	94.6	Matrin-3 [Source:UniProtKB/Swiss-Prot;Acc:P43243]
11	*090211_04_NW_C6.mgf*	ENSP00000354522	3.36	1	-4.5	9.3	90.7	DNA topoisomerase 1 (EC 5.99.1.2)(DNA topoisomerase I) [Source:UniProtKB/Swiss-Prot;Acc:P11387]
27	*090211_22_NW_C14.mgf*	ENSP00000354932	4.04	1	-1.1	6.6	91.2	Toll-like receptor 1 Precursor (Toll/interleukin-1 receptor-like protein)(TIL)(CD281 antigen) [Source:UniProtKB/Swiss-Prot;Acc:Q15399]
8	*090213_10_NW_S4.mgf*	ENSP00000355258	4.6	1	-3.1	9.9	24.8	60S ribosomal protein L10a (CSA-19)(Neural precursor cell expressed developmentally down-regulated protein 6)(NEDD-6) [Source:UniProtKB/Swiss-Prot;Acc:P62906]
9	*090213_11_NW_C5.mgf*	ENSP00000355258	4.19	2	-4.5	9.9	24.8	60S ribosomal protein L10a (CSA-19)(Neural precursor cell expressed developmentally down-regulated protein 6)(NEDD-6) [Source:UniProtKB/Swiss-Prot;Acc:P62906]
10	*090213_12_NW_S5.mgf*	ENSP00000355258	3.46	1	-4.6	9.9	24.8	60S ribosomal protein L10a (CSA-19)(Neural precursor cell expressed developmentally down-regulated protein 6)(NEDD-6) [Source:UniProtKB/Swiss-Prot;Acc:P62906]
31	*090211_27_NW_C16.mgf*	ENSP00000355258	5.68	5	-7.2	9.9	24.8	60S ribosomal protein L10a (CSA-19)(Neural precursor cell expressed developmentally down-regulated protein 6)(NEDD-6) [Source:UniProtKB/Swiss-Prot;Acc:P62906]
32	*090211_28_NW_S16.mgf*	ENSP00000355258	4.69	1	-1.3	9.9	24.8	60S ribosomal protein L10a (CSA-19)(Neural precursor cell expressed developmentally down-regulated protein 6)(NEDD-6) [Source:UniProtKB/Swiss-Prot;Acc:P62906]
38	*090213_14_NW_S19.mgf*	ENSP00000355258	3.88	1	-2.3	9.9	24.8	60S ribosomal protein L10a (CSA-19)(Neural precursor cell expressed developmentally down-regulated protein 6)(NEDD-6) [Source:UniProtKB/Swiss-Prot;Acc:P62906]
43	*090213_20_NW_C22.mgf*	ENSP00000355258	3.5	1	-1.4	9.9	24.8	60S ribosomal protein L10a (CSA-19)(Neural precursor cell expressed developmentally down-regulated protein 6)(NEDD-6) [Source:UniProtKB/Swiss-Prot;Acc:P62906]
44	*090213_21_NW_S22.mgf*	ENSP00000355258	3.5	1	-1.2	9.9	24.8	60S ribosomal protein L10a (CSA-19)(Neural precursor cell expressed developmentally down-regulated protein 6)(NEDD-6) [Source:UniProtKB/Swiss-Prot;Acc:P62906] ENSP00000355258
13	*090211_06_NW_C7.mgf*	ENSP00000355356	3.41	1	-1.3	9.5	179.4	
9	*090213_11_NW_C5.mgf*	ENSP00000355759	4.32	1	-2.5	9	113	Poly [ADP-ribose] polymerase 1 (PARP-1)(EC 2.4.2.30)(ADPRT)(NAD(+) ADP-ribosyltransferase 1)(Poly[ADP-ribose] synthetase 1) [Source:UniProtKB/Swiss-Prot;Acc:P09874]
10	*090213_12_NW_S5.mgf*	ENSP00000355759	3.56	2	-9.1	9	113	Poly [ADP-ribose] polymerase 1 (PARP-1)(EC 2.4.2.30)(ADPRT)(NAD(+) ADP-ribosyltransferase 1)(Poly[ADP-ribose] synthetase 1) [Source:UniProtKB/Swiss-Prot;Acc:P09874]
40	*090213_17_NW_S20.mgf*	ENSP00000355809	3.49	1	-1.1	6.5	66.5	Protein enabled homolog [Source:UniProtKB/Swiss-Prot;Acc:Q8N8S7]
13	*090211_06_NW_C7.mgf*	ENSP00000356264	5.64	2	-8.1	8.6	162.6	Neuron navigator 1 (Steerin-1)(Pore membrane and/or filament-interacting-like protein 3)(Unc-53 homolog 1)(unc53H1) [Source:UniProtKB/Swiss-Prot;Acc:Q8NEY1]
5	*090213_06_NW_C3.mgf*	ENSP00000356520	3.76	2	-6.1	6.4	140.9	ATP-dependent RNA helicase A (EC 3.6.1.-)(Nuclear DNA helicase II)(NDH II)(DEAH box protein 9) [Source:UniProtKB/Swiss-Prot;Acc:O08211]
5	*090213_06_NW_C3.mgf*	ENSP00000356881	5.22	13	-23.3	6.8	14.5	40S ribosomal protein S12 [Source:UniProtKB/Swiss-Prot;Acc:P25398]
6	*090213_07_NW_S3.mgf*	ENSP00000356881	4.93	9	-24.4	6.8	14.5	40S ribosomal protein S12 [Source:UniProtKB/Swiss-Prot;Acc:P25398]
29	*090211_25_NW_C15.mgf*	ENSP00000356881	4.25	1	-2.2	6.8	14.5	40S ribosomal protein S12 [Source:UniProtKB/Swiss-Prot;Acc:P25398]
13	*090211_06_NW_C7.mgf*	ENSP00000357002	5.17	1	-1.1	6.6	13.3	Putative thiosulfate sulfurtransferase KAT (EC 2.8.1.1) [Source:UniProtKB/Swiss-Prot;Acc:Q8NFU3]
8	*090213_10_NW_S4.mgf*	ENSP00000357284	4.17	2	-9.7	6.4	65.1	Lamin-A/C (70 kDa lamin)(Renal carcinoma antigen NY-REN-32) [Source:UniProtKB/Swiss-Prot;Acc:P02545]
10	*090213_12_NW_S5.mgf*	ENSP00000357284	3.52	1	-8.9	6.4	65.1	Lamin-A/C (70 kDa lamin)(Renal carcinoma antigen NY-REN-32) [Source:UniProtKB/Swiss-Prot;Acc:P02545]
5	*090213_06_NW_C3.mgf*	ENSP00000357673	3.25	1	-5.2	5.2	42.9	Interleukin enhancer-binding factor 2 (Nuclear factor of activated T-cells 45 kDa) [Source:UniProtKB/Swiss-Prot;Acc:Q12905]
9	*090213_11_NW_C5.mgf*	ENSP00000357673	5.03	1	-6.7	5.2	42.9	Interleukin enhancer-binding factor 2 (Nuclear factor of activated T-cells 45 kDa) [Source:UniProtKB/Swiss-Prot;Acc:Q12905]
10	*090213_12_NW_S5.mgf*	ENSP00000357673	4.27	1	-7.9	5.2	42.9	Interleukin enhancer-binding factor 2 (Nuclear factor of activated T-cells 45 kDa) [Source:UniProtKB/Swiss-Prot;Acc:Q12905]
11	*090211_04_NW_C6.mgf*	ENSP00000357673	5.83	6	-7	5.2	42.9	Interleukin enhancer-binding factor 2 (Nuclear factor of activated T-cells 45 kDa) [Source:UniProtKB/Swiss-Prot;Acc:Q12905]
12	*090211_05_NW_S6.mgf*	ENSP00000357673	4.33	1	-3.4	5.2	42.9	Interleukin enhancer-binding factor 2 (Nuclear factor of activated T-cells 45 kDa)
37	090213_13_NW_C19.mgf	ENSP00000357673	3.42	1	-1.2	5.2	42.9	Interleukin enhancer-binding factor 2 (Nuclear factor of activated T-cells 45 kDa) [Source:UniProtKB/Swiss-Prot;Acc:Q12905]
40	*090213_17_NW_S20.mgf*	ENSP00000357673	3.87	1	-3.9	5.2	42.9	Interleukin enhancer-binding factor 2 (Nuclear factor of activated T-cells 45 kDa) [Source:UniProtKB/Swiss-Prot;Acc:Q12905]
37	090213 13 NW C19.mgf	ENSP00000357791	3.53	1	-4.3	10	282.2	Hornerin [Source:UniProtKB/Swiss-Prot;Acc:Q86YZ3]
38	*090213_14_NW_S19.mgf*	ENSP00000357791	3.89	2	-24.4	10	282.2	Hornerin [Source:UniProtKB/Swiss-Prot;Acc:Q86YZ3]
40	*090213_17_NW_S20.mgf*	ENSP00000357791	3.89	2	-16.4	10	282.2	Hornerin [Source:UniProtKB/Swiss-Prot;Acc:Q86YZ3]
5	*090213_06_NW_C3.mgf*	ENSP00000358027	6.06	6	-1.9	7.7	18.9	Decaprenyl-diphosphate synthase subunit 2 (EC 2.5.1.-)(Decaprenyl pyrophosphate synthetase subunit
6	*090213_07_NW_S3.mgf*	ENSP00000358027	4.41	1	-2.2	7.7	18.9	Decaprenyl-diphosphate synthase subunit 2 (EC 2.5.1.-)(Decaprenyl pyrophosphate synthetase subunit 2)(Candidate tumor suppressor protein) [Source:UniProtKB/Swiss-Prot;Acc:Q86YH6]
8	*090213_10_NW_S4.mgf*	ENSP00000358089	3.43	1	-2.4	8.1	43.4	Nucleolysin TIAR (TIA-1-related protein) [Source:UniProtKB/Swiss-Prot;Acc:Q01085]
37	090213 13 NW C19.mgf	ENSP00000358089	3.72	1	-1.1	8.1	43.4	Nucleolysin TIAR (TIA-1-related protein) [Source:UniProtKB/Swiss-Prot;Acc:Q01085]
40	*090213_17_NW_S20.mgf*	ENSP00000358089	3.43	1	-2	8.1	43.4	Nucleolysin TIAR (TIA-1-related protein) [Source:UniProtKB/Swiss-Prot;Acc:Q01085]
13	*090211_06_NW_C7.mgf*	ENSP00000358123	3.81	1	-1.1	5.1	64.6	E3 ubiquitin-protein ligase HACE1 (EC 6.3.2.-)(HECT domain and ankyrin repeat-containing E3 ubiquitin-protein ligase 1) [Source:UniProtKB/Swiss-Prot;Acc:Q8IYU2]
8	*090213_10_NW_S4.mgf*	ENSP00000358417	4.21	2	-13.5	6.3	56.6	D-3-phosphoglycerate dehydrogenase (3-PGDH)(EC 1.1.1.95) [Source:UniProtKB/Swiss-Prot;Acc:O43175]
35	*090211_32_NW_C18.mgf*	ENSP00000358417	3.88	1	-1.1	6.3	56.6	D-3-phosphoglycerate dehydrogenase (3-PGDH)(EC 1.1.1.95) [Source:UniProtKB/Swiss-Prot;Acc:O43175]
37	090213_13_NW_C19.mgf	ENSP00000358417	3.45	1	-6.3	6.3	56.6	D-3-phosphoglycerate dehydrogenase (3-PGDH)(EC 1.1.1.95) [Source:UniProtKB/Swiss-Prot;Acc:O43175]

38	*090213_14_NW_S19.mgf*	ENSP00000358417	3.33	1	-6.9	6.3	56.6	D-3-phosphoglycerate dehydrogenase (3-PGDH)(EC 1.1.1.95) [Source:UniProtKB/Swiss-Prot;Acc:O43175]
40	*090213_17_NW_S20.mgf*	ENSP00000358417	3.72	1	-7	6.3	56.6	D-3-phosphoglycerate dehydrogenase (3-PGDH)(EC 1.1.1.95) [Source:UniProtKB/Swiss-Prot;Acc:O43175]
8	*090213_10_NW_S4.mgf*	ENSP00000358799	4.26	1	-1.2	10	107.1	Putative RNA-binding protein 15 (RNA-binding motif protein 15)(One-twenty two protein) [Source:UniProtKB/Swiss-Prot;Acc:O96T37]
9	*090213_11_NW_C5.mgf*	ENSP00000358857	4.12	1	-1.2	5.3	29	Emerin [Source:UniProtKB/Swiss-Prot;Acc:P50402]
48	*090213_26_NW_S24.mgf*	ENSP00000358943	3.58	1	-3.7	5.9	23.7	Tumor protein D54 (hD54)(Tumor protein D52-like 2) [Source:UniProtKB/Swiss-Prot;Acc:O43399]
17	*090211_11_NW_C9.mgf'*	ENSP00000358998	4.56	2	-14.1	8.8	144.9	Myosin-VI (Unconventional myosin VI) [Source:UniProtKB/Swiss-Prot;Acc:O9UM54]
5	*090213_06_NW_C3.mgf*	ENSP00000359002	5.01	6	-38.1	8.8	146	Myosin-VI (Unconventional myosin VI) [Source:UniProtKB/Swiss-Prot;Acc:O9UM54]
6	*090213_07_NW_S3.mgf*	ENSP00000359002	4.32	2	-10.5	8.8	146	Myosin-VI (Unconventional myosin VI) [Source:UniProtKB/Swiss-Prot;Acc:O9UM54]
8	*090213_10_NW_S4.mgf*	ENSP00000359002	4.51	4	-39.4	8.8	146	Myosin-VI (Unconventional myosin VI) [Source:UniProtKB/Swiss-Prot;Acc:O9UM54]
9	*090213_11_NW_C5.mgf*	ENSP00000359002	4.68	4	-10.5	8.8	146	Myosin-VI (Unconventional myosin VI) [Source:UniProtKB/Swiss-Prot;Acc:O9UM54]
10	*090213_12_NW_S5.mgf*	ENSP00000359002	3.56	1	-3.5	8.8	146	Myosin-VI (Unconventional myosin VI) [Source:UniProtKB/Swiss-Prot;Acc:O9UM54]
11	*090211_04_NW_C6.mgf'*	ENSP00000359002	4.27	1	-2.2	8.8	146	Myosin-VI (Unconventional myosin VI) [Source:UniProtKB/Swiss-Prot;Acc:O9UM54]
20	*090211_14_NW_S10.mgf*	ENSP00000359002	3.44	1	-1.9	8.8	146	Myosin-VI (Unconventional myosin VI) [Source:UniProtKB/Swiss-Prot;Acc:O9UM54]
38	*090213_14_NW_S19.mgf*	ENSP00000359002	3.64	1	-1.7	8.8	146	Myosin-VI (Unconventional myosin VI) [Source:UniProtKB/Swiss-Prot;Acc:O9UM54]
39	*090213_16_NW_C20.mgf*	ENSP00000359002	3.54	1	-2	8.8	146	Myosin-VI (Unconventional myosin VI) [Source:UniProtKB/Swiss-Prot;Acc:O9UM54]
40	*090213_17_NW_S20.mgf*	ENSP00000359002	3.69	1	-1.5	8.8	146	Myosin-VI (Unconventional myosin VI) [Source:UniProtKB/Swiss-Prot;Acc:O9UM54]
5	*090213_06_NW_C3.mgf*	ENSP00000359345	4.18	2	-7.2	9.7	34.3	60S ribosomal protein L5 [Source:UniProtKB/Swiss-Prot;Acc:P46777]
10	*090213_12_NW_S5.mgf*	ENSP00000359438	3.5	1	-5.1	7.7	38.9	Erlin-1 (Endoplasmic reticulum lipid raft-associated protein 1)(Stomatin-prohibitin-flotillin-HflC/K domain-containing protein 1)(SPFH domain-containing protein 1)(Protein KE04) [Source:UniProtKB/Swiss-Prot;Acc:O75477]
6	*090213_07_NW_S3.mgf*	ENSP00000359508	3.51	1	-11.2	7.3	65.8	Fragile X mental retardation 1 protein (Protein FMR-1)(FMRP) [Source:UniProtKB/Swiss-Prot;Acc:O06787]
17	*090211_11_NW_C9.mgf'*	ENSP00000359508	4.08	1	-1.4	7.3	65.8	Fragile X mental retardation 1 protein (Protein FMR-1)(FMRP) [Source:UniProtKB/Swiss-Prot;Acc:O06787]
9	*090213_11_NW_C5.mgf*	ENSP00000359645	5.06	2	-6	10	42.3	Heterogeneous nuclear ribonucleoprotein G (hnRNP G)(RNA-binding motif protein, X chromosome)(Glycoprotein p43) [Contains Processed heterogeneous nuclear ribonucleoprotein G] [Source:UniProtKB/Swiss-Prot;Acc:P38159]
10	*090213_12_NW_S5.mgf*	ENSP00000359645	3.93	2	-5.4	10	42.3	Heterogeneous nuclear ribonucleoprotein G (hnRNP G)(RNA-binding motif protein, X chromosome)(Glycoprotein p43) [Contains Processed heterogeneous nuclear ribonucleoprotein G] [Source:UniProtKB/Swiss-Prot;Acc:P38159]
5	*090213_06_NW_C3.mgf*	ENSP00000360034	3.98	3	-11	8.7	44.9	Plasminogen activator inhibitor 1 RNA-binding protein (PAI1 RNA-binding protein 1)(PAI-RBP1)(SERPINE1 mRNA-binding protein 1) [Source:UniProtKB/Swiss-Prot;Acc:O8NC51]
6	*090213_07_NW_S3.mgf*	ENSP00000360034	3.44	1	-5.9	8.7	44.9	Plasminogen activator inhibitor 1 RNA-binding protein (PAI1 RNA-binding protein 1)(PAI-RBP1)(SERPINE1 mRNA-binding protein 1) [Source:UniProtKB/Swiss-Prot;Acc:O8NC51]
8	*090213_10_NW_S4.mgf*	ENSP00000360034	4.57	3	-8	8.7	44.9	Plasminogen activator inhibitor 1 RNA-binding protein (PAI1 RNA-binding protein 1)(PAI-RBP1)(SERPINE1 mRNA-binding protein 1) [Source:UniProtKB/Swiss-Prot;Acc:O8NC51]
11	*090211_04_NW_C6.mgf'*	ENSP00000360034	4.38	1	-5.9	8.7	44.9	Plasminogen activator inhibitor 1 RNA-binding protein (PAI1 RNA-binding protein 1)(PAI-RBP1)(SERPINE1 mRNA-binding protein 1) [Source:UniProtKB/Swiss-Prot;Acc:O8NC51]
26	*090211_21_NW_S13.mgf*	ENSP00000360293	3.86	3	-6.8	6.4	142.4	Sorbin and SH3 domain-containing protein 1 (Ponsin)(c-Cbl-associated protein)(CAP)(SH3 domain protein 5)(SH3P12) [Source:UniProtKB/Swiss-Prot;Acc:Q9BX66]
8	*090213_10_NW_S4.mgf*	ENSP00000360709	4.07	2	-12.3	5	83.2	Heat shock protein HSP 90-beta (HSP 90)(HSP 84) [Source:UniProtKB/Swiss-Prot;Acc:P08238]
22	*090211_16_NW_S11.mgf'*	ENSP00000361269	4.71	1	-1.3	5.8	123.6	Rap guanine nucleotide exchange factor 1 (Guanine nucleotide-releasing factor 2)(C3G protein)(CRK SH3-binding GNRP) [Source:UniProtKB/Swiss-Prot;Acc:O13905]
9	*090213_11_NW_C5.mgf*	ENSP00000361288	5.76	3	-7.4	10	24.2	40S ribosomal protein S8 [Source:UniProtKB/Swiss-Prot;Acc:P62241]
10	*090213_12_NW_S5.mgf*	ENSP00000361288	4.82	6	-7.9	10	24.2	40S ribosomal protein S8 [Source:UniProtKB/Swiss-Prot;Acc:P62241]
13	*090211_06_NW_C7.mgf*	ENSP00000361290	4.18	2	-9.6	9.3	165.7	Collagen alpha-6(IV) chain Precursor [Source:UniProtKB/Swiss-Prot;Acc:Q14031]
5	*090213_06_NW_C3.mgf*	ENSP00000361626	3.9	3	-11	9.9	35.9	Nuclease-sensitive element-binding protein 1 (Y-box-binding protein 1)(Y-box transcription factor)(YB-1)(CCAAT-binding transcription factor I subunit A)(CBF-A)(Enhancer factor I subunit A)(EFI-A)(DNA-binding protein B)(DBPB) [Source:UniProtKB/Swiss-Prot;Acc:P67809]
37	090213_13_NW_C19.mgf	ENSP00000361920	4.54	3	-2.4	11	14.9	60S ribosomal protein Fragment [Source:UniProtKB/TrEMBL;Acc:Q5T8W0]
40	*090213_17_NW_S20.mgf*	ENSP00000361920	3.89	2	-2.3	11	14.9	60S ribosomal protein Fragment [Source:UniProtKB/TrEMBL;Acc:Q5T8W0]
17	*090211_11_NW_C9.mgf'*	ENSP00000361927	5.22	2	-10.9	5.9	49.2	60S ribosomal protein L36a (60S ribosomal protein L44)(Cell migration-inducing gene 6 protein) [Source:UniProtKB/Swiss-Prot;Acc:P83881]
5	*090213_06_NW_C3.mgf*	ENSP00000362211	3.73	1	-1.1	6.4	80.2	Kelch-like protein 4 [Source:UniProtKB/Swiss-Prot;Acc:Q9C0H6]
5	*090213_06_NW_C3.mgf*	ENSP00000362744	4.44	3	-19.8	10	29.6	40S ribosomal protein S4, X isoform (Single copy abundant mRNA protein)(SCR10) [Source:UniProtKB/Swiss-Prot;Acc:P62701]
6	*090213_07_NW_S3.mgf*	ENSP00000362744	3.59	1	-3.4	10	29.6	40S ribosomal protein S4, X isoform (Single copy abundant mRNA protein)(SCR10) [Source:UniProtKB/Swiss-Prot;Acc:P62701]
37	090213_13_NW_C19.mgf	ENSP00000362744	4.19	2	-3	10	29.6	40S ribosomal protein S4, X isoform (Single copy abundant mRNA protein)(SCR10) [Source:UniProtKB/Swiss-Prot;Acc:P62701]
38	*090213_14_NW_S19.mgf*	ENSP00000362744	3.96	2	-3.4	10	29.6	40S ribosomal protein S4, X isoform (Single copy abundant mRNA protein)(SCR10) [Source:UniProtKB/Swiss-Prot;Acc:P62701]
40	*090213_17_NW_S20.mgf*	ENSP00000362744	4.24	1	-3.3	10	29.6	40S ribosomal protein S4, X isoform (Single copy abundant mRNA protein)(SCR10) [Source:UniProtKB/Swiss-Prot;Acc:P62701]
34	*090211_30_NW_S17.mgf*	ENSP00000362768	3.83	1	-1.6	7.3	120.8	Retinoblastoma-like protein 1 (PRB1)(107 kDa retinoblastoma-associated protein)(p107) [Source:UniProtKB/Swiss-Prot;Acc:P28749]
38	*090213_14_NW_S19.mgf*	ENSP00000362820	3.41	1	-1.6	12	19.3	Splicing factor, arginine/serine-rich 3 (Pre-mRNA-splicing factor SRP20) [Source:UniProtKB/Swiss-Prot;Acc:P84103]
40	*090213_17_NW_S20.mgf*	ENSP00000362820	4.11	1	-3.4	12	19.3	Splicing factor, arginine/serine-rich 3 (Pre-mRNA-splicing factor SRP20) [Source:UniProtKB/Swiss-Prot;Acc:P84103]
10	*090213_12_NW_S5.mgf*	ENSP00000363006	4.17	2	-5.6	9.7	29.1	Transcription factor A, mitochondrial Precursor (mtTFA)(Mitochondrial transcription factor 1)(MtTF1)(Transcription factor 6-like 2) [Source:UniProtKB/Swiss-Prot;Acc:Q00059]
21	*090211_15_NW_C11.mgf'*	ENSP00000363006	4.68	1	-3.6	9.7	29.1	Transcription factor A, mitochondrial Precursor (mtTFA)(Mitochondrial transcription factor 1)(MtTF1)(Transcription factor 6-like 2) [Source:UniProtKB/Swiss-Prot;Acc:Q00059]
5	*090213_06_NW_C3.mgf*	ENSP00000363021	4.41	5	-2.8	5.7	29.2	Replication protein A 32 kDa subunit (RP-A p32)(RP-A p34)(Replication factor A protein 2)(RF-A protein 2) [Source:UniProtKB/Swiss-Prot;Acc:P15927]
6	*090213_07_NW_S3.mgf*	ENSP00000363021	3.65	2	-1.3	5.7	29.2	Replication protein A 32 kDa subunit (RP-A p32)(RP-A p34)(Replication factor A protein 2)(RF-A protein 2) [Source:UniProtKB/Swiss-Prot;Acc:P15927]
17	*090211_11_NW_C9.mgf'*	ENSP00000364802	4.82	2	-10.6	5.5	70	Heat shock 70 kDa protein 1 (HSP70.1)(HSP70-1/HSP70-2) [Source:UniProtKB/Swiss-Prot;Acc:P08107]
8	*090213_10_NW_S4.mgf*	ENSP00000364805	4.16	2	-10.5	5.8	70.3	Heat shock 70 kDa protein 1L (Heat shock 70 kDa protein 1-like)(Heat shock 70 kDa protein 1-Hom)(HSP70-Hom) [Source:UniProtKB/Swiss-Prot;Acc:P34931]
9	*090213_11_NW_C5.mgf*	ENSP00000365238	4.42	1	-2.2	5.7	126.7	Ankyrin repeat domain-containing protein 26 [Source:UniProtKB/Swiss-Prot;Acc:Q9UPS8]
5	*090213_06_NW_C3.mgf*	ENSP00000365458	4.27	3	-13.5	5.2	51	Heterogeneous nuclear ribonucleoprotein K (hnRNP K)(Transformation up-regulated nuclear protein)(TUNP) [Source:UniProtKB/Swiss-Prot;Acc:P61978]
10	*090213_12_NW_S5.mgf*	ENSP00000365458	3.83	1	-3	5.2	51	Heterogeneous nuclear ribonucleoprotein K (hnRNP K)(Transformation up-regulated nuclear protein)(TUNP) [Source:UniProtKB/Swiss-Prot;Acc:P61978]
6	*090213_07_NW_S3.mgf*	ENSP00000366013	3.38	1	-6.3	8	29.7	Guanine nucleotide-binding protein subunit beta-2-like 1 (Guanine nucleotide-binding protein subunit beta-like protein 12.3)(Receptor of activated protein kinase C 1)(RACK1)(Receptor for activated C kinase) [Source:UniProtKB/Swiss-Prot;Acc:P63244]
8	*090213_10_NW_S4.mgf*	ENSP00000366013	4.17	1	-1.1	8	29.7	Guanine nucleotide-binding protein subunit beta-2-like 1 (Guanine nucleotide-binding protein subunit beta-like protein 12.3)(Receptor of activated protein kinase C 1)(RACK1)(Receptor for activated C kinase) [Source:UniProtKB/Swiss-Prot;Acc:P63244]
37	090213_13_NW_C19.mgf	ENSP00000366190	3.4	1	-1.8	5.1	23.2	Dr1-associated corepressor (Dr1-associated protein 1)(Negative co-factor 2-alpha)(NC2-alpha) [Source:UniProtKB/Swiss-Prot;Acc:Q14919]
22	*090211_16_NW_S11.mgf'*	ENSP00000366620	4.34	1	-2.1	6.8	89.9	GDH/6PGL endoplasmic bifunctional protein Precursor [Includes Glucose 1-dehydrogenase(EC 1.1.1.47)(Hexose-6-phosphate dehydrogenase);6-phosphogluconolactonase(6PGL)(EC 3.1.1.31)] [Source:UniProtKB/Swiss-Prot;Acc:O95479]
37	090213_13_NW_C19.mgf	ENSP00000366702	3.99	1	-4.3	8.4	50.5	ERBB receptor feedback inhibitor 1 (Mitogen-inducible gene 6 protein)(Mig-6) [Source:UniProtKB/Swiss-Prot;Acc:O9UJM3]
39	*090213_16_NW_C20.mgf*	ENSP00000366702	4.52	2	-2.9	8.4	50.5	ERBB receptor feedback inhibitor 1 (Mitogen-inducible gene 6 protein)(Mig-6) [Source:UniProtKB/Swiss-Prot;Acc:O9UJM3]
40	*090213_17_NW_S20.mgf*	ENSP00000366702	4.39	2	-4.2	8.4	50.5	ERBB receptor feedback inhibitor 1 (Mitogen-inducible gene 6 protein)(Mig-6) [Source:UniProtKB/Swiss-Prot;Acc:O9UJM3]
11	*090211_04_NW_C6.mgf'*	ENSP00000367025	4.06	1	-3.3	5.3	53	keratin 25D Source: RefSeq_peptide NP_853513
8	*090213_10_NW_S4.mgf*	ENSP00000367044	3.61	1	-5	8.7	152.4	Ribosome-binding protein 1 (Ribosome receptor protein)(180 kDa ribosome receptor homolog)(ES/130-related protein) [Source:UniProtKB/Swiss-Prot;Acc:Q9P2E9]
19	*090211_13_NW_C10.mgf*	ENSP00000367336	3.9	1	-4.5	10	14.8	60S ribosomal protein L23 (Ribosomal protein L17) [Source:UniProtKB/Swiss-Prot;Acc:P62829]
12	*090211_05_NW_S6.mgf*	ENSP00000367643	3.92	1	-1.1	5.8	138.1	PR domain zinc finger protein 16 (PR domain-containing protein 16)(Transcription factor MEL1) [Source:UniProtKB/Swiss-Prot;Acc:O9HAZ2]
15	*090211_08_NW_C8.mgf*	ENSP00000367643	5.05	1	-1.3	5.8	138.1	PR domain zinc finger protein 16 (PR domain-containing protein 16)(Transcription factor MEL1) [Source:UniProtKB/Swiss-Prot;Acc:O9HAZ2]
10	*090213_12_NW_S5.mgf*	ENSP00000367806	4.76	5	-10.3	11	17.1	40S ribosomal protein S16 [Source:UniProtKB/Swiss-Prot;Acc:P62249]
13	*090211_06_NW_C7.mgf*	ENSP00000367865	4.54	1	-1.2	6.1	21.1	Transmembrane protein 52 Precursor [Source:UniProtKB/Swiss-Prot;Acc:O8NDY8]
22	*090211_16_NW_S11.mgf'*	ENSP00000368543	3.86	1	-1.6	9.4	72.5	Vitrin Precursor [Source:UniProtKB/Swiss-Prot;Acc:Q6UXI7]
5	*090213_06_NW_C3.mgf*	ENSP00000368883	4.51	4	-14.6	4.5	17.3	Myosin light polypeptide 6 (Smooth muscle and nonmuscle myosin light chain alkali 6) (Myosin light chain alkali 3) (Myosin light chain 3) (MLC-3) (LC17). Source: Uniprot/SWISSPROT P60660
10	*090213_12_NW_S5.mgf*	ENSP00000369129	3.79	1	-1.3	6.4	331.6	Desmoplakin (DP)(250/210 kDa paraneoplastic pemphigus antigen) [Source:UniProtKB/Swiss-Prot;Acc:P15924]
21	*090211_15_NW_C11.mgf'*	ENSP00000369129	4.31	1	-1.2	6.4	331.6	Desmoplakin (DP)(250/210 kDa paraneoplastic pemphigus antigen) [Source:UniProtKB/Swiss-Prot;Acc:P15924]
37	090213_13_NW_C19.mgf	ENSP00000369129	3.8	1	-4.2	6.4	331.6	Desmoplakin (DP)(250/210 kDa paraneoplastic pemphigus antigen) [Source:UniProtKB/Swiss-Prot;Acc:P15924]
38	*090213_14_NW_S19.mgf*	ENSP00000369129	4.01	1	-6.4	6.4	331.6	Desmoplakin (DP)(250/210 kDa paraneoplastic pemphigus antigen) [Source:UniProtKB/Swiss-Prot;Acc:P15924]
15	*090211_08_NW_C8.mgf*	ENSP00000369245	7.14	2	-1.1	7	36	Ig gamma-4 chain C region. Source: Uniprot/SWISSPROT P01861
16	*'090211_09_NW_S8.mgf*	ENSP00000369245	5.32	1	-1.8	7	36	Ig gamma-4 chain C region. Source: Uniprot/SWISSPROT P01861
17	*090211_11_NW_C9.mgf'*	ENSP00000369245	7.01	2	-1.4	7	36	Ig gamma-4 chain C region. Source: Uniprot/SWISSPROT P01861
21	*090211_15_NW_C11.mgf'*	ENSP00000369245	6.36	2	-6.5	7	36	Ig gamma-4 chain C region. Source: Uniprot/SWISSPROT P01861

25	090211_20_NW_C13.mgf	ENSP00000369245	5.61	2	-1.1	7	36	Ig gamma-4 chain C region. Source: Uniprot/SWISSPROT P01861
5	090213_06_NW_C3.mgf	ENSP00000369757	4.5	3	-8.9	11	28.7	40S ribosomal protein S6 (Phosphoprotein NP33) [Source:UniProtKB/Swiss-Prot;Acc:P62753]
6	090213_07_NW_S3.mgf	ENSP00000369757	4.02	2	-1.7	11	28.7	40S ribosomal protein S6 (Phosphoprotein NP33) [Source:UniProtKB/Swiss-Prot;Acc:P62753]
5	090213_06_NW_C3.mgf	ENSP00000369957	4.65	4	-20.5	7.9	76.5	Interleukin enhancer-binding factor 3 (Nuclear factor of activated T- cells 90 kDa) (NF-AT-90) (Double-stranded RNA-binding protein 76) (DRBP76) (Translational control protein 80) (TCP80) (Nuclear factor associated with dsRNA) (NFAR) (M-phase phosphoprote Source: Uniprot/SWISSPROT Q12906
6	090213_07_NW_S3.mgf	ENSP00000369957	4.24	2	-4.3	7.9	76.5	Interleukin enhancer-binding factor 3 (Nuclear factor of activated T- cells 90 kDa) (NF-AT-90) (Double-stranded RNA-binding protein 76) (DRBP76) (Translational control protein 80) (TCP80) (Nuclear factor associated with dsRNA) (NFAR) (M-phase phosphoprote Source: Uniprot/SWISSPROT Q12906
8	090213_10_NW_S4.mgf	ENSP00000369957	3.67	1	-6.3	7.9	76.5	Interleukin enhancer-binding factor 3 (Nuclear factor of activated T- cells 90 kDa) (NF-AT-90) (Double-stranded RNA-binding protein 76) (DRBP76) (Translational control protein 80) (TCP80) (Nuclear factor associated with dsRNA) (NFAR) (M-phase phosphoprote Source: Uniprot/SWISSPROT Q12906
9	090213_11_NW_C5.mgf	ENSP00000369957	3.95	1	-4.5	7.9	76.5	Interleukin enhancer-binding factor 3 (Nuclear factor of activated T- cells 90 kDa) (NF-AT-90) (Double-stranded RNA-binding protein 76) (DRBP76) (Translational control protein 80) (TCP80) (Nuclear factor associated with dsRNA) (NFAR) (M-phase phosphoprote Source: Uniprot/SWISSPROT Q12906
12	090211_05_NW_S6.mgf	ENSP00000369957	5.03	3	-3.7	7.9	76.5	Interleukin enhancer-binding factor 3 (Nuclear factor of activated T- cells 90 kDa) (NF-AT-90) (Double-stranded RNA-binding protein 76) (DRBP76) (Translational control protein 80) (TCP80) (Nuclear factor associated with dsRNA) (NFAR) (M-phase phosphoprote Source: Uniprot/SWISSPROT Q12906
23	090211_18_NW_C12.mgf	ENSP00000369957	3.99	2	-2.6	7.9	76.5	Interleukin enhancer-binding factor 3 (Nuclear factor of activated T- cells 90 kDa) (NF-AT-90) (Double-stranded RNA-binding protein 76) (DRBP76) (Translational control protein 80) (TCP80) (Nuclear factor associated with dsRNA) (NFAR) (M-phase phosphoprote Source: Uniprot/SWISSPROT Q12906
38	090213_14_NW_S19.mgf	ENSP00000369957	3.54	1	-1.3	7.9	76.5	Interleukin enhancer-binding factor 3 (Nuclear factor of activated T- cells 90 kDa) (NF-AT-90) (Double-stranded RNA-binding protein 76) (DRBP76) (Translational control protein 80) (TCP80) (Nuclear factor associated with dsRNA) (NFAR) (M-phase phosphoprote Source: Uniprot/SWISSPROT Q12906
41	090213_18_NW_C21.mgf	ENSP00000369957	3.39	1	-1.4	7.9	76.5	Interleukin enhancer-binding factor 3 (Nuclear factor of activated T- cells 90 kDa) (NF-AT-90) (Double-stranded RNA-binding protein 76) (DRBP76) (Translational control protein 80) (TCP80) (Nuclear factor associated with dsRNA) (NFAR) (M-phase phosphoprote Source: Uniprot/SWISSPROT Q12906
31	090211_27_NW_C16.mgf	ENSP00000370540	3.98	2	-8.2	8.7	26.2	Transmembrane emp24 domain-containing protein 4 precursor. Source: Uniprot/SWISSPROT Q7Z7H5
10	090213_12_NW_S5.mgf	ENSP00000370589	3.54	1	-4.7	9.2	66	Nucleolar protein 5A (Nucleolar protein Nop56) [Source:UniProtKB/Swiss-Prot;Acc:O00567]
40	090213_17_NW_S20.mgf	ENSP00000370601	3.49	1	-3.5	10	23.3	ATP synthase O subunit, mitochondrial precursor (EC 3.6.3.14) (Oligomycin sensitivity conferral protein) (OSCP). Source: Uniprot/SWISSPROT P48047
14	090211_07_NW_S7.mgf	ENSP00000370782	4.25	1	-1.4	5.9	24.7	
5	090213_06_NW_C3.mgf	ENSP00000371275	3.71	2	-13.7	8.6	47	Creatine kinase, ubiquitous mitochondrial Precursor (EC 2.7.3.2)(U-MtCK)(Acidic-type mitochondrial
6	090213_07_NW_S3.mgf	ENSP00000371275	4.18	3	-13.8	8.6	47	Creatine kinase, ubiquitous mitochondrial Precursor (EC 2.7.3.2)(U-MtCK)(Acidic-type mitochondrial creatine kinase)(Mia-CK) [Source:UniProtKB/Swiss-Prot;Acc:P12532]
20	090211_14_NW_S10.mgf	ENSP00000371275	3.79	1	-3	8.6	47	Creatine kinase, ubiquitous mitochondrial Precursor (EC 2.7.3.2)(U-MtCK)(Acidic-type mitochondrial
5	090213_06_NW_C3.mgf	ENSP00000371283	4.95	3	-8.3	9.7	70	Polyadenylate-binding protein 3 (Poly(A)-binding protein 3) (PABP 3) (Testis-specific poly(A)-binding protein). Source: Uniprot/SWISSPROT Q9H361
6	090213_07_NW_S3.mgf	ENSP00000371283	4.32	2	-9.2	9.7	70	Polyadenylate-binding protein 3 (Poly(A)-binding protein 3) (PABP 3) (Testis-specific poly(A)-binding protein). Source: Uniprot/SWISSPROT Q9H361
17	090211_11_NW_C9.mgf'	ENSP00000371283	3.56	1	-1.7	9.7	70	Polyadenylate-binding protein 3 (Poly(A)-binding protein 3) (PABP 3) (Testis-specific poly(A)-binding protein). Source: Uniprot/SWISSPROT Q9H361
18	090211_12_NW_S9.mgf	ENSP00000371283	3.62	1	-7.3	9.7	70	Polyadenylate-binding protein 3 (Poly(A)-binding protein 3) (PABP 3) (Testis-specific poly(A)-binding protein). Source: Uniprot/SWISSPROT Q9H361
8	090213_10_NW_S4.mgf	ENSP00000371363	4.73	3	-8.7	10	20.1	Ribosomal protein S10-like pseudogene. Source: Uniprot/SPTREMBL Q9NQ39
19	090211_13_NW_C10.mgf	ENSP00000371647	4.67	2	-7.9	9.5	121.6	Myosin-Ic (Myosin I beta) (MMI-beta) (MMIb). Source: Uniprot/SWISSPROT O00159
47	090213_25_NW_C24.mgf	ENSP00000371891	3.29	1	-1.7	9.2	59.3	Caskin-1 (CASK-interacting protein 1) [Source:UniProtKB/Swiss-Prot;Acc:Q8WXD9]
13	090211_06_NW_C7.mgf	ENSP00000372170	3.22	1	-1.2	10	31.3	Homeobox protein MSX-1 (Msh homeobox 1-like protein)(Hox-7) [Source:UniProtKB/Swiss-Prot;Acc:P28360]
10	090213_12_NW_S5.mgf	ENSP00000372218	3.79	1	-2	5.2	48.4	Serpin B12 [Source:UniProtKB/Swiss-Prot;Acc:Q96P63]
34	090211_30_NW_S17.mgf	ENSP00000372500	5.25	2	-3.9	8.6	27.9	60S RIBOSOMAL L5
24	090211_19_NW_S12.mgf	ENSP00000372520	4.9	1	-1.1	6.3	59	Ig gamma-1 chain C region. Source: Uniprot/SWISSPROT P01857
29	090211_25_NW_C15.mgf	ENSP00000372520	4.66	2	-6.1	6.3	59	Ig gamma-1 chain C region. Source: Uniprot/SWISSPROT P01857
38	090213_14_NW_S19.mgf	ENSP00000372524	3.36	1	-1.4	10	16.7	Uncharacterized protein ENSP00000372524 [Source:UniProtKB/TrEMBL;Acc:A6NH90]
42	090213_19_NW_S21.mgf	ENSP00000372524	3.49	1	-2.7	10	16.7	Uncharacterized protein ENSP00000372524 [Source:UniProtKB/TrEMBL;Acc:A6NH90]
17	090211_11_NW_C9.mgf'	ENSP00000372554	4.55	1	-1.3	11	9.8	40S ribosomal protein S18 (Ke-3)(Ke3) [Source:UniProtKB/Swiss-Prot;Acc:P62269]
19	090211_13_NW_C10.mgf	ENSP00000372554	4.92	1	-1.3	11	9.8	40S ribosomal protein S18 (Ke-3)(Ke3) [Source:UniProtKB/Swiss-Prot;Acc:P62269]
20	090211_14_NW_S10.mgf	ENSP00000372554	3.87	1	-1.4	11	9.8	40S ribosomal protein S18 (Ke-3)(Ke3) [Source:UniProtKB/Swiss-Prot;Acc:P62269]
35	090211_32_NW_C18.mgf	ENSP00000372648	3.97	1	-8.7	6.9	192.6	complement component 4B preproprotein [Source:RefSeq peptide;Acc:NP_001002029]
9	090213_11_NW_C5.mgf	ENSP00000372873	3.99	2	-21	7.1	47.3	Flotillin-1 [Source:UniProtKB/Swiss-Prot;Acc:O75955]